Thesis

"Novel Therapeutic Targets for Chordoma"

submitted by

Dr. med.univ.
Susanne SCHEIPL

for the Academic Degree of a

Doctor of Medical Science
(Dr. scient. med.)

at the

Medical University of Graz
Department of Orthopaedics and Orthopaedic Surgery

under the Supervision of

Assoc.-Prof. PD Dr. Bernadette LIEGL-ATZWANGER

2016

Declaration

I hereby declare that this thesis is my own original work and that I have fully acknowledged by name all of those individuals and organisations that have contributed to the research for this thesis. Due acknowledgement has been made in the text to all other material used. Throughout this thesis and in all related publications I followed the "Standards of Good Scientific Practice and Ombuds Committee at the Medical University of Graz".

Graz, July 20th, 2016

X

Dr. med. univ. Susanne Scheipl

Foreword

This project, which focuses on the development of new therapeutic agents for chordoma, is part of a major international collaborative effort that seeks to understand the pathogenesis of chordoma, a primary malignant bone tumour, with the aim of delivering more effective treatments for this rare disease. The Chordoma Foundation (http://www.chordomafoundation.org) unifies this international project of which the Austrian research group is a member. The interdisciplinary Austrian project on chordoma (Department of Orthopaedics and Orthopaedic Surgery, and the Institute of Pathology, Medical University of Graz, in close collaboration with the Departments of Neurosurgery and Otorhinolaryngology, Medical University of Graz) was initiated in 2007 and is part of this collaborative effort, as is the National Center for Spinal Disorders, Budapest, Hungary. Our research efforts in this area have resulted in several publications. I was the first author of two of these publications, and they are a part of this thesis (1, 2).

Since our Austrian research group has a commitment to chordoma research, it is crucial to work with others in the field. Univ.-Prof. Dr. Adrienne M. Flanagan, Academic Head of University College London (UCL) Pathology, Lead of the Genetics & Cell Biology Sarcoma Group in the UCL Cancer Institute, and Head of the Department of Pathology, Royal National Orthopaedic Hospital (RNOH) Stanmore, is recognised as a leader in the field of chordoma research. She and her team have studied chordoma for more than twelve years (3-10). Not only was her laboratory the first to establish *T* (brachyury) as the molecular hallmark of chordoma (8), but it also showed through various approaches that brachyury is pivotal in the pathogenesis of this disease (5, 7-9). The Austrian group has already established a good relationship with Professor Flanagan's laboratory, as demonstrated by the two co-authored, peer-reviewed manuscripts that have resulted (3, 7).

I was awarded several short-term fellowships (Erasmus staff training 2010, "Bank Austria Visiting Scientists Programme" 2013), which allowed me to visit the Flanagan laboratory at the UCL Cancer Institute, London, UK. In 2013, a "Marietta Blau Scholarship" (OeAD, ICM-2012-01605) enabled me to spend a year in Professor Flanagan's laboratory and to conduct a pilot study. On the basis of this work, in 2014 I was awarded an "Erwin Schroedinger fellowship" by the Austrian Science Fund (FWF, J3640). In total, I spent almost four years (January 2013 until October 2016) in Professor Flanagan's laboratory at the UCL Cancer Institute, where I conducted a focused compound screen involving more

than 1,000 small molecule kinase inhibitors. My fellowships gave me the opportunity to learn new methods and skills, which I can apply not only to chordoma and my thesis, but also to a wide range of other diseases and research questions. What is more, my work at the UCL Cancer Institute enabled me to become part of an international research network and to publish my work in the renowned "Journal of Pathology" (11). I would like to thank all funding bodies and supporters at my home university, the Medical University of Graz, Graz, Austria, as well as at the UCL Cancer Institute, London, UK, for providing me with this singular opportunity. I look forward to applying this newly acquired knowledge to my future research and work back home in Austria.

Disclosures

Permission of copyright holders of materials included in this work (John Wiley & Sons, Inc., Hoboken, NJ, USA; Assoc.-Prof. PD Dr. Bernadette Liegl-Atzwanger, Institute of Pathology, Medical University of Graz; Univ.-Prof. Dr. Andreas Leithner, head of the Department of Orthopaedics and Orthopaedic Surgery, Medical University Graz; Josh Sommer, Executive Director of the Chordoma Foundation, Durham, NC, USA) are attached to this thesis (**Appendix 3**). Co-authors who actively contributed to the resulting publications are listed below, and their contributions are stated. They have all provided written permission for the use of these data (**Appendix 3**). Copies of the original manuscripts are in the Appendix (with kind permission from John Wiley & Sons, Inc.) (**Appendix 2**).

The following individuals and co-authors contributed to the work published by Scheipl *et al.* in 2012 (1): Assoc.-Prof. PD Dr. Bernadette Liegl-Atzwanger (BL), Institute of Pathology, and Univ.-Prof. Dr. Andreas Leithner (AL), Dept. of Orthopaedics and Orthopaedic Surgery, Medical University of Graz, planned and initialised this project. BL supervised the project. Univ.-Prof. Dr. Reinhard Windhager (Dept. of Orthopaedics and Orthopaedic Surgery, Medical University of Graz), Univ.-Prof. Dr. Michael Mokry (Dept. of Neurosurgery, Medical University of Graz), Univ.-Prof. Dr. Heinz Stammberger (Dept. of Otorhinolaryngology, Medical University of Graz), Univ.-Prof. Dr. Stefan Gattenloehner, as well as Univ.-Prof. Dr. Peter P. Varga (PPV) and Dr. Aaron Lazáry (AL) (both National Center for Spinal Disorders, Buda Health Center, Budapest, Hungary) were heads and/or representatives of the departments that contributed to the diagnosis and treatment of chordoma patients whose samples were included in our analysis. Dr. Elke V. Froehlich (EVF) (Medical University of Graz) collected these samples and the baseline patients' data. BL and Univ.-Prof. Dr. Alfred Beham (AB) (Institute of Pathology, Medical University of Graz) revised the histological diagnoses prior to the inclusion of samples in this study. Margit Gogg-Kamerer and Elisabeth Grygar, both of the Institute of Pathology, Medical University of Graz, conducted the immunohistochemical stainings. Dr. Susanne Scheipl (SS) and BL evaluated the immunohistochemical slides. SS conducted the semiquantitative analysis and updated the follow-up and the clinical data. Dr. Franz Quehenberger (FQ) (Institute of Medical Informatics, Statistics and Documentation, Medical University of Graz) conducted the statistical analyses. SS and BL wrote the manuscript. Dr. Sara Crockett, PD Dr. Gerald Gruber, Dr. Werner Maurer-Ertl and Dr.

Joerg Friesenbichler revised the manuscript. Univ.-Prof. Dr. Reinhard Windhager, Univ.-Prof. Dr. Heinz Stammberger and Univ.-Prof. Dr. Stefan Gattenloehner have terminated their employment with the Medical University of Graz and have not returned their signed permission forms. However, they gave their written permission prior to the manuscript's publication. All other co-authors gave written consent to the use of these data in this thesis. The research underlying this manuscript was further supported by the Austrian Musculo-Skeletal Oncology Society (AMSOS) and by a grant from the National Bank of Austria (Jubilaeumsfondprojekt no. 13459).

The work reported by Scheipl *et al.* in 2013 was supported by the following co-authors and contributors (2): BL and SS initialised the project, contributed to the outline of the experimental designs and semiquantitatively analysed the immunohistochemcial sections. BL supervised, and SS coordinated the project. Univ.-Prof. Dr. Johannes Haybaeck (Institute of Pathology, Medical University of Graz) contributed his HDAC antibodies. PPV and AL provided follow-up data on the Hungarian patients. And, EVF and AL provided clinical information on the Austrian patients. BL, Margit Gogg-Kamerer and Elisabeth Grygar created the tissue micro array (TMA) and conducted the immunohistochemical stainings. PD Mag. Dr. Birgit Lohberger (Head of the Research Laboratory of the Dept. of Orthopaedics and Orthopaedic Surgery, Medical University Graz) contributed to the outline of the experimental designs, supervised the laboratory work, conducted the experimental data analysis and provided a draft on the methods employed. Ass.-Prof. PD Mag. Dr. Beate Rinner (Center for Medical Research, former Cell Culture Facility, Medical University of Graz) contributed to the outline of the experimental designs, provided the chordoma cell lines studied and conducted the cell cycle analysis. FQ analysed the clinical data. Heike Kaltenegger and Nicole Stuendl (NS), technicians at the Research Laboratory of the Dept. of Orthopaedics and Orthopaedic Surgery, Medical University of Graz, conducted the laboratory experiments. NS was co-funded by a grant from the Austrian Musculo-Skeletal Oncology Society (AMSOS), which was awarded to SS in 2010. SS wrote the manuscript. All co-authors provided written consent permitting the use of these data in this thesis.

Finally, the work published by Scheipl *et al.* in 2016 was co-authored and/or supported by the following individuals (11): Univ.-Prof. Dr. Adrienne M. Flanagan (AMF) (University College London [UCL] Cancer Institute, London, UK, and Department of Histopathology, Royal National Orthopaedic Hospital [RNOH] Stanmore, Stanmore, UK) initiated and

supervised the project. AMF and SS coordinated the project. SS, Michelle Barnard (MB), SenSci, Cancer Research Technology (CRT) Discovery Laboratories, Cambridge, UK and the UCL Cancer Institute outlined the screening cascade. SS and MB conducted the experiments. Dr. Lucia Cottone (LC) and Dr. Mette Jorgensen, both of the UCL Cancer Institute, contributed to the tissue culture work and the focused compound screen, and helped to arrange the Western blots (LC). MB conducted the data analysis. SS and AMF wrote the manuscript. Dr. Fabrice Turlais (CRT Discovery Laboratories) oversaw and advised on compound screening and data analysis. James A. Smith, CRT Discovery Laboratories, was responsible for the compound plate preparation. GlaxoSmithKline (GSK) donated the Published Kinase Inhibitor Sets (PKIS) used in the focused compound screen. Univ.-Prof. Dr. David Drewry and Univ.-Prof. Dr. William J. Zuercher, both of the Structural Genomics Consortium (SGC)-UNC, UNC Eshelman School of Pharmacy, University of North Carolina at Chapel Hill, NC, USA, both former employees of GSK, helped organise the GSK compounds and the biochemical selectivity data and advised on data analysis and data preparation for publication. Dr. Hongtao Ye (Dept. of Histopathology, RNOH Stanmore) performed FISH analysis. Dr. Ana P. Leite (APL) (UCL Cancer Institute) and Dr. Nischalan Pillay (UCL Cancer Institute and Dept. of Histopathology, RNOH Stanmore) supported data analysis and next-generation sequencing mutation analysis. APL conducted MSigDB enrichment analysis. Dr. Naomi Guppy (UCL Advanced Diagnostics, London, UK) performed immunohistochemistry. Dr. Sandra J. Strauss (UCL Cancer Institute) advised on the clinical relevance of the findings. AL provided organisational support and clinical advice. Univ.-Prof. Dr. Möller, Univ.-Prof. Dr. Thomas Barth and Dr. Silke Brüderlein, Institute of Pathology, Ulm University, Ulm, Germany, established the U-CH7 primary culture and helped to provide us with (new) chordoma cell lines. Dr. Fernanda Amary and Dr. Roberto Tirabosco contributed with their clinicopathological expertise. The Chordoma Foundation (CF, an international chordoma patient advocacy group), in particular Josh Sommer and Patty Cogswell (PC), provided administrative support and support with cell line validation. PC provided a statement regarding the methodology employed for the animal studies. *In vivo* studies were generated through the CF Drug Screening Pipeline at South Texas Accelerated Research Therapeutics (START), San Antonio, TX, USA under International Animal Care and Use Committee-approved protocols. Staff members from Cancer Research Technology Discovery Laboratories, particularly Mathew Rushbrook, and Dr. Ariadna Mendoza-Naranjo (UCL Cancer Institute) contributed with technical support and reagents. David

Allen, as well as Dr. Naomi Guppy, UCL Advanced Diagnostics, helped with the creation of the IHC images. Univ.-Prof. Dr. Paolo Salomoni and Dr. Aikaterini Lampada, UCL Cancer Institute, provided scientific and technical advice. Dr. Silke Brüderlein has retired from Ulm University and has not returned her signed permission form. However, her successor, Univ.-Prof. Dr. Thomas Barth, provided written consent. All other co-authors have provided written consent permitting the use of these data in this thesis.

Acknowledgements

I offer my warmest thanks to my parents and my brother. Without their continuous help and support, I would not have been able to go abroad and/or complete the studies underlying this thesis. I would also like to thank my friends in Austria and in London, who always were willing to listen and to offer advice.

I am grateful and proud to have been mentored by outstanding supervisors, to whom I am much obliged: Assoc.-Prof. PD Dr. Bernadette Liegl-Atzwanger, Institute of Pathology, Medical University of Graz, supervised my PhD thesis and has been a mentor and friend throughout my scientific career. Univ.-Prof. Dr. Andrea Langmann, former vice rector of the Medical University of Graz, encouraged and inspired me to undertake a research fellowship. Univ.-Prof. Dr. Adrienne M. Flanagan, UCL Cancer Institute, trained me to become a clinical scientist, as well as supervised and educated me throughout my research fellowship in London. I would also like to thank Univ.-Prof. Dr. Andreas Leithner, Medical University Graz, who gave consent to be absent from clinical rounds during my fellowship.

Several funding bodies have substantially supported my research fellowship: the Austrian Science Fund (FWF) (Erwin-Schroedinger fellowship, J3640) (October 2014 - October 2016), the OeAD GmbH (Marietta Blau fellowship; ICM-2012-01605) (2013) and Chordoma UK (166854) (April - November 2014). Dr. Tibor Szabó (OeAD-GmbH) and Mr. Gass (Austrian Science Fund) have been extremely supportive and helpful regarding any questions or issues related to these fellowships. The research underlying this thesis was further supported by a grant from the Austrian Musculoskeletal Oncology Society (AMSOS), awarded in 2010.

I would like to thank the Chordoma Foundation (CF), in particular Josh Sommer, for permitting me to use the *in vivo* data that was generated via the foundation's Drug Screening Pipeline. Special thanks are also dedicated to my co-authors and collaborators for their important contributions, constructive criticism and advice.

Dr. Christopher Barrington helped with various computational issues and with editing this manuscript.

There are many more people whose help and support were crucial for bringing this thesis to its fruitful completion, and even though I cannot mention all of them in this section, I offer my warmest thanks to each of them.

List of Contents

List of Abbreviations

4E-BPs: eukaryotic translation initiation factor 4E binding proteins (such as 4E-BP1)

ACTR2: activin A receptor, type IIB

ADCC: antibody-dependent cellular cytotoxicity

ADP: adenosine diphosphate

AKR1B10: aldo-keto reductase family 1 member B10

AKT, AKT1: protein kinase B alpha or PKB

ALK: anaplastic lymphoma kinase

ALK5: activin receptor-like kinase 5 (ALK5) (alias: TGFB1)

AMP: adenosine monophosphate

AMPK: adenosine monophosphate (AMP)-activated protein kinase

AMSOS: Austrian Musculo-Skeletal Oncology Society

ANOVA: analysis of variance

AR: amphiregulin

Arg: arginine

ATCC: American Type Culture Collection

ATP: adenosine-5‘-triphosphate

AXL: Anexelekto (Greek word for “uncontrolled”), AXL receptor tyrosine kinase

AZD8931: sapitinib

BCA: bicinchoninic acid assay

BCL2: B-cell CLL/lymphoma 2

BIBW 2992: afatinib

BIM: gene encoding B-cell CLL/lymphoma 2 (BCL2)-like 11

BNCT: benign notochordal cell tumours

BRAF: B-RAF (rapidly accelerated fibrosarcoma) proto-oncogene, serine/threonine kinase

BTC: betacellulin

BTK: bruton agammaglobulinemia tyrosine kinase

C: cytosine

CA: California

cAMP: cyclic adenosine monophosphate

CD: cluster of differentiation

CDKN2A: cyclin-dependent kinase inhibitor 2A

cDNA: complementary deoxyribonucleic acid

CEN: centromeric

CI: confidence interval

CK19: cytokeratin 19

c-KIT: stem-cell factore receptor, receptor tyrosine kinase CD117

CLL: chronic lymphocytic leukaemia

CML: chronic myelogenous leukaemia

CNV: copy number variation

CO_2: carbon dioxide

COI: combination index

COSMIC: catalogue of somatic mutations in cancer

CpG: CG dinucleotides ("CpGs": cytosine – phosphate - guanine)

CRT: Cancer Research Technology Discovery Laboratories, Cambridge, UK

CS: Cowden syndrome

CS: cytostatic profile

CT: computed tomography

CT: Connecticut

CTLA4: cytotoxic T lymphocyte-associated antigen 4

Dept.: Department

Dil.: dilution

DNA: deoxyribonucleic acid

EC_{50}: half-maximal effective concentration

EDTA: ethylenediaminetetraacetic acid

EED: embryonic ectoderm development

EGF: epidermal growth factor

EGFR: epidermal growth factor receptor

EGTA: ethylene glycol tetraacetic acid

eIF4E: eukaryotic translation initiation factor 4E

ELISA: enzyme-linked immunosorbent assay

EMA: epithelial membrane antigen

EMSOS: European Muscolo-Skeletal Oncology Society

EMT: epithelial-mesenchymal transition

EPR: epiregulin

ER: estrogen receptor

ERBB (-1, -2, -3, -4): erythroblastic leukaemia viral oncogene homolog (-1, -2, -3, -4)

ERK1/2: extracellular signal-regulated kinases ½

ESMO: European Society for Medical Oncology

FACS: fluorescence-activated cell sorting

FBS: fetal bovine serum

FDA: U.S. Food and Drug Administration

FDR: false discovery rate

FISH: fluorescence in situ hybridisation

FITC: fluorescein isothiocyanate

FKBP-12: FK506-binding protein 12

G: guanine

GAPDH: Glyceraldehyde 3-phosphate dehydrogenase

GH: growth hormone

GIST: gastrointestinal stromal tumour

Gly: glycine

GPCR: G-protein coupled receptor

Grb-2: growth factor receptor-bound protein-2

GSK: GlaxoSmithKline

GTP: guanosine-5‘-triphosphate

GyE: gray equivalent

H&E: haematoxylin and eosin

H: hour

H1 (H2A, H2B, H3, H4): histone 1 (2A, 2B, 3, 4)

HAT: histone acetyl transferase

HB-EGF: heparin-binding growth factor

HDAC: histone deacteylase

HeLa: immortalised cell line originating from cervical cancer cells of Henrietta Lacks

HER (-1, -2, -3, -4): human epidermal growth factor receptor (-1, -2, -3, -4)

HGF: hepatocyte growth factor

HSP90: heat shock protein 90

HSR(s): homogeneously staining region(s)

IC_{50}: half-maximal inhibitory concentration

ID: identity

IGF: insulin-like growth factor

IGF-1: insulin-like growth factor1

IGF-1R: insulin-like growth factor (IGF-) receptor 1

IGF-2: insulin-like growth factor2

IGF-2R: insulin like growth factor receptor type 2

IGFBP 1-6: IGF-binding proteins 1-6

IHC: immunohistochemistry, immunohistochemical

IL-6: interleukin-6

IMDM: Iscove's Modified Dulbecco's medium

IN: Indiana

Inc.: Incorporated

IR: insulin receptor

IR-A: fetal isofom of the insulin receptor

IRS-1 to IRS-4: insulin receptor substrates 1 to 4

ITS: insulin/transferrin/sodium selenite

JAK2: janus-kinase 2

kDa: kilodaltons (molecular weight)

KDR: kinase insert domain receptor (a type III receptor tyrosine kinase) (alias: VEGFR-2)

KGaA: Kommanditgesellschaft Auf Aktien (German for "limited partnership on shares")

LBH-589: panobinostat

LCK: lymphocyte-specific protein tyrosine kinase

LKB1: liver kinase B1 (also known as serine-threonine kinase 11 or STK11)

LYN: v-yes-1 Yamaguchi sarcoma viral related oncogene homolog

Lys: lysine

µg: microgram

µm: micrometer

μM: micro-molar

mAbs: monoclonal antibodies

MAP: mitogen-activated protein kinase

MD: medicinae doctor, doctor of medicine

MDC: multidrop combi

MEK (1 and 2): MAP (mitogen-activated protein) kinase/ERK (extracellular signal-regulated kinase) kinase (1 and 2), or MAPK/ERK kinases (1 and 2), or MEK1 and MEK2

Met: methionine

MET: protein (receptor tyrosine kinase) encoded by the *MET* gene

MI: maximum percentage inhibition

min.: minimum

Min: minute(s)

miRNA: micro-RNA

mM: milli-molar

MPNST: malignant peripheral nerve sheath tumours

MRI: magnetic resonance imaging

mTOR: mammalian target of rapamycin

mTORC1 and 2: mammalian target of rapamycin complex 1 and 2

MUG: Medical University of Graz

MUG-Chor1: "Medical University of Graz Chordoma 1", chordoma cell line

n: number (of repeats, of samples, of compounds)

NaCl: sodium chloride

NaF: sodium fluoride

NAHDF: normal adult human dermal fibroblasts

NCI-N87: human gastric carcinoma cell line

NF1: neurofibromatosis type 1

NGS: next generation sequencing

NJ: New Jersey

Nonidet P-40: octylphenoxypolyethoxyethanol

NOS: not otherwise specified

NOV120101; HM781-36B: poziotinib

NRAS: neuroblastoma RAS

NRG: neuroregulin

NSCLC: non-small cell lung cancer

NT: not tested

NY: New York

OSI-774: erlotinib

p: phospho-

Pan-CK: pan-cytokeratin

PARP: poly Adenosine diphosphate (ADP) ribose polymerase

PASW: predictive analytics software

PBS: phosphate-buffered saline

PCR: polymerase chain reaction

PDGF: platelet-derived growth factor

PDGFR: platelet-derived growth factor receptor

PDK1: 3-phospho-inositide-dependent protein kinase-1

PDX: patient derived xenograft(s)

Pen/Strep: penicillin/streptomycin

PET: positron emission tomography

pH: pH scale as a chemical measure of acid and base properties

PhD: philosophiae doctor, doctor of philosophy

PI: propidium iodide

PI3K: phosphoinositide 3-kinase; (also called phosphatidylinositol-4,5-bisphosphate 3 kinase), enzyme encoded by the PIK3CA gene

PIK3CA: phosphatidylinositol-4,5-bisphosphate 3-kinase catalytic subunit alpha; gene encoding for PI3K

PIKK: phosphatidylinositol-kinase-related kinase

PIP2: phosphatidylinositol-4,5-biphosphate

PIP3: phosphatidylinostiol-3,4,5-triphosphate

PJS: Peutz-Jeghers syndrome (PJS)

PKC: protein kinase C

PKIS: published kinase inhibitor set (GSK)

PLC-γ: phospholipase-C-γ

PNQ (SS): potency not quantified due to a small activity span

POS: positive controls

PR: progesterone receptor

PRC2: polycomb repressive complex 2

PRKACA: protein kinase, cAMP-dependent, catalytic, alpha

PTEN: phosphatase and tensin homolog

PXD101: belinostat

q-RT-PCR: quantitative real-time polymerase chain reaction

RAF: rapidly accelerated fibrosarcoma kinase

RAS: rat sarcoma viral oncogene homolog, small GTP(guanosine triphosphate)ase

RASSF1: RAS association domain family protein 1

RCC: renal cell carcinoma

RECIST: response evaluation criteria in solid tumours

REDD1 and 2: regulated in development and DNA damage responses protein 1 and 2

Rheb: RAS homologue enriched in brain

RIPA: radioimmunoprecipitation assay lysis buffer

RNA: ribonucleic acid

RNOH: Royal National Orthopaedic Hospital Stanmore, UK

ROCK1: rho-associated, coiled-coil containing protein kinase 1

Rpm: revolutions per minute

RPMI: Roswell Park Memorial Institute medium

RPS6: 40S ribosomal protein S6

RTK: receptor tyrosine kinases

S (for instance S4/S5); sacral vertebrae (4 or 5)

S100: name of a low-molecular weight protein

S6K1: ribosomal protein S6 kinase

SAHA: vorinostat; suberoylanilide hydroxyamic acid

SD: standard deviation(s)

SDS: sodium dodecyl sulfate

SDS-PAGE: sodium dodecyl sulfate polyacrylamide gel electrophoresis

SenSci: senior scientist

Ser: serine

Shc: Src homology and collagen domain protein

SNC: selectivity not calculated

SOS: son of sevenless

SRC: v-src sarcoma (Schmidt-Ruppin A-2) viral oncogene homolog (avian)

SRPN: staurosporine

START: South Texas Accelerated Research Therapeutics

STAT(3; 5): signal transducer and activator of transcription (3; 5)

STR: short tandem repeat

SUZ12: suppressor of zeste 12 homolog

T: brachyury

TGFB1: transforming growth factor, beta receptor 1 (alias: ALK5)

TGF-α: transforming growth factor α

Thr: threonine

TKI: tyrosine kinase inhibitor

TLR: toll-like receptor

TMA: tissue micro array

TNM: UICC staging system for malignant tumours (T describes the primary tumour site, N regional lymph node involvment, and M the presence or abscence of distant metastases)

TOR: target of rapamycin

Tris-HCL: tris(hydroxymethyl)aminomethane hydrochloride

Trp: tryptophan

TSC: tuberous sclerosis complex

TSC1: tuberous sclerosis complex 1; hamartin

TSC2: tuberous sclerosis complex 2; tuberin

TV: tumour volume

TX: Texas

Tyr: tyrosine

U-CH1, -2, -7, -10: ”Ulm Chordoma-1, -2, -7, -10”, chordoma cell lines

UCL: University College London, London, UK

UICC: Union for International Cancer Control

UK: United Kingdom

USA: United States of America

Val: valine

VEGF: vascular endothelial growth factor

VEGFR: vascular endothelial growth factor receptor

WB: western blot analysis

WHO: World Health Organisation

YAP(1): yes-associated protein (1)

ZD1839: gefitinib

List of Figures

List of Tables

Abstract

Chordomas are rare malignant bone tumours with a poor prognosis. The mainstay of treatment is surgery. Even though there have been advances in irradiation therapy, therapeutic options are limited, particularly in advanced and metastasising disease. In view of this unmet need, the author conducted three studies in order to identify potential therapeutic targets for chordoma. These approaches are summarised in this thesis.

The first study assesses whether the insulin-growth factor-1 (IGF-1) receptor (IGF-1R) could be a potential target for specific inhibition in chordomas. For that reason we studied the immunohistochemical (IHC) expression of IGF-1R and its ligands, IGF-1 and IGF-2, in a series of 50 clinical chordoma samples (34 primary tumours, 16 recurrences). These were obtained from 44 patients (27 males, 17 females). Thirty-eight chordomas (76%) expressed IGF-1R, 46 (92%) stained positive for IGF-1 and 25 (50%) for IGF-2. Staining was strong and diffuse in 18 (36%; IGF-1R), 32 (64%; IGF-1) and 8 (16%; IGF-2) chordomas, respectively. In summary, we could show that IGF-1R and IGF-1 were expressed in the majority of clinical chordoma samples.

In a second study, we investigated histone deacetylase (HDAC) inhibitors as potential epigenetic therapeutics. We performed IHC on 50 chordoma samples using antibodies against HDACs 1-6. We then tested three pan-HDAC inhibitors, vorinostat (SAHA), panobinostat (LBH-589) and belinostat (PXD101), in our chordoma cell line, MUG-Chor1, by Western blots, cell cycle analysis and various apoptosis assays. IHC was negative for HDAC1, positive for HDAC2 in the majority of specimens (n=36; 72%) and positive for HDACs 3-6 in all available specimens (n=43; 86%). Expression for HDAC6 was strongest. The HDAC inhibitors SAHA and LBH-589 induced a significant increase of G2/M phase cells and cleaved caspase-3 (p=0.0003 and p=0.0014 after 72h, respectively), while PXD101 did not. For SAHA and LBH-589, a peak in caspase 3/7 activity and PARP cleavage confirmed apoptosis. In conclusion, this study indicated that our chordoma series expressed HDACs 2-6 and that SAHA and LBH-589 significantly increased apoptosis and changed cell cycle distribution *in vitro*.

At the University College London (UCL) Cancer Institute we chose a more comprehensive approach and undertook a phenotypic compound screen against 1,097 compounds on three well-characterised chordoma cell lines. A total of 154 compounds were selected from the single concentration screen (1 μM) and further profiled in a 10-point dose-response (EC_{50})

format. EC_{50} profiling was conducted in chordoma cell lines as well as in normal dermal fibroblasts. The latter were included as we aimed to identify compounds which selectively targeted chordoma cells but not fibroblasts. Twenty-seven of these 154 compounds displayed chordoma selective growth-inhibitory effects. Twenty-one of these 27 compounds (78%) targeted the epidermal growth factor receptor/erythroblastic leukaemia viral oncogene homolog (EGFR/ERBB) family. EGFR inhibitors in clinical development were then studied on an extended cell line panel of seven chordoma cell lines, four of which were responsive to EGFR inhibition. Sapitinib (AstraZeneca) emerged as our most promising compound, followed by gefitinib (AstraZeneca) and erlotinib (Roche/Genentech). These compounds were shown to induce apoptosis in responsive cell lines and to suppress phospho-EGFR and its downstream-markers in a dose-dependent manner. Analyses of chemical trends and substituent patterns suggested that EGFR inhibitors with small aniline substituents in the 4-position of the quinazoline ring were more effective than inhibitors with large substituents in that position. Sapitinib significantly reduced tumour growth in two xenograft mouse models. One of the resistant cell lines (U-CH2) was shown to express high levels of phospho-MET, which is a recognised bypass signalling pathway to EGFR. Neither amplifications (*EGFR*, *ERBB2*, *MET*) nor mutations in *EGFR, ERBB2, ERBB4, PIK3CA, BRAF, NRAS, KRAS, PTEN, MET* or other cancer gene hotspots were detected. Our findings were consistent with the (phospho-) EGFR expression reported in the majority of clinical samples. Furthermore, our results provided evidence for exploring the efficacy of EGFR inhibitors in the treatment of patients with chordoma and for studying possible resistance mechanisms to these compounds both *in vitro* and *in vivo*. Based on the promising preclinical data on EGFR inhibition, Chordoma Foundation and associated researchers and clinicians are currently planning a prospective, randomised clinical trial, which will involve a second-generation EGFR inhibitor in advanced chordoma.

In summary, the approaches we have chosen to identify therapeutic targets for chordoma have become more functional and comprehensive during the time I spent on this thesis. Finally, a phenotypic screening approach, which reduces mechanistic assumptions regarding the nature and/or the structure of a potential target, has led to the identification of the EGFR/ERBB family as a promising therapeutic target for this orphan disease. Based on these findings, which have been shared by other laboratories, an EGFR-inhibitor is now going to enter the first prospective, randomised clinical trial in chordoma.

Zusammenfassung

Bei Chordomen handelt es sich um seltene, bösartige Knochentumoren, welche aufgrund eingeschränkter therapeutischer Optionen eine schlechte Prognose besitzen. Dies trifft insbesondere auf fortgeschrittene und metastasierende Stadien dieses Tumors zu. In Hinblick auf unzureichende Behandlungsmöglichkeiten fasst diese Arbeit drei von der Autorin durchgefuehrte Studien zusammen, welche den Anspruch verfolgen, potentielle Zielstrukturen für neue Behandlungsansätze zu identifizieren:

Zunächst wurden in einer ersten Studie 50 klinische Chordomproben untersucht. Diese setzten sich aus 34 Primärtumoren und 16 Rezidiven von 44 PatientInnen (27 männlich, 17 weiblich) zusammen. Die Chordomproben wurden immunhistochemisch auf deren Expression des IGF-1-Rezeptors (IGF-1R) bzw. von IGF-1 und IGF-2, den Liganden dieses Rezeptors, überprüft. Dabei konnte festgestellt werden, dass 38 dieser Proben (76%) IGF-1R exprimierten, 46 (92%) IGF-1, und 25 (50%) IGF-2. Wir beobachteten eine starke und diffuse Expression des IGF-1-Rezeptors in 18 Chordomen (36%). Die Liganden waren in 32 Tumoren (64%; IGF-1) bzw. in acht Chordomen (16%; IGF-2) stark und diffus exprimiert.

In einer zweiten Studie wurden Histon-Deacetylase (HDAC) - Hemmer als potentielle epigenetische Therapeutika für Chordome evaluiert. In einem ersten Schritt untersuchten wir dazu unsere 50 Chordomproben immunhistochemisch auf eine Expression der HDACs 1-6. Anschließend testeten wir in unserer Chordom-Zelllinie MUG-Chor1 mittels Western Blotting, Zellzyklusanalyse und diverser Apoptose-Assays drei pan-HDAC Inhibitoren, nämlich Vorinostat (SAHA), Panobinostat (LBH-589), und Belinostat (PXD101). Während HDAC1 immunhistochemisch nicht nachweisbar war, zeigte HDAC2 eine Expression in der Mehrzahl der Fälle (n=36; 72%). HDACs 3 bis 6 waren in allen überprüfbaren Proben in unterschiedlichem Maße exprimiert (n=43; 86%); HDAC6 zeigte dabei die stärkste Expression. Die HDAC Inhibitoren SAHA and LBH-589, nicht jedoch PXD101, bewirkten einen signifikanten Anstieg der Cleaved Caspase-3 (p=0.0003, bzw. p=0.0014 nach 72h) sowie jener Zellen, welche sich in der G2/M Phase des Zellzyklus befanden. SAHA und LBH-589 induzierten weiters einen Caspase 3/7-Anstieg sowie eine Spaltung von PARP. Das kann als Beweis für die apoptotische Aktivität dieser Inhibitoren angesehen werden. Zusammenfassend konnten wir in dieser zweiten Studie somit eine Expression der HDACs 2-6 in unseren Chordomproben nachweisen bzw. zeigen, dass die

HDAC-Inhibitoren SAHA und LBH-589 proapoptotisch wirken und den Zellzyklus in Chordomzellen beeinflussen.

Am University College London (UCL) Cancer Institute wählten wir – in einer dritten Studie - einen umfassenderen Ansatz und testeten 1097 Substanzen in drei gut charakterisierten Chordom-Zelllinien. Die Testung erfolgte im Rahmen eines phänotypischen Substanzscreenings. Im Zuge des initialen Screens wurden alle Substanzen in einer singulären Konzentration (1 μM) getestet, wobei 154 der Substanzen die Hit-Selektionskriterien erfüllten. Diese Hits wurden weiters in 10 ansteigenden Konzentrationen auf ihre Wirksamkeit und ihr Kurvenprofil hin untersucht (EC_{50}). Diese EC_{50}-Bestimmung erfolgte sowohl in Chordom-Zelllinien als auch in dermalen Fibroblasten. Durch die Testung in Fibroblasten konnten unter den initialen 154 Hits jene 27 Substanzen identifiziert werden, welche selektiv Chordomzellen in ihrem Wachstum hemmten. Hierbei erwiesen sich 21 dieser 27 Substanzen (78%) als Inhibitoren der *Epidermal Growth Factor Rezeptor/Erythroblastic Leukaemia Viral Oncogene Homolog (EGFR/ERBB)*-Familie. In einem nächsten Schritt wurden EGFR Inhibitoren, welche sich bereits in klinischer Anwendung bzw. Erprobung befanden, in einem erweiterten Panel von sieben Chordomzelllinien getestet. Vier dieser sieben Zellinien sprachen auf diese Inhibitoren an. Sapitinib (AstraZeneca) erwies sich als vielversprechendste Substanz, gefolgt von Gefitinib (AstraZeneca) und Erlotinib (Roche/Genentech). Diese EGFR/ERBB Inhibitoren wirkten proapoptotisch und riefen eine dosisabhängige Suppression von phosho-EGFR und dessen nachgeschalteten intrazellulären Effektoren hervor. Eine chemische Strukturanalyse ergab, dass EGFR Inhibitoren mit kleinen Anilin-Substituenten in Position 4 des Quinazolinringes bessere Ergebnisse zeigten als solche mit groβen Anilin-Substituenten in dieser Position. Sapitinib bewirkte eine signifikante Größenreduktion in zwei Xenograft-Maus-Modellen. Eine jener Zelllinien, welche sich als resistent gegenüber EGFR Inhibitoren erwiesen hatte (U-CH2), zeigte eine starke Expression von phospho-MET, einem anerkannten EGFR-Umgehungskreislauf. Wir konnten weder Amplifikationen (*EGFR*, *ERBB2*, *MET*), noch Mutationen in *EGFR, ERBB2, ERBB4, PIK3CA, BRAF, NRAS, KRAS, PTEN, MET* bzw. anderen Cancer Gene Hotspots identifizieren. Unsere Ergebnisse decken sich mit der Literatur, in welcher eine Expression von (phospho-) EGFR in der Mehrzahl der klinischen Proben beschrieben wird. Darüber hinaus liefern sie die Grundlage für weiterführende *in vitro* und *in vivo* Studien über die Wirksamkeit von EGFR Inhibitoren bei Chordom-PatientInnen sowie für die

Erforschung von potentiellen Resistenz-Mechanismen gegen diese Inhibitoren. Basierend auf vielversprechenden präklinischen Daten befindet sich derzeit eine prospektiv-randomisierte klinische Studie in Planung, welche die Wirksamkeit eines EGFR Inhibitors der zweiten Generation bei PatientInnen mit fortgeschrittenen Chordomerkrankungen untersuchen wird.

Zusammenfassend zeigt sich im Verlauf eine zunehmend umfassende und funktionelle Ausrichtung dieser Studien. Durch ein ausgedehntes Substanzscreening, bei welchem die mechanistischen Grundannahmen betreffend möglicher Zielstrukturen wesentlich reduziert waren, konnten EGFR-Inhibitoren als potentiell therapeutisch relevante Substanzgruppe identifiziert werden. Basierend auf dieser Erkenntnis, welche unabhängig von dieser Arbeit auch von anderen Gruppen gewonnen wurde, soll nun eine erste prospektiv-randomisierte klinische Studie für diese seltene Tumorerkrankung durchgeführt werden.

Introduction

Chordoma

Epidemiology and Sites of Involvement

Chordoma is an extremely rare primary malignant bone tumour, accounting for approximately 1 to 4% of all primary bone malignancies (12, 13). Chordoma occurs with a reported incidence of 0.08 in 100,000/year (14) and has a prevalence of less than 1 in 100,000 (15). This neoplasm mainly arises in the axial skeleton, occurring from the base of skull to the coccyx. Its distribution has been reported as involving cranial, spinal and sacral sites almost equally (32%, 33% and 29% of cases, respectively) (12, 14, 16). However, other reports, such as the *European Society for Medical Oncology (ESMO) Clinical Practice Guidelines on bone sarcoma 2014*, consider chordoma to occur more frequently in the sacrum and the skull base as compared to the mobile spine (50% sacrum, 30% skull base, 20% mobile spine) (15, 17, 18). Whereas clival chordomas affect both genders equally, there is a male-to-female ratio of approximately 2:1 for sacrococcygeal neoplasms (16). The overall median age of diagnosis is 58 years (14). Chordomas appear in low incidence in patients younger than 40 years (12, 16), and they seldom affect children and adolescents (12). Paediatric chordomas (<5% of all chordoma cases) occur as base of skull tumours and with a familial chordoma history more frequently than chordomas arising in the older population (12, 13, 19-21). Although rare (14, 22, 23), chordoma forms the most common primary malignant bone tumour of the sacrum, accounting for more than 50% of tumours in this region (12, 13, 24).

Rare Variants of Chordoma

In addition to axial chordomas, a number of publications have reported the occurrence of extra-axial chordomas. These tumours have the same morphological features as axial chordomas, and they also express brachyury and cytokeratins, and they may express S100 (10, 16, 25, 26). These lesions are exceptionally rare and have been observed in various skeletal locations and in (juxta-articular) soft-tissue (25, 27). The lesions are slow-growing but recur if not fully excised. Metastatic disease has not been reported, but as only a very limited number of cases have been studied, the disease's true behaviour is not fully understood.

Aetiology

Chordomas are thought to develop from notochordal remnants in the axial skeleton (16, 18, 28). Notochordal cells originate from the mesoderm and are involved in the formation of the neural plate and the vertebral column. Additionally, they provide support for the development of the axial skeleton (29). However, the notochord regresses during fetal development (29), but remnants may persist until three years of age and very rarely into adulthood (29). There is anecdotal evidence that benign notochordal cell tumours (BNCT) are precursor lesions for chordomas, although most do not develop into demonstrable tumours (29). These lesions arise in the same anatomic locations as axial chordoma; they express brachyury, and they have been found lying adjacent to classical variants of chordoma. They do not require surgical intervention and are generally detected at autopsy (30, 31). Although most chordomas arise as sporadic disease, a small number occur in a familial setting, with inheritance compatible with an autosomal dominant trait (10). Yang *et al.* (2009) reported that familial chordoma is associated with a duplication of the chromosomal region 6q27, which only contains the *T* (brachyury) gene (10, 19). A duplication of *T* has been reported in approximately 7% of sporadic chordomas (7, 10). There is also a recognised, although rare, association of chordoma with tuberous sclerosis complex (TSC) (10, 32). TSC is an inherited autosomal dominant neurocutaneous disorder (TSC1: chromosome 9q34; TSC2: chromosome 16p13.3), characterised by the potential for hamartoma formation in almost every organ (33). TSC-associated chordoma is generally observed in children (10, 32, 34).

Macroscopy, Histopathology and Immunophenotype

Chordomas are lobulated, grey to bluish-white tumours with a gelatinous cut surface, although other areas might reveal a more solid chondroid texture (10, 35). They are typified by a lobular architecture with fibrous strands separating groups of epitheloid cells embedded in a basophilic extracellular matrix rich in mucin and glycogen (16, 35). Necrosis is frequently present and can be extensive (10). Chordomas were first characterised microscopically by Virchow in 1857 (12, 13). A characteristic feature of chordomas are their polygonal large cells with abundant pink to clear cytoplasm and unique, intracellular, bubbly vacuoles. Virchow described these as “physaliphorous”, derived from the Greek word for “bubbles” (10, 12, 16, 36). These characteristic physaliphorous cells are immunoreactive for mesodermal and epidermal markers and thus express cytokeratins (10). Chordomas also express S100 protein, epithelial membrane

antigen (EMA) (10, 16) and brachyury (8, 16). However, they are negative for high molecular weight keratins.

T (brachyury), a transcription factor, belongs to the embryonal *T*-box genes (37), and it is now recognised as the diagnostic hallmark of chordoma (8, 19). Depending on their morphology, chordomas can be subclassified into three different histopathologic subtypes: Subtype one includes chordomas not otherwise specified (NOS) (also referred to as "conventional", or "classic", chordomas), and this is the most common subtype (10). The second subtype describes chondroid chordomas, which display a matrix that mimics hyaline cartilaginous tumours. However, chondroid chordomas (in contrast to cartilaginous tumours) express brachyury and keratins (10). The third subtype refers to dedifferentiated chordoma, which accounts for less than 10% of chordomas (approximately 5%, according to Stacchiotti *et al.* (2015) (15). Dedifferentiated chordoma is the most aggressive variant (10, 15-17). Immunoreactivity to brachyury, keratins, EMA and S100 is likely to be lost in the dedifferentiated component of a dedifferentiated chordoma (8, 10, 15).

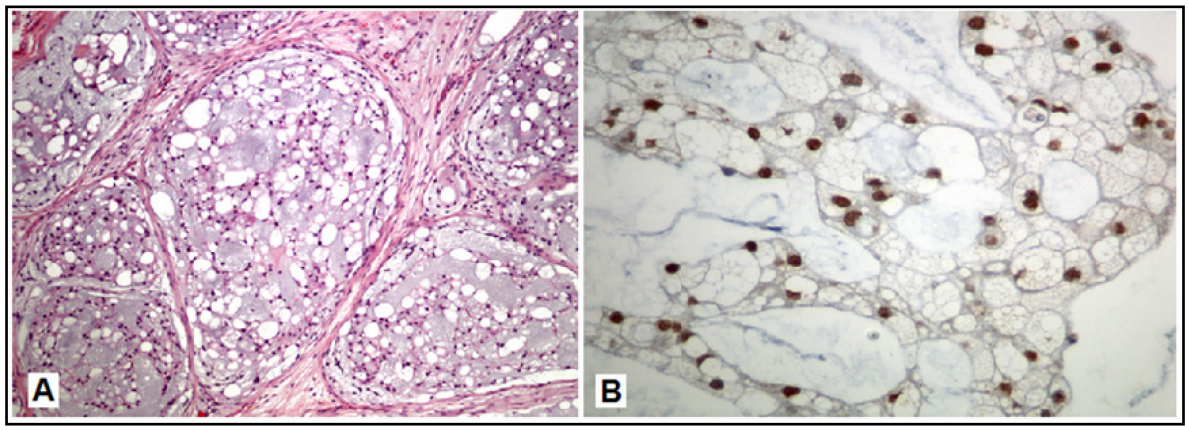

Figure 1. Chordoma histology.
(A) Chordomas possess a characteristic morphological and immunohistochemical profile, composed of **lobules of typical polygonal, vacuolated - "physaliphorous" – cells**, as shown in this case of a "classic", or "conventional", chordoma NOS (10) **(B) *T* (brachyury)**, a transcription factor belonging to the embryonal T-box family of genes (37), decorates the nuclei of the tumour cells. This marker has recently been established as the diagnostic hallmark of chordoma (8). With the kind permission of Assoc.-Prof. PD Dr. Bernadette Liegl-Atzwanger, Institute of Pathology, Medical University of Graz.

Clinical Presentation

The mean survival period from diagnosis is only seven years, although this disease can have a protracted course (14, 38, 39). Chordomas are indolent, slow-growing and locally destructive (22, 24), and early clinical symptoms are often unspecific (13). Clinical

presentation varies and is dependent on a tumour's location and size (12, 13), so that patients are often diagnosed after a significant delay (23). Once advanced, these neoplasms eventually become symptomatic via invasion, particularly the compression of surrounding tissues, including neural structures (12, 13). Because of their late presentation, by the time they are first diagnosed, approximately 5% of chordomas have already metastasised to the lungs, bone, skin or brain (13). In advanced disease, particularly after local recurrence (15), approximately 30-40% of chordomas metastasise to the lungs, bone, liver, lymph nodes (10, 17) and subcutaneous tissue (10, 15). Other authors have even reported a metastatic potential of up to 65% (12, 13). Dedifferentiated tumours appear to have a worse prognosis (10). However, the chordoma's local aggressiveness, rather than its metastatic potential, is primarily responsible for clinical effects (15).

Diagnosis

It is now commonly recognised that not only chordoma treatment, but also chordoma diagnosis, requires a high level of specialisation and disease-specific reference networks. Diagnosis and treatment should thus be conducted in specialised referral centres (15).

In terms of imaging, conventional radiographs in two planes are routinely recommended for initial imaging of tumours of the mobile spine and sacrum (15, 17). However, magnetic resonance imaging (MRI) is the best diagnostic modality for chordoma diagnosis, as it helps distinguish tumour borders, as well as different (soft-tissue) tumour components and spinal metastases (15, 17). To rule out spinal metastases, images of the primary tumour site and the whole spine are generally recommended (15). MRI images should always include three axis images, with detailed guidelines listed in a position paper by Stacchiotti *et al.* (2015) (15). On T1-weighted MRI images, most chordomas are iso- or hypointense compared to muscle. Furthermore, on T2-weighted images, they have a high signal intensity that reflects their high water content (15). Most chordomas demonstrate little to moderate enhancement after the application of gadolinium-based contrast medium (15). According to the *ESMO Clinical Practice Guidelines on bone sarcoma 2014* and Stacchiotti *et al.* (2015), computed tomography (CT) should be used in cases of diagnostic doubt. Moreover, CT imaging can better visualise calcifications, periosteal bone formations or cortical destructions; serve as a guide for biopsy and for surgical strategy planning; and substitute when an MRI is contraindicated (15, 17). Both imaging modalities (MRI and CT) are suitable for visualising residual tumour components after surgical resections, and case-based reasoning should be used to select the appropriate tool(s) (15).

MR angiography and/or CT angiography can help to assess the (local) vascular situation, for instance, in cases where the vertebral or carotid artery is suspected to be involved (15).

Typical clinical, radiological and pathological differential diagnoses of chordoma include: benign notochordal cell tumours, chondrosarcomas, sacral schwannomas, other bone sarcomas (particularly osteo- and Ewing's sarcomas), myxopapillary ependymomas, lymphomas, multiple myeloma and metastases from other cancers (15).

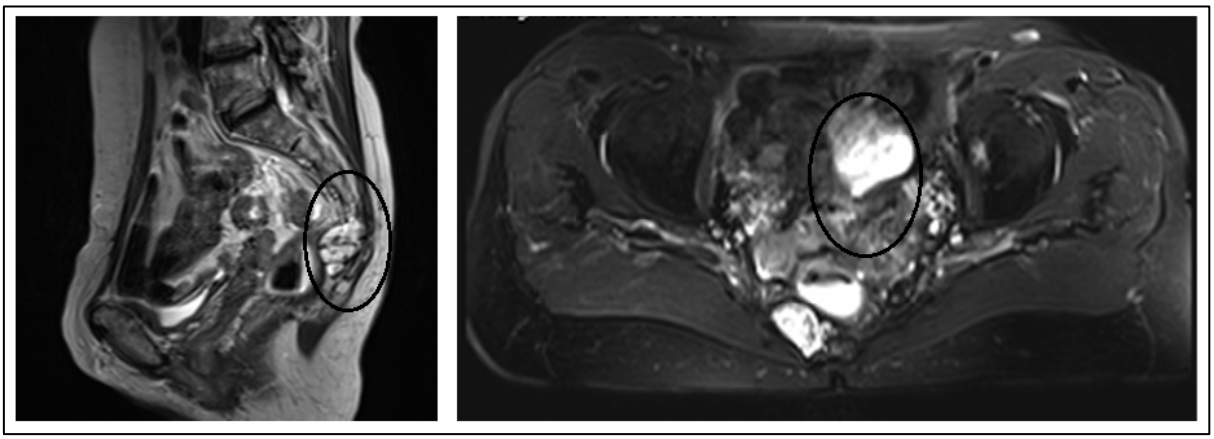

Figure 2. MRI displaying chordoma.
T2-weighted MRI images in sagittal (left) and transverse (right) planes, of a **sacral chordoma in a 68-year-old Caucasian female** patient. MRI reveals a high-signal sacral tumour (S4/S5) with extra-osseous masses. With the kind permission of Univ.-Prof. Dr. Andreas Leithner, Dept. of Orthopaedic Surgery, Medical University of Graz.

Treatment

Treatment options for chordoma are limited and are mainly restricted to surgical excision (22-24), since chordomas have proven to be largely resistant to conventional ionising radiation and chemotherapy (16, 23, 24). The European Sarcoma Network Working Group (17), as well as an international expert panel participating in the first European Society for Medical Oncology Chordoma Workshop (15), further emphasised the importance of a multidisciplinary treatment approach for chordomas in specialised referral centres. Treatment should involve experts in all fields of musculo-skeletal oncology, that is, expert pathologists, radiologists, orthopaedic surgeons, medical and radiation oncologists, as well as a palliative care team. Preoperative core needle biopsy is recommended for histological diagnosis, except for selected cases of skull base chordoma in which the risk of unrecoverable seeding of tumour cells is deemed too high (15). Final surgical resection should always include the biopsy track, which, as a general rule, should be posterior and midline for sacral chordomas (15). Research has shown adequate surgery to be the most

important prognostic factor in ***primary tumour treatment*** (15). Thus, R0 (en-bloc) resection, according to the Union for International Cancer Control (UICC) TNM classification system (40), is considered the surgical standard treatment of primary chordomas, with an estimated 5-year recurrence-free survival of 50% (15, 17). En-bloc removal of the tumour with a cuff of healthy tissue at both the bone stump and surrounding soft tissues is required to obtain microscopic negative margins all around the tumour, which is crucial to avoid recurrences and intraoperative spillage (15, 17). However, this is not always feasible and/or possible. This particularly the case for tumours of the skull base and the cervical spine, as well as for tumours that have spilled into the spinal canal or if the patient does not consent to surgery, due to the risk of surgical morbidities caused by a (wide) resection (15). In all of these latter cases, the aim is to achieve a maximum tumour resection (if obtainable, R1 resection). This goal should be balanced with the preservation of both (neurological) function and quality of life (15). After macroscopic complete surgery, adjuvant radiotherapy is recommended (15), and the latter constitutes the treatment of choice for inoperable patients (15). For sacral chordomas, surgery is the first treatment choice for tumours arising from S4 and below (15, 17). ***Surgery*** should also be offered as first line treatment for tumours originating from S3, particularly if the S2 nerve roots can be preserved (15, 17). This course of treatment is recommended for such tumours, since the pudendal nerve (S2-4), and particularly its fibres from the S2 and S3 roots, innervate the rhabdosphincter around the urethra, the levator ani muscle and the pelvic floor. Their loss causes an inability to control urination and/or defecation and thus is a major impairment to a patient's quality of life (41). For sacral chordomas originating above S3, surgery needs to be discussed in the context of possible alternatives (for instance, radiotherapy), as surgery in these anatomical regions is always followed by severe neurological deficits (15, 17). In thoracolumbar sites, en-bloc R0 resection is the approach of choice if applicable, although possible alternatives (for instance, radiotherapy) should be discussed with the patient (15). In cases when the transection of posterior elements (performed in the course of a vertebrectomy) unavoidably passes the tumour, surgery should be followed by radiotherapy (15). Unfortunately, due to the fact that chordomas often present at advanced stages of local disease and occur in anatomically challenging sites, en-bloc resections with negative microscopic margins cannot be obtained and/or are not feasible in many cases (12, 22, 24), resulting in high residual tumour and local relapse rates (15, 24, 42, 43).

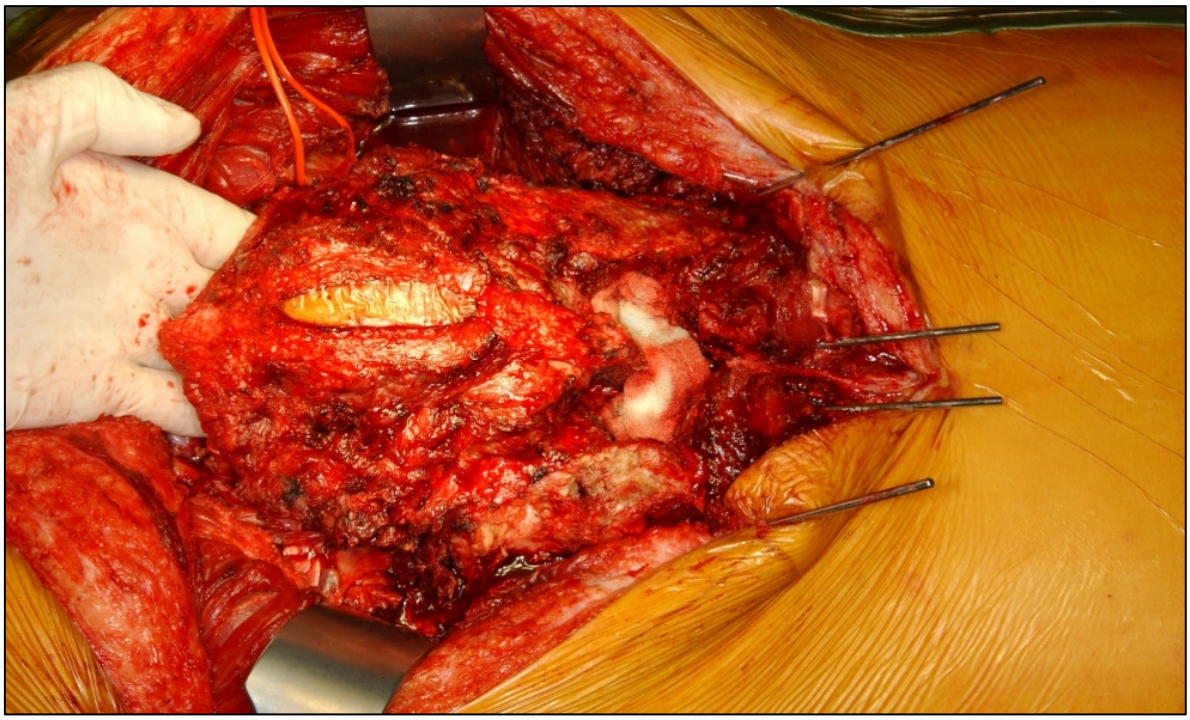

Figure 3. Surgical image of a sacral chordoma.
Sacral chordoma (S4/S5) in a 68-year-old Caucasian female patient, which was **resected en-bloc with wide margins**. With the kind permission of Univ.-Prof. Dr. Andreas Leithner, Dept. of Orthopaedic Surgery, Medical University of Graz.

Radiotherapy is the treatment of choice in unresectable tumours, inoperable patients and in cases when the surgical morbidities are not accepted by the patient (15, 17, 44). There is an increasing body of evidence that hadrons (i.e. high-dose protons and carbon ions) are superior to photons in their physical effect on chordoma, and particularly in their dose-sparing effect on the surrounding tissues (17, 45, 46). However, to date, there are no randomised trials on this topic that would allow for final recommendations (17). When protons or ions are not available, advanced technology photons can be used as an alternative if the photons permit delivery of similar dose distributions on the target and adjacent structures (17). As chordomas are hardly radiosensitive in general, the delivery of a high dose (at least 74 GyE) in conventional fractionation (1.8-2 GyE) is required for both photon and proton therapy (15, 17).

Cytotoxic chemotherapy has shown to be generally inactive in chordomas (15, 17). However, there is anecdotal evidence of single responses to chemotherapeutic treatment. These were observed in dedifferentiated and paediatric chordomas (15, 17, 47-50). Currently, no ***drugs*** are approved for the treatment of (advanced) chordoma (15). Moderate responses were obtained in a non-radomised clinical trial with imatinib mesylate

(Glivec®/Gleevec®, Novartis Pharma AG, Basel, Switzerland) (15, 51). One out of 50 patients (2%) showed a distinct volumentric response, and 20% showed minor respones (that is, less than a 30% decrease of their tumour's maximum diameter) (15, 51). Due to a lack of more sufficient alternatives, the ESMO consensus group suggested that "efforts are needed to make imatinib accessible for patients with advanced disease (15)". Moderate responses were also observed in two non-randomised phase II trials with antiangiogenic multi-kinase inhibitors, sunitinib (Sutent®, Pfizer, New York City, NY, USA) (15, 52), and sorafenib (Nexavar®, Bayer AG, Leverkusen, Germany and Onxy Pharmaceuticals, South San Francisco, CA, USA) (53). Furthermore, isolated case reports have shown positive effects upon treatment with several EGFR inhibitors (15, 54-59).

Local relapse has extremely poor survival rates, and patients are unlikely to be cured (17). Thus, the treatment approach for a recurrent tumour is of palliative intent rather than of curative intent, and it seeks to balance morbidity and quality of life (15, 17). Treatment options include surgery and/or radiation therapy and/or systemic treatment, and should incorporate supportive care from the beginning (15, 17). In selected cases of ***oligometastatic disease***, possible treatment options might be surgery, radiofrequency ablations or stereotactic irradiation of metastases (17).

Targeted Therapies

In the past few decades, significant progress has been made in understanding the molecular mechanisms that contribute to carcinogenesis (60). Scientists are studying molecular expression profiles, and we are now able to analyse cancer genomes for potential driver mutations. We can also study cancer epigenetics, such as DNA methylation patterns and post-translational protein modifications, including: phosphorylation, acetylation, and ubiquitylation, non-coding RNAs (mRNAs) and others (61). Standard therapeutic approaches have also been evolving in parallel with this gain in knowledge concerning cancer biology and genetics. Surgery, which for decades was the mainstay of treatment in bone and soft tissue sarcomas, has been supported by improvements in chemo- and radiotherapeutic regimens since the 1970s. This is especially true for osteo- and Ewing's sarcomas. These developments have significantly improved both local tumour control and patients' survival (44, 62, 63). However, problems and side effects arise from the systemic administration of cytotoxic drugs, as these drugs have to cross several biological barriers (e.g. blood vessels, tissues, organs and cells) when administered (60). More problems stem from the fact that these drugs exert systemic (that is, off-target), toxicities.

Chemotherapeutic drugs have nonspecific mechanisms of action and basically interfere with central cellular events, such as DNA replication and microtubule assembly (60). Furthermore, it is necessary to administer comparatively high doses of these drugs to achieve adequate local drug concentrations (60). In addition, some entities (including chordomas) have not been able to benefit from these advances in chemo- and radiotherapeutic regimens to the same extent as other tumours, since they have proven largely resistant to conventional chemo- and radiotherapy (15, 17). Thus, researchers are making efforts to identify and target specific tumour-related mechanisms, with the goal of achieving ideal anti-tumour effects while keeping off-target toxicities low (60, 64). With increasing knowledge about cancer pathogenesis, tailored therapeutic options, such as gene/immune therapies, are being explored. This development is relevant to bone and soft tissue sarcomas, as well as chordomas (65-70). Even though these new approaches seem promising, they are still experimental and require further research and development (65). Other treatment strategies focus on the overexpression, mutation or selective expression of cancer surface antigens and/or their downstream signalling pathways, as well as on the dense (though leaky) vascular system within a tumour, as a basis for a tumour-targeting strategy (60, 71). The German physician, Paul Ehrlich, who won the Nobel prize for Physiology or Medicine in 1908, first introduced the concept of a "magic bullet" approach via drug-targeting (60, 72). His concept was based on observations of infectious disease treatments: treatments were less likely to damage the host organism if the drugs targeted receptors specific to the invading parasites (72). Ehrlich thus developed the vision of a targeted medicine that selectively hits pathogens but does not harm healthy tissues (72). One hundred years later, his vision had evolved to a basic principle, thanks to work by a number of other researchers. In 1986, biochemist Stanley Cohen was awarded the Nobel prize in Physiology and Medicine for describing the first cell-growth controlling cell surface receptor, the epidermal growth factor receptor (EGFR), and its ligand, the epidermal growth factor (EGF) (72, 73). And, the 1970s and 1980s saw the descriptions of various oncogenes, tumour suppressor genes and cell signalling pathways (72). These discoveries paved the way for today's modern targeted therapies, in which drugs (such as antibodies and their derivatives, peptides or small molecules) specifically bind to a receptor that is unique to, mutated in or overexpressed by the target tissue (60, 71). This concept aims to increase the concentration of the drug in the target tissue, which is often (but not necessarily) neoplastic tissue, and to enhance the interaction between a ligand and its target cells (60). One obvious advantage of a targeted approach is that target cells have

preferential access to drugs; a second advantage lies in the fact that the localisation and expression of these specific targets potentially function as biomarkers for the target cell population throughout treatment (60). A successful example of a rationally designed drug, created to hit a target strongly expressed in disease-specific tissue is the chimeric monoclonal anti-CD20 antibody, rituximab (Rituxan™/MabThera®, Roche/Genentech Inc., Basel, Switzerland), which was the first U.S. Food and Drug Administration (FDA)-approved monoclonal antibody (1997) for the symptomatic treatment of cluster of differentiation (CD) 20 positive follicular non-Hodgkin's lymphoma (72). It is now also approved for treating otherwise non-responsive rheumatoid arthritis when used in combination with the antimetabolitic drug, methotrexate, and for treating other rheumatoid diseases (e.g. polyangiitis) when used in combination with glucocorticoids (72, 74, 75). In 1998, the first humanised monoclonal antibody gained FDA approval: trastuzumab (Herceptin®, Roche/Genentech Inc.), which targets ERBB2 (also referred to as HER2/neu) alone or in combination with chemotherapeutics in the treatment of ERBB2 positive (that is, ERBB2 amplified or overexpressing) breast cancers (64, 72, 76). Imatinib mesylate is an example of a small molecule inhibitor targeting BCR/ABL, the constitutively active tyrosine kinase, which results from the Philadelphia chromosome translocation t(9; 22) (77-79). This translocation fuses the ABL with the BCR gene; the *ABL* gene is located on chromosome 9q34 and encodes for a nonreceptor tyrosine kinase involved in protein-protein signalling and signal transduction, and the *BCR* gene is located on chromosome 22q11.2 and mediates signal transduction (77-79). When fused, these two genes confer the leukaemic phenotype in chronic myelogenous leukaemia (CML) (77-79). The BCR/ABL fusion oncoprotein functions as a dysregulated, constitutively active tyrosine kinase that promotes growth and replication via its interference with multiple downstream pathways (80). Imatinib mesylate was approved by the FDA for the treatment of CML in 2001 (64, 72, 81). Based on another principle proposed by Paul Ehrlich ("wir muessen chemisch zielen lernen"/"we have to learn how to aim chemically" (72)), Imatinib mesylate was the first small molecule kinase inhibitor that was rationally designed to selectively target a specific tumour-driving mechanism present in tumour cells but not in normal tissue. It became a paradigm for targeted cancer therapeutics (64, 72). In addition to BCR/ABL, Imatinib mesylate also inhibits two cell surface tyrosine kinases, the platelet-derived growth factor receptors α and β (PDGFR-α and -β), as well as the stem-cell receptor (c-KIT, CD117) (79). It is consequently used in the treatment of KIT-positive (and particularly, KIT-mutated) malignant gastrointestinal stromal tumours (GISTs) and

diseases associated with dysregulated PDGFR-α/β activity driven by activating mutations and/or translocations of these receptors, such as myeloproliferative disorders (a subset of PDGFR-α mutated GISTs) or dermatofibrosarcoma protuberans (79, 82, 83).

Targeted therapeutic approaches currently employ two major strategies, monoclonal antibodies (mAbs) and small molecule inhibitors, reviewed in the following paragraphs (60, 64). However, according to Toporkiewics *et al.* (2015), several other targeted approaches exist (60). The first of these two major approaches is based on monoclonal antibodies, which specifically bind to their targets and exert a high binding affinity in the nanomolar range (60, 71). To avoid unwanted immune responses, therapeutic mAbs are usually produced as either chimeric, humanised or fully human antibodies (60, 84, 85). In chimeric antibodies, the entire variable antibody domain derives from a host animal (e.g. a mouse), while the original constant region is replaced with a human sequence (84, 85). Examples of chimeric antibodies include rituximab (Rituxan™/MabThera®, Roche/Genentech) and cetuximab (Erbitux®, Merck KGaA, Darmstadt, Germany/Bristol Meyers Squibb, New York City, NY, USA) (85). In humanised mAbs, only the antigen binding site (and not the whole variable domain) derives from a rodent, and the rest of the antibody is of human origin. And, fully human mAbs do not contain any rodent structures at all (60, 84, 85). The anti-ERBB2 antibody, trastuzumab (Herceptin®, Roche/Genentech Inc.), and the anti-VEGF antibody, bevacizumab (Avastin®, Roche/Genentech Inc.), serve as examples of humanised mAbs, whereas the anti-EGFR mAb, panitumumab (Vectibix®, Amgen, Thousand Oaks, CA, USA), is an example of a fully human antibody (85). Monoclonal antibodies can exert a "kill effect" on tumour cells via various mechanisms, both direct and indirect (60, 71). Direct mechanisms of action include receptor blockade or activation, with subsequent induction of apoptosis. Indirect mechanisms of action, such as antibody-dependent cellular cytotoxicities (ADCC) or T-cell regulation (60, 71), are based on immune modulations. In addition, antibodies can deliver specific drugs that are conjugated to the antibody or that target a tumour's vascular system and/or stroma (60, 71). In clinical applications, mAbs have become well known in the context of EGFR/ERBB-family targeting, for example, in colorectal cancer (85, 86). In this type of cancer, a constitutive EGFR activation is thought to be brought about by paracrine/autocrine receptor stimulation rather than by *EGFR* mutations (85, 86). To exert their effect on the target, mAbs follow two courses of action. First, mAb (such as cetuximab or panitumubab) compete with the natural ligand (for instance, EGF) for the receptor's ligand binding site,

so as to inhibit its ligand-mediated activation. Or, mAbs (such as matuzumab) block the domain rearrangement required for high-affinity ligand binding and receptor dimerisation and subsequent activation (60, 87, 88). In addition to EGFR/ERBB-family targeting, mAbs have also become particularly established in the treatment of various haematologic malignancies, the targets of which include several cluster of differentiation (CD) markers (such as CD20, CD30 and CD52). Moreover, mAbs against the cytotoxic T lymphocyte-associated antigen 4 (CTLA4, also known as CD152) are used in immune-modulating therapies, and have been approved by the FDA for treating advanced melanoma. Another example is the use of mAbs in targeting a tumour's vascular system with anti-angiogenetic antibodies (71, 74, 89-92).

The second major targeted therapeutic strategy utilises small molecule inhibitors. Small molecule inhibitors are particularly applied in the targeted inhibition of protein kinases (64, 85, 93, 94). In this context, protein kinases have become the most intensively pursued class of chemically tractable drug targets (93, 94). Protein kinases are enzymes that modify protein functions by catalysing the transfer of a γ-phosphate from adenosine-5′-triphosphate (ATP) or guanosine-5′-triphosphate (GTP) onto a protein, thus phosphorylating the protein, while protein phosphatases dephosphorylate proteins by transferring the phosphate from a phospho-protein to a water molecule (95). Protein (de-)phosphorylation is the most prevalent form of post-translational protein modification, and it regulates a wide spectrum of protein functions and structures, including complex functions, such as signal transduction, differentiation, migration, angiogenesis, cell-cycle, metabolism and even cell fate (85, 95, 96). This importance of protein (de-)phosphorylation is further signified by the fact that, even though protein kinases are encoded by only 2% of most eukaryotic genomes, they phosphorylate more than 30% of all cellular proteins (95). There are two types of kinases, according to the amino acids they phosphorylate: tyrosine kinases, which phosphorylate tyrosines, and serine-threonine kinases, which phosphorylate serine or threonine (96, 97). The majority of tyrosine kinases form cell surface receptors for hormones and growth factors ("receptor tyrosine kinases" or RTKs), whereas serine-threonine kinases are mainly involved in intracellular signal transduction (96, 97). In addition, a variety of non-receptor tyrosine kinases exist, and there is one known example of serine-threonine kinases forming cell surface receptors, which are receptors belonging to the transforming growth factor beta (TGF-β) family (97, 98). Dysregulated kinase functions have been implicated in many disorders, including not

only various cancers, but also neurological diseases, such as Alzheimer's or Parkinson's disease, as well as immunological, metabolic and infectious diseases (94, 95). Small molecule inhibitors work by competitively displacing ATP, which binds to the active site of a protein (93, 94). Rather than acting indirectly via immune responses such as mAbs, small-molecule kinase inhibitors directly target kinases and thus kinase-bearing tumour cells, particularly when a tumour cell has an "oncogene addiction" to a certain (constitutively activated) kinase function (85, 94). Many kinases have highly specific functions, and so it is not surprising that more than 30 kinase inhibitors have already entered phase 1 clinical trials, and several protein kinase inhibitors have been approved by the FDA (64, 93, 94). Well known examples of FDA-approved small molecule kinase inhibitors include the BCR/ABL/c-KIT/PDGFR inhibitor, Imatinib mesylate (Glivec®/Gleevec®, Novartis Pharma AG, Basel, Switzerland), for the treatment of chronic myelogenous leukaemia (CML), GIST, and dermatofibrosarcoma protuberans; and the EGFR inhibitors, erlotinib (Tarceva®, Roche/Genentech Inc.) and gefitinib (Iressa®, AstraZeneca, London, UK) (64, 85, 99). The latter have been approved for *EGFR*-mutated non-small cell lung cancer (NSCLC), and the dual EGFR/ERBB2 inhibitor, lapatinib (Tykerb®/Tyverb®, GlaxoSmithKline (GSK), Brentford, London, UK), has been approved for the treatment of metastatic ERBB2-positive breast cancer (64, 85, 99). Other examples of FDA-approved kinase inhibitors are antiangiogenic multi-kinase inhibitors, such as pazopanib (Votrient®, GSK), sorafenib or sunitinib, which are utilised in the treatment of advanced renal cell carcinoma (RCC), Imatinib-resistant GIST (sunitinib) and/or certain types of soft tissue sarcomas (pazopanib) (64, 85, 99). Another example is the proteasome inhibitor, bortezomib (Velcade®, Millennium Pharmaceuticals, Cambridge, MA, USA), which has become established in the treatment of multiple myeloma (64, 85, 99).

In contrast to mAbs, which are large proteins (approximately 150 kDa), small molecule inhibitors are small chemicals (approximately 500 Da) (85). According to Imai and Takaoka (2006) (85), these size disparities, together with differences in their chemical structures (proteins versus chemicals), might contribute to the observed difference in the half lives of these two agents ($\geq$ 3 days for mAbs versus $\leq$ 3 days for small molecule inhibitors used in anti-EGFR treatment) and in tissue penetration, tumour retention and/or blood clearance abilities (85). In addition, small molecule inhibitors – but not mAbs – can pass into the cytoplasm and thus target molecules regardless of their cellular localisation (85). Also, the modes of delivery differ; mAbs are delivered via intravenous injections,

whereas small molecule inhibitors are given orally (85). Together with the high binding-specificity of mAbs, these facts might help to explain why mAbs have become particularly successful in the treatment of haematological malignancies, while small molecule kinase inhibitors are more frequently applied in the treatment of solid tumours (85). Of course, as shown by the examples of cetuximab (colon cancer), transtuzumab (ERBB2-positive breast cancer), imatinib (CML) and bortezomib (multiple myeloma), exemptions apply.

Despite the fact that the use of targeted therapeutics has led to remarkable achievements, these approaches also have disadvantages (64). Thus, these targeted treatment options are likely to be profitable for only a small subset of patients, and the figure is estimated to be 10-20% of patients in unselected populations (64). Thus, it has become apparent that predictive biomarkers associated with an increased likelihood of clinical response (e.g. the presence of a sensitising *EGFR* mutation) must be identified and utilised to stratify patients to treatment (64). For that reason, predictive biomarkers have become increasingly integrated in early stage drug discovery as well as in (FDA) drug approval processes (64). However, another problem lies in the short-lived duration of the effects of targeted monotherapies, irrespective of cancer and treatment types. Even if, for instance, 75% of patients harbouring an activating *EGFR* mutation show an initial response to EGFR-targeting therapies in NSCLC, the benefits of these treatments only last for an average of 6-12 months, and are invariably followed by resistance (64, 100). Primary or intrinsic resistance describes a tumour that has never responded to a certain targeted therapeutic approach. Acquired resistance, according to "Jackman's" criteria, describes a neoplasm harbouring a sensitising mutation that initially shows objective responses to a type of treatment and that subsequently progresses during 30 days of continuous treatment without intervening systemic therapies (101). Inter- and intratumoural heterogeneity are the main causes of primary and acquired resistance (64, 102). These describe pre-existing disparities between different tumours or within different regions of single tumours on the genetic, epigenetic, transcriptomic and proteomic level (64, 102). Genetic instabilities, as well as constantly on-going clonal selection processes within every tumour, contribute to these heterogeneities, as does the fact that a tumour constantly adapts to its environment and/or to selection pressures (64, 102). What is more, differences among tumours are being increasingly recognised due to improving molecular and genetic techniques. This results in a more extensive subtyping of cancerous entities based on their genetic and epigenetic alterations and/or their molecular expression profiles (64). Thus, the pathological

landscape is currently being altered, and the manner in which these (sub-) entities are (sub) classified, diagnosed and possibly treated is changing (64). Adaptational processes and clonal selections occur as evolutionary mechanisms in every tumour, as well as during the course of antitumoural treatments (102). As there may be various mechanisms of resistance for any given therapy, this can result in a tumour becoming resistant via multiple resistance routes simultaneously, a circumstance also referred to as polycloncal resistance (102, 103). Well-described resistance mechanisms include the activation of bypass-signalling pathways in order to circumvent a therapeutic signalling blockade, such as, for instance, signalling via other ERBB family members (in particular, ERBB2 and ERBB3) and/or amplification in *ERBB2*, which has been well-described in resistance to EGFR-blocking targeted treatments (100, 101, 104). Similarly, MET signalling is a well reported bypass signalling pathway, particularly in EGFR blocking therapies (64, 101, 104). It has been reported that *MET* amplifications account for up to 20% of resistance to EGFR inhibitors (64, 101, 104). In addition, targeted treatments result in the selection of resistant subclones, such as, for instance, *MET*-amplified subclones, or subclones carrying the common T790M-*EGFR* resistance mutation (64, 102, 104, 105). The T790M "gatekeeper" mutation of *EGFR* enhances the affinity of the ATP binding pocket of this receptor for ATP rather than for the small molecule inhibitor and thus accounts for approximately 50% of acquired resistance to the reversible small molecule inhibitor gefitinib (AstraZeneca) in NSCLC (64, 101, 104, 105). In this context, a tumour's microenvironment might also contribute to resistance (64, 104). So can, for instance, stromal fibroblasts' (over-) production of the MET-ligand hepatocyte growth factor (HGF) stimulate MET-sensitive subclones, thus conferring resistance to EGFR/ERBB inhibition (64, 104). Mutations of a receptor kinase's downstream signalling effectors (such as *PIK3CA*, *BRAF* or *KRAS*) are also well-established causes of a tumour's resistance to EGFR inhibitors (100, 101, 104). *BIM* polymorphisms and, in rare cases, *EGFR* T790M mutations have been described as germline events and can thus confer primary resistance (64, 104). In addition to the aforementioned mechanisms, a variety of other resistance mechanisms have been reported in recent years, many of them in NSCLC. These include: translocations of the *ALK* gene, the activation of AXL (Anexelekto, a receptor kinase), a polymorphism altering the pro-apoptotic function of a protein called B-cell CLL/lymphoma 2 (BCL2)-like 11 (BIM), the activation of yes-associated protein 1 (YAP1), epithelial-to-mesenchymal transition (EMT), the loss of PTEN expression and many others (100, 101, 104-107). However, in up to 30% of cases, the detailed mechanisms of resistance have yet to be explained (100, 101).

In summary, over the last few decades there has been a great shift in our understanding of tumour biology and genetics and in our approaches towards their treatment. We have moved from "one-for-all" treatment strategies, such as chemotherapies, towards more personalised approaches, following the "magic bullet" concept of Paul Ehrlich (64, 72). However, as technologies advance and experience increase, it is now becoming apparent that this concept faces a diverse landscape of inter- and intratumoural heterogeneities, as well as tumoural evolutions arising from selectional pressures that lead to intrinsic and acquired (polyclonal) resistance issues (64, 102, 103, 108). Single agent therapies have not shown lasting success, and it has become apparent that biomarkers indicating response and/or resistance to a certain type of treatment ("predictive biomarkers"), as well as sufficient biomarkers measuring treatment response ("biomarkers of response"), must be sought (64). This will allow for a more efficient patient stratification, and it will enable treatment teams to monitor whether a neoplasm is resistant or is starting to become resistant. However, efficient biomarker discovery requires a sufficient panel of adequate model systems capable of representing the range of human cancer(s) (64). These model systems must include a broad range of cancer cell lines. Furthermore, a sufficient amount of patient-derived xenograft (PDX) models need to be established (64). Tumour evolution must be constantly monitored in patients and/or xenografts, such as, for instance, in co-clinical trials where these two populations are treated and monitored in parallel (64). If a tumour is resistant or becomes resistant, consecutive treatment modifications need to be undertaken, with a focus on personalised combination therapies (64, 100). Recent developments to overcome resistance have concentrated on second- and third-generation TKIs, which have been specially designed to overcome resistance by forming irreversible bonds with the EGF receptor's ATP binding site (100). Further approaches involve epigenetic and immune-checkpoint modulators, as it is increasingly recognised that a tumour's microenvironment, particularly the immune system, plays an important role in a tumour's response to treatment (64, 109). While many exciting approaches exist, it remains to be proven whether this new era of personalised cancer therapy will be able to resolve the broad variety of outstanding challenges and develop into a truly efficient "magic bullet" (64).

Selected Target Classes

The following section outlines selected target classes, which include the receptor tyrosine kinases, EGFR and IGF-1R, and their key downstream effectors, as well as epigenetic

histone modulators, the so-called histone deacetylases (HDACs). These targets have attracted particular attention in the context of personalised medicine, and this study explores them in further detail.

The EGFR/ERBB System

The epidermal growth factor receptor (EGFR) is a 185 kDA receptor tyrosine kinase (RTK) localised on the plasma membrane and activated upon ligand binding (110). EGFR is one of four transmembrane growth factor receptor proteins that forms the EGFR/ERBB (epidermal growth factor receptor/erythroblastic leukaemia viral oncogene homolog) family (111). The four members of this family have similarities in their structures and functions (111). EGFR (also known as ERBB1, HER1), ERBB2 (HER2/neu), ERBB3 (HER3) and ERBB4 (HER4) are all receptor tyrosine kinases (112-114). They consist of an extracellular ligand binding domain, a single hydrophobic transmembrane domain and an intracellular tyrosine kinase-containing domain (**Figure 4**) (114). Two of these family members show peculiarities; ERBB2 does not bind any ligands (114-116), and ERBB3 lacks activity in its cytoplasmic tyrosine kinase domain (114, 117). Consequently, neither of these receptor family members can function as homodimers (114, 116, 117). However, they do form (highly) active heterodimers with one another and with other ERBB family members (114, 116, 117). In fact, ERBB2/ERBB3 heterodimers have been reported to be the most potent signalling complex in terms of cell proliferation and *in vitro* transformation (114, 116, 117).

ERBB receptors are activated by the binding of growth factors from the EGF family. These can be secreted in an autocrine manner (that is, by the receptor-bearing cells themselves) or in a paracrine manner (by the surrounding cells) (114). Growth factors of the EGF family consist of three groups (114). The first group contains EGF, transforming growth factor alpha (TGF-α) and amphiregulin (AR), all of which bind specifically to EGFR (114). Betacellulin (BTC), heparin-binding growth factor (HB-EGF) and epiregulin (EPR) form the second group, binding to EGFR, as well as to ERBB4 (114). The third group includes the neuroregulins (NRGs), and members are divided into two subgroups based on their potential to bind both ERBB3 and ERBB4 (NRG-1 and -2) or to bind only ERBB4 (NRG-3 and -4) (114). Recently, epigen was also identified as a ligand to EGFR (115), thus increasing the number of EGF-like family members to 11 (EGF, TGF-α, AR, BTC, HB-EGF, EPR, NRG-1-4 and epigen), and the number of EGFR ligands to 7 (EGF, TGF-α, AR, BTC, HB-EGF, EPR and epigen) (**Figure 4**) (115). Ligand binding induces either

homo- or heterodimerization of the EGFR/ERBB receptors, resulting in a *trans*-autophosphorylation of their cytoplasmic domains (114, 115, 118).

Receptor activation initiates several major downstream pathways, including the phospholipase-C-γ/protein kinase C (PLC-γ/PKC) pathway (119, 120), the RAS (rat sarcoma)/RAF (rapidly activated fibrosarcoma kinase)/MEK (MAP [mitogen-activated protein] kinase/ERK [extracellular-signal-regulated kinase] kinase) pathway, the PI3K (phosphoinositide 3-kinase)/AKT (protein kinase B alpha)/mTOR(C1) (mammalian target of rapamycin [complex1]) pathway and the JAK2 (janus-kinase 2)/STAT3 (signal transducer and activator of transcription 3) pathway (110, 112-114, 121). These downstream pathways regulate changes in gene expression, cytoskeletal rearrangements and apoptosis inhibition, as well as increased cell proliferation, and are thus important for physiological cell survival (113). Much research has focused on ERBB RTKs signalling from the plasma membrane, but there is also evidence that these receptors are translocated to the nucleus where they participate in cell signalling (122). In cases of malignant transformation, these various effects of ERBB signalling contribute to tumour growth, progression and survival (110, 113). Thus, aberrant tyrosine kinase activity of ERBB family members has been implicated in the pathogenesis of various cancer types, including lung, breast, stomach, brain, head and neck, pancreatic and colorectal cancers (112, 114, 122). Examples of how aberrant EGFR/ERBB signalling is involved in the pathogenesis of some of these neoplasms are provided throughout this document.

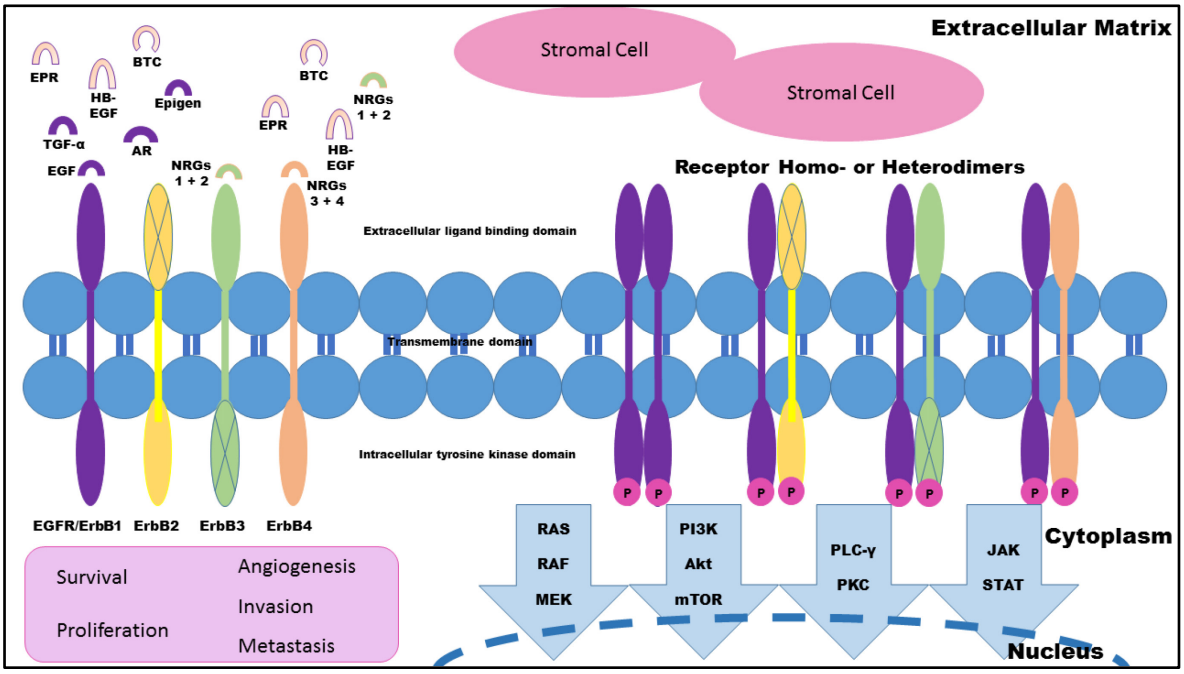

Figure 4. EGFR/ERBB signalling.
EGFR/ERBB receptors form homo- or heterodimers upon ligand binding and subsequently activate intracellular signalling pathways. EGFR/ERBB signalling thus influences cell survival, proliferation and angiogenesis, as well as invasion and metastasis (114, 123).

The IGF System

The insulin-like growth factor (IGF) system, and particularly the type 1 insulin-like growth factor receptor (IFG-1R) pathway, has emerged as a promising candidate for a selective signalling blockade. In the last two decades, several approaches have sought to target elements of this pathway – not only in carcinomas, but also in sarcomas (124-130). On the physiological level, the IGF system plays central role in pre- and postnatal growth and tissue differentiation (125, 127, 129). Thus, alterations of the IGF axis have also been reported in malignancies (127). In particular, IGF-1R signalling has been linked to tumourigenesis, metastases and resistance to cytotoxic drugs (125, 127, 128). So, IGF-1R has been implied in the pathogenesis of various sarcomas, such as Ewing's, osteo- and rhabdomyosarcoma (128, 131-133). However, several clinical attempts with IGF-1R inhibitory monotherapies have not lived up to researchers' and clinicians' expectations (131, 133, 134). Thus, researchers need to gain deeper insights into the role of IGF-1R in sarcoma, resistance mechanisms and patient stratification (132, 133).

The IGF system is composed of three ligands (IGF-1, IGF-2 and insulin), four cell-membrane receptors (the IGF receptor type 1 [IGF-1R], the insulin receptor [IR], hybrid

receptors between IR and IGF-1R and the IGF receptor type 2 [IGF-2R]), at least six high-affinity IGF-binding proteins (IGFBP-1-6) (128) and binding protein proteases (**Figure 5**) (127, 130).

Both the insulin receptor and IGF-1R are transmembrane receptors formed by two half-receptors, each consisting of an extracellular ligand-binding *a*-subunit and a transmembrane *b*-subunit, which possess an intracellular tyrosine kinase domain (125, 128, 130). Receptors are activated by ligand binding to the extracellular site, resulting in an autophosphorylation of the intracellular tyrosines at the kinase domains of the receptors (125). IGF-1R is activated by the binding of IGFs (IGF-1, as well as IGF-2, as outlined below) (125, 128), while IR is activated by insulin, which is secreted by the pancreas after food intake (125). There are two isoforms of the insulin receptor, IR-A and IR-B, generated by alternative splicing of exon 11 (125, 128). IR-B (exon 11+) is physiologically active in adult tissue, and under normal conditions it regulates glucose (125, 128), whereas IR-A forms the fetal isoform (125, 128). IR-A preferentially binds to insulin, but it also binds to IGF-2, and it is upregulated in several malignant tumours, such as breast cancer and colon cancer (128, 135). Whereas interactions of IR-A with insulin are primarily metabolic, interactions of IR-A with IGF-2 have been reported to exert primarily mitogenic intracellular effects (135).

Due to structural homologies between the two receptors (128), IRs and IGF-1Rs may form hybrid receptors, consisting of a half-receptor of each (125, 128). If hybrid receptors contain IR-B, they bind IGF-1 with high affinity; if they contain IR-A, they are activated by IGF-1, IGF-2 and insulin (128, 130).

In contrast to IR and IGF-1R, IGF-2R lacks an intracellular domain (128). This receptor regulates the extracellular IGF-2 concentration by internalising this growth factor after its binding to the extracellular receptor domain, subsequently degrading it in lysosomes (128).

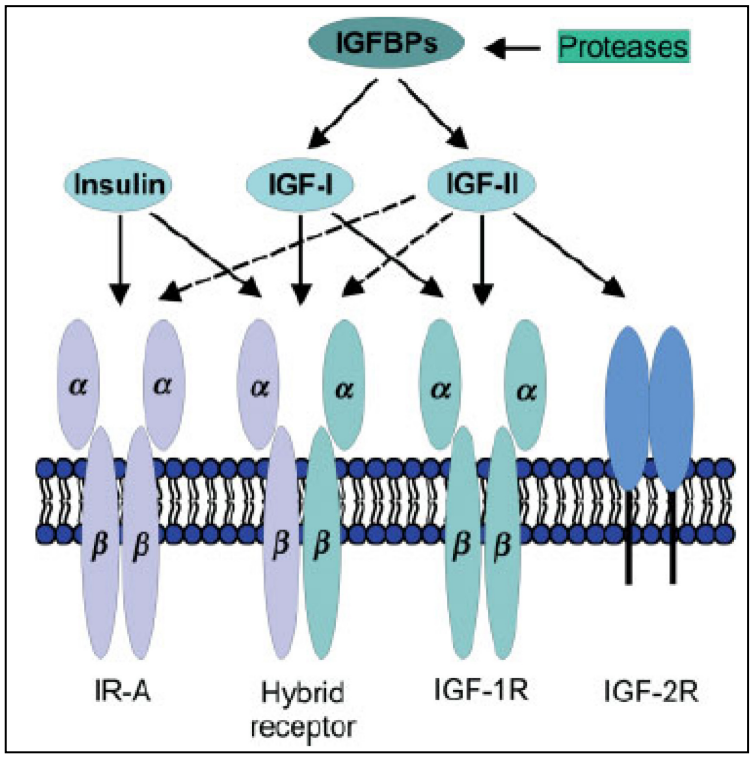

Figure 5. The receptors and ligands in the IGF/IR signalling system.
Figure from p. 470: Rikhof, de Jong, Suurmeijer, *et al.* The insulin-like growth factor system and sarcomas. J Pathol. 2009 Mar;217(4):469-82 (128). With the kind permission of John Wiley & Sons, Inc., Hoboken, NJ, USA (**Appendix 3**).

The Type 1 Insulin-Like Growth Factor (IGF-1R) Pathway

As the reviews by Rikhof *et al.* (2009) (128) and Chitnis *et al.* (2008) (125) noted, IGF-1R is activated by binding of IGF-1 or IGF-2. These IGFs are produced by the liver, as well as by extrahepatic sites (128). In contrast to IGF-1, the expression of IGF-2, which is the predominant circulating IGF in humans, is not stimulated by growth hormone (GH) (128).

IGF-1R activation via ligand binding causes an autophosphorylation of tyrosines at the receptor's intracellular kinase site. This leads to the recruitment of several adaptor proteins, such as insulin receptor substrates 1 to 4 (IRS-1 to IRS-4) and Src homology and collagen domain protein (Shc) (125, 127, 128, 136). Thereby, at least two major intracellular signal transduction pathways are activated (**Figure 6**) (125, 128), including the phosphatidylinositol-3-kinase (PI3K)-AKT pathway and the RAS/RAF/mitogen-activated protein kinase (MAPK) pathway (125, 127, 128). Activation of these pathways results in cell proliferation and apoptosis inhibition (128). Protein synthesis and cell growth are stimulated by AKT's activation of the mammalian target of rapamycin complex 1 (mTORC1). The extracellular signal-regulated kinases-1 and -2 (ERK1 and ERK2) (which

are activated by the MAPK/ERK kinases, MEK1 and MEK2) have many target proteins. These regulate, for instance, cell proliferation, survival, differentiation and migration (**Figure 6**) (128, 136).

Since a functional IGF-1R is required for cell growth and proliferation, survival and migration (127, 129), this pathway is also likely to be important for the development and progression of malignant neoplasms (125, 127, 128). What is more, IGF-1R activation seems to protect tumour cells against a hypoxic microenvironment (which is typical of large neoplasms) (127), as well as against killing by cytotoxic drugs (129). Furthermore, IGF-1R activation is associated with an increased likelihood of invasion and metastases (127).

Key Downstream Pathways of RTKs

The PI3K/AKT/mTOR Pathway

The phosphatidylinositide 3-kinase (also called phosphatidylinositol-4,5-bisphosphate 3 kinase, PI3K)/AKT/mammalian target of rapamycin (mTOR) pathway is a key intracellular downstream pathway of receptor tyrosine kinases. These include EGFR (110, 113), IGF1-R (**Figure 6**) (125, 128), *MET* proto-oncogene (c-MET) (137) and others.

The binding of growth factors to their (trans-) membrane-receptors (e.g. ERBB family receptors) results in the recruitment of PI3K. PI3K belongs to a family of lipid kinases that catalyses the phosphorylation of phosphatidylinositol-4,5-biphosphate (PIP2) to phosphatidylinostiol-3,4,5-triphosphate (PIP3) at the cell-membrane (138). As illustrated in **Figure 6**, this chemical reaction results in the activation of AKT (also referred to as protein kinase B or PKB) via the 3-phospho-inositide-dependent protein kinase-1 (PDK1). PDK1 is inhibited by the lipid phosphatase "phosphatase and tensin homolog" (PTEN (138)) (136). Activated AKT subsequently leads to the inactivation of tuberin (tuberous sclerosis complex 2 [TSC2]), thus initiating the activation of the mTOR complex 1 (mTORC1). This process is mediated by the rat sarcoma viral oncogene homolog (RAS) (139) -related small GTPase "RAS homologue enriched in brain" (Rheb (138)) (136). Additional factors involved in the regulation of mTORC1 activation in cases of cellular stress or low cellular energy are the adenosine monophosphate (AMP)-activated protein kinase (AMPK); the tumour suppressor protein liver kinase B1 (LKB1) (also known as serine-threonine kinase 11 or STK11), which is an upstream kinase of AMPK; the homologous proteins "regulated in development and DNA damage responses protein 1 and

2 (140)" (REDD1 and REDD2); and RAS and its effector-molecules along the RAS/mitogen-activated kinase (MAPK) pathway (**Figure 6**) (136, 139).

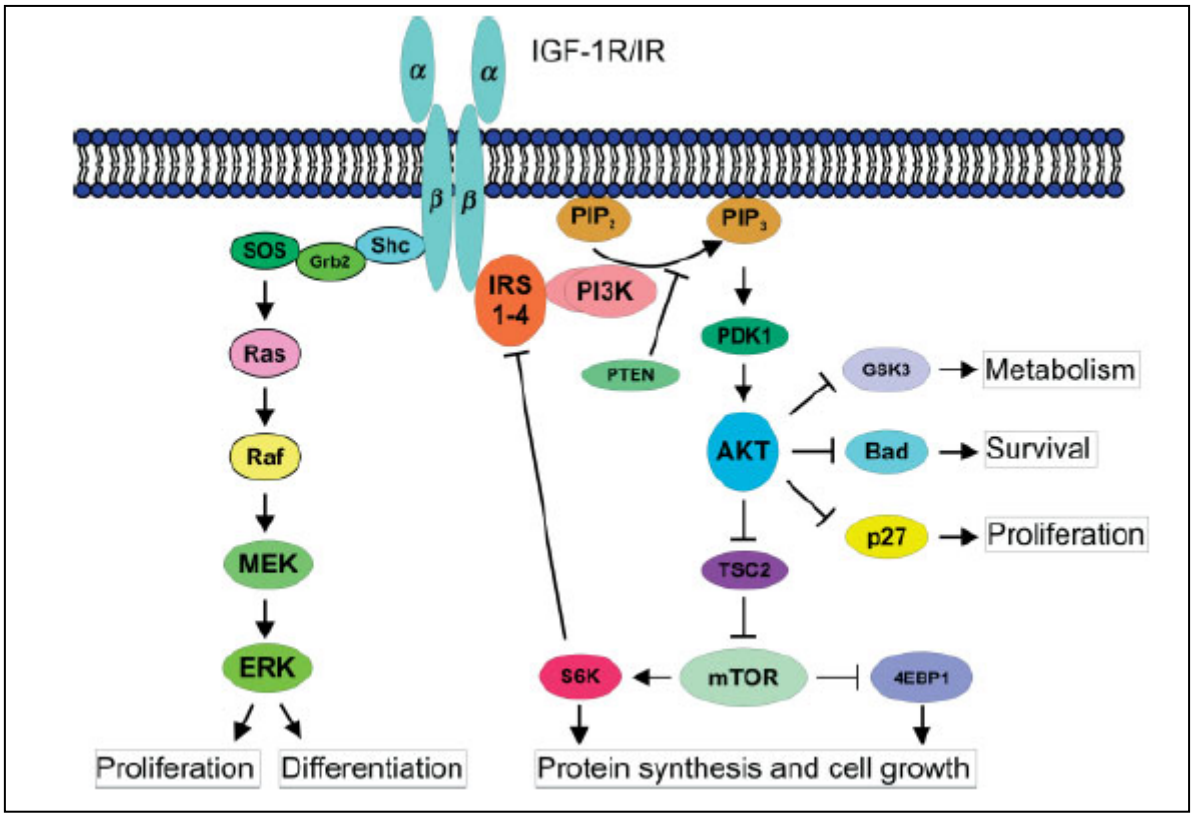

Figure 6. RTK downstream signalling.
The IGF-1R is an example of a receptor tyrosine kinase. The figure illustrates downstream signalling via the PI3K/AKT/mTOR and the RAS/RAF pathways.
Figure from p. 471: Rikhof, de Jong, Suurmeijer, *et al.* The insulin-like growth factor system and sarcomas. J Pathol. 2009 Mar;217(4):469-82 (128). With the kind permission of John Wiley & Sons, Inc., Hoboken, NJ, USA (**Appendix 3**).

When rapamycin, a macrocyclic lactone produced by a bacterial strain *(Streptomyces hygroscopicus)*, was discovered in the 1970s, it was found to inhibit the proliferation of mammalian cells (136). Further investigation of the underlying mechanisms led to the identification of target of rapamycin (TOR), a highly conserved serine-threonine kinase belonging to the phosphatidylinositol-kinase-related kinase (PIKK) family, which was shown to be the rapamycin target in mammalian cells ("mTOR" = "mammalian target of rapamycin") (136).

As a review by Wullschleger, Loewith and Hall (2006) stated, (m)TOR plays a central role in the control of cell growth (136, 140, 141). mTOR exists in two molecular complexes, mTORC1 and mTORC2 (6, 136, 140), although only one of these two complexes,

mTORC1, is sensitive to rapamycin (136). The latter forms a complex with FK506-binding protein 12 (FKBP-12) (139, 140) and thus inhibits TOR (136, 140, 141). Whereas mTORC1 is believed to regulate temporal aspects of cell growth, mTORC2 is insensitive to rapamycin and seems to be involved in actin cytoskeleton organisation (136, 140). Signalling via mTOR has mainly been studied in and for mTORC1 (136).

The regulation of mTOR activity is complex; mTOR signalling seems to be initiated by various factors, particularly by the binding of growth factors to receptor tyrosine kinases upstream of mTOR. Nutrients (particularly amino-acids), energy and stress are other factors that can influence mTOR signalling (136, 141). The central mechanism by which mTOR is activated is the inactivation of the tuberous sclerosis proteins, TSC1 (hamartin) and TSC2 (tuberin) (136, 140, 141). These proteins form a heterodimer, which exerts a negative regulatory function on mTOR signalling (136, 140, 141).

Downstream targets of activated mTORC1 are molecules involved in ribosomal biosynthesis and protein translation. These include the ribosomal protein S6 kinase (S6K1), which phosphorylates the 40S ribosomal protein S6 (RPS6); eukaryotic translation initiation factor 4E (eIF4E) binding proteins (4E-BPs, such as 4E-BP1); and eukaryotic initiation factors, such as the eukaryotic initiation factor 4E (eIF4E) (136, 140, 141).

Many factors involved in mTORC1 signalling have been linked to tumourigenesis (136, 138, 139, 142). A dysregulated activity with hyperactivation of the PI3K/mTORC1 pathway is a characteristic feature in various syndromes, such as the Peutz-Jeghers syndrome (PJS), the tuberous sclerosis complex syndrome (TSC) and the Cowden syndrome (CS) (136, 138, 142). Although benign, the neoplasms associated with these syndromes form a cancer predisposition (136, 138, 142). These syndromes particularly involve the tumour suppressor proteins TSC1/TSC2, PTEN and LKB1, all of which are known to cause dysregulations in the mTORC1 signalling cascade (136, 138, 142). Neurofibromatosis type 1 is also thought to be linked to the PI3K/mTOR pathway, as this disease is caused by a mutation in the gene product of *NF1*, which is a Ras GTPase activating protein (142).

Dysregulated mTORC1 signalling has also been linked to the pathogenesis of various malignant tumours (32, 136, 139, 143-152). Thus, inhibitors of the mTORC1 pathway, such as rapamycin (also known as sirolimus) (144-149) or the dual AKT/mTOR inhibitor, PI-103 (152, 153), form potential therapeutic agents in cancer therapy, particularly in a

combinatorial setting (139, 143-149, 151, 152, 154-156). Due to promising preclinical data, mTOR inhibitors (such as sirolimus, everolimus and ridaforolimus) have entered clinical trials (139, 154-158). Responses upon treatment with mTOR inhibitors have been reported in, for example, angiomyolipomas related to TSC syndromes (157). And, single modest responses have been reported in myxoid/round cell liposarcomas with *PI3KCA* mutations, PTEN loss, AKT activation and/or IGF-1R overexpression (157, 159). What is more, a phase 3 study exploring ridaforolimus versus placebo in 702 patients with metastasising sarcoma (soft tissue or bone sarcoma with prior response to chemotherapy) reported a small but significant effect of this mTOR inhibitor in delaying tumour progression (158).

The RAS/RAF/MAPK Pathway

Another major cell-signalling pathway is the RAS/rapidly accelerated fibrosarcoma (RAF)/mitogen-activated protein (MAP) kinase pathway, which is also initiated by ligand binding to various cell surface receptors (**Figure 6**) (125, 128). Upon ligand binding to the receptor, Shc, growth factor receptor-bound protein-2 (Grb-2) and son of sevenless (SOS) interact to activate RAS (128). RAS subsequently activates the RAF kinases, which are a group of three serine/threonine kinases (128). RAF then phosphorylates the mitogen-activated protein kinase (MAPK)/extracellular signal-regulated kinase (ERK) kinases (MEK1 and MEK2), which is followed by an activation of the extracellular signal-regulated kinases-1 and -2 (ERK1 and ERK2) (125, 128). Activation of this pathway results in the phosphorylation of many target proteins regulating a variety of cellular functions, including, for instance, cell proliferation, survival, differentiation and migration (128). As this pathway triggers crucial cellular functions, it has been implicated in various types of cancer. Activating *BRAF* mutations, particularly the V600E mutation (previously designated as the V599E mutation) (160-162), have been found in more than 50% of melanomas (160, 162-164). The high percentage of activating V600E mutations in *BRAF* (50-70%), as well as other activating mutations in the MAPK/ERK pathway (such as *NRAS* mutations [10-30%]), provide evidence that melanoma is a disease linked to oncogenic MAPK/ERK signalling (161, 165). These insights have led to altered treatment approaches for this disease, and several therapeutics targeting the MAPK/ERK pathway (e.g. vemurafenib [PLX4032; Zelboraf; Genentech/Plexxikon, Berkeley, CA, USA]) have been approved for melanoma therapy after having shown promising results in clinical trials (165). The V600E *BRAF* mutation has also been reported in various carcinomas, although

with a lower frequency. For example, this mutation was found in a subset comprising 8-10% of colorectal carcinomas (166), as well as in 1 to 4% of NSCLC (167, 168). It has also been reported in thyroid cancers (162) and other cancers (160). There is evidence for activation of the RAS/RAF system in chordomas (4, 169), and reports of chromosomal losses of *RAF* in patients' samples include regions involved in the RAS/RAF system (170). However, thus far several laboratories have failed to reveal recurrent point mutations in *KRAS*, *NRAS*, *HRAS* or *BRAF* in chordomas (3, 10, 171-173).

JAK/STAT(3) Signalling

As two reviews by Yu *et al.* (2007) and (2014) (121, 174) pointed out, signalling via the janus kinase (JAK)/signal transducer and activator of transcription (STAT) pathway mediates biological processes that are crucial for cancer progression (121). STAT is a family of transcription factors known to be involved in the regulation of various cellular processes, including apoptosis and cell cycle (175). The cytoplasmic transcription factor, STAT3, is a particularly well-known member of this family, as it has been implicated in various types of cancer (175-177). Physiologically, STAT3 is known to play a dominant role in the regulation of the cell cycle and anti-apoptosis (175). Furthermore, it regulates HIF-1α expression in the nucleus, and it is involved in cancer cell metabolism and in the Warburg effect, which describes a cancer-related non-oxidative glycolytic mode of energy generation (175). In addition to its role as a transcription factor, STAT3 has recently been shown to regulate gene expression via epigenetic modulations, such as DNA methylation and chromatin remodelling, and it seems to be involved in the regulation of mitochondrial functions (121). STAT3 also plays an important role in tumour-mediated immunosuppression, which restrains anti-tumour immune responses (121, 174). Activated JAK/STAT3 signalling has also been reported to facilitate the formation of clusters of myeloid cells, which serve as "pre-metastatic niches" and are favourable microenvironments for disseminated tumour cells at distant sites to grow and form metastases (121). Due to these crucial functions, it is not surprising that STAT3 has been implicated in tumour cell proliferation and invasion, angiogenesis and immunosuppression in various types of cancer (e.g. breast, lung and prostate cancer), as well as in haematopoietic malignancies (121). Furthermore, STAT3 is thought to be involved in epithelial-mesenchymal transition (EMT) in carcinomas (178, 179). The JAK/STAT3 pathway is activated by various receptors, including cytokine receptors (121). Of these cytokine receptors, the interleukin-6 (IL-6) receptor is the best-known activator of STAT3

(121). In addition to cytokine receptors, Toll-like receptors (TLRs); G-protein coupled receptors (GPCRs); and various receptor tyrosine kinases (e.g. EGFR, ERBB2, IGF-1R, the vascular endothelial growth factor receptor [VEGFR], PDGFR and cMET) (121, 174) can also activate JAK/STAT3 signalling. For instance, it was recently reported that EGFR/STAT3 signalling promotes malignant transformation in xenografts of malignant peripheral nerve sheath tumours (MPNST) (180). However, in contrast to RTKs, cytokine receptors (e.g. the IL-6 receptor), TLRs and GPCRs lack intrinsic activity but undergo transformational changes upon ligand binding, which initiates the interaction of adapor proteins with these receptors, thus starting the signalling cascade (121). When the cytokine IL-6 is bound to IL-6 receptors, cytosolic STAT3 is phosphorylated at tyrosine (Tyr) 705 by the intracellular nonreceptor tyrosine kinases, JAK1 and JAK2, and is thus activated (121). Activated STAT3 dimers then diffuse into the nucleus, where they bind to gene promotors and regulate gene expression (121). Since IL-6 acts as a mediator of various inflammatory responses and is a key activator of JAK/STAT3 signalling, JAK/STAT signalling has also been implicated in inflammatory processes, as well as in inflammation-mediated cancer (121). There are many reasons to believe that STAT3 might form an interesting target for cancer (immune-) therapy (121, 174). However, as STAT3 lacks its own enzymatic activity, and as it has a complex role in cancer, it is hard to develop STAT3-targeting therapeutics (121). Nevertheless, STAT3 inhibition should be further explored as a therapeutic target, not only in carcinomas, but also in sarcomas (121, 174, 180).

The "Epigenetic Landscape" as a New Area for Cancer Research

In the last few decades, scientists have increasingly recognised that many changes in cancer cells (e.g. silencing of tumour suppressor genes, activation of oncogenes, chromosomal instability or impaired DNA repair mechanisms) are not always due to genetic alterations/mutations. Rather, epigenetic mechanisms that regulate gene expression can also trigger such changes (181, 182). The British embryologist and geneticist, Conrad Hal Waddington, first introduced the model of an "epigenetic landscape" in the first half of the twentieth century (183). Epigenetic mechanisms allow cells of a multicellular organism – even though they are genetically uniform – to become structurally and functionally heterogeneous and to thus fulfil various different functions during development and differentiation, as well as in the adult organism (182). What is more, epigenetic mechanisms allow an organism to respond and/or to adapt to environmental influences via

changes in gene expression, as epigenetic changes can be inherited mitotically in somatic cells (182, 184). Environmental factors occurring in the prenatal or early postnatal period, (e.g. nutritional factors, chemicals and low-dose irradiation) can alter the risk of developing (chronic) diseases later in life by changing the epigenomic programming (184). What is more, increasing evidence supports the hypothesis that epigenetic alterations can also be inherited between generations of individuals ("transgenerational inheritance") (184). While it is well-recognised that epigenetic alterations are common in cancer, researchers are currently discussing whether epigenetic disruptions in cancer cell precursors might precede genetic gate-keeper alterations, such as the inhibition of tumour suppressor genes or the activation of oncogenes (185). Epigenetic mechanisms include post synthetic modification of the DNA itself or of proteins closely associated with the DNA, so-called histones (182). These mechanisms involve the organisational control of the higher-level chromatin structure within the nucleus that affects the accessibility of DNA for transcription factors. Epigenetic mechanisms furthermore include non-coding RNAs (such as microRNAs), as well as DNA (de-)methylation, and histone modifications (181, 182, 184, 186). DNA methylation is carried out by various methyltransferases, and it restricts transcription. In contrast, demethylation is catalysed by demethylases and has the opposite effect (182). Vertebrate genomes are mainly methylated at the dinucleotide CpG ("CpG": cytosine – phosphate - guanine) and largely depleted in CpG dinucleotides, since methylated cytosine has mutagenic properties (187, 188). However, there are short (approximately 1,000 base-pair long) DNA regions that contain high percentages of cytosines ("C"), guanines ("G") and CpG dinucleotides and that are predominantly non-methylated. These are referred to as "CpG islands" (187, 188). CpG islands are sites of transcription initiation and are often associated with promotor regions, particularly in housekeeping genes, but also in tissue-specific and developmental regulator genes (187, 188). During carcinogenesis, however, the genome typically undergoes hypomethylation with simultaneous hypermethylation of CpG islands (182). Alterations in DNA methylation profiles can contribute to tumorigenesis in several ways (182). On the one hand, hypermethylation can result in the silencing (and consequent inactivation) of tumour suppressor genes (182). Demethylation, on the other hand, might induce oncogene activation (182). Demethylation can also reverse the epigenetic silencing of repetitive (transposable) elements, thereby enabling them to replicate, transpose and potentially cause insertional mutagenesis (184). Furthermore, methylation changes can lead to the loss of genomic imprinting. Genomic imprinting is monoallelic gene expression resulting from

somatic inactivation of either the paternal or the maternal allele of a gene, as is observed, for example, in females' somatic X-chromosome inactivation (182, 184). Loss of imprinting might result in a biallelic (over) expression of, for instance, imprinted growth factors, which could stimulate tumour growth (182). Moreover, changes in methylation can also induce secondary genetic alterations contributing to tumorigenesis. Thus, point mutations in CpG islands are more likely to occur if the CpG islands are hypermethylated (182). Microsatellite instability can result from methylation-induced silencing of mismatch repair genes, and genome-wide hypomethylation can induce overall genomic instability (182). Another key mechanism of epigenetic control of gene expression lies in histone modifications (182, 186). Histones are highly conserved proteins found in the nuclei of all eukaryotic cells (186). They provide a scaffold for the packaging of the deoxyribonucleic acid (DNA) double helix, which wraps around the histone complexes (186). There are five different histone proteins: H2A, H2B, H3, H4 and the H1 linker histone (186). Together, histones and DNA form the chromatin structure (186). Chromatin consists of basic functional units called nucleosomes, and each nucleosome consists of 147 base pairs of DNA wrapped around an octamer of histone proteins (186). Each octamer is built of two copies of H2A, H2B, H3 and H4, respectively (186). In addition to these histone types, several histone variants (or isoforms) exist, which are "subspecies" that differ from the major histone species in their amino-acid sequences and that carry out distinct functions (189, 190). While the histone subtypes are usually present to package newly replicated DNA, histone variants are present in a replication-independent manner (190). For instance, the histone H3 has several different variants: H3.1, H3.2, H3.3, the centromeric variant CENPA, the testes-specific H3t and the testes-specific H3.5 (189). Of these variants, H3.3 and CENPA have been extensively studied (189). Modifications of histones can fundamentally alter the organisation and function of chromatin (186). This is why post-translational histone modifications (e.g. [de-]acetylation, [de-]phosphorylation, [de-]methylation and citrullation [or "deimination"]) (191) play an important role in the regulation of DNA-based processes, such as transcription, DNA repair and replication (186, 192, 193). Whereas most currently known histone modifications refer to alterations located in the N-terminal flexible histone tail that protrudes from the nucleosome, recent studies have revealed modifications affecting the actual histone cores (191). Histone tail modifications alter the regulatory functions of histones by affecting their binding affinities for effector proteins, while histone core modifications alter the structures of nucleosomes (191). Histone tail modifications occur at different amino acid sites of histone tails, are

catalysed by specific enzymes and have specific functions in gene regulation and other DNA-associated processes (191). For example, histone acetylation has been associated with increased gene expression (191). Histone lysine methylation has been correlated with increased or decreased gene expression, depending upon methylation sites and the extent of methylation (that is, mono-, di- or tri-methylation) (191). Thus, it is not surprising that mutations in epigenetic modifiers (such as in enzymes catalysing histone modifications or in genes encoding histonic proteins) have been linked to tumourigenesis. Recently, two research groups reported genetic alterations in malignant peripheral nerve sheath tumours (MPNSTs) other than the well-established *NF1* mutations (194, 195). These research groups found somatic alterations in *CDKN2A* (cyclin-dependent kinase inhibitor 2A) in 81% of MPNSTs, as well as somatic mutations/loss-of-function alterations of the epigenetic regulatory *PRC2* (polycomb repressive complex 2) components, *EED* (embryonic ectoderm development) and/or *SUZ12* (suppressor of zeste 12 homolog), in the majority of MPNSTs (194, 195). PRC2 catalyses the methylation of histone H3 at lysine 27 (H3K27), resulting in H3K27me1, H3K27me2 or H3K27me3, respectively (196). Thus, the mutations observed in MPNST result in a loss of trimethylation at lysine 27 in the tail of the histone H3 (H3K27me3) (194). This trimethylation was restored once the lost PRC2 component was replaced, resulting in reduced tumour cell growth (194). In 2013, Behjati *et al.* reported that specific driver mutations affect the histone variant H3.3 in two rare bone tumours, chondroblastomas and giant cell tumours of bone (197). These mutations were located in two different genes encoding for an identical protein, the replication-independent histone H3.3 (197). These genes are called *H3F3A* and *H3F3B*, and they are located on chromosomes 1 and 17, respectively (197). As many as 95% of chondroblastomas showed a single nucleotide alteration in *H3F3B* (p.Lys36Met: H3 lysine 36-to-methionine; H3K36M), and 92% of giant cell tumours of bone carried a mutation in *H3F3A* (p.Gly34Trp/Leu: H3 glycine 34–to–tryptophan/leucine; G34W/L) (197). Both mutations were located in the stromal cell population of these mesenchymal neoplasms and did not affect the osteoclasts, which are thus thought to be reactive (197). In the context of previously reported *H3F3A* mutations in childhood brain tumours (p.Lys27Met: lysine 27–to–methionine [K27M], p.Gly34Arg, or p.Gly34Val: glycine 34–to–arginine/valine [G34R/V] mutations), these reports indicate a specificity of mesenchymal/glial tumours for histone H3.3 driver mutations, indicating distinct functions of these histonic proteins,

mutations and genes (197, 198). Recent evidence found that the H3K36M mutation interferes with cells' chondrocytic differentiation capacities, which can account for the accumulation of immature chondroblasts observed in chondroblastomas (199). However, the full functional changes induced by these mutations, particularly the G34W mutations, still need to be clarified (197).

Targeting Epigenetic Modulators: Histone Deacetylase (HDAC) Inhibitors

Histone acetylation is mediated by histone acetyltransferases (HATs), and histone deacetylases (HDACs) catalyse the removal of acetyl groups from amino acids on histone tails (2, 181). These epigenetic modifications alter the accessibility of transcription factors to DNA gene promoter regions (2, 200). In diseases such as cancer, the balance between histone acetylation and deacetylation is often disturbed and dysregulated (2, 181). To date, at least 18 human HDACs have been identified, and these can be grouped into four classes based on their homology to yeast proteins (2, 181, 200-202). Classes I, II and IV are zinc (Zn^{2+})-dependent and include the HDACs 1 to 11, whereas class III HDACs (so-called sirtuins) function independent of Zn^{2+} (2, 181, 200, 201). Apart from histone modifications, HDACs also catalyse the reactions of non-histonic proteins, such as transcription factors, cytoplasmic proteins and signalling molecules (2, 200). In the past few years, HDAC inhibitors have been studied as a comparatively new class of small-molecule anti-cancer drugs targeting the Zn^{2+}-dependent human HDACs 1 to 11 (2, 181, 200). So far, no inhibitors are available for the less frequently studied class III HDACs, the sirtuins (203). Several HDAC inhibitors have been tested in clinical trials as monotherapies and/or in combination with other anticancer drugs, and an increasing number has been approved by the FDA (2, 200, 203). In 2006, Vorinostat (Zolinza®, Merck KGaA, Darmstadt, Germany) became the first FDA-approved HDAC inhibitor (204), followed by Romidepsin (Istodax®, Celgene, Summit, New Jersey, USA) in 2009 (205). Both of these are used in the treatment of cutaneous T-cell lymphoma. Since then, other HDAC inhibitors have been approved by the FDA. Examples include Belinostat (Beleodaq®, Spectrum Pharmaceuticals, Inc., New York, USA), approved in 2014 for the treatment of peripheral T-cell lymphoma (206), and Panobinostat (Farydak®, Novartis, Basel Switzerland), approved in 2015 for the treatment of multiple myeloma (2, 203, 207).

Aims of the Subsequent Studies

To identify new targets for chordoma treatment, the author undertook three studies, which are subsequently reported and summarised: In 2010 and 2011, we examined clinical chordoma samples for their expression of IGF-1R and the correlating growth factors, IGF-1 and IGF-2 (1), as the IGF system was at that time reported to be involved in the pathogenesis of bone tumours (e.g. Ewing's sarcoma) (128, 132). Both 2012 and 2013 brought prominent reports of histone mutations in chondroblastomas and in giant cell tumours of bone (197). Since post-translational modifications of histones play an important role in epigenetic regulation and have been linked to tumorigenesis (208), and as several HDAC inhibitors were being approved by the FDA for clinical use in haematological malignancies (203), we studied the effect of HDAC inhibitors in chordoma cell lines (2). We examined the immunohistochemical expression profiles of HDACs in a series of 50 chordomas, and we evaluated the effect of the pan-HDAC-inhibitors, SAHA (Vorinostat; Suberoylanilide hydroxyamic acid), LBH-589 (Panobinostat) and PXD101 (Belinostat) in the well established chordoma cell line, MUG-Chor1, to assess whether these substances had a suppressive effect on chordoma cell growth *in vitro* (2). In parallel to our studies, an increasing number of reports have focused on agents exerting some activity in chordoma. For example, imatinib, which is a PDGFR inhibitor, demonstrated limited activity in a non-randomised phase II study and when used in a compassionate program (11, 209, 210). In addition, there were encouraging results, in the form of anecdotal reports, on the response of chordoma to EGFR (54-58, 211) and vascular endothelial growth factor (VEGF) inhibitors (11, 17, 54, 55, 212). Advances in radiation technology with particles or photons have allowed higher doses of radiation to be delivered (12, 15), and this has been shown to be beneficial for local disease control. However, there are still no approved agents for treatment of patients with inoperable and/or metastatic chordoma (15), and data from prospective randomised clinical trials are still lacking (11, 17, 212). Thus, we employed a drug-discovery approach to identify new therapeutic targets for chordoma. Target-based drug discovery represents a major strategy for planning new cancer treatments (213, 214), and this approach has demonstrated remarkable successes. For example, the FDA approved the ABL-inhibitor, imatinib, which is a drug specifically designed to target the Philadelphia chromosome in chronic myelogenous leukaemia (213). However, target-based drug discovery does not seem to be the method of choice for chordoma. This is because chordomas lack tractable targets, such as recurrent mutations in receptor tyrosine kinases.

And, current potentially tractable targets, such as *PIK3CA* mutations, are only infrequently detected in a small subset of these tumours (3, 173, 215, 216). In view of this unmet need for effective treatment of patients with chordoma, we decided on a phenotypic approach, which means that potential drugs were screened on the basis of a measure of phenotype rather than on a defined target (213). This phenotypic effect can be driven by a combination of direct and indirect effects upon a number of (potential) targets, yielding a summative effect upon the phenotype (213). Phenotypic approaches have been reported to be more successful than target-based approaches in identifying drug candidates with clinically relevant mechanisms of action (214, 217, 218), even though the underlying target may not be discovered until years later. Aspirin, the most widely used drug in the world, is an example of such a drug. It was marketed as an anti-inflammatory drug as early as 1899, but its suppressive effect on the synthesis of prostaglandins was not discovered until 1971 (213, 219). For that reason, we undertook a large-scale phenotypic compound screen on three chordoma cell lines that were available when we started this study. Furthermore, we validated the key target(s) in an extended panel of seven chordoma cell lines that had become available, in order to identify potential new therapeutic options and to contribute to an understanding of the mechanisms by which this disease develops (11).

Materials and Methods

Clinical Samples

As reported by Scheipl *et al.* (2012) (1) and (2013) (2), 50 formalin-fixed paraffin-embedded chordoma specimens (34 primary lesions and 16 recurrences) from 44 patients were available for these studies. The blocks were obtained from the Institute of Pathology at the Medical University of Graz and the National Center for Spinal Disorders in Budapest, Hungary. Two pathologists (Univ.-Prof. Dr. Alfred Beham, Assoc.-Prof. PD Dr. Bernadette Liegl-Atzwanger) reviewed all samples prior to their inclusion in the respective analyses. All tumours demonstrated an immunohistochemical (IHC) expression of *T (brachyury)* and a co-expression of Pan-CK, CK19, EMA, S100 and vimentin (**Table 1**) (2). Morphological sub-classification according to the World Health Organisation (WHO) criteria was performed (10), and conventional chordoma not otherwise specified (NOS) formed the prevailing subtype (*n*=47) (1, 2). Three chordomas (two primary specimens and one recurrence) were of the chondroid subtype (1, 2). The studies were approved by the local Ethics Committee of the Medical University of Graz (18-192 ex 06/07) (1, 2).

Clinical Data

The samples were obtained from 27 males and 17 females (1, 2). The patients' median age at presentation was 54 years (range 24 to 90 years) (1, 2). The tumours originated from the sacrum/coccyx (n=20), the mobile spine (n=13; cervical 4, thoracic 2, lumbar 7) and the scull base (n=11) (1). Primary tumours (n=34) occurred in the sacrum/coccyx (n=17), the mobile spine (n=9; cervical 3, thoracic 2, lumbar 4) and the skull base (n=8) (2). Recurrences (n=16) were situated in the sacrum/coccyx (n=6), the mobile spine (n=6; cervical 1, thoracic 1, lumbar 4) and the skull base (n=4), respectively (2). Tumour volume could be calculated in 39 cases (1). The median volume of the primary tumours was slightly larger than the median volume of the recurrent chordomas (median 75.6 cm^3 [range 0.6 to 2295 cm^3] vs. median 75.0 cm^3 [range 1.5 to 2720 cm^3]) (1).

Patients' follow-up data, which were obtained from the medical records, was available for 43/44 (98%) patients (1). The mean follow-up period was 78 months (median 73 months) (range 2 to 196 months) (2). Three patients had died of disease after 2, 16 and 19 months, respectively (2). The remaining patients had a minimum of 22 months follow-up at the time of last follow-up (2). By then, 15 (34%) patients had died of disease, 10 (23%) were alive with disease, 14 (32%) were without evidence of disease and 4 (9%) had died of

other causes (cardiorespiratory insufficiency and lung cancer) (2). One patient had developed pulmonary metastases, and two others developed local lymph-node metastases (2).

Immunohistochemistry

For our IGF-1R study, we used the following antibodies: IGF-1R, subunit α, (Neomakers, Lab Vision, Thermo Fisher Scientific, CA, USA; mouse monoclonal 24-31; dilution [dil.] 1:50), IGF-1 (Santa Cruz Biotechnology, Santa Cruz, CA, USA; rabbit polyclonal H-70; dil. 1:200) and IGF-2 (Santa Cruz; rabbit polyclonal H-103; dil. 1:100) (1). Antigen retrieval was performed using Dako target retrieval solution at ph9 (Dako, Glostrup, Denmark) and microwave pretreatment (1). For detections, we used the Dako Real Detection System K5001 (Dako) and the Dako immunostainer (Dako) (1). The expression levels of IGF-1R, IGF-1 and IGF-2 were evaluated in a semi-quantitative manner (1): Staining distribution was evaluated as negative (0) if less than 10% of tumour cells stained positive, focal (1) if 11% to 25% of tumour cells stained positive, patchy (2) if 26% to 49% of tumour cells stained positive and diffuse (3) if 50-100% of tumour cells staining positive (1). Staining intensity of each specimen was considered as: negative (-) in cases where no staining was observed, weak (+), moderate (++) or strong (+++) (1).

For our HDAC study, we produced tissue micro arrays (TMAs) according to standard protocols (2). The tumour samples could be obtained from soft-tissue parts of the neoplasms in the majority of cases (2). If this was not possible and/or feasible, the bone was decalcified with ethylenediaminetetraacetic acid (EDTA) (2). The following antibodies were used for IHC: Brachyury (Santa Cruz, dilution 1:50), mouse monoclonal HDAC1 (10E2, dil. 1:500), rabbit monoclonal HDAC2 (Y461, dil. 1:500), rabbit monoclonal HDAC 3 (Y415, dil. 1:100), rabbit polyclonal HDAC4 (dil. 1:100), HDAC5 (dil. 1:25) and HDAC6 (dil. 1:100) (Abcam, Cambridge, UK) (2). Antigen retrieval and detections were performed as described above. Adequate positive and negative controls were included in all studies (1, 2).

Table 1. Immunohistochemical antibodies used for chordoma diagnosis. Adapted from Scheipl *et al.* (2013) (2).

Antibody	Source	Clone	Dilution	Antigen Retrieval	Detection System	Immunostainer

Brachyury	Santa Cruz	H-210 Rabbit Polyclonal	1:50	CC1 mild	ultra View DAB	Ventana
Pan-CK	Dako	MNF 116 Mouse Monoclonal	1:100	P1 8 Min	iView DAB	Ventana
CK 19	Dako	RCK 108 Mouse Monoclonal	1:100	Protease Type XXIV 10 Min	Dako K5001 AEC	Dako
EMA	Dako	E29 Mouse Monoclonal	1:200	P1 8 Min	iView DAB	Ventana
S-100	Dako	Rabbit Polyclonal rab-a-cow	1:2000	P2 12 Min	iView DAB	Ventana
Vimentin	Linaris	V9 Mouse Monoclonal	ready to use	none	Dako K5001 DAB	Ventana

Footnote to Table 1. Abbreviations: Linaris, Wertheim, Germany; CC1 predilute (retrieval buffer) (Ventana Medical Systems Inc., Roche, Basel, Switzerland); P1: Protease 1 (Ventana); Protease Typ XXIV 0,1% (Sigma-Aldrich, St. Louis, MO, USA); P2: Protease 2 (Ventana); ultraView DAB Detection Kit (Ventana); Dako Real Detection System Peroxidase/DAB rabbit/mouse K5001 (Dako); iView DAB Detection Kit (Ventana); AEC (Dako) (2).

For our focused compound screen, we used antibodies against PTEN (clone 6H2.1, mouse, Dako, Agilent Technologies, Glostrup, Denmark), phospho (p)-MET (Tyr1234/1235, clone D26, rabbit, Cell Signaling Technology, Leiden, The Netherlands) and E-Cadherin (clone NCH-38, mouse, Dako) (11). All antibodies were used in a 1:100 dilution. Pretreatment was conducted with Bond TM Epitope Retrieval Solution 2 (Leica Biosystems, Milton Keynes, UK) (11). Immunohistochemistry was carried out on the Leica Bond-III detection platform using the Bond Polymer Refine Detection system (Leica) (11). Compared to the relevant positive and negative controls, expression was evaluated semiquantitatively as reported previously (3, 11): 0-"negative" in absence of immunoreactivity, 1-"weak" if the staining intensity was weaker than the positive control, 2-"moderate" if the staining was as intense as the positive control and 3-"strong" if the staining intensity was stronger than the positive control (3, 11). A minimum of 10% of immunoreactive cells was required for a sample to be considered as immunoreactive (10-25% of immunoreactive cells: +, 26-49% of immunoreactive cells: ++, ≥50% of immunoreactive cells: +++) (3, 11).

Tissue Culture Methods

For the HDAC project, we studied the chordoma cell lines, MUG-Chor1 and U-CH1 (2, 220, 221), which were incubated in a standard incubator at 37°C in a humidified

atmosphere with 5% CO_2. The cells were cultured in IMDM/RPMI 4:1 (PAA Laboratory, Pasching, Austria), to which we added 10% fetal bovine serum (FBS; PAA Laboratory), 1% Insulin/Transferrin/Sodium Selenite (ITS; PAA Laboratory), 2 mM glutamine and 1% Penicillin/Streptomycin (Pen/Strep; PAA Laboratory) (2). Periodic checks for mycoplasma were undertaken as part of standard quality control procedures (2).

For the focused compound screen and its validation experiments, we used seven human chordoma cell lines (U-CH1, U-CH2, U-CH7, U-CH10, MUG-Chor1, JHC7 and UM-Chor1) and cultured them according to previously reported conditions (221-224); http://www.chordomafoundation.org/) (1, 2, 11). The cell lines were either obtained from our collaborators (U-CH1: Dr. Silke Brüderlein, Ulm, Germany; U-CH2 and MUG-Chor1: Dr. Beate Rinner, Graz, Austria) or from the Chordoma Foundation (JHC7, U-CH10, UM-Chor1) (11). U-CH7 was established as reported above (11). All chordoma lines included in this study derived from sacral tumours, except UM-Chor1, which derived from a clival neoplasm (http://www.chordomafoundation.org/) (220-224). The cell lines were periodically quality controlled by short-tandem-repeat (STR) analysis (DNA Diagnostic Center, London, UK) (**Suppl. Table 1**) and mycoplasma testings (11, 220-224). For immunohistochemistry and FISH, we had cell pellets from the chordoma cell lines formalin-fixed and paraffin-embedded, and 3 µm sections were cut (3, 11). The gastric cancer cell line NCI-N87 (which expresses ERBB2 [ATCC® CRL-5822™])(225), and human dermal fibroblasts (ATCC® PCS-201-012™) were included as non-neoplastic control cell populations. Both were cultured according to ATCC guidelines (11): Normal adult human dermal fibroblasts were cultured in Fibroblast Basal Medium (ATCC® PCS-201-030™), which was supplemented with Fibroblast Growth Kit-Low serum (ATCC® PCS-201-041™) (11). NCI-N87 cells were grown in RPMI 1640 (Gibco) containing 10% FBS (Life Technologies) and 1% Pen/Strep (Gibco) (11). For the drug screening experiments as described below, the cells were plated at the following densities: 156 cells/mm^2 (U-CH1, U-CH7, U-CH10, MUG-Chor1, JHC7, UM-Chor1 and NCI-N87), 78 cells/mm^2 (U-CH2) and 14 cells/mm^2 (human dermal fibroblasts) (11).

Professor Adrienne M. Flanagan obtained ethical approval from the Cambridgeshire 2 Research Ethics Service (reference 09/H0308/165) and the UCL Biobank for Health and Disease Ethics Committee.

Protein Extraction and Western Blot Analysis

For our HDAC study in 2013 (2), the cells were re-suspended in lysis buffer (50 mM Tris-HCL pH 7.4, 150 mM NaCl, 50 mM NaF, 1 mM EDTA, 10% Nonidet P-40 [NP-40], 1% Triton-X and protease inhibitors), incubated on ice for 10 minutes and centrifuged at 15,000 rpm for 15 minutes (2). We then separated 20 µg aliquots of protein extracts on 12% SDS-PAGE and electroblotted these onto 0.45 µm Hybond ECL nitrocellulose membranes (Amersham Biosciences, Little Chalfont, UK) (2). The membranes were blocked with 3% milk blocking buffer for 1 hour and then incubated with the primary antibodies for 2 hours at room temperature (2). We applied the following antibodies: polyclonal rabbit HDAC2 (ab32117) and HDAC6 (ab1440) (both Abcam, Cambridge, UK), as well as the polycloncal mouse antibody PARP (#9542; New England Biolabs, Frankfurt, Germany) (2). The blots were developed at room temperature for 1 hour using horseradish peroxidase-conjugated secondary antibodies (Dako, Vienna, Austria) and the SuperSignal® West Pico Chemoluminescent Substrate (Thermo Scientific, Rockford, IL) according to the manufacturers' protocol (n=3) (2).

In the course of the focused compound screen and its validation experiments (11), cells were lysed on ice with RIPA buffer (20 mM Tris-HCL pH 7.4, 150 mM NaCl, 50 mM NaF, 1 mM EGTA, 1 mM EDTA, 1% NP-40, 0.5% Sodium-Deoxycholate, 1% SDS) containing EDTA-free protease (Roche) and phosphatase inhibitors (Sigma-Aldrich, Gillingham, UK) (11). Total protein concentrations were determined using a Pierce™ BCA Protein Assay Kit (Thermo Scientific) according to the manufacturer's instructions (11). Protein aliquots (25µg) were resolved on an acrylamide gel (Criterion™ TGX (Tris-Glycine eXtended) Stain-Free™ Any KD, Bio-Rad Laboratories Ltd., Hemel Hempstead, UK) and blotted on nitrocellulose Whatman® Protran® Membranes (GE Healthcare Life Sciences, Chalfont St Giles UK) (11). Filters were developed using an Odyssey Infrared Imaging System (LI-COR Biotechnology, Cambridge, UK) (11). The primary and secondary antibodies that were used are listed in **Table 2**. We conducted a minimum of n=2 biological replicates of each Western blot.

Table 2. Antibodies and conditions used for Western blot analysis. Adapted from Scheipl *et al.* (2016) (11).

Protein (Clone)	kDA	Supplier	Cat. Number	Species	Clonality	Dilution
Akt	60	Cell Signaling	9272	Rabbit	polyclonal	1:1000
Beta Actin (AC-15)	42	Sigma-Aldrich	A5441	Mouse	monoclonal	1:5000
Brachyury (A-4)	49	Santa Cruz	Sc-374321	Mouse	monoclonal	1:500
cMET (D1C2)	140	Cell Signaling	8198	Rabbit	monoclonal	1:500
EGFR	175	Cell Signaling	2232	Rabbit	polyclonal	1:500
ERBB2	185	Sigma-Aldrich	HPA001383	Rabbit	polyclonal	1:500
ERBB3 (1B2E)	185	Cell Signaling	4754	Rabbit	monoclonal	1:500
ERBB4 (111B2)	185	Cell Signaling	4795	Rabbit	monoclonal	1:500
HGF	83	Abcam	83760	Rabbit	polyclonal	1:500
p44/42 MAPK (ERK1/2) (3A7)	44/42	Cell Signaling	9107	Mouse	monoclonal	1:1000
p-Akt (Ser473) (193H12)	60	Cell Signaling	4058	Rabbit	monoclonal	1:1000
p-EGFR (Tyr1068) (D7A5)	175	Cell Signalling	3777	Rabbit	monoclonal	1:500
p-EGFR (Tyr1173)	170	Merck Millipore	04-341	Rabbit	monoclonal	1:500
p-ERBB2 (Tyr 1248)	185	Cell Signalling		Rabbit	monoclonal	1:500
p-ERBB3 (Tyr1222) (EPR5807)	185	Merck Millipore	MABN1119	Rabbit	monoclonal	1:500
p-ERBB4 (Tyr1284) (21A9)	180	Cell Signalling		Rabbit	monoclonal	1:500
p-MET (Tyr1234/1235) (D26)	145	Cell Signaling	3077	Rabbit	monoclonal	1:500
p-p44/42 MAPK (ERK1/2) (Thr202/Tyr204) (D13.14.4E)	44/42	Cell Signaling	4370	Rabbit	monoclonal	1:500
p-STAT3 (Tyr705) (D3A7)	79/86	Cell Signaling	9145	Rabbit	monoclonal	1:500
PTEN (6H2.1)	54	Merck Millipore	04-035	Mouse	monoclonal	1:1000
p-YAP (Ser127) (D9W2I)	65	Cell Signaling	13008	Rabbit	monoclonal	1:500
STAT3 (124H6)	79/86	Cell Signaling	9139	Mouse	monoclonal	1:500
YAP (D8H1X)	65	Cell Signaling	14074	Rabbit	monoclonal	1:500

Footnote to Table 2. The antibodies were stored, prepared, and used according to the manufacturers‘ instructions. Sigma: Sigma-Aldrich. Millipore: Merck Millipore. Cell Sign.: Cell Signaling.

Additional methods "HDAC Study"

Cell Proliferation Assay

Cell proliferation was assessed with the CellTiter 96® aqueous nonradioactive cell proliferation assay (Promega, Mannheim, Germany), which was used according to the manufacturer's instructions (2). We seeded $1x10^4$ chordoma cells and incubated these with increasing drug concentrations for 24, 48 and 72 hours to determine IC_{50} values (2). This experiment was run in technical replicates (n=12). The HDAC inhibitors SAHA (vorinostat; Suberoylanilide hydroxyamic acid), LBH-589 (panobinostat) and PXD101 (belinostat) were purchased from Alinda Chemistry Ltd (Moscow, Russia) (2). The drug concentrations used in this experiment were 10-50 µM for SAHA, 50-500 nM for LBH-589 and 1-50 µM for PXD101 (2). Untreated control cells were included for each experiment.

Caspase-Glo® 3/7Assay

We plated 10^4 cells/well (100µl) from two chordoma cell lines, MUG-Chor1 and U-CH1, and after 24 hours, we treated these with their IC_{50} concentrations of SAHA, LBH-589 and PXD101 for 3, 6, 24, 48 and 72 hours (2). In addition to untreated cells, we included skin fibroblasts from the MUG-Chor1 patient as additional controls (fibro-MUG-Chor1) (2). Caspase activation was studied using the Caspase-Glo® 3/7 Assay (Promega, Mannheim, Germany) according to the manufacturer's instructions (2). Luminescence was measured after 30 minutes of incubation with the Caspase-Glo® 3/7 Reagent (Caspase-Glo® substrate and buffer) (2). Each experiment was conducted n=3 times.

Cleavage of Caspase-3

We harvested MUG-Chor1 cells by trypsinization 24, 48 and 72 hours after incubation with the respective IC_{50}s of the HDAC inhibitors, fixed them with formaldehyde for 10 minutes at 37°C (2×10^6 cells/ml) and permeabilised the cells with methanol (2). Untreated cells were included as a negative control (2). The pellets were re-suspended in an incubation buffer consisting of PBS and FBS in a 1:200 ratio and stained with a FITC-conjugated monoclonal active caspase-3 antibody (Cell Signaling Technology, Danvers, MA) (2). Flow cytometry (FACSCalibur, BD Biosciences) was performed with FACSDiva software. FCS3 express software (De Novo software) was used to create the histograms (2). The experiment was conducted n=3 times.

Cell Cycle Analysis

We incubated MUG-Chor1 cells with the IC_{50}s of SAHA, LBH-589 and PXD101 for 24, 48, and 72 hours and harvested the cells by trypsinization (2). Cells ($5x10^5$) were fixed for 10 minutes at 4°C in ice cold ethanol (70%) (2). The cell pellets were washed and re-suspended in propidium iodide (PI) (50 µl/ml PI, RNAse A; Beckman Coulter, Krefeld, Germany) (2). Cells were incubated in PI staining buffer for 15 minutes at 37°C (2). Cell cycle distribution was determined using FACSCalibur (BD Biosciences, San Diego, CA, USA) and ModFit software (2).

Statistical Analysis

Statistical analyses for our IGF-1R study were conducted using R version 2.11.1 (http;//www.r-project.org, University of Economics and Business, Vienna, Austria) (1). Survival times were calculated from the date of tumour diagnosis to the date of death or last follow-up (1). We considered *p*-values ≤ 0.05 as obtained from Cox regression to be significant (1).

For our HDAC study in 2013 (2), the PASW Statistics 18 Software (IBM Corporation, Somers, NY) was used for the statistical analysis, and the SigmaPlot® software (Systat Software Inc., San Jose, CA, USA) generated graphs (2). All outcome variables were expressed as mean values (± SD) (2). We applied the Student's unpaired *t*-test and the exact Wilcoxon's test to study potential differences between the groups, and we considered *p*-values ≤ 0.05 to be statistically significant (2). Four parameter logistic curves were applied to determine IC_{50} values (2).

Additional methods "Focused Compound Screen"

Protein Kinase Inhibitors and Compound Libraries

We selected 1,097 compounds for the screen (**Suppl. Table 2**), which was conducted in collaboration with Cancer Research Technology Limited UK (CRT) (11). Of these 1,097 compounds, 886 small molecule kinase inhibitors were provided by GlaxoSmithKline (GSK), and these made up two compound sets of 365 ("PKIS") and 521 ("PKIS2") compounds, respectively, on which there are published data (**Suppl. Table 2**) (11, 226, 227). We further included 160 Calbiochem kinase inhibitors (Merck KGaA, Darmstadt, Germany) provided by CRT, an Anticancer Library (n=43) (Selleckchem, Houston, TX, USA), as well as eight compounds reported to be inhibitors of Aldo-Keto Reductase

Family 1 Member B10 (AKR1B10) (Selleckchem) (11, 228). Six commercially available EGFR/ERBB family inhibitors were purchased (Selleckchem), and these had either been approved by the FDA or were in clinical trials at the time of research (122, 229-231). These were: erlotinib (OSI-774), gefitinib (ZD1839), sapitinib (AZD8931), afatinib (BIBW 2992), poziotinib (NOV120101; HM781-36B) and lapatinib (Tykerb®; GSK) (11).

Focused Compound Screen* (*Figure 1)

The compounds, which had undergone quality control at CRT, were tested at a single concentration of 1 μM using a non-randomised plate layout in a 96-well plate format (80 compounds per plate) (min. n=3) (11). Three chordoma cell lines (U-CH1, U-CH2 and MUG-Chor1) were included in this single concentration screen (11). We seeded the cells in 90 μl of medium per well using a Multidrop Combi (MDC, Thermo Fisher Scientific, Loughborough, UK) and cultured them for 24 hours before adding the compounds (11). CRT diluted 10mM compound stocks with an ECHO 550 liquid handler (LabCyte, Sunnyvale, CA, USA) to create 10X compound plates (11). From these 10X plates, compounds (10 μL/well) were added to the cell plates using a Biomek FX (Beckman Coulter, Brea, CA, USA) (11). Following 96 hours of compound treatment, we assessed cell survival using the Water Soluble Tetrazolium Salt (WST1) assay (Roche Diagnostics Limited, Burgess Hill, UK), according to manufacturers' recommendations (11).

Hit Selection

Hit selection thresholds were calculated independently for each cell line (11). Percentage inhibition for each compound at 1 μM was calculated from the raw data relative to the controls on each plate (11). Mean percentage inhibition and standard deviations (SD) were calculated for each cell line by combining the results of different libraries (Calbiochem, Anticancer) or by analysing data from libraries independently (PKIS, PKIS2) (11). Based on the spread of data, we applied a hit selection threshold of 2X SD (PKIS) or 1.5X SD (other libraries) for each line (11).

Hit Confirmation

We evaluated the potencies of the inhibitory 'hits' identified in the single concentration screen by testing their half maximal effective concentration (EC_{50}) in a 10-point dose response format (11). The dose response testing was conducted in three chordoma cell lines (U-CH1, U-CH2 and MUG-Chor1) and in dermal fibroblasts. We tested each compound in three independent experiments, with two replicates per experiment (11). The

highest concentration tested was 30 μM with a subsequent 1:3 dilution (11). We recorded the maximum percentage inhibition (MI) that was obtained at the highest concentration of each compound (11). Staurosporine (SRPN; Sigma-Aldrich) was used as a positive control, and its EC_{50} value(s) were monitored to ensure reproducibility between the runs (11). An arbitrary threshold of an EC_{50} <5 μM in chordoma cell lines and >10 μM in dermal fibroblasts was applied to select compounds that killed chordoma cells but not dermal fibroblasts (11). Selectivity was defined as the fold difference between a compound's EC_{50} in fibroblasts and in chordoma cells (11).

Hit Validation

Analysis of Cell Death. To determine induction of apoptosis and cell viability, we used the Caspase-Glo® 3/7 Assay (Promega, Southampton, UK) and the CellTiter-Glo® Luminescent Cell Viability Assay (Promega), respectively (11). Profiling was conducted in a dose-dependent manner with a 1:3 serial dilution starting from 20 μM (11). A minimum of two independent experiments was carried out for each compound (11). Data were analysed with XLfit version 5.0 (IDBS, Guildford, UK) (11).

Biochemical Selectivity Analysis. GSK chemists selected 11 GSK compounds based on their structural homologies. These compounds (as well as sapitinib, erlotinib and gefitinib [Selleckchem]) were sent for biochemical IC_{50} determination against EGFR, ERBB2 and ERBB4 (Reaction Biology Corporation, Malvern, PA, USA) **(Table 12)** (11). No test set was available for ERBB3.

ELISA. Lysates of chordoma cell lines were prepared and experiments performed using the Human Total EGFR (#DYC1854) and the Human Phospho-EGFR/ERBB1 (#DYC1095B) ELISA kits (R&D Systems Ltd., Abingdon, UK) according to the manufacturer's instructions (11). We used 60 μg of protein per sample, and each experiment was conducted a minimum n=2 times.

Combination Study of Sapitinib with the MET Inhibitor Crizotinib. We tested the ALK/MET inhibitor crizotinib (Xalkori®, Pfizer, NY, USA) (232) in combination with sapitinib, applying a non-randomised plate layout in a 384-well format (11). U-CH2 cells were seeded in 70 μl of medium and cultured for 24 hours (11). Profiling was conducted in a 7-point dose response matrix starting from a maximum concentration of 1 μM in a 1:3 serial dilution (11). Raw data were corrected for background (which was media only) and tested in 16 replicates per plate (11). The CalcuSyn software version 2.1 (Biosoft,

Cambridge, UK) was used to determine synergy (11). A combination index (COI) was calculated and evaluated as synergistic (COI ≤ 0.9), additive (COI = 0.9 to 1.1) or antagonistic (COI ≥ 1.1), on the basis of the literature (11, 233). We conducted statistical analysis in GraphPad version 6.0 (Prism, CA) using the Students t-test, and we considered p-values ≤ 0.05 (**) to be significant (11).

Real-time quantitative PCR. We extracted RNA from frozen cell line pellets using the miRNeasy Mini Kit (Qiagen GmbH, Hilden, Germany), and quantified its yield by Nanodrop® spectrophotometry (Thermo Fisher Scientific, Wilmington, DE, USA) (11). We then transcribed 500 µg of RNA into cDNA, applying the High Capacity cDNA Reverse Transcription Kit (Applied Biosystems, Foster City, CA, USA) according to the manufacturer's instructions (9, 11). Fast SYBR® Green MasterMix (Applied Biosystems) was used to carry out quantitative real-time PCR (q-RT-PCR) according to the manufacturer's instructions (11). We used primers that had been previously published by our group: *T (brachyury)*: 5'- CCCGTCTCCTTCAGCAAAGTC-3' forward; 5'-TGGATTCGAGGCTCATACTTATGC-3' reverse; *GAPDH*: 5'-GGAGTCAACGGATTTGGTCGTA-3' forward; *GAPDH* reverse: 5'-GGCAACAATATCCACTTTACCAGAGT-3' reverse (9, 11). Water samples served as controls (11). *T* expression in human chordoma cell lines was analysed using the $2^{-\Delta CT}$ method with normalisation to *GAPDH* expression (9, 11). U-CH1 served as the reference by which to compare *T* expression in different chordoma cell lines (9, 11).

FISH Analysis of EGFR, ERBB2 and MET. For FISH analysis, we used commercial probes for EGFR/CEP7, HER2/CEP17 (Abbott Molecular, Des Plaines, IL, USA) and MET/CEN7 (Zytovision, Bremerhaven, Germany). Evaluation was performed as follows: EGFR/HER2/MET status was scored as the average number of EGFR/HER2/MET red/green/green signals per nucleus and as the ratio between EGFR/HER2/MET red/green/green signals and centromeric (CEN) CEN7/CEN17/CEN7 green/red/red signals, respectively (3, 11). Results were reported according to the Colorado criteria, as previously described by Shalaby *et al.* (2012) (3, 11). The FISH-positive group included two categories, which were high-level polysomy of chromosome 7/17/7 (≥ 4 copies of the gene of interest and CEN7/17/7 per cell in ≥ 40% of cells) and amplification (≥ 15 gene copies per cell in ≥10% of analysed cells, regardless of the number of CEN7/17/7 signals) (11). The FISH-negative group consisted of cell lines with low-level polysomy (≥ 2 copies of the gene of interest and CEN7/17/7 per cell in ≤ 40% of cells, and 3 copies of the gene of

interest per cell in ≥40% of cells) or disomy (≤ 2 copies of the gene of interest and CEN7/17/7 in ≥ 90% of the cells) (3, 11).

Analysis for Mutations in Cancer Gene Hotspots of Chordoma Cell Lines. We had the hotspots in 22 cancer-related genes analysed for mutations using the Ion AmpliSeq™ Colon and Lung Cancer Research Panel v2 (Thermo Scientific) (11). Sequencing was conducted at the UCL Advanced Diagnostics-Sarah Cannon Research Laboratories, London, UK (11). This facility employed an Ion Torrent Personal Genome Machine (PGM) (Life Technologies) using Ion PGM™ Sequencing 200 Kit v2 chemistry (Thermo Fisher), as well as a 318v2 chip (Thermo Fisher) (11). The laboratory analysed the data with Torrent suite v4.0.2 and Variant Caller v4.0 (r76860) (Thermo Fisher) (11) and grouped the Variant Caller output into categories based on an in-house developed script (UCL Advanced Diagnostics - Sarah Cannon Research Laboratories) (11). Only variants reported with a frequency of > 2.5% in a minimum of 100 high-quality unbiased reads were considered "detected" (11).

In vivo Studies. Chordoma Foundation tested sapitinib (AstraZeneca) at South Texas Accelerated Research Therapeutics (START) through its Drug Screening Pipeline (11). Antitumour activity of this drug was tested on two chordoma mouse models: a cell line-derived xenograft (U-CH1) (220) and a patient-derived xenograft (SF8894) (11, 234). All animal studies were conducted under protocols approved by the International Animal Care and Use Committee (11). Xenografts were established by implanting tumour fragments from host animals subcutaneously into six- to eight-week-old athymic nude mice (Charles River Laboratories Inc., Wilmington, MA, USA) (11). The mice were matched by tumour volume (TV) and randomised to the control or the treatment group, respectively, after their tumours had reached an average volume of 150-250 mm^3 (11). In the treatment group, the mice received an oral gavage of sapitinib 50 mg/kg (25 mg/kg twice daily). This dosing schedule was chosen based on the literature (11, 235). Initial dosing started at Day 0 and continued for a minimum of 4 weeks (28 days for SF8894, and 42 days for U-CH1) (11). Throughout this period, the mice were observed daily and weighed twice a week with their TVs and weights recorded electronically using a digital calliper and scale (11). Based on the formula, $TV\ (mm^3) = width^2\ (mm^2) \times length\ (mm) \times 0.52$, tumour dimensions were converted into tumour volumes (11). A mean control TV of approximately 1–2 cm^3 formed the primary endpoint (11). Based on initial and final tumour measurements, percent growth inhibition values were calculated for both the treatment and the control group (11). For

statistical analyses, a two-way analysis of variance (ANOVA) was conducted, followed by the Dunnett's multiple comparisons test (11).

Results

Correlation with Clinical Data

At 5 years, the overall survival rate was 72.8% (95% confidence interval [CI] 50.1%-86.4%) (1). This rate dropped to 45.3% after 10 years (95% CI 18.0%-69.4%) (1) (**Figure 7**).

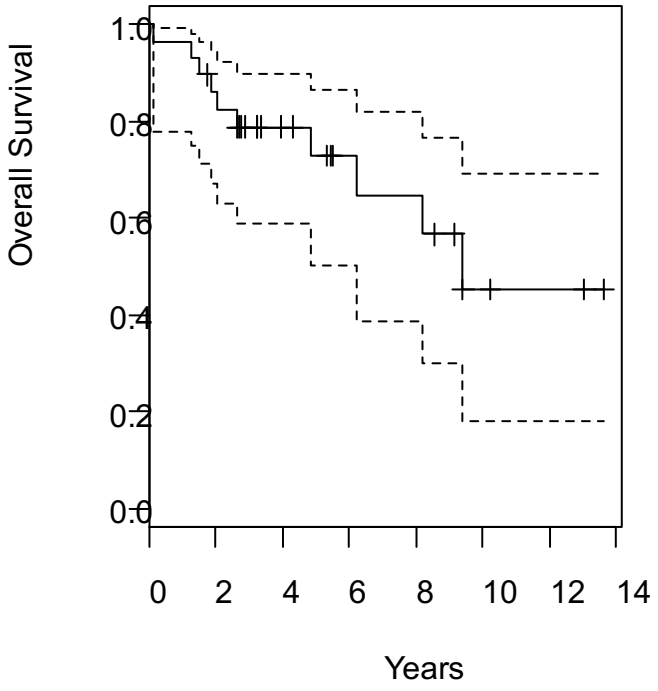

Figure 7. Kaplan-Meier graph illustrating overall survival rates of chordoma patients.

Survival was significantly influenced by patients' age ($p = 0.01$), putting elderly patients at a disadvantage (1). In addition, tumour volume ($p = 0.002$), as well as tumour location ($p = 0.029$), significantly influenced survival of patients with chordoma (1). Patients with tumours occurring in the distal parts of the axial skeleton showed significantly lower survival rates compared to patients whose neoplasms were located in the proximal areas of the axial skeleton (1).

IGF-1R, IGF-1 and IGF-2 in Chordomas

Expression Levels of IGF-1R, IGF-1 and IGF-2 in Chordomas

All markers investigated (IGF-1R, IGF-1 and IGF-2) stained immunohistochemcally to varying degrees in the chordoma samples analysed: The staining obtained with IGF-1R

displayed a combined membranous and cytoplasmic pattern (1). In contrast, IGF-1 and IGF-2 stained exclusively cytoplasmic (1). In two cases, staining patterns could not be evaluated due to a lack of sufficient material (1). The staining results are listed in detail in **Table 3**, and they are illustrated in **Figure 8**. In summary, IGF-1R was expressed by 38/50 (76%) chordomas (25/34 primary tumours and 15/16 recurrences) (1). The majority of tumours (46/50, 92%) stained positive for IGF-1 (30/34 primary lesions and all 16 recurrent tumours), and half of them expressed IGF-2 (25/50, 16/34 primary tumours and 9/16 recurrent lesions) (1). Moderate/strong and diffuse expression of IGF-1R was observed in 18 chordomas (36%, 12/34 primary tumours, 6/16 recurrences) (1). IGF-1 was expressed moderately/strongly and diffusely in 32 chordomas (64%, 24/34 primary and 8/16 recurrent tumours), and IGF-2 in 8 chordomas (16%, 5/34 primary and 3/16 recurrent tumours) (1). We did not observe that high levels of ligand expression were correlated significantly with high levels of receptor expression (1). However, there was a positive correlation between tumour volume and IGF-1R staining intensity in primary tumours (p = 0.042) and in recurrent neoplasms (p = 0.052) (1). Though no statistical significance could be obtained, when a recurrent tumour was directly compared to the primary neoplasm of the same patient, there was a trend for the recurrent chordomas to show a more distinct staining for IGF-1R, IGF-1 and IGF-2. (1). One case proved an exception to this statement, as IGF-1R expression, which was observed weakly in the primary neoplasm, disappeared in the recurrent tumour (1).

Table 3. Expression profile of IGF-1R, I-GF1 and I-GF2 in chordomas (n=50). Adapted from Scheipl *et al.* (2012) (1).

Expression Profile of IGF-1R, IGF-1 and IGF-2 in Chordomas.			
n=50			
	IGF-1R	**IGF-1**	**IGF-2**
Staining Distribution			
Diffuse (3)	26	46	8
Patchy (2)	8	0	5
Focal (1)	4	0	12
Negative (0)	10	2	23
NA	2	2	2
Total Expression (∑)	**38 (76%)**	**46 (92%)**	**25 (50%)**
Staining Intensity			
Strong (+++)	12	20	0

Moderate (++)	6	12	16
Weak (+)	20	14	9
Negative (-)	10	2	23
NA*	2	2	2
Strong/Moderate ≥ 50% (∑)*	**18 (36%)**	**32 (64%)**	**8 (16%)**

Footnote to Table 3. Staining distribution (percentage of chordoma cells staining positive by IHC): diffuse (3) 50-100%, patchy (2) 26 - 49%, focal (1) 11-25%, negative (0) = less than 10% of tumour cells staining positive; NA: specimens not available for analysis. Staining intensity: strong (+++), moderate (++), weak (+), negative (-). *Strong or moderate staining intensity in ≥ 50% of tumour cells (1).

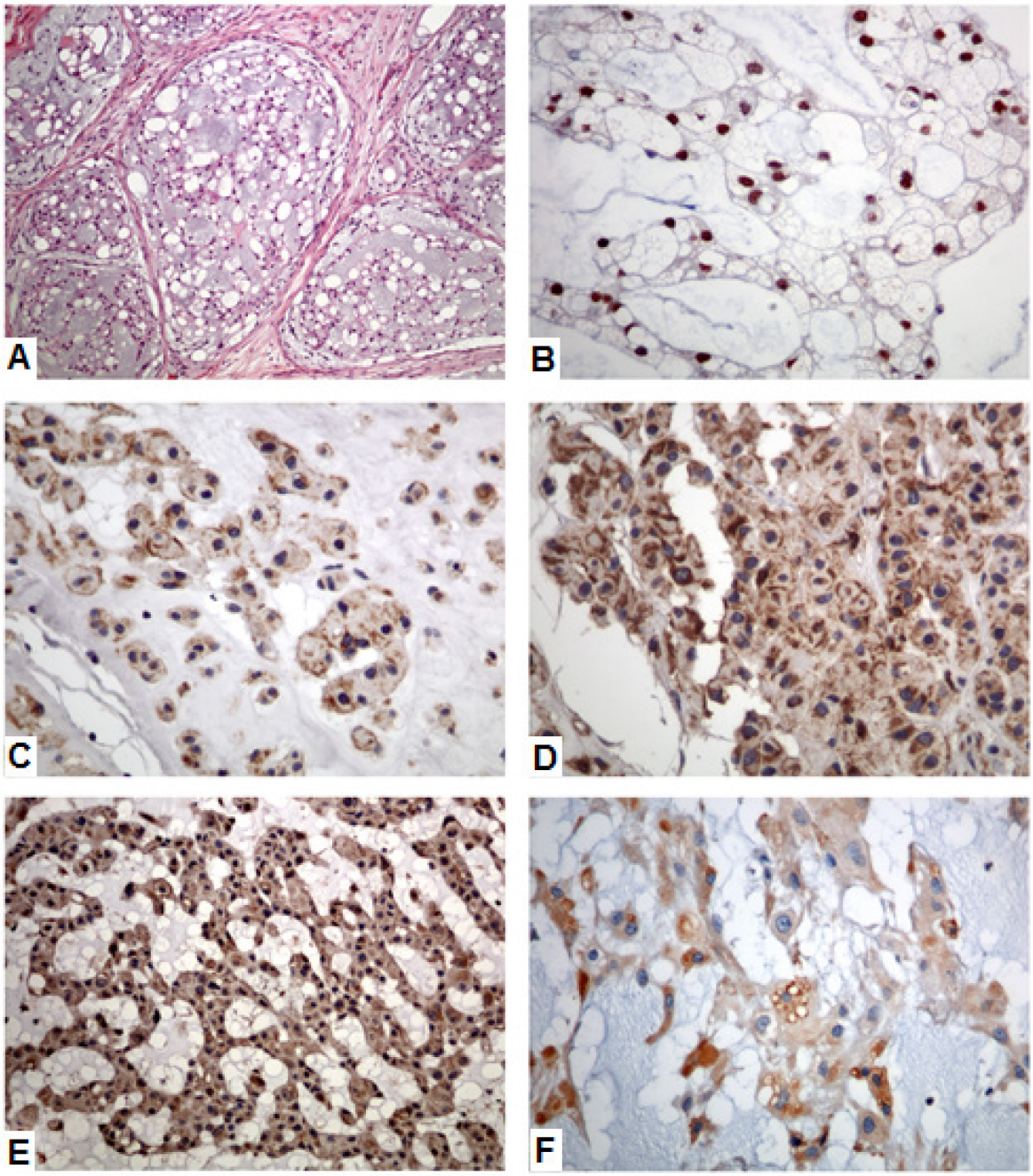

Figure 8. IHC analysis of IGF-1R, IGF-1, and IGF-2 expression profiles in chordoma specimens.
Adapted from Scheipl *et al.* (2012) (1). **(A)** H&E staining of a chordoma, showing the lobular growth pattern of this neoplasm. The lobules consist of cords and strands of tumour cells embedded in a myxoid matrix (1). **(B)** Chordoma cells are characterised by their nuclear staining for *T* (brachyury) (1). **(C)** Combined membranous and cytoplasmic staining profile for IGF-1R, which shows a moderate staining intensity in a case of primary chordoma (1). **(D)** Strong membranous and cytoplasmic staining for IGF-1R in a case of recurrent chordoma (1). **(E)** Strong cytoplasmic IGF-1 staining of a primary chordoma (1). **(F)** Moderate cytoplasmic IGF-2 staining of a primary chordoma (1). Images were taken at a x10 (A) and a x20 (B-F) magnification.

Evaluating Expression Levels of HDACs in Chordomas and Studying the Effect of HDAC Inhibitors on Chordoma Cell Lines

Expression Levels of HDACs 1-6 in Chordomas

The detailed IHC results are listed in **Table 4**. In summary, HDAC1 showed a weak nuclear staining in a subset of tumours (n=5, 10%) but was cytoplasmically negative in all cases available for analysis (n=48, 96%) (2). HDAC2 stained cytoplasmically positive in 36 cases (72%) and negative in 11 cases (22%) (2). A nuclear co-expression of this marker was observed in 27 tumours (54%) (2) (**Table 4**). HDACs 3 and 4 were cytoplasmically expressed to varying degrees in all cases evaluated (2). There was a nuclear positivity for HDAC3 in 13 (26%) cases, and HDAC4 showed nuclear expression in 2 cases (4%) (2). Immunoreactivity for HDACs 5 and 6 was found to be exclusively cytoplasmic (2) (**Table 4**). The strongest expression levels were obtained for HDAC6, with all of the specimens analysed demonstrating moderate (n =3, 6%) or strong (n = 41, 82%), diffuse staining for this marker (**Figure 9E, Table 4**) (2). None of the expression profiles of any of the markers tested significantly differed between primary and recurrent lesions (2). Nor did we observe any correlations with tumour size, tumour location, development of recurrence or survival in Bonferroni-corrected analysis (2). Expression of HDACs 2 and 6 was additionally confirmed by Western Blot analysis in both chordoma cell lines analysed, U-CH1 and MUG-Chor1 (**Figure 9F**) (2).

Table 4. Summary of IHC results for HDACs 1-6. Adapted from Scheipl *et al.* (2013) (2).

Staining Intensity				Staining Distribution				Nuclear Staining		NA	Total
- *(%)*	1+ *(%)*	2+ *(%)*	3+ *(%)*	0 *(%)*	1 *(%)*	2 *(%)*	3 *(%)*	neg *(%)*	pos *(%)*	n *(%)*	n *(Total %)*
HDAC1				**HDAC1**				**HDAC1**		**HDAC1**	**HDAC1**
48 *(96)*	0 *(0)*	0 *(0)*	0 *(0)*	48 *(96)*	0 *(0)*	0 *(0)*	0 *(0)*	43 *(86)*	5 *(10)*	2 *(4)*	50 *(100)*
HDAC2				**HDAC2**				**HDAC2**		**HDAC2**	**HDAC2**
11 *(22)*	22 *(44)*	9 *(18)*	5 *(10)*	11 *(22)*	1 *(2)*	4 *(8)*	31 *(62)*	20 *(40)*	27 *(54)*	3 *(6)*	50 *(100)*
HDAC3				**HDAC3**				**HDAC3**		**HDAC3**	**HDAC3**
0 *(0)*	14 *(28)*	21 *(42)*	8 *(16)*	0 *(0)*	0 *(0)*	0 *(0)*	43 *(86)*	30 *(60)*	13 *(26)*	7 *(14)*	50 *(100)*
HDAC4				**HDAC4**				**HDAC4**		**HDAC4**	**HDAC4**
0 *(0)*	18 *(36)*	18 *(36)*	7 *(14)*	0 *(0)*	0 *(0)*	0 *(0)*	43 *(86)*	41 *(82)*	2 *(4)*	7 *(14)*	50 *(100)*

HDAC5				**HDAC5**				**HDAC5**		**HDAC5**	**HDAC5**
0	30	13	0	0	0	0	43	43	0	7	50
(0)	*(60)*	*(26)*	*(0)*	*(0)*	*(0)*	*(0)*	*(86)*	*(86)*	*(0)*	*(14)*	*(100)*
HDAC6				**HDAC6**				**HDAC6**		**HDAC6**	**HDAC6**
0	0	3	41	0	0	0	44	44	0	6	50
(0)	*(0)*	*(6)*	*(82)*	*(0)*	*(0)*	*(0)*	*(88)*	*(88)*	*(0)*	*(12)*	*(100)*

Footnote to Table 4. Cytoplasmic staining intensity of each specimen is described as: negative (-) in cases where no staining was observed, weak (+), moderate (++), or strong (+++) (2). Cytoplasmic staining distribution is evaluated as: negative (0) = less than 10% of tumour cells staining positive; focal (1) = 11% to 25%; patchy (2) = 26% to 49%; and diffuse (3) = 50-100% of tumour cells staining positive (2). Nuclear staining is reported as positive (pos) or negative (neg) (2). NA: specimens not available for analysis (2).

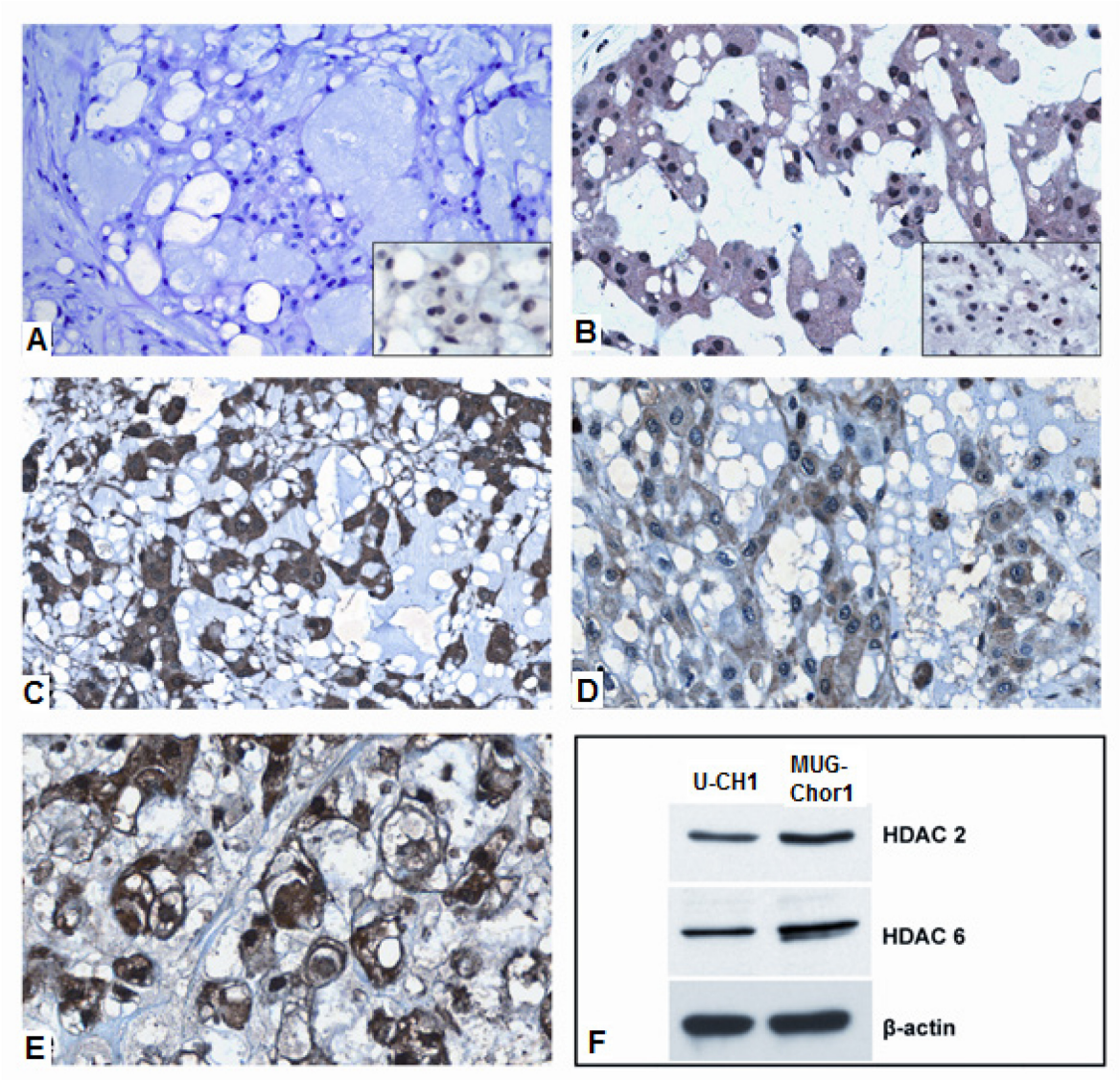

Figure 9. IHC analysis of HDAC expression profiles in chordoma specimens.
Adapted from Scheipl *et al.* (2013) (2). **(A)** H&E staining of a conventional chordoma NOS, the inset showing nuclear staining for T (brachyury). **(B)** Chordoma sample demonstrating moderate cytoplasmic and nuclear (inset) expression of HDAC2. **(C)** Chordoma displaying strong cytoplasmic IHC expression of HDAC4. **(D)** Chordoma showing moderate cytoplasmic expression of HDAC5. **(E)** Strong cytoplasmic HDAC6 expression in another chordoma sample. All images were taken at a 20X magnification. **(F)** Western Blot analysis confirms expression of HDACs 2 and 6 in the chordoma cell lines U-CH1 and MUG-Chor1. Beta-Actin served as a loading control (2).

HDAC Inhibitors Showed Dose-Dependent Effects on Cell Proliferation

All HDAC inhibitors showed a time- and dose-dependent inhibition of cell proliferation. The IC_{50} values after 48 hours of incubation were 50 µM (SAHA), 1 µM (LBH-589) and 0.5 µM (PXD101) (2).

The HDAC Inhibitors SAHA and LBH-589 Induced Apoptosis in Chordoma Cell Lines

HDAC inhibitor-induced apoptosis was studied via three different methods, which were described above: caspase 3/7 induction, cleaved caspase-3 and PARP cleavage. As shown in **Figure 10**, caspase 3/7 levels increased in U-CH1 and MUG-Chor1 upon treatment with SAHA and LBH-589, indicating apoptosis (2, 236). Caspase 3/7 levels increased from 6 hours onwards and peaked 48 hours after compound treatment in U-CH1 (**Figure 10A and B**). In MUG-Chor1, an increase could be observed from 24 hours onwards, with a peak at 72 hours (**Figure 10A and B**). For both cell lines, the compounds' effect upon tumour cells was more distinct compared to their effect upon normal skin fibroblasts. The latter were obtained from the patient whose tumour tissue served as the origin of the MUG-Chor1 cell line (fibro-MUG-Chor1) (**Figure 10A and B**). In contrast to the results obtained with SAHA and LBH-589, no relevant induction of caspase 3/7 was observed when these two chordoma cell lines were treated with PXD101 (**Figure 10C**) (2). When cleaved caspase-3 was measured by flow cytometry, similar results were obtained. For this experiment, MUG-Chor1 cells were treated with the IC_{50} concentrations of the 3 HDAC inhibitors studied for 24, 48, and 72 hours (**Figure 10D, Table 5**) (2). **Figure 10** shows FACS histograms obtained after 72 hours of compound treatment. Untreated control cells are shown in black filling, SAHA-treated cells indicated by a light grey line, LBH-589-treated cells with a dark grey line and PXD101-treated cells with an area filled with vertically stripped lines (**Figure 10D**) (2). Detailed values for all time points are listed in **Table 5**. For all three compounds tested, there was a significant increase of cleaved caspase-3 over time compared to untreated control cells (p = 0.0003 for SAHA-, p = 0.0198 for PXD101- and p = 0.0014 for LBH-589-treated cells after 72 h, see **Table 5**). At 72 hours, cleaved caspase-3 levels were 54.5 ± 7.4% (mean ± SD) in SAHA-treated cells and 63.1 ± 13.2% in LBH-589-treated cells, indicating apoptotic induction in these cells (**Table 5**) (2, 236). However, cleaved caspase-3 levels were lower in PXD101-treated cells (8.2 ± 3.4%) (**Table 5, Figure 10D**) (2). **Figure 10E** illustrates, by Western Blot analysis, SAHA- and LBH-589-induced cleavage of PARP in MUG-Chor1 cells, which is indicative of apoptosis (237). PXD101 treatment resulted in subtotal PARP cleavage (**Figure 10E**) (2).

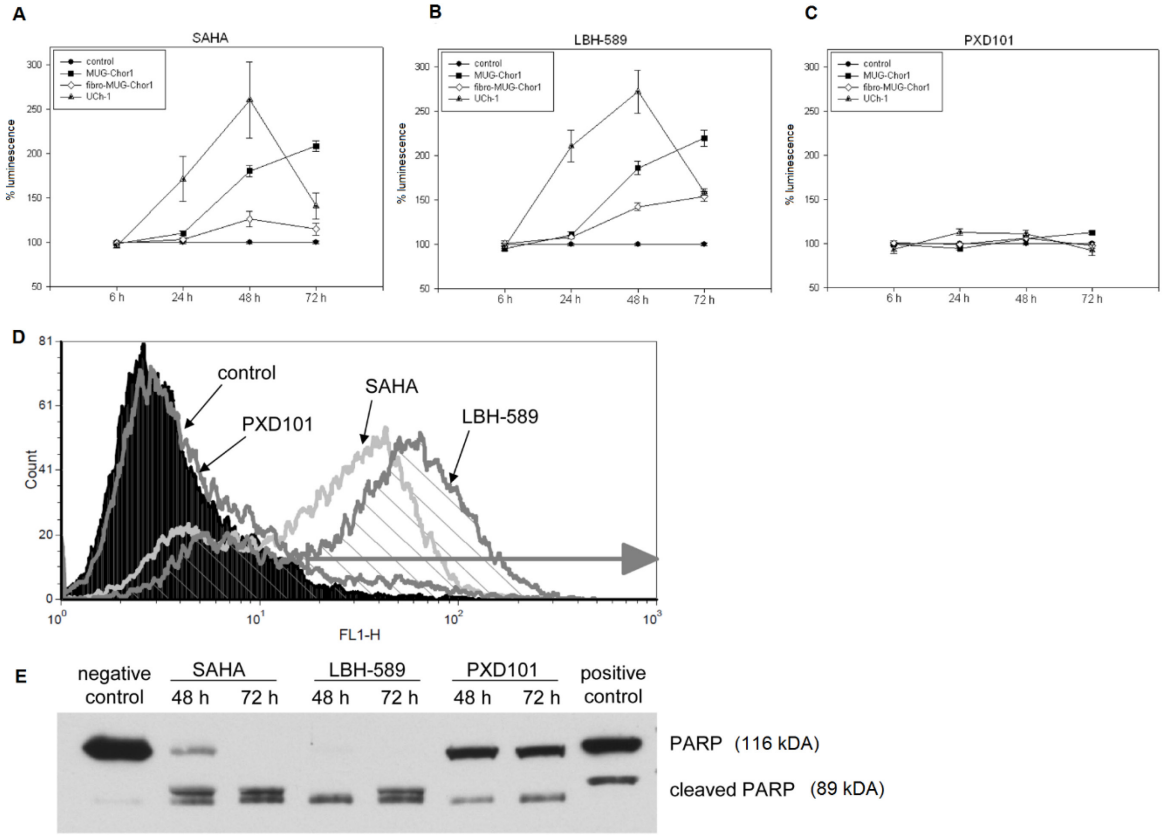

Figure 10. HDAC-inhibitor induced apoptosis.
Adapted from Scheipl *et al.* (2013) (2). The HDAC inhibitors SAHA and LBH-589 induced apoptosis in chordoma cell lines (2). Treatment with SAHA **(A)** and LBH-589 **(B)**, but not PXD101 **(C)** resulted in induction of caspase 3/7, as measured by the Caspase-Glo® 3/7 Assay (2). **(D)** Cleaved caspase-3 levels increased after treatment with SAHA and LBH-589, but not PXD101. **(E)** SAHA and LBH-589 treatment led to cleavage of PARP, which remained subtotal after PXD101 treatment (2).

Table 5. Statistical analysis of the cleaved caspase-3 apoptosis assay. Adapted from Scheipl *et al.* (2013) (2).

	Control	SAHA	PXD101	LBH-589
24 h	2.0 ± 0.9	4.9 ± 2.0, *p=0.0312*	2.7 ± 0.4	3.7 ± 1.1, *p=0.0269*
48 h	2.42 ± 1.1	25.0 ± 5.1, *p=0.0013*	5.2 ± 0.5	30.8 ± 0.9, *p=6.21E-09*
72 h	2.7 ± 1.5	54.5 ± 7.4, *p=0.0003*	8.2 ± 3.3, *p=0.0198*	63.1 ± 13.1, *p=0.0014*

Footnote to Table 5. MUG-Chor1 cells were treated with SAHA, PXD101 and LBH-589 for 24, 48 and 72 h, and cleaved caspase-3 was measured by flow cytometry. Treated groups were compared to untreated controls (n=3, mean ± SD) (2).

The HDAC Inhibitors SAHA and LBH-589 Cause Cell Cycle Arrest in MUG-Chor1

We next investigated the effects of HDAC inhibitors on the cell cycle (2). For that purpose, MUG-Chor1 cells were treated with the IC_{50} concentrations of SAHA, LBH-589 and PXD101, and the effects were compared to untreated controls (n=3) (**Figure 11, Table 6**) (2). Results are displayed in **Table 6** and illustrated in **Figure 11** (2). The cumulative findings indicated that treatment with SAHA (**Figure 11B**) and LBH-589 (**Figure 11D**) decreased the number of cells in the G1 phase and increased the number of cells in the G2/M phase after 48 and 72 hours, thus showing an arrest of cells in the G2/M phase (**Table 6**) (2). In line with the results obtained from apoptotic assays (see previous paragraph), a subG1 peak (which is indicative of apoptosis) was observed in cells treated with SAHA and LBH-589, and less distinctly in cells treated with PXD101 (**Figure 11, Table 6**) (2).

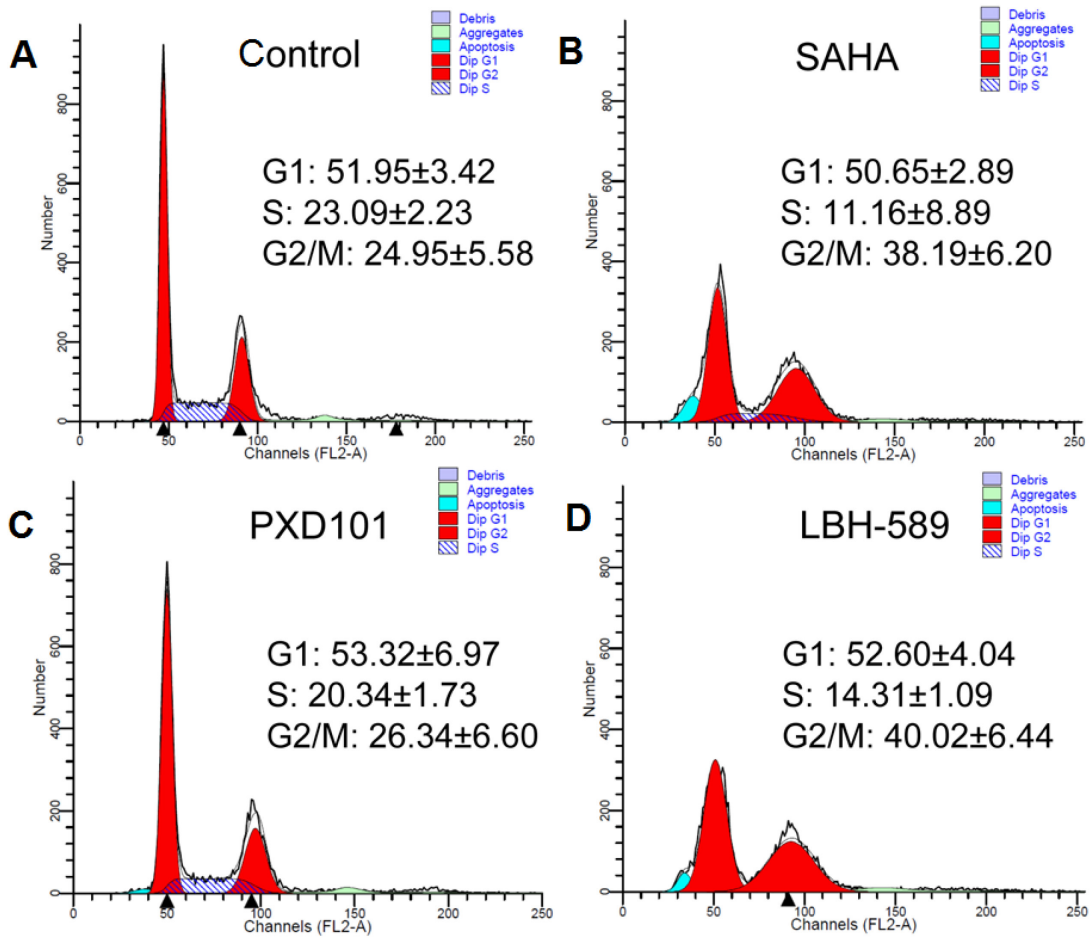

Figure 11. Influence of HDAC inhibitors on the cell cycle distribution in MUG-Chor1 cells.
Adapted from Scheipl *et al.* (2013) (2). **(A)** Untreated cells served as controls. **(B-D)** MUG-Chor1 cells were treated with the HDAC inhibitors SAHA, PXD101 and LBH-589

and analysed by flow cytometry. The reported values represent the percentage of cells in the G1, S and G2/M phases (mean ± SD) (2). A subG1 peak (coloured in turquoise) indicates apoptosis (B, D > C).

Table 6. Cell cycle distribution. Adapted from Scheipl *et al.* (2013) (2).

24 h	Control	SAHA	PXD101	LBH-589
G1	46.86 ± 5.87	48.65 ± 1.98	48.09 ± 5.22	49.63 ± 4.46
S	27.25 ± 3.32	11.01 ± 1.55	15.92 ± 0.94	9.23 ± 2.79
G2/M	25.90 ± 7.35	40.34 ± 0.43	35.99 ± 4.58	41.14 ± 4.30
subG1	1.64 ± 0.45	4.59 ± 4.43	1.34 ± 1.21	1.22 ± 1.11
48 h	**Control**	**SAHA**	**PXD101**	**LBH-589**
G1	50.77 ± 4.23	43.73 ± 6.72	58.71 ± 7.48	46.53 ± 3.64
S	26.18 ± 2.28	20.69 ± 2.63	15.53 ± 3.50	16.93 ± 5.60
G2/M	23.05 ± 5.15	35.58 ± 8.98	25.77 ± 4.70	36.55 ± 7.79
subG1	0.46 ± 0.09	12.75 ± 2.14	1.52 ± 1.05	10.78 ± 2.21
72 h	**Control**	**SAHA**	**PXD101**	**LBH-589**
G1	51.95 ± 3.42	50.65 ± 2.89	53.32 ± 6.97	52.60 ± 4.04
S	23.10 ± 2.23	11.16 ± 8.89	20.34 ± 1.73	14.32 ± 1.10
G2/M	24.95 ± 5.59	38.19 ± 6.20	26.34 ± 6.60	40.02 ± 6.44
subG1	0.52 ± 0.31	12.96 ± 7.29	1.47 ± 0.21	14.03 ± 8.45

Footnote to Table 6. MUG-Chor1 cells lines after 24, 48, and 72 h of exposure to the HDAC inhibitors SAHA, PXD101 and LBH-589 (n=3, mean ± SD) (2).

Establishment of a New Chordoma Cell Line, U-CH7

U-CH7 was established from tumour tissue obtained from a patient at Royal National Orthopaedic Hospital Stanmore, UK (RNOH) (11). Samples were acquired from a primary sacral chordoma (90 x 75 x 60 mm) of a 33-year-old Caucasian male after partial sacrectomy in September 2011 (11), which was followed by adjuvant radiotherapy (11). Histological diagnosis revealed conventional chordoma not otherwise specified (NOS) (11). The patient was alive with no evidence of relapse after 50 months of follow-up (11). The resected tumour tissue was submitted to our collaborator, Dr. Silke Brüderlein, Ulm, Germany, for establishment of the primary cultures, according to her previously established and reported methods (11, 223, 224). When the culture had reached a steady state containing approximately 30–40% of physaliferous cells, it was returned to the UCL

Cancer Institute, London, UK (11). Throughout the procedure, cells were cultured in 4:1 Iscove's Modified Dulbecco's Medium (IMDM) (Gibco, Paisley, UK): RPMI 1640 (Gibco) with 10% FBS (Life Technologies, Inchinnan, UK) and 1% Pen/Strep (Gibco) (11). The chordoma cell culture was successfully passaged 55 times over a 36-month period, with regular mycoplasma testings remaining negative (11). STR analysis (DNA Diagnostic Center, London, UK) verified the origin of U-CH7 from the tumour from which it was originally derived (**Table 7, Suppl. Table 1**) (11). Chordoma Foundation forwarded the newly established cell line for validation to Vala Sciences, San Diego, CA, USA. **Figure 13** was taken at the UCL Cancer Institute and shows the U-CH7 cell morphology. Detailed validation data are available from the Chordoma Foundation (11). In line with the typical features of chordoma, U-CH7 cells were shown to express high levels of *T (brachyury)* **(Figure 12)**, and this new cell line is presently available as a bioresource from the American Type Culture Collection (ATCC) (11).

Table 7. STR analysis of U-CH7 and its parental tumour. Adapted from Scheipl *et al.* (2016) (11).

STR-Analysis	U-CH7 Cell Line UCL		U-CH7 Primary Tumour	
Marker	**Allele 1**	**Allele 2**	**Allele 1**	**Allele 2**
D3S1358	17		16	17
TH01	7		7	
D21S11	30	33.2	30	33.2
D18S51	16		16	18
Penta E	12	15	12	15
D5S818	12	13	12	13
D13S137	10		10	12
D7S820	10	11	10	11
D16S539	10	12	10	12
CSF1PO	12		12	
Penta D	12	13	12	13
AMEL	X	Y	X	Y
vWA	16	17	16	17
D8S1179	14	16	14	16
TPOX	8	11	8	11
FGA	22	24	22	24
D19S433	13	14	13	14
D2S1338	23		23	

Footnote to Table 7. STR results for the U-CH7 cell line and the primary chordoma from which this cell line derived.

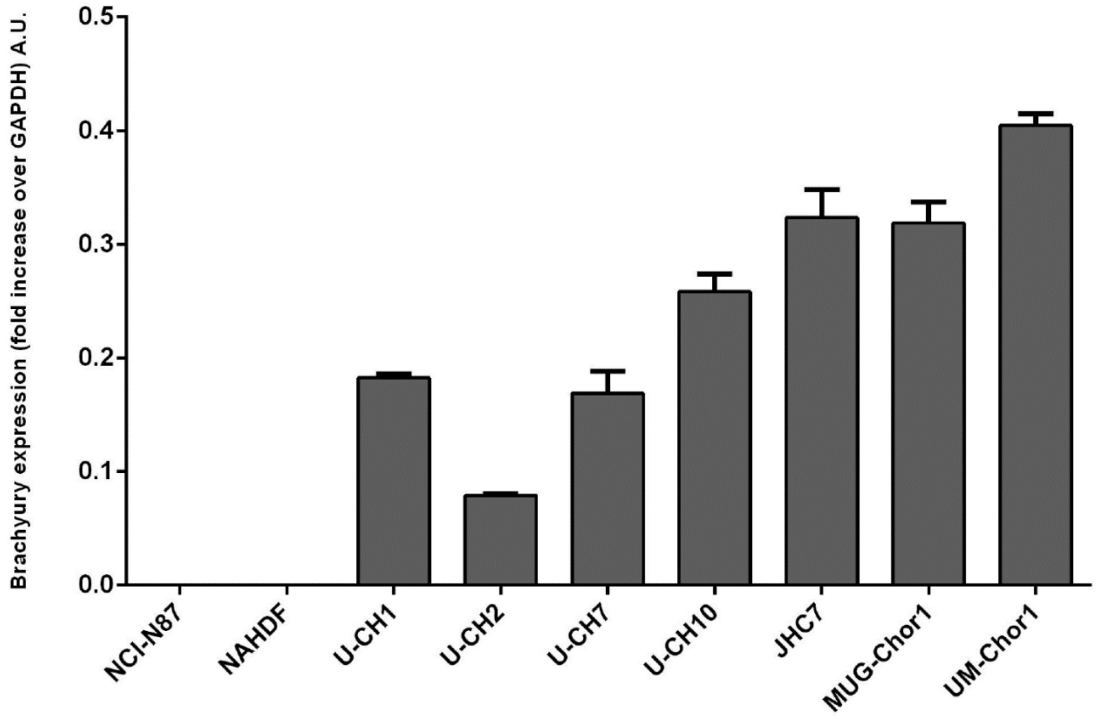

Figure 12. T (brachyury) expression of the chordoma cell line panel.
Adapted from Scheipl *et al.* (2016) (11). *T* (brachyury) expression of the chordoma cell line panel, as determined by real time quantitative PCR. Real-time quantitative PCR was conducted as described by Nelson et al. 2012 (9, 11). The panel includes the newly established human chordoma cell line U-CH7 (11). NAHDF: normal adult human dermal fibroblasts. All seven chordoma cell lines, but not the controls (NAHDF, NCI-N87), expressed high levels of T (11).

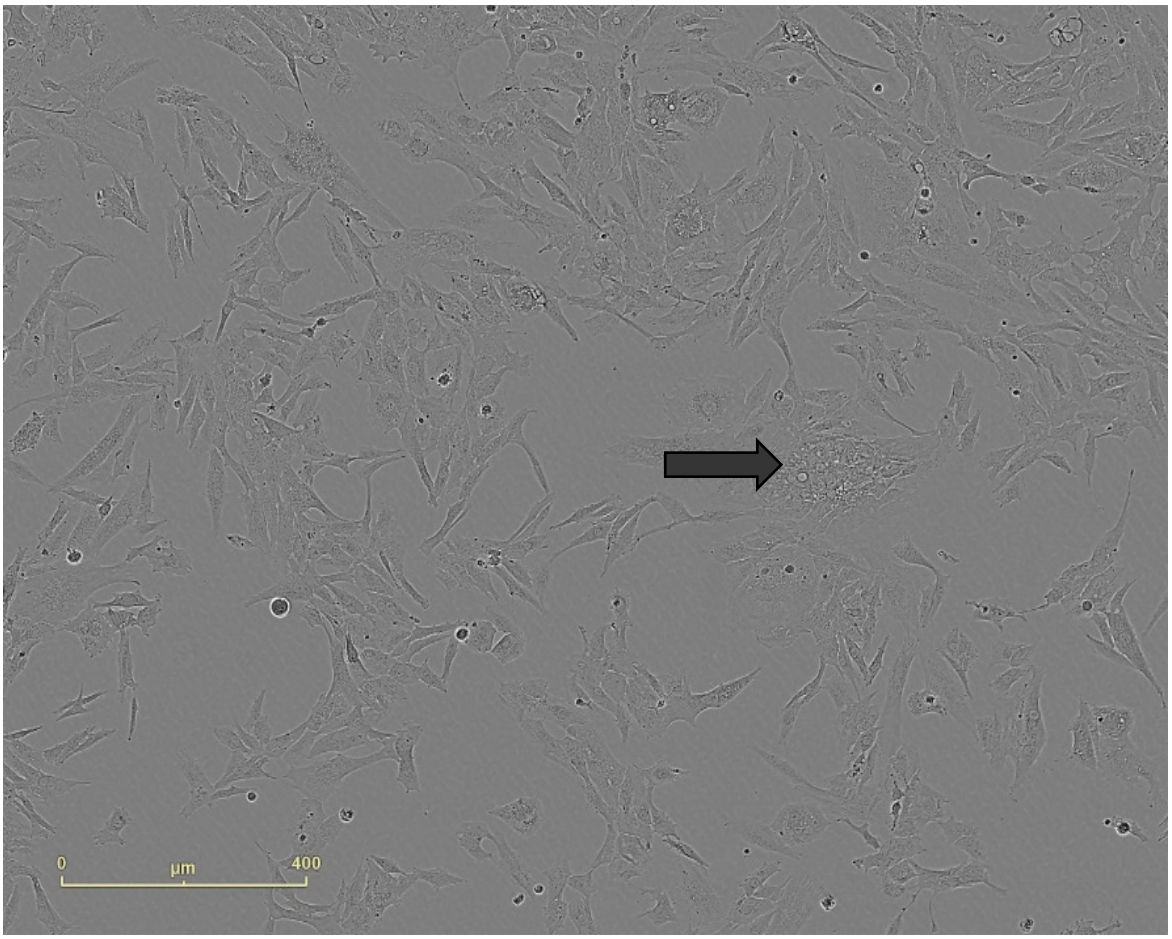

Figure 13. Morphology of U-CH7 cells.
The image was taken at a 20X magnification. The arrow indicates a physaliferous cell, which is a characteristic feature of chordoma cell lines.

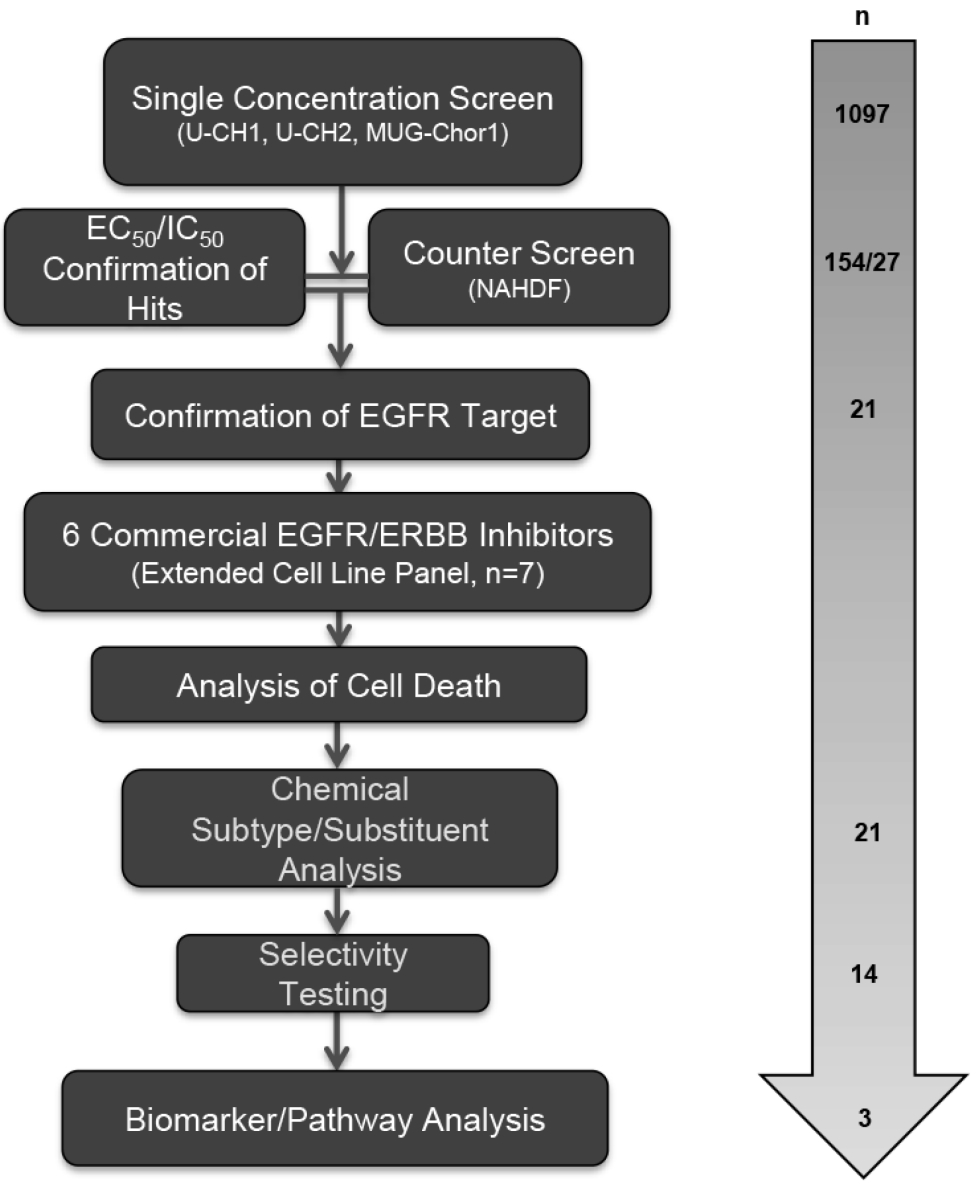

Figure 14. Screening cascade.
Adapted from Scheipl *et al.* (2016) (11). Outline of the screening cascade of the focused compound screen. On the right-hand side, n indicates the numbers of compounds relevant for each step of the cascade.

EGFR/ERBB Family Inhibitors Selectively Targeted Chordoma Cells in a Focused Compound Screen

Of the 1,097 compounds that we screened at a single concentration of 1µM in three human chordoma cell lines (U-CH1, U-CH2, MUG-Chor1) (**Suppl. Table 2**), a subset of 154

compounds met our hit selection criteria (**Figure 14, Suppl. Table 2**) (11). This represents an overall hit rate of 14% (154/1,097) (**Table 8**). The hit rates for the individual libraries can be taken from **Table 8** (11). These 154 hit compounds were tested in a 10-point EC_{50} format in three human chordoma cell lines (U-CH1, U-CH2, MUG-Chor1) and in human dermal fibroblasts (**Figure 14**). Twenty-seven of these 154 compounds selectively inhibited chordoma cell growth but did not target normal dermal fibroblasts (**Figure 14, Table 9**) (11). Of these 27 chordoma-selective compounds, 21 (78%) were EGFR/ERBB family inhibitors (**Figure 14, Table 9**) (11). Five EGFR/ERBB family inhibitors also co-targeted B-Raf proto-oncogene, serine/threonine kinase (BRAF) **(Table 9**) (11). We obtained reproducible results across all cell lines when we tested two different batches of compounds (data not shown) (11). These 21 EGFR/ERBB family inhibitors displayed maximum effects and the highest potency in U-CH1, whereas they exerted practically no activity in U-CH2 (**Table 9**) (11).

Table 8. Hit rates across all compound libraries. Adapted from Scheipl *et al.* (2016) (11).

Library	Library Compounds	Library Hits	Library Hit Rate
ID	**n**	**n**	**%**
Anticancer	43	23	53.49
Calbiochem	160	23	14.38
GSK PKIS	365	37	10.14
GSK PKIS2	521	71	13.63
AKR1B10	8	0	0.00
All Libraries	**1097**	**154**	**14.04**

Footnote to Table 8. Inhibitory hit rates across all compound libraries that were included in the single-concentration focused compound screen (11).

Table 9. Chordoma-selective hit compounds (n=27). Adapted from Scheipl *et al.* (2016) (11).

Cpd	Library	Target	Drug Potency (Geomean EC_{50} [µM])					Compound Selectivity Compared to Fibroblasts				Maximum Percentage Inhibition at Highest Drug Concentration				
ID			NAHDF	U-CH1	U-CH2	MUG-Chor1	U-CH7	U-CH1	U-CH2	MUG-Chor1	U-CH7	NAHDF	U-CH1	U-CH2	MUG-Chor1	U-CH7
AG 1478	Calbiochem	EGFR	20.744	PNQ (SS)	18.817	0.083	NT	SNC	1	248	NT	10	76	52	64	NT
Compound 56	Calbiochem	EGFR	22.794	0.566	20.000	0.010	0.216	40	1	2349	105	77	86	27	62	50
CRT0103079	Calbiochem	EGFR/ERBB2/4	12.912	0.179	16.695	0.024	0.775	72	1	548	17	96	79	38	64	61
PD174780	Calbiochem	EGFR	30.000	0.209	19.663	0.101	0.270	143	2	296	111	29	80	35	55	49
PD174265	Calbiochem	EGFR	30.000	0.384	13.248	0.149	0.332	78	2	201	90	11	75	43	70	71
GDC-0941	Anticancer	*PIK3CA Class 1A*	3.987	2.676	3.630	3.573	NT	1	1	1	NT	85	93	79	71	NT
GW461104A	GSK PKIS1	EGFR/ERBB2	17.082	2.023	30.000	2.057	1.912	8	1	8	9	85	80	32	58	51
GW410563A	GSK PKIS1	*VEGFR-2*	22.028	1.906	19.392	4.406	NT	12	1	5	NT	68	80	67	47	NT
GW282449A	GSK PKIS1	EGFR/ERBB2	29.295	0.800	20.883	1.796	1.360	37	1	16	22	55	65	34	45	58
GW576609A	GSK PKIS1	EGFR/ERBB2	12.099	4.060	23.038	Biphasic	NT	3	1	SNC	NT	85	77	38	49	NT
GW583373A	GSK PKIS1	EGFR/ERBB2	10.958	1.391	17.931	30.000	0.476	8	1	1	23	62	71	44	32	44
GW616030X	GSK PKIS1	EGFR/ERBB2	19.400	0.538	30.000	1.624	0.454	36	1	12	43	53	69	27	39	55
GW680191X	GSK PKIS1	EGFR/ERBB2	30.000	1.259	17.833	0.369	3.149	24	2	81	10	41	86	61	45	61
GI230329A	GSK PKIS2	EGFR	16.871	Biphasic	20.000	0.188	0.371	SNC	1	90	45	96	94	40	41	71
GSK1307810A	GSK PKIS2	*AKT1*, ROCK1, PKCα	13.652	16.442	1.847	5.683	NT	1	7	2	NT	100	61	64	30	NT
GSK1660437A	GSK PKIS2	*BRAF,* Src1, LCK, LYN, BTK, ALK5, ERBB4, ActR2	3.024	15.407	1.001	18.443	NT	1	3	1	NT	78	45	58	56	NT
GSK198271A	GSK PKIS2	ERBBs, BRAF	3.702	0.337	3.089	0.217	0.335	11	1	17	11	48	78	43	50	58
GSK299495A	GSK PKIS2	Src, ERBBs, BRAF	20.000	1.485	3.895	6.538	NT	13	5	3	NT	38	79	49	38	NT
GSK326180A	GSK PKIS2	ERBBs, BRAF	20.000	0.891	0.431	2.956	1.201	22	46	7	17	35	74	44	48	69
GSK357952A	GSK PKIS2	Src, ERBBs, BRAF	20.000	1.987	6.191	20.000	NT	10	3	1	NT	17	61	40	31	NT
GSK361061A	GSK PKIS2	BRAF, ERBB4	22.134	1.512	22.894	11.257	NT	15	1	2	NT	17	56	28	33	NT
GW569716A	GSK PKIS2	ERBB2/EGFR	8.767	4.744	13.484	0.592	2.197	2	1	15	4	99	81	71	46	47
GW582764A	GSK PKIS2	ERBB2/EGFR	21.096	1.717	22.894	22.134	NT	12	1	1	NT	78	54	20	25	NT
GW583340C	GSK PKIS2	ERBB2/ EGFR	15.130	1.060	13.083	20.000	7.093	14	1	1	2	55	66	40	34	39
GW876731X	GSK PKIS2	*ALK5,* ROCK1	8.881	10.922	0.577	12.763	NT	1	15	NT	NT	83	94	74	39	NT
SKF-97184	GSK PKIS2	Unknown	20.000	19.170	20.000	6.369	NT	1	1	3	NT	9	55	24	42	NT
GW582764A	GSK PKIS2	ERBB2/EGFR	21.096	1.717	22.894	22.134	NT	12	1	1	NT	78	54	20	25	NT

nM µM 0% 100%

Scheipl S., 2016

Footnote to Table 9. Table xy displays hit compounds (n=27) that exerted a chordoma-selective inhibitory effect compared to normal dermal fibroblasts (11). In cases of low percentage inhibition where no plateau was observed (indicating inactivity of these compounds), EC_{50} values were extrapolated (Geomean $EC_{50} \geq$ 30µM) (11). NAHDF (normal adult human dermal fibroblasts) served as controls. NT: Not tested. PNQ (SS): Potency not quantified due to a small activity span. Biphasic: The potency was not quantified due to a biphasic curve profile (11). SNC: Selectivity not calculated (11). The key targets of the non-EGFR hit compounds are indicated in italics (11).

The non-EGFR hit compounds (n=6) targeted the activin receptor-like kinase 5 (ALK5), PI3K, BRAF and protein kinase B alpha (AKT1) (11, 238-241). One of these non-EGFR hit compounds was pazopanib (Votrient®, GSK), which is an angiogenesis inhibitor targeting the VEGFR-2, the PDGFR and c-Kit. It has been FDA-approved for renal cell carcinoma and soft tissue sarcomas (11, 157, 242). These key targets in bold print in **Table 10**. The target for one of the compounds is still unknown (11). When we looked at a potential enrichment of these targets in signalling pathways (243), VEGFR-1/2 signalling was identified as the pathway covering the majority of the non-EGFR target genes (**Suppl. Table 2**) (11).

Table 10. Target genes of non-EGFR hit compounds (n=6). These genes were used in the enrichment in pathways analysis. Adapted from Scheipl *et al.* (2016) (11).

Entrez Gene ID	Gene Symbol	Gene Description	Aliases	Compound
673	**BRAF**	v-raf murine sarcoma viral oncogene homolog B1		**GSK1660437A**
3932	LCK	lymphocyte-specific protein tyrosine kinase		GSK1660437A
4067	LYN	v-yes-1 Yamaguchi sarcoma viral related oncogene homolog		GSK1660437A
6714	SRC	v-src sarcoma (Schmidt-Ruppin A-2) viral oncogene homolog (avian)	Src1	GSK1660437A
10097	ACTR2	Activin A Receptor, Type IIB	ActR2	GSK1660437A
7046	**TGFBR1**	transforming growth factor, beta receptor 1	ALK5	GSK1660437A, GW876731X
2066	ERBB4	V-Erb-B2 Avian Erythroblastic Leukemia Viral Oncogene Homolog 4	HER4	GSK1660437A
695	BTK	Bruton Agammaglobulinemia Tyrosine Kinase	AGMX1	GSK1660437A
207	**AKT1**	v-akt murine thymoma viral oncogene homolog 1	AKT	GSK1307810A
5566	PRKACA	protein kinase, cAMP-dependent, catalytic, alpha	PKA; PKC-Alpha	GSK1307810A
6093	ROCK1	Rho-associated, coiled-coil containing protein kinase 1		GSK1307810A, GW876731X
5290	**PIK3CA**	phosphoinositide-3-kinase, catalytic, alpha polypeptide		GDC-0941
3791	**KDR**	kinase insert domain receptor (a type III receptor tyrosine kinase)	VEGFR-2	GW410563A

Footnote to Table 10. This table displays targets of the non-EGFR hit compounds, as stated in the literature (11, 238-241). **The compounds' key targets are indicated in bold** (11).

Chemical Substituents Correlated with the Activity of EGFR/ERBB Family Inhibitors in Chordoma Cell Lines

GSK selected 21 EGFR/ERBB family inhibitors for structural analysis, based on the phenotypic (viability) potencies of these drugs/compounds (**Table 11**) (11). GSK chemists found that these compounds consisted of two basic chemotypes, pyrimidines and quinazolines (11). The quinazolines were sub-divided into two subgroups, one of which was characterised by large substituents on the aniline group in the 4-position of the quinazoline ring (hereafter referred to as "quinazolines large"). The other subgroup was characterised by small substituents on the aniline ring in that position ("quinazolines small") (11). The latter group included erlotinib, gefitinib and sapitinib, and this group showed a trend towards greater potency in chordoma cell lines compared to "quinazoline large" compounds (**Table 11**) (11). Neither subtype showed any relevant activity on U-CH2 (11). When a selection of these compounds (n=14) was biochemically assessed for their effects on EGFR, ERBB2 and ERBB4 (for ERBB3, no test kit was available), it became apparent that the size of the substituent group on the aniline ring, as well as the structure of the tail portion of the molecule that extends towards the solvent front of the kinase, had an impact on a compound's potencies on these three targets (**Table 12**) (11). **Figure 15** shows the varying effects of a selection of these EGFR hit compounds on phospho-EGFR and EGFR on the three human chordoma cell lines (U-CH1, U-CH2 and MUG-Chor1), as studied by Western blot analysis (**Figure 15**) (11). Western blots for erlotinib, gefitinib and sapitinib are provided in the **Figures 16, 17, 18** and **19**.

Table 11. Chemical substituent trend analysis of selected EGFR/ERBB inhibitors (n=21). Adapted from Scheipl *et al.* (2016) (11).

Cpd ID	Library	Target	Chemical Substituent	Drug Potency (Geomean EC_{50} [µM])				
				NAHDF	U-CH1	U-CH2	MUG-Chor1	U-CH7
GSK198271A	GSK PKIS2	ERBB family, BRAF	Pyrimidine	3.702	0.337	3.089	0.217	0.335
GSK326180A	GSK PKIS2	ERBB family, BRAF		20.000	0.891	0.431	2.956	1.201
Lapatinib	Anticancer	EGFR	Quinazoline large	4.542	6.163	14.697	1.527	6.225
GW282449A	GSK PKIS1	EGFR/ERBB2		29.295	0.800	20.883	1.796	1.360
GW583373A	GSK PKIS1	EGFR/ERBB2		10.958	1.391	17.931	30.000	0.476
GW616030X	GSK PKIS1	EGFR/ERBB2		19.400	0.538	30.000	1.624	0.454
GW569716A	GSK PKIS2	ERBB2/EGFR		8.767	4.744	13.484	0.592	2.197
GW582764A	GSK PKIS2	ERBB2/EGFR		21.096	1.717	22.894	22.134	NT
GW583340C	GSK PKIS2	ERBB2/ EGFR		15.130	1.060	13.083	20.000	7.093
Compound 56	Calbiochem	EGFR	Quinazoline small	22.794	0.566	20.000	0.010	0.216
CRT0103079	Calbiochem	EGFR/ERBB2/ERBB4		12.912	0.179	16.695	0.024	0.775
PD174780	Calbiochem	EGFR		30.000	0.209	19.663	0.101	0.270
PD174265	Calbiochem	EGFR		30.000	0.384	13.248	0.149	0.332
Canertinib	Selleckchem	EGFR/ERBB2		5.186	0.125	9.302	CS	0.248
Erlotinib	Selleckchem	EGFR		14.755	0.396	10.866	0.299	0.861
Gefitinib	Selleckchem	EGFR		18.669	0.226	16.983	0.150	0.410
GW461104A	GSK PKIS1	EGFR/ERBB2		17.082	2.023	30.000	2.057	1.912
GW680191X	GSK PKIS1	EGFR/ERBB2		30.000	1.259	17.833	0.369	3.149
GI230329A	GSK PKIS2	EGFR		16.871	CS	20.000	0.188	0.371
Sapitinib (AZD 8931)	Selleckchem	EGFR/ERBB2		20.003	0.054	10.160	0.015	0.046
Afatinib	Selleckchem	EGFR/ERBB2		5.448	CS	9.160	CS	10.756

nM  µM

Footnote to Table 11. Quinazoline large: large substituent on the aniline ring in the 4 position of the quinazoline ring system (11). Quinazoline small: small substituent on the aniline ring in the 4-position of the quinazoline ring system (11). NAHDF (normal adult human dermal fibroblasts) served as controls. In cases of low percentage inhibition where no plateau was observed (indicating inactivity of these compounds),

EC_{50} values were extrapolated (Geomean $EC_{50} \geq$ 30µM) (11). CS: due to a cytostatic profile no potency was calculated. NT: Not tested. In this analysis, the irreversible EGFR TKI poziotinib (Selleckchem) was replaced by canertinib (Selleckchem) (11).

Table 12. Biochemical selectivity data. Data for EGFR, ERBB2, and ERBB4 of selected EGFR/ERBB inhibitors (n=14). Adapted from Scheipl *et al.* (2016) (11).

Cpd ID	Parent Compound	Chemical Substituent	Biochemical Potency		
			EGFR IC_{50} [µM]	ERBB2 IC_{50} [µM]	ERBB4 IC_{50} [µM]
GW282449A	GW282449	Quinazoline large	0.0011	0.070	0.00051
GW583373A	GW583373		0.0011	0.039	0.0082
GW582764A	GW582764		0.0047	0.907	0.044
GW616030X	GW616030		0.0014	0.03	0.014
GW583340C	GW583340		0.0097	0.082	0.0235
GW569716A	GW569716		0.0256	0.079	0.00383
GW582764A	GW582764		0.0407	0.442	0.0859
GW459135A (Erlotinib)	GW459135	Quinazoline small	0.00022	0.474	0.317
GI261607A	GI261607		0.00035	0.062	0.105
GW461104A	GW461104		0.0005	0.039	0.197
GW459125X (Gefitinib)	GW459125		0.0024	0.750	0.322
GW680191X	GW680191		0.00002	0.0064	0.105
GI230329A	GI230329		0.00018	0.0273	0.0558
GSK3413714A (Sapitinib)	GSK3413714		0.00051	0.0089	0.011

Footnote to Table 12. ERBB3 was not studied as no test kit was available (11). Quinazoline large: large substituent on aniline in 4-position of the quinazoline ring system (11). Quinazoline small: small substituent on aniline in 4-position of the quinazoline ring system (11).

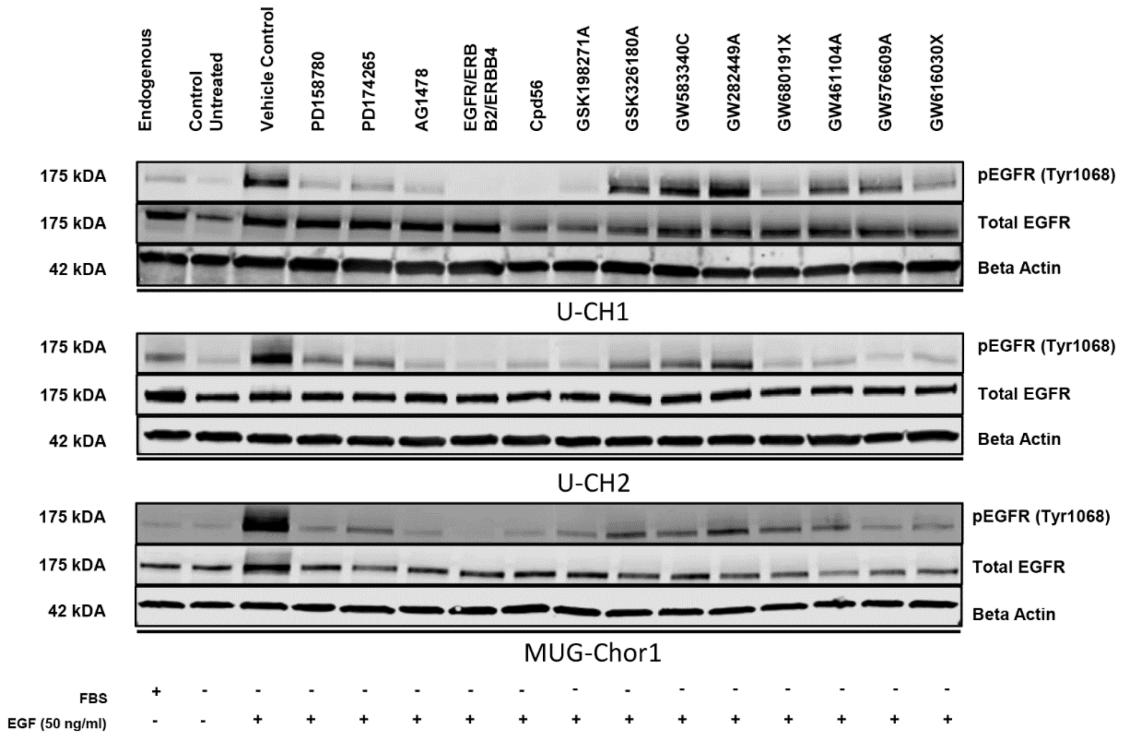

Figure 15. Effects of hit compounds on phospho-EGFR and EGFR levels.
Adapted from Scheipl *et al.* (2016) (11). Of the 21 EGFR compounds that selectively targeted chordoma cells in our single concentration screen, the impact of 13 of these was studied by Western blots on 3 chordoma cell lines (U-CH1, U-CH2, MUG-Chor1) (11). These 13 compounds comprised a selection of hit compounds across the libraries and chemical structures tested (listed in **Tables 9** and **11**) (11). Eight compounds were hit compounds from the GSK PKIS libraries: two of these were Pyrimidine compounds (GSK198271A, GSK326180A), three were compounds that had large substituents on the aniline ring in the 4-position of the quinazoline ring system (GW583340C, GW282449A and GW616030X), two had small substituents in that position (GW680191X, GW461104A) and one compound had an unknown target (GW576609A). Five compounds were Calbiochem compounds: AG1478, Compound 56, the EGFR/ERBB2/ERBB4 inhibitor CRT0103079, PD174780 and PD174265. The cells were serum-starved overnight and treated with EGFR inhibitors (250 nM) for 4 h before they were exposed to EGF (50 ng/ml) for 15 min (11). Endogenous controls (non-serum-starved, non-EGF-spiked), untreated controls (serum-starved, non-EGF-spiked) and vehicle controls (serum-starved, treated with 2.5% DMSO, EGF-spiked) were included in this experiment (11).

Commercially Available EGFR/ERBB Family Inhibitors Showed High Activity in an Extended Chordoma Cell Line Panel

The majority of the compounds investigated thus far have not yet been approved by the FDA but are still under development and/or were created for test purposes only (11). We thus continued our studies on a set of six commercially available EGFR/ERBB family inhibitors, which were approved by the FDA and/or had been used in clinical trials (11,

122, 229, 231). These inhibitors included four reversible drugs (erlotinib, sapitinib, gefitinib, lapatinib) and two irreversible drugs (afatinib, poziotinib), and they were studied in an extended panel consisting of seven human chordoma cell lines (11) (**Table 13**). This panel included those three cell lines that had previously been studied (U-CH1, U-CH2, MUG-Chor1) (11). Human dermal fibroblasts (ATCC® PCS-201-012™) and the gastric cancer cell line NCI-N87 served as negative and positive controls, respectively (11) (**Table 13**). We observed that four of these cell lines (U-CH1, U-CH7, UM-Chor1 and MUG-Chor1) were responsive to EGFR inhibition, as indicated by EC_{50}s being generally below 1 μM (11) (**Table 13**). In contrast, U-CH2, U-CH10 and JHC7 proved largely resistant (11) (**Table 13**). Three out of the four reversible agents (erlotinib, gefitinib and sapitinib), showed high potencies in the four "responsive" cell lines, with EC_{50}s in the nanomolar range (11). The fourth reversible compound, lapatinib, was potent on UM-Chor1 (EC_{50} of 314 nM and 98% MI), moderately potent on MUG-Chor1 (EC_{50} > 1 μM < 3 μM) and inactive on the other cell lines ($EC_{50} \geq 3$ μM) (**Table 13**) (11). The irreversible inhibitor, afatinib, exerted a high potency on UM-Chor1 (EC_{50} of 26 nM and 89% MI) and displayed a cytostatic profile on U-CH1 and MUG-Chor1 (11). Poziotinib showed a cytostatic profile on U-CH1, MUG-Chor1 and UM-Chor1, and neither of the two irreversible compounds was active on U-CH7 (**Table 13**) (11). In our study, the highest potencies were displayed by sapitinib, a "quinazoline small compound", which displayed nanomolar EC_{50} concentrations in the four "responsive" chordoma cell lines (11). These concentrations were comparable to those reported in NSCLC and in head and neck cancer cell models defined as sensitive to EGFR inhibition. For both cancer types, responses to sapitinib were observed in related mouse xenograft models (11, 235). The other active compounds were erlotinib and gefitinib, two drugs with FDA approval and of the "quinazoline small" chemotype (**Table 13**) (11).

Table 13. Phenotypic activities of commercially available EGFR/ERBB inhibitors. These inhibitors (n=6) were tested on an extended chordoma cell line panel. Adapted from Scheipl *et al.* (2016) (11).

Drug	Drug Potency (Geomean EC_{50} [µM])									Maximum Percentage Inhibition at Highest Drug Concentration								
ID	U-CH1	U-CH2	U-CH7	U-CH10	JHC7	MUG-Chor1	UM-Chor1	NAHDF	NCI-N87	U-CH1	U-CH2	U-CH7	U-CH10	JHC7	MUG-Chor1	UM-Chor1	NAHDF	NCI-N87
Erlotinib	0.396	10.866	0.861	30.000	30.000	0.299	0.516	14.755	2.957	66	45	61	33	36	74	71	51	84
Gefitinib	0.226	16.983	0.410	30.000	17.928	0.150	0.304	18.669	1.674	64	61	61	42	56	72	78	50	100
Lapatinib	6.163	14.697	6.225	12.285	14.336	1.527	0.314	4.542	0.027	102	73	81	100	91	95	98	80	103
Sapitinib	0.054	10.160	0.046	8.565	26.132	0.015	0.040	20.003	0.128	74	69	65	58	53	78	79	57	103
Afatinib	CS	9.160	10.756	11.913	8.937	CS	0.026	5.448	<0.005	103	100	109	94	99	102	89	85	105
Poziotinib	CS	4.900	7.495	18.439	14.008	CS	CS	3.382	<0.005	91	89	73	47	77	88	82	95	103

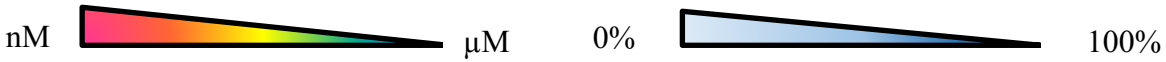

Footnote to Table 13. In cases of low percentage inhibition where no plateau was observed (indicating inactivity of these compounds), EC_{50} values were extrapolated (Geomean $EC_{50} \geq$ 30µM) (11). NAHDF (normal adult human dermal fibroblasts) and the gastric cancer cell line NCI-N87 served as positive and negative controls, respectively. CS: due to acytostatic profile no potency was calculated (11).

EGFR/ERBB Family Inhibitors Suppressed phospho-EGFR and EGFR Downstream Effectors in EGFR-sensitive Chordoma Cell Lines

In ELISA and Western Blot analysis, we observed that the three compounds that had been most potent in our phenotypic screen (sapitinib>gefitinib>erlotinib) suppressed the biomarker, phospho-EGFR, in a dose-dependent manner (11). This effect was observed for both EGFR-phosphorylation sites studied (Tyr1068 and Tyr1173), with similar results obtained for EGF-spiked/serum-starved (**Figures 16** and **17**) and non-spiked/non-starved conditions (**Figures 18** and **19**) (11). This suppression was seen in all chordoma cell lines (except U-CH10, which was not studied, as it was very slow-growing, so that sufficient protein lysate was not available), thus confirming that the drugs hit their key target (11). Also, key effectors of EGFR signalling, such as phospho-AKT (PI3K/AKT/mTOR) and phospho-ERK1/2 (Ras/Raf/MEK/ERK1/2 = MAPK/ERK1/2), were dose-dependently suppressed by the drugs, although we did not observe significant effects on phospho-STAT3 (**Figures 16, 17** and **18, 19**) (11). Sapitinib was shown to suppress phospho-EGFR and its downstream targets at lower doses compared to erlotinib or gefitinib. **Figure 20** displays the endogenous/baseline status for all markers tested (11).

EGFR/ERBB Family Inhibitors Induced Apoptosis in EGFR-sensitive Chordoma Cell Lines

The EGFR/ERBB family inhibitors induced apoptosis in a dose-dependent manner in the EGFR sensitive chordoma cell lines, resulting in a decreased cell viability from 24 hours onwards (**Figures 21** and **22**) (11). In cases where EGFR inhibitors induced a cytostatic profile (such as lapatinib in U-CH1), we observed minimal caspase 3/7 activity (~30%) in support of these phenotypic data (**Figures 21** and **22**) (11).

Sapitinib Caused a Significant Reduction in Tumour Growth in Chordoma Mouse Models

Chordoma Foundation had our most promising compound, sapitinib, tested in two chordoma mouse models via their Drug Screening Pipeline (11). These *in vivo* tests were conducted at the START laboratories in Texas, USA. One of the models studied was a xenograft derived from the human chordoma cell line, U-CH1, which had been highly responsive to EGFR inhibition in our screen (11, 220). The other model was a patient-derived chordoma xenograft model (SF8894) (234). Sapitinib caused a significant reduction tumour growth in both chordoma mouse models, as shown in **Figure 16C** and **16D**.

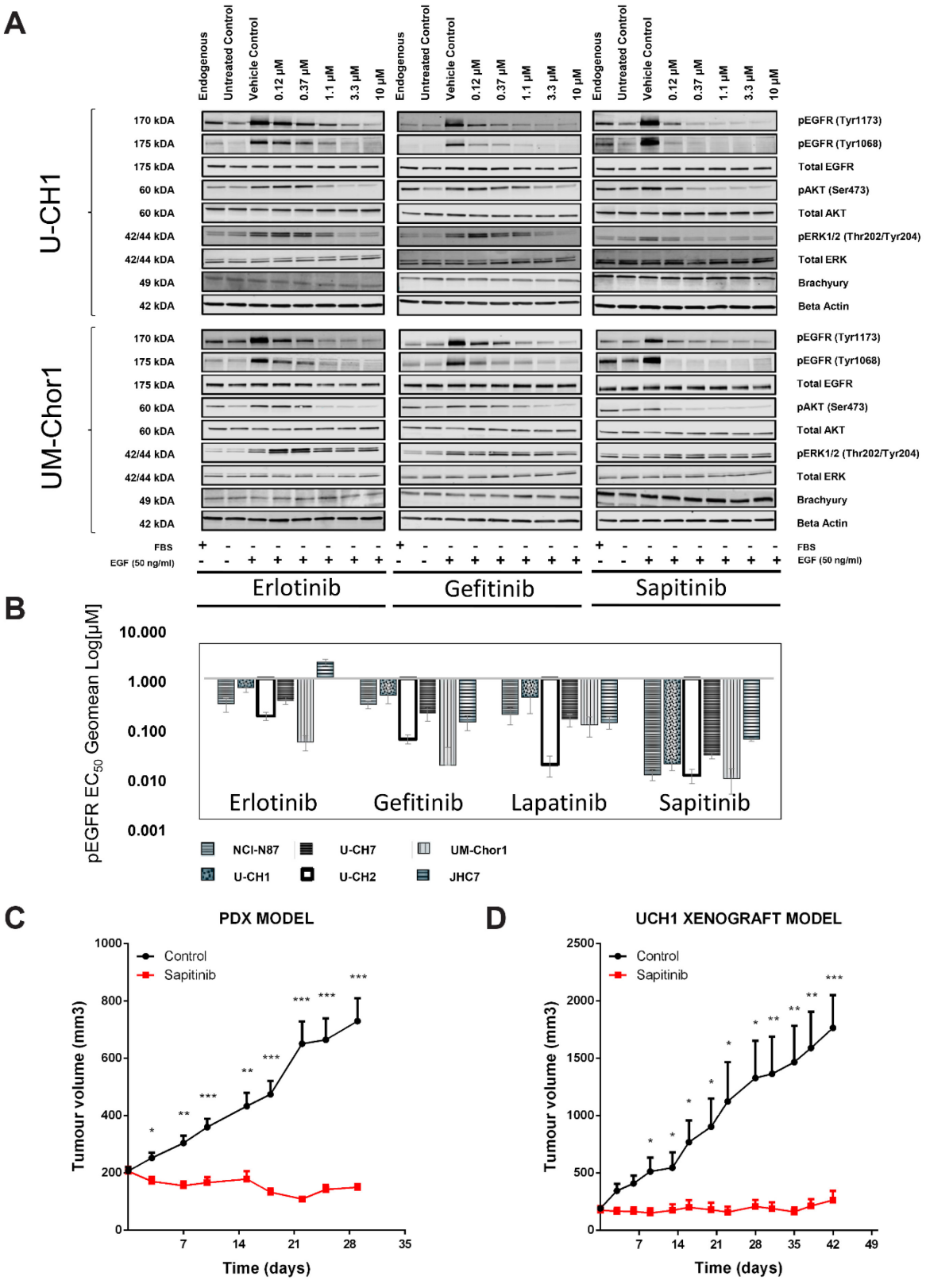

Figure 16. Western blot, ELISA, and *in vivo* studies.
Adapted from Scheipl *et al.* (2016) (11). **Western blot (A) and ELISA (B) analysis confirmed suppression of the biomarker phospho-EGFR** upon treatment with EGFR TKIs (erlotinib, gefitinib, sapitinib) in U-CH1 and UM-Chor1 (11). We serum-starved the chordoma cells overnight before we treated them with a range of concentrations of the EGFR inhibitors erlotinib, gefitinib and

sapitinib for 4 h (11). Cells were then spiked with EGF (50 ng/ml) for 15 min to accentuate the effects (11). However, similar results were obtained in non-spiked/non-starved experiments (Figures 18 and 19). We included the following controls: endogenous (non-serum-starved, non-EGF-spiked), untreated (serum-starved, non-EGF-spiked) and vehicle controls (serum-starved, treated with 2.5% DMSO, EGF-spiked) (11). Suppression of phospho-EGFR levels was studied by Western blot and by ELISA (11). The Western Blot results for the other chordoma cell lines studied (U-CH2, U-CH7, JCH7 and MUG-Chor1) are displayed in Figure 17. **(C, D)** Sapitinib (25 mg/kg twice daily oral gavage) induced a significant growth reduction in the patient-derived **xenograft SF8894 (C)** and in the **U-CH1 xenograft (D)** (* $p \leq 0.05$; ** $p \leq 0.01$; *** $p \leq 0.001$).

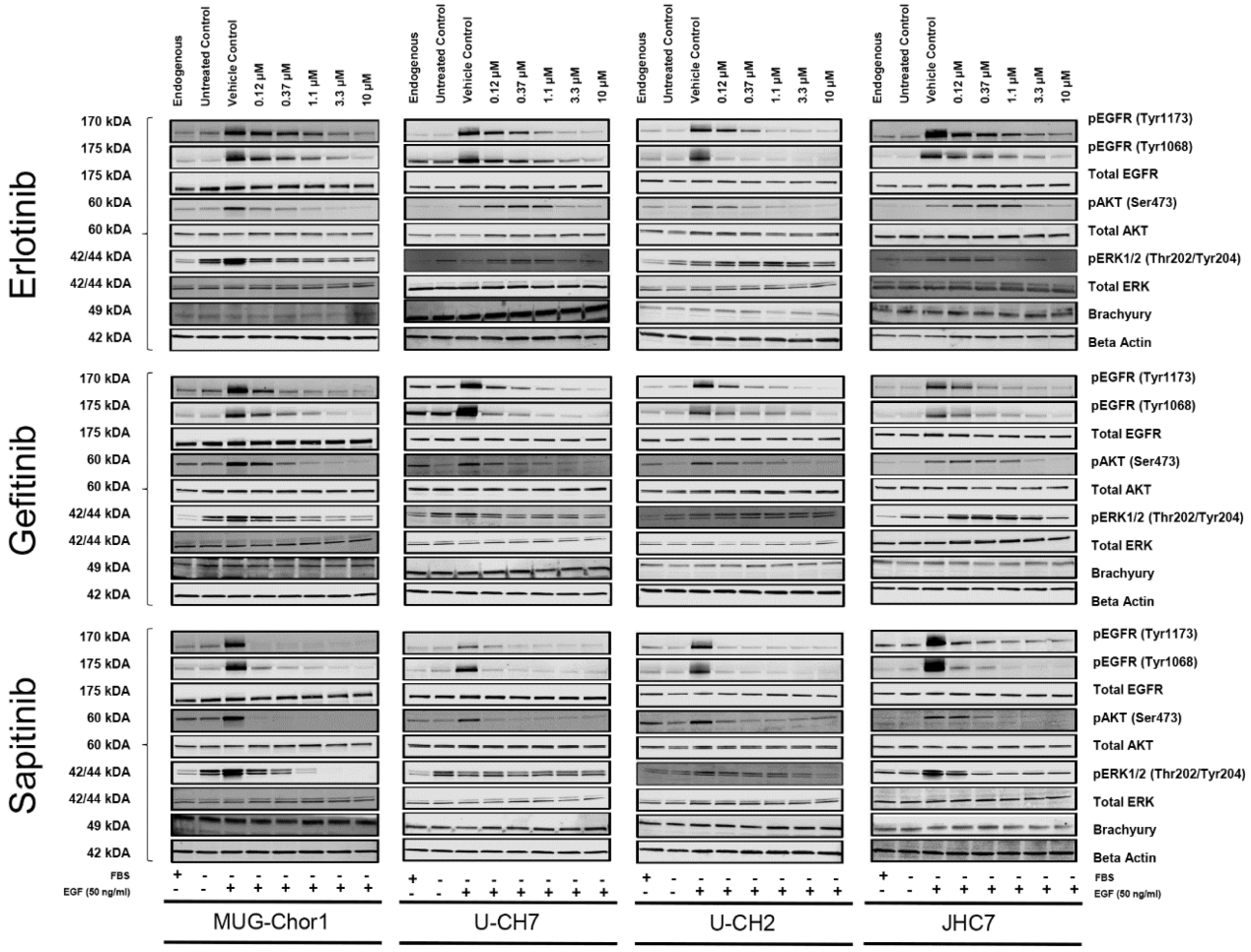

Figure 17. Western blot analysis in MUG-Chor1, U-CH7, U-CH2 and JHC7 (EGF-spiked, serum-starved).

Adapted from Scheipl *et al.* (2016) (11). Western Blot analysis for the effects of EGFR TKIs on phospho-EGFR and its downstream effectors in the chordoma cell lines MUG-Chor1, U-CH7, U-CH2 and JCH7 (EGF spiked, serum-starved) (11). For a detailed description, see the legend of Figure 16.

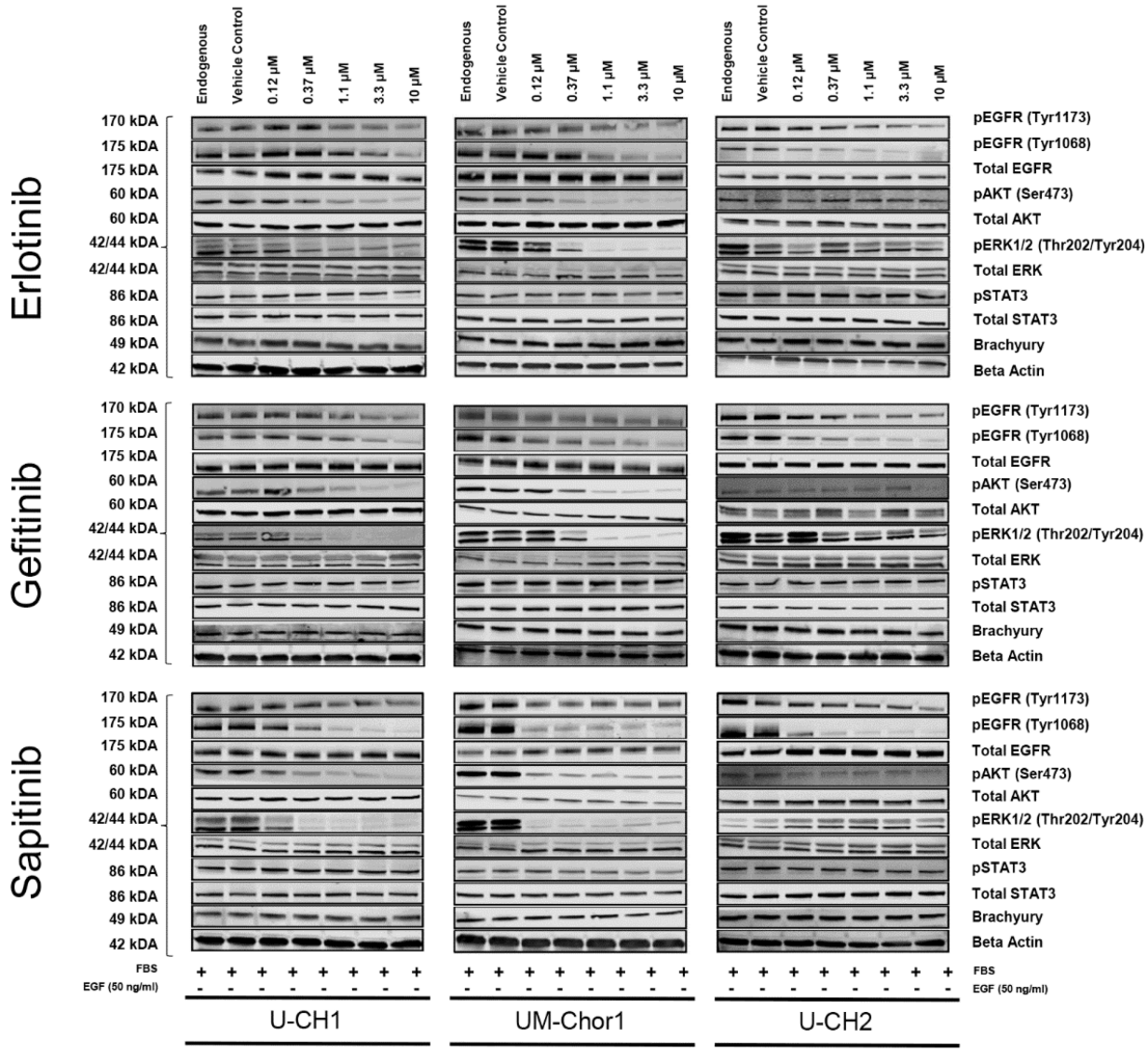

Figure 18. Western blot analysis of U-CH1, UM-Chor1 and U-CH2 (not EGF-spiked, not serum-starved).

Adapted from Scheipl *et al.* (2016) (11). Western blots of U-CH1, UM-Chor1 and U-CH2 in the absence of serum-starving and EGF-spiking (11). Cells were treated with a range of concentrations of the EGFR inhibitors, erlotinib, gefitinib and sapitinib for 4 h (11).

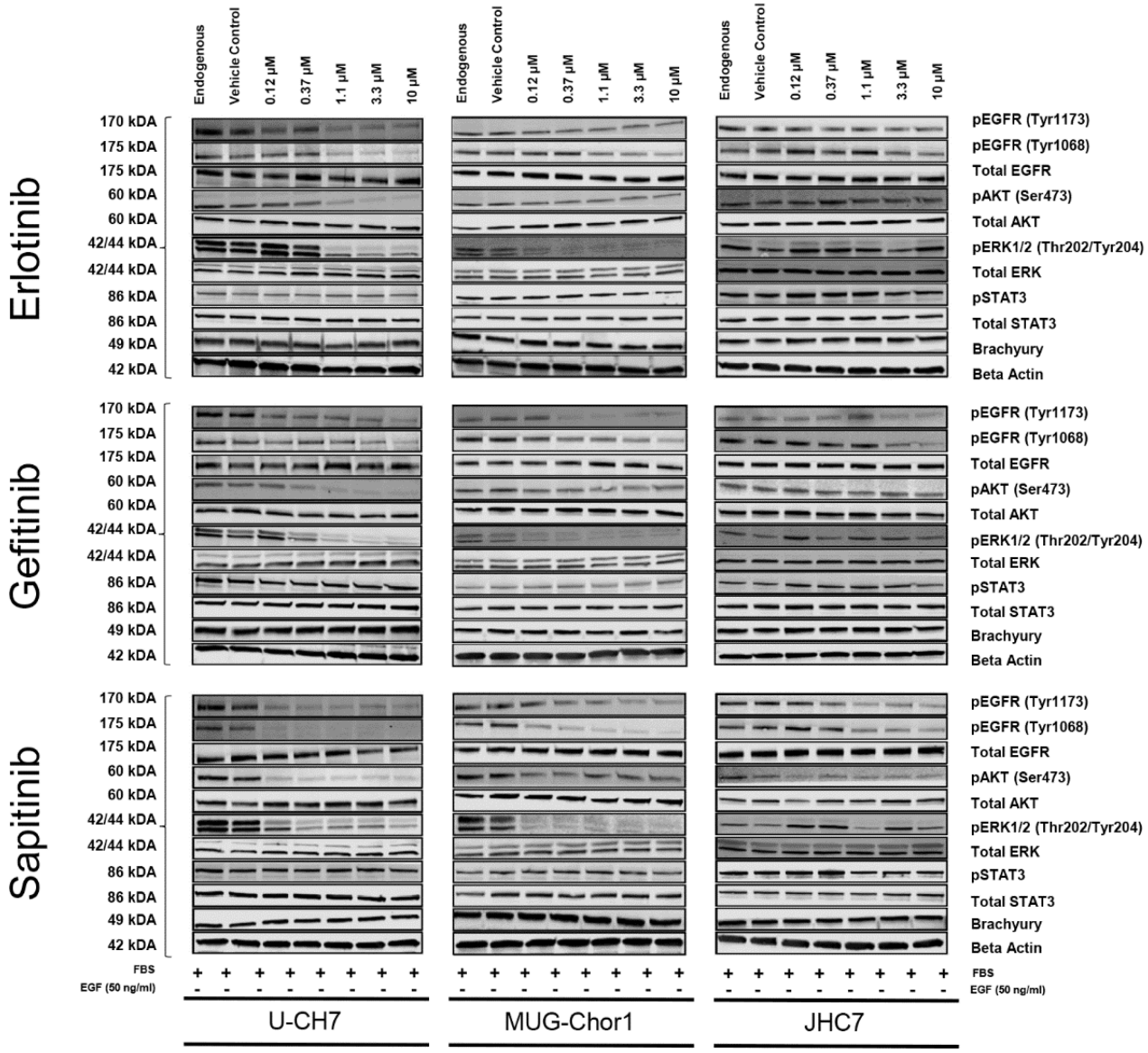

Figure 19. Western blot analysis in U-CH7, MUG-Chor1 and JHC7 (not EGF-spiked, not serum-starved).

Adapted from Scheipl *et al.* (2016) (11). Western blots of U-CH7, MUG-Chor1 and JHC7 in the absence of serum-starving and EGF-spiking (11). For details, see the legend to Figure 18.

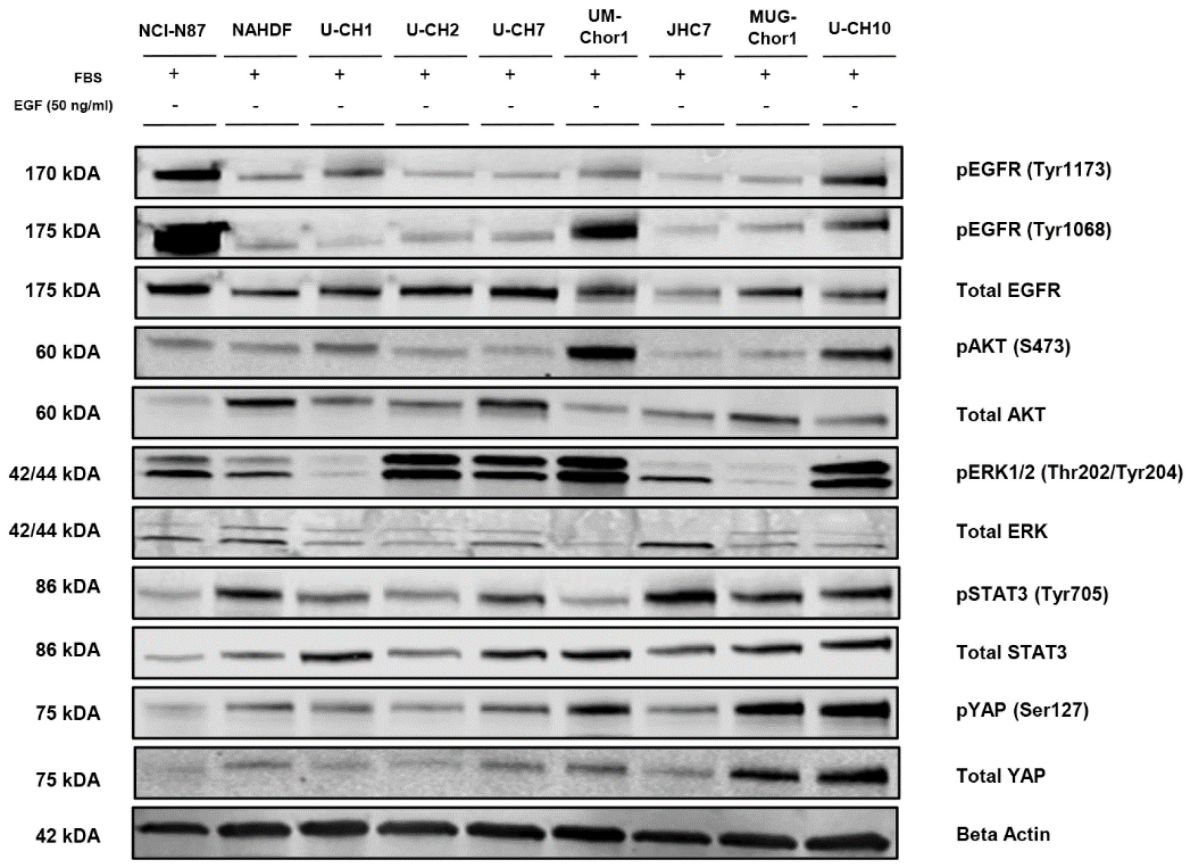

Figure 20. Endogenous status for the markers studied.
Adapted from Scheipl *et al.* (2016) (11). Endogenous/baseline status for the markers studied in the chordoma cell line panel and controls (NAHDF/normal adult human dermal fibroblasts and NCI-N87) (11).

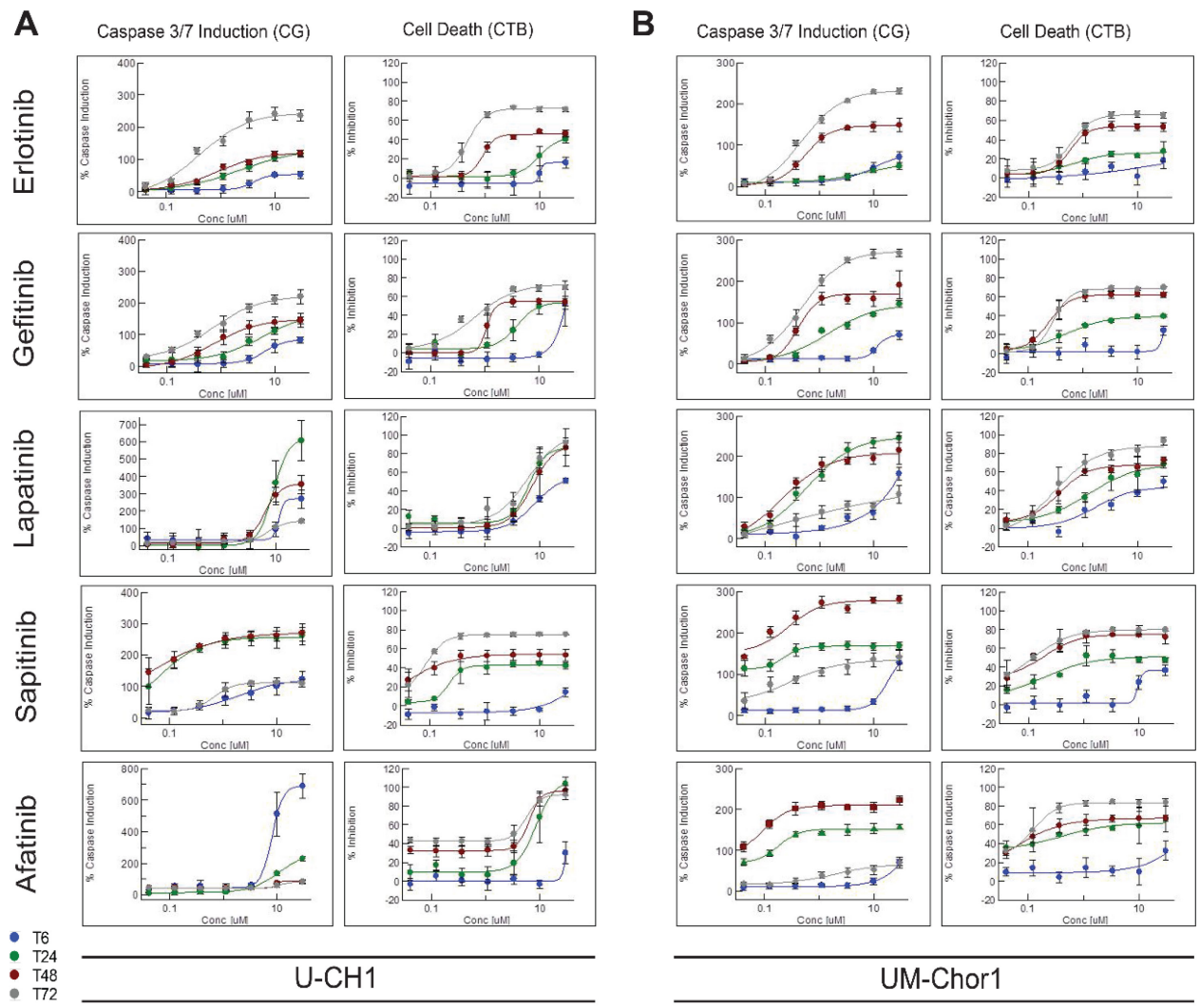

Figure 21. Apoptotic induction in U-CH1 and UM-Chor1.
Adapted from Scheipl *et al.* (2016) (11). **Apoptotic induction in the human chordoma cell lines U-CH1 (A) and UM-Chor1 (B).** In order to monitor cell viability and to determine induction of apoptosis upon treatment with erlotinib, gefitinib, sapitinib, afatinib and lapatinib, we used the Caspase-Glo® 3/7 Assay (CG) and the CellTiter-Blue® Luminescent Cell Viability Assay (CTB) on separate assay plates (11). Read-outs were conducted at 4 time points (6 h, 24 h, 48 h and 72 h), the results of which are expressed in different colours (11). We performed two independent experiments for each compound (n = 3 for sapitinib and erlotinib) (11). The results for U-CH7 and MUG-Chor1 are displayed in Figure 22.

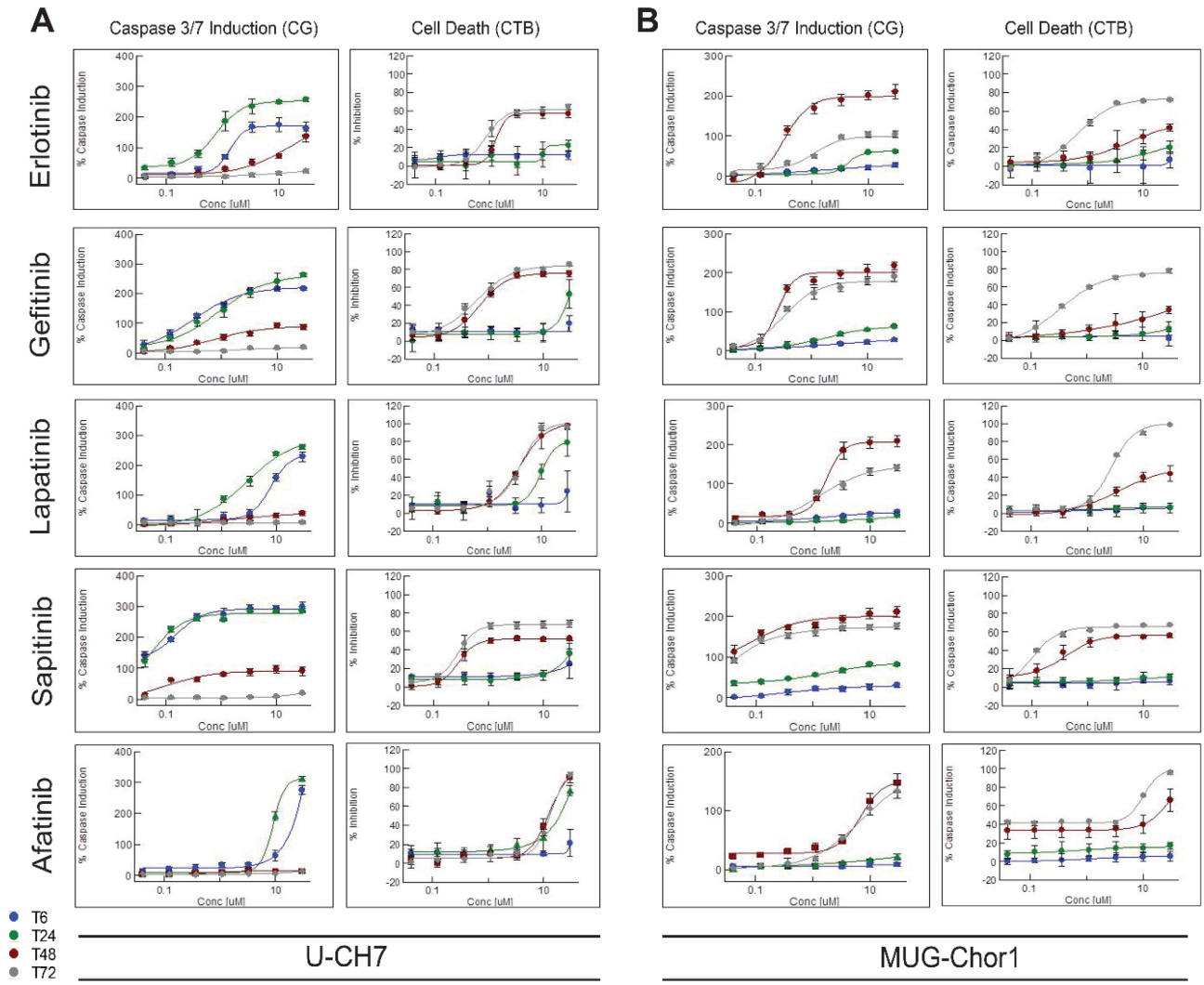

Figure 22. Apoptotic induction in U-CH7 and MUG-Chor1.
Adapted from Scheipl *et al.* (2016) (11). **Apoptosis data for U-CH7 (A) and MUG-Chor1 (B).** For details see the legend to Figure 21.

Investigation into Resistance Mechanisms of U-CH2, JHC7 and U-CH10

In the next step, we tried to identify reasons why our most active compounds were not effective in the three resistant cell lines (U-CH2, JHC7 and U-CH10) (11). We addressed this issue by looking into mechanisms of resistance to EGFR tyrosine kinase inhibitors, which have been reported in other cancer types (11). However, we were unable to detect mutation in the hotspots of 22 tumour-related genes, including *EGFR*, *ERBB2* and *ERBB4* and their downstream effectors (*KRAS, BRAF, PIK3CA, AKT1, PTEN, NRAS, MAPK*) by next-generation sequencing, which might have provided an obvious genetic explanation for sensitivity and/or resistance patterns observed in our chordoma cell lines (11).

Activation of bypass signalling pathways (e.g. via ERBB2 and MET) has also been reported to induce resistance (11, 101, 244). However, we did not detect amplifications in *EGFR*, *ERBB2* or *MET* in any of our cell lines by FISH analysis (**Table 14**) (11). What is more, no mutations were detected in *MET* (11). In addition, amplifications of *MET* were only observed in 2 (non-clival) of 114 clinical chordoma samples when assessed by FISH analysis (11). The majority of these samples (n=66) were located along the spinal axis, and 48 were situated in the clivus (11). However, when we studied MET expression in our chordoma cell line panel by Western blot analysis and immunohistochemistry, we observed strong phospho-MET expression in U-CH2 (**Figure 23A** and **Figure 24B**) (11).

Table 14. FISH data of the chordoma cell line panel. Adapted from Scheipl *et al.* (2016) (11).

Cell Line	FISH Data		
ID	***EGFR***	***ERBB2/HER2***	***MET***
U-CH1	***Polysomy*** 70% 3-5G + 3-5R	***Polysomy*** 30% 3-5G + 3-5R	***Polysomy*** 70% 3-5G + 3-5R
U-CH2	***Polysomy*** 70% 3-6G + 3-6R	***Polysomy*** 30% 3-5G + 3-5R	***Polysomy*** 80% 3-7G + 3-7R
U-CH7	***Disomy*** 2G + 2R	***Disomy*** 2G + 2R	***Disomy*** 2G + 2R
U-CH10	***Polysomy*** 90% 3-9R + 3-9G	***Polysomy*** 90% 3-13R + 3-13G	***Polysomy*** 90% 3-6R + 3-6G
JHC7	***Polysomy*** 40% 3-7R + 3-7G	***Polysomy*** 40% 3-7G + 3-7R	***Polysomy*** 40% 3-8G + 3-8R
MUG-Chor1	***Polysomy*** 80% 3-6G + 3-6R	***Polysomy*** 70% 3-4G + 3-4R	***Polysomy*** 80% 3-5G + 3-5R
UM-Chor1	***Polysomy*** 90% 3-5R + 3-5G	***Polysomy*** 90% 3-4R + 3-4G	***Polysomy*** 90% 3-6R + 3-4G (R>G)

Footnote to Table 14. EGFR/CEN 7: EGFR in red (R), centromeric 7 in green (G). HER2/CEN 17: HER2 in green (G), centromeric 17 in red (R). MET/CEN 7: MET in green (G), centromeric 7 in red (R) (3, 11).

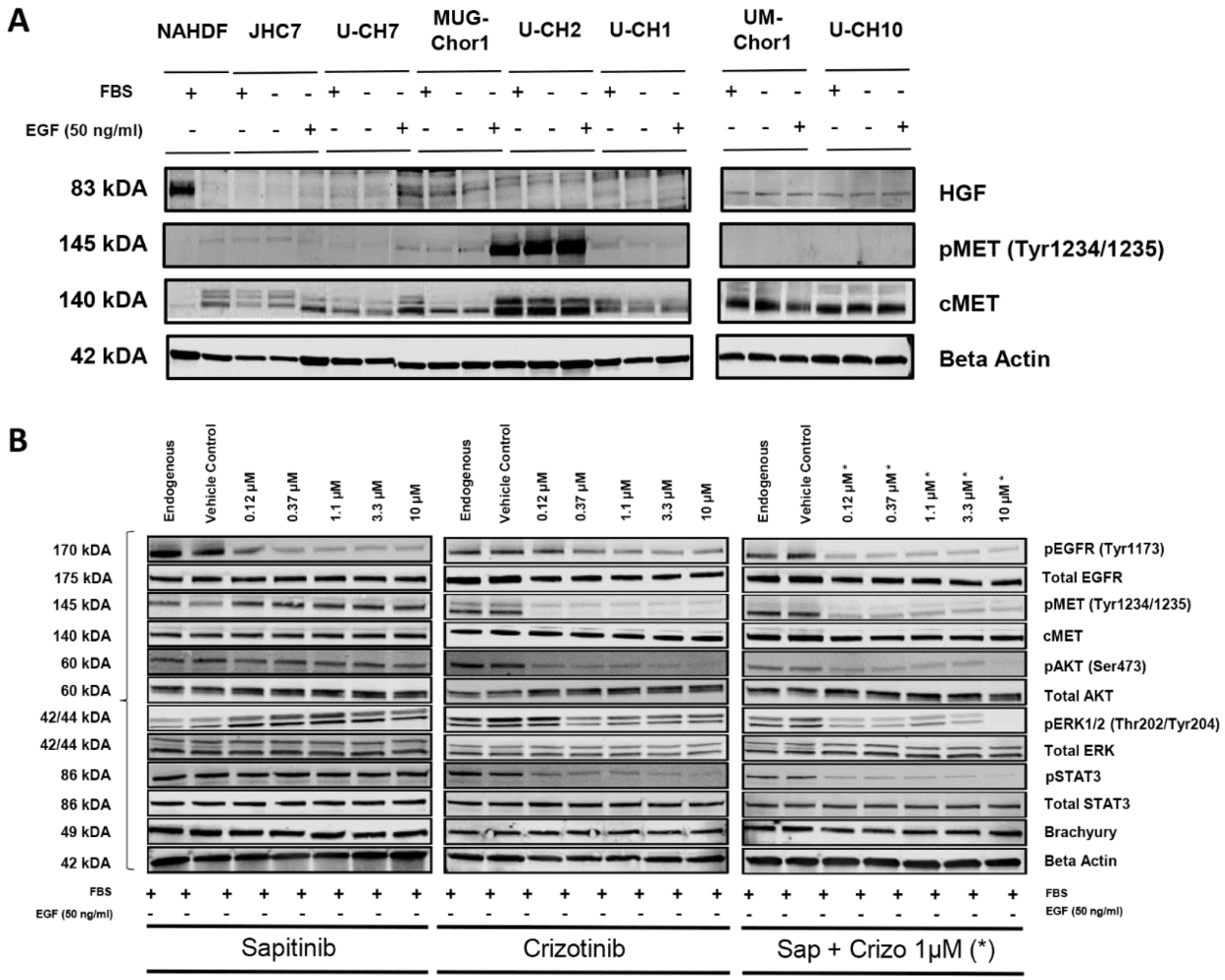

Figure 23. MET expression.
Adapted from Scheipl *et al.* (2016) (11). (**A) MET expression in the chordoma cell line panel.** MET expression in the cell line panel was analysed by Western blotting (11). These blots were run on endogenous (non-serum-starved, non-EGF-spiked), serum-starved (serum-starved, non-EGF-spiked) and EGF-spiked (serum-starved, EGF-spiked) samples for each chordoma cell line (11). Normal adult human dermal fibroblasts (NAHDF) were included as a control. In Western blots and immunohistochemistry (data shown in **Figure 24B**) there was strong phospho-MET expression in the resistant cell line, U-CH2, but not in the other chordoma cell lines studied (11). (**B) Effects of sapitinib and crizotinib on (phospho-) EGFR and its downstream pathways in U-CH2.** Western blots of U-CH2 treated with the reagents indicated (sapitinib, crizotinib and both drugs in combination) for 4 h (11).

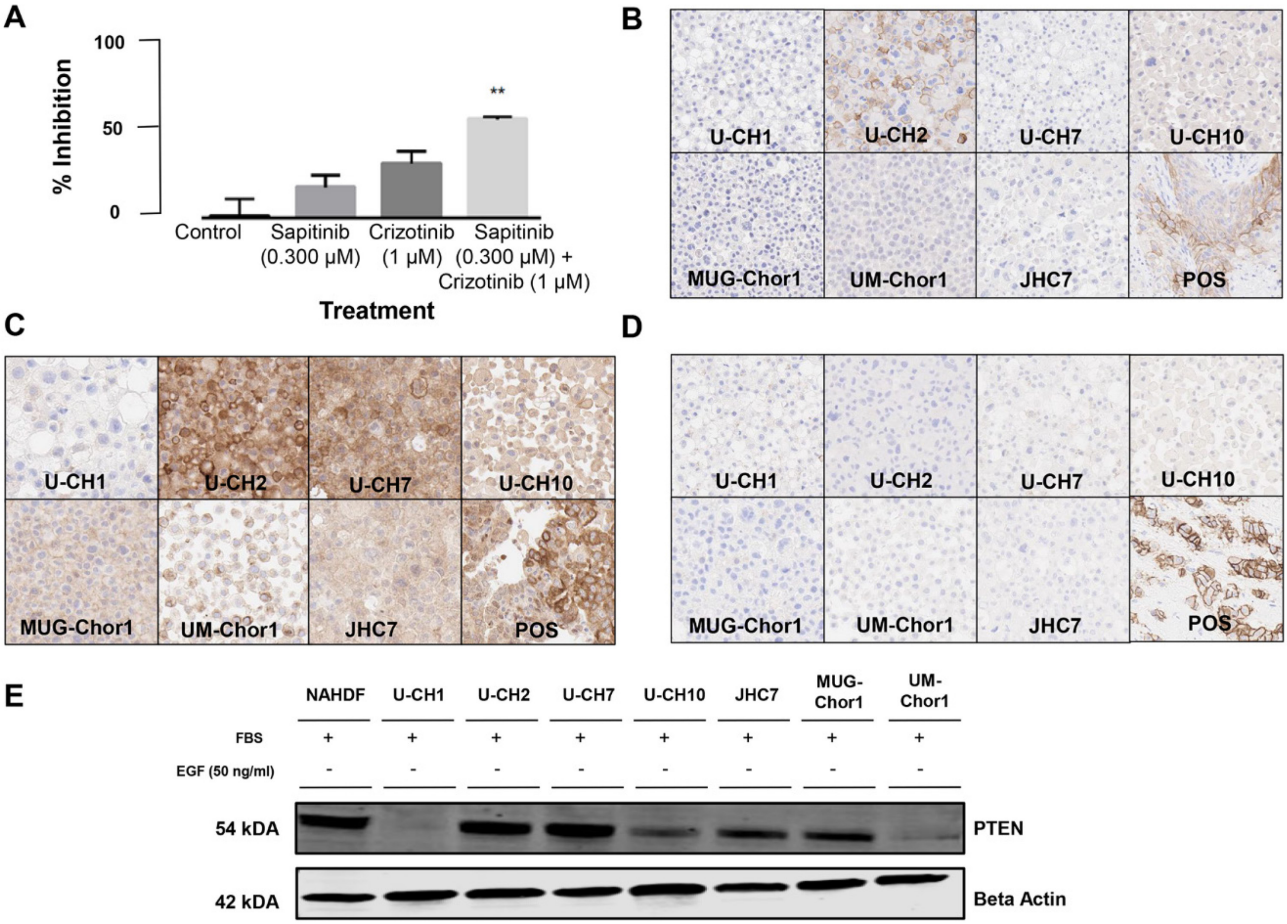

Figure 24. Combination treatment.
Adapted from Scheipl *et al.* (2016) (11). **Combination treatment of the EGFR inhibitor, sapitinib, and the MET/ALK inhibitor, crizotinib, resulted in a significant synergistic effect** (11)**. (A)** We plated U-CH2 cells in a 384-well format using a Multidrop-Combi (11). Twenty-four hours after plating the cells, we treated them with crizotinib for 72 h, followed by sapitinib for another 24 h (11). Experiments were conducted n=4 times for the combination treatment and n=3 times for the compounds alone (11). We calculated a combination index (COI) to evaluate synergistic (COI < 0.9), additive (COI = 0.9 to 1.1) and antagonistic (COI > 1.1) effects (11, 233). There was a significant synergistic effect for a combined treatment of U-CH2 cells with sapitinib (300 nM) and crizotinib (1 µM) (MI 58%; COI = 0.121; combination versus control, p = 0.0047, **) (11). **(B)** Immunohistochemistry was performed on formalin-fixed and paraffin-embedded pellets of all seven human chordoma cell lines, as well as on normal adult human dermal fibroblasts (NAHDF) and on adequate positive controls (POS) (11). Images were taken at a x20 magnification (11). Concordant to the results obtained from Western Blot analysis (**Figure 23A**), there was a strong phospho-MET expression in U-CH2 but not in the other cell lines (11). **(C)** PTEN expression was negative in U-CH1, weak in UM-Chor1 and positive to varying degrees in the other chordoma cell lines (11). **(D)** E-Cadherin expression was weak and only focal in U-CH7 and MUG-Chor1, and negative in the other cell lines (11). **(E)** Western blot analysis on the seven human chordoma cell lines and NAHDF confirmed the IHC results: an absence of PTEN in U-CH1, weak expression in UM-Chor1 and varying expression levels in the other cell lines **(C)** (11).

Loss and decreased expression of the tumour suppressor, PTEN, have also been correlated with resistance to EGFR TKIs (11, 244, 245). As illustrated in **Figure 24C,** our IHC results showed that

all cell lines (apart from U-CH1) expressed PTEN to varying degrees. There was strong immunoreactivity in U-CH2 and U-CH7; moderate reactivity in MUG-Chor1, JHC7 and U-CH10; and weak reactivity in UM-Chor1 (11). These results were confirmed by Western blot analysis, as shown in **Figure 24E** (11). Also, the loss of E-Cadherin expression has been linked to resistance against EGFR TKIs, as it has been suggested that E-Cadherin loss is implicated in epithelial mesenchymal transition (EMT) and the associated increase in cell motility (11, 244, 245). Immunoreactivity for E-Cadherin was weak and only focal in U-CH7 and MUG-Chor1. It was absent in the remaining five chordoma cell lines (**Figure 24D**). The Hippo downstream effector, Yes-associated protein (YAP) (246, 247), has been associated with EGFR TKI resistance (11, 107, 248, 249). We saw a strong positivity for YAP in the resistant chordoma cell line, U-CH10, in Western blot analysis (**Figure 20**) (11). However, the protein was also strongly expressed in another cell line, MUG-Chor1, which was responsive to EGFR inhibition in our screen (**Figure 20**) (11). Based on the results obtained from our cell line panel, protein expression levels of PTEN, E-Cadherin and YAP do not seem to be correlated with the presence and/or the absence of resistance to EGFR TKIs (11).

ERBB3 (HER3) has recently attracted attention for its putative role in resistance to EGFR and/or ERBB family inhibitors (117, 250, 251). Resistance is thought to be induced via a compensatory activation of common RTK downstream pathways (such as AKT/mTOR, RAS/RAF/MAPK and JAK/STAT signalling) in the presence of EGFR- or ERBB2-blocking (117). When we looked into upregulation of other ERBB family members upon spiking with the EGFR-specific ligand, EGF, (114), we observed that phospho-ERBB3 was upregulated in the resistant cell lines, U-CH2 and JHC7. This upregulation was not observed in the responsive cell lines, U-CH1, U-CH7 and MUG-Chor1 **(Figure 25)**. However, this experiment was conducted as a pilot study to further investigate resistance mechanisms, and data for UM-Chor1 and U-CH10 are lacking to date of submission of this thesis.

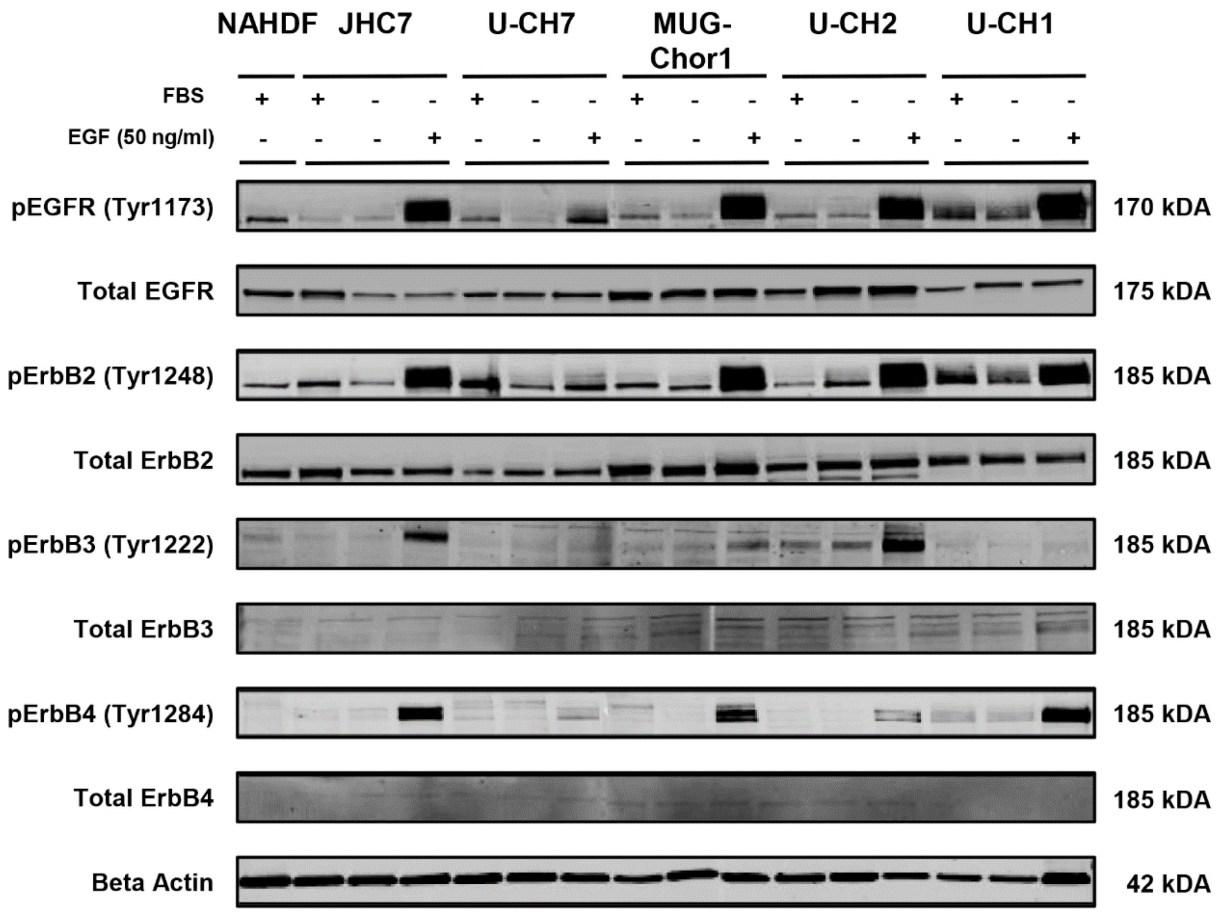

Figure 25. ERBB family heterodimerization.
ERBB family heterodimerization in chordoma cell lines. These blots were run on endogenous (non-serum-starved, non-EGF-spiked), serum-starved (serum-starved, non-EGF-spiked) and EGF-spiked (serum-starved, EGF-spiked) samples for each chordoma cell line. Normal adult human dermal fibroblasts (NAHDF) were included as a control.

Discussion

Chordoma is a rare primary malignant bone tumour of notochordal origin, and it usually develops in the bones of the base of skull, the vertebral bodies and the sacro-coccygeal region (10-12, 15). In addition, there are occasional reports of extra-axial and soft tissue lesions (10, 11, 25). Due to the slow growth of this disease, the median survival of patients with chordoma is seven years (11, 12, 15). Advances in radiation technology with either particles or photons have allowed delivery of higher doses of radiation (12, 15) and can be beneficial for local disease control (11). However, up to 30-40% of chordomas have been reported to metastasise, and there are currently no approved agents for treatment of patients with inoperable and/or metastatic chordoma (11, 15). Cytotoxic chemotherapy is not active in this entity (11, 15, 17). Imatinib, a PDGFR inhibitor, has shown only limited activity in a phase II study and when used in a compassionate program (11, 209, 210). However, there are encouraging anecdotal reports of responses to EGFR (54-58, 211) and VEGF inhibitors (17, 54, 55, 212), although data from prospective randomised clinical trials are lacking (11, 17, 212).

The expression of the transcription factor, *T (brachyury*), is a hallmark of chordoma (8), and there is a body of evidence supporting its critical role in this disease (7, 11). Specifically, study of the *T* regulatory network by Nelson *et al.* (2011) (9) revealed that EGF (as well as, among others, transforming growth factor alpha [TGFA] and fibroblast growth factor 1 [FGF1]) is a direct product of *T*-mediated transcription (9, 11). These findings are supported by a strong immuno-expression of these (phosphorylated) proteins in chordoma (3, 11, 171, 172, 252).

Genotype-directed therapy represents a major strategy for developing new cancer treatments. Its success has been demonstrated by, for instance, improving the outcome in close to 70% of patients with NSCLC harbouring *EGFR* mutations, although these cancers are known to develop resistance after 1-2 years (11, 101). However, despite the fact that chordomas are immunoreactive for the activated form of EGFR (phospho-EGFR), they lack *EGFR* mutations and infrequently show other current, potential tractable targets, such as *PIK3CA* mutations (3, 11, 173, 215, 216). In 2010 and 2011, the IGF system was reported to be involved in the pathogenesis of bone tumours, such as Ewing's sarcoma (128, 132). Moreover, an increasing number of protein kinase inhibitors had been approved by the FDA for treatment of various cancers (93). This is why we studied IGF-1R and its ligands in our clinical chordoma series to examine whether there was a rationale for IGF-1R inhibition in chordoma (1). Subsequently, following prominent reports of histone mutations in chondroblastomas and giant cell tumours of bone (197), and given that several HDAC inhibitors

were being approved by the FDA for clinical use in haematological malignancies (203), we studied the effect of HDAC inhibitors in chordoma cell lines (2).

Finally, during my research fellowship in Professor Flanagan's laboratory at the UCL Cancer Institute, London, UK, we chose a more comprehensive approach (11). We conducted a large-scale phenotypic compound screen on three chordoma cell lines and validated the key target in an extended panel of seven cell lines (11). Our aim was to identify new therapies and understand the mechanism by which this disease develops (11). We chose a phenotypic screening approach, as it had become clear that chordomas lacked known tractable targets (3, 11, 173, 215, 216). In addition, phenotypic approaches had been reported to be more successful than target-based approaches in identifying innovative drug candidates with clinically relevant mechanisms of action (11, 214, 217, 218). The results of these three studies (IGF-1R, HDAC and the phenotypic compound screen) are discussed below.

The IGF-1R Pathway in Sarcomas and Chordomas

Sekyi-Otu *et al.* (1995) showed that primary human sarcomas express IGF-1R and its ligands, IGF-1 and IGF-2 (253). In their review, Scotlandi and Picci (2008) summarised why sarcomas are likely to be suitable candidates for IGF-1R-targeting in clinical trials (130). In their review, Rikhof *et al.* (2009) illustrated that IGF-1R inhibition induced tumour-suppressive effects in preclinical studies on rhabdomyosarcoma, the most common soft tissue sarcoma in childhood (128). Similar effects were observed in Ewing's sarcoma (128).

Regarding the Ewing's family of tumours, Toretsky *et al.* (1997) reported that the characteristic EWS/FLI-1 fusion protein requires the IGF-1R pathway to transform cells (254). They further stated that the fusion protein itself seems to be involved in altering the IGF-1R pathway (254), probably via IGFBP-3 and/or IGF-1 (130). Therefore, it is not surprising that IGF-1R-targeting was considered as a therapeutic option, particularly in Ewing's sarcoma (128, 255, 256). In 2011, Pappo *et al.* described the results of a multicentre clinical trial using the IGF-1R inhibitory antibody, R1507, in 115 patients with refractory or recurrent Ewing's sarcoma (132). They reported an overall complete or partial response rate of 10%, with a median response duration of 29 weeks (132). Ten of 11 patients eliciting a response presented with primary bone tumours. The drug was well-tolerated, with the most common grade 3/4 adverse events being: pain (15%), anaemia (8%), thrombocytopenia (7%) and asthenia (5%) (132). The overall response to R1507 was judged as moderate, and the authors concluded that, to increase the efficacy of this therapeutic approach, predictive markers for patient

stratification and resistance mechanisms need to be identified and understood, and the treatment itself needs to be optimised (132).

Expression of IGF-1, IGF-2 and IGF-1R has also been reported in osteosarcoma (124, 128, 130). In this entity, expression was functionally related to malignant growth and invasion (130). Osteosarcoma forms the most common primary malignant tumour of bone. It occurs (similar to Ewing's sarcoma) mainly during puberty, so growth hormone (GH) is believed to play a central role in tumourigenesis (128, 130, 255). However, GH cannot be blocked, as this would cause major side effects on physiological development (128, 130, 255). In contrast, IGF-1R inhibitors have shown promising results in preclinical (osteo-)sarcoma models (126, 128). These results include the sensitisation of tumour cells to chemotherapeutic agents (126). Avnet *et al.* (2009) emphasised IGF-2 rather than IGF-1 as the predominant growth factor secreted by osteosarcoma cells (124). They hypothesised that IGF-2 maintains an autocrine loop via binding not only to IGF-1R, but also to a fetal isoform of the insulin receptor (IR-A), as well as to hybrid receptors consisting of IR-A and IGF-1R (124). Thus, according to Avnet *et al.* (2009), co-targeting of IR-A and IGF-1R might prove more effective in inhibiting osteosarcoma cell growth than targeting IGF-1R on its own (124).

IGF-1R blockade has also shown promising results in preclinical studies on rhabdomyosarcoma. In this entity, an overexpression of IGF-2 has been reported (128). IGF-2 was thought to nourish an autocrine/paracrine loop involving the growth factor receptor, IGF-1R (128). The latter had been shown to be consistently expressed in this type of sarcoma cell (128). As feedback mechanisms with IGF-1R downstream pathways are supposed to diminish the effects of an IGF-1R blockade, a combined IGF-1R and mTOR inhibition was expected to yield superior results (128). This observation was supported by Kurmasheva *et al.* (2009) (257), who reported that neither an IGF-1R-blocking antibody nor the mTOR-inhibitor, rapamycin, provided as single agents, induced tumour regression in xenograft models of various sarcomas, including rhabdomyosarcoma, Ewing's sarcoma and osteosarcoma. However, a combination of these two agents exerted synergistic effects, which resulted in a total remission of 5 out of 13 xenografts (257).

We aimed to provide a rationale for IGF-1R-targeting in chordomas by studying the immunohistochemical expression of the receptor tyrosine kinase (RTK) and its ligands (1). This aim was supported by previous reports, as Mitsuhashi *et al.* (258, 259) had demonstrated IGF-1R expression in 3 chordomas (2006) and 14 chordomas (2008), respectively, in two published abstracts. To further explore IGF-1R expression in chordomas, we studied a series of 50 chordoma samples and found an IGF-1R expression in the majority (76%) of these samples (1). Semiquantitative

analysis yielded a total of 18 chordomas (36%) that showed a moderate or strong staining intensity for IGF-1R in the majority (≥ 50%) of tumour cells, indicating that this subpopulation might particularly respond to anti-IGF-1R treatment (1). Our findings were supported by the data of Sommer *et al.* (2010) (260), who reported an expression of activated (that is, phosphorylated) IGF-1R/insulin receptor (IR) in a comparable percentage of chordomas (41%) (1). What is more, we found that there was a correlation between tumour volume and IGF-1R staining, which further nourishes the hypothesis that IGF-1R signalling might be involved in chordoma growth (1). The ligand, IGF-1, was expressed in a higher percentage of chordomas (92%) as compared to IGF-2 (50%), and strong expression of IGF-1 was more common (64%) than strong expression of IGF-2 (16%) (1). These data were in line with the reported findings of Mitsuhashi *et al.* (2006) and (2008) (258, 259) and possibly indicate that IGF-1 is the preferred ligand in stimulating IGF-1R in chordomas (1). In addition, there have been reports showing an activation of important RTK downstream effectors (such as AKT and mTOR) in this entity (1, 6). In summary, these results seemed to be supportive of further pursuit of IGF-1R inhibition in chordoma (1).

Targeting the IGF-1R Pathway in Sarcomas

As IGF-1R downregulation has been shown to inhibit tumour growth and metastases, and to enhance sensitivity to cytotoxic drugs and irradiation (128, 129), this made the IGF-1R pathway an attractive candidate for selective inhibition (128, 129, 261). As outlined above, IGF-1R has also been implied in the pathogenesis of various sarcomas, such as Ewing's, osteo- and rhabdomyosarcoma (128, 131-133). Thus, there have been several approaches used to target elements of this pathway, not only in carcinomas, but also in sarcomas (124-130). In particular, monoclonal anti-IGF-1R antibodies have been studied preclinically and in early-phase clinical trials (128, 134, 255, 261-263). Monoclonal antibodies selectively block the interaction of IGF-1R with its ligands, IGF-1 and IGF-2, and consecutively lead to receptor downregulation via endocytosis (127, 128), without severely interfering with the related insulin receptor (128). Examples of anti-IGF-1R monoclonal antibodies include: R1507 (F. Hoffmann-La Roche, Basel Switzerland), cixutumumab (IMC-A12, Imclone Systems Inc., now Eli-Lilly and Company, Indianapolis, IN, USA), figitumumab (CP-751 871, Pfizer, New London, CT, USA), dalotuzumab (MK-0646, Merck & Co Inc., Kenilworth, NJ, USA) and ganitumab (AMG-476, Amgen, Thousand Oaks, CA, USA) (132, 264). Linsitinib (OSI-906, OSI Pharmaceuticals Inc., Farmingdale, NY, USA), also a dual anti-IGF-1R/IR small molecule inhibitor, has been explored in clinical trials (134, 265, 266).

Encouragingly, initial positive clinical responses with IGF-1R inhibitory agents were reported, and there were few serious side effects (255). The authors reported occasional occurrences of

hyperglycaemia, which presented in mild forms (255). However, several clinical attempts with IGF-1R inhibitory monotherapies have not quite lived up to researchers' and clinicians' expectations, although they did show modest responses in select patients (131, 133, 134). In a phase 1 study on 28 patients with multiple sarcoma subtypes, one patient showed a total response and one a partial response (both with Ewing's sarcoma), and eight patients had a prolonged disease stabilisation (six with Ewing's sarcoma, one with synovial sarcoma and one with fibrosarcoma, respectively) upon treatment with figitumumab (CP-751 871, Pfizer) (157). Ewing's sarcoma was found to be the most sensitive histotype, although several side effects were reported (157). Some partial responses were also obtained with figitumumab in solitary fibrous tumours (157). Yet, Pappo *et al.* (2014) presented disappointing results from a phase 2 trial of the IGF-1R blocking antibody, R1507, in sarcoma patients: A total of 163 patients from 33 institutions with recurrent or refractory rhabdomyosarcoma, osteosarcoma, synovial sarcoma and other soft tissue sarcomas were enrolled in this trial, which was large for a sarcoma trial (131, 133). The primary endpoint of this study was the best objective response rate according to WHO criteria. To the disappointment of clinicians and researchers alike, treatment with R1507 resulted in a response rate of only 2.5%; four patients showed a partial response (two with osteosarcoma, one with embryonal rhabdomyosarcoma and one with alveolar soft part sarcoma) (131, 133). What is more, the duration of the responses were short-lived, with a median length of only 12 weeks (131, 133). Four additional patients (three with rhabdomyosarcoma, and one with myxoid liposarcoma) had a ≥50% decrease in tumour size that lasted for <4 weeks (133). The positive aspects were that the drug was well-tolerated and not associated with severe side effects (131, 133). The most common grade 3/4 toxicities were metabolic (12%), haematologic (6%), gastrointestinal (4%) and general constitutional symptoms (8%) (133). However, as a recent systematic review by Ma H *et al.* (2014) (264) pointed out, there seem to be differences in the side effects caused by individual anti-IGF-1R mAbs (264). So, the monoclonal anti-IGF-1R antibody, R1507 (132, 264), had a worse adverse-event profile as compared to cixutumumab or figitumumab (264). Furthermore, a higher rate of toxicity was observed in combinations of anti-IGF-1R antibodies with, for instance, EGFR inhibitors or with cytotoxic chemotherapeutic drugs (264). Also, younger patients who mainly received anti-IGF-1R mAbs for the treatment of (Ewing's) sarcoma showed higher toxicity rates compared to older patients (264). In summary, the results from this trial prompted Roche to discontinue development of R1507 (131). And, other pharmaceutical companies have lost interest in supporting IGF-1R inhibitory trials in sarcoma, as a personal communication with Dr. Silvia Stacchiotti, Milan, Italy, revealed in 2013 (Department of Cancer Medicine, Adult Sarcoma Medical Oncology Unit, Fondazione IRCCS Istituto Nazionale Tumori, Milan, Italy). Several authors concluded that additional studies are warranted to help to identify predictive factors

associated with clinical benefits in selected histologies, such as rhabdomyosarcoma or Ewing's sarcoma (133, 134).

In summary, mono-therapeutic approaches in IGF-1R inhibition have not yielded the expected results in sarcomas thus far (132, 133). However, in diseases in which the IGF-1R pathway provides an interesting target (such as Ewing's sarcoma), efforts need to be made to gain deeper insights into the role of IGF-1R and to identify reliable biomarkers for resistance, patient stratification and combinatory therapeutic approaches (132-134, 267, 268). As the IGF-1R pathway is influenced by its downstream pathways via various feedback-mechanisms (127, 128), a combined blockade at different levels of the pathway has repeatedly been discussed as a favourable alternative to monotherapies with anti-IGF-1R blockers (128, 130, 257). What is more, IGF-1R inhibitors have been shown to be of greater efficacy when combined with chemotherapeutic agents (and vice versa) (127-130, 261). These observations seem to support combination therapies of anti-IGF-1R blockers with other targeted therapeutics and/or cytotoxic chemotherapeutic drugs (130, 134). Future approaches will thus have to balance potential (side) effects with the benefits of various combination regimens (134, 263). Most importantly, efforts need to be made to better understand the role of IGF-1R in sarcoma, potential resistance mechanisms and the identification of biomarkers for patient stratification to anti-IGF-1R (combination) therapies (132, 133).

Studying HDACs in Chordoma

HDACs have been shown to influence malignant transformation by altering histonic and nonhistonic proteins (2, 208). In particular, histone modifications have been recognised as a central mechanism of epigenetic transcription regulation (2, 208). In the absence of recurrent genetic alterations in chordoma (3, 10, 173, 215, 216), and based on the fact that mutations in histone genes have been described in other bone tumours (197), we were interested to examine HDACs and study their expression in clinical chordoma samples. However, we had little data for comparison, as published data on HDAC expression in chordomas were sparse (2). Duan *et al.* (2010) (269) studied miRNAs in chordomas and reported the expression of HDAC4 in chordoma cell lines (including U-CH1) and in eight chordoma clinical samples. In our study, we confirmed immunohistochemical expression of HDAC4 and, furthermore, we showed that HDACs 2-6 were expressed in our series of chordoma samples (2). Since we were aware that decalcification might negatively influence our IHC results, we tried to generate our tissue micro array from soft tissue parts of tumours (2). We did not observe differences in IHC expression between primary tumours and recurrences, nor between specimens that had been EDTA decalcified and others that had not (2). Of all HDACs studied, HDAC6 showed the strongest immunoreactivity in our series (2). Expression of HDAC6 was further confirmed by

Western blot analysis in the chordoma cell lines, U-CH1 and MUG-Chor1 (2). In line with the published literature, we found that HDAC6 expression was exclusively localised in the cytoplasm (2, 181, 200, 270). HDAC6 has several features that distinguishes it from other HDACs: It interacts with the microtubule network (tubulin alpha) and with heat shock protein (HSP) 90 in an ubiquitin-dependent manner (2, 270-273). These features characterise HDAC6 as a crucial player in the management of cellular stress, which can be caused by cytotoxic accumulations of misfolded proteins (2, 270-273). Thus, it might be of interest for future research to study the role of HDAC6 and its potential implications in chordoma pathogenesis (2). Having verified the expression of various HDACs in our clinical chordoma specimens, we were interested to study the effect of three pan-HDAC inhibitors in our well-established chordoma cell line, MUG-Chor1 (2, 221). Two of these inhibitors, SAHA and LBH589, significantly induced apoptosis in MUG-Chor1 cells *in vitro* ($p \leq 0.0003$ for SAHA, and $p \leq 0.0014$ for LBH589 after 72h of incubation, respectively) (2). This SAHA- and LBH589-induced apoptosis was reproduced in another well-established chordoma cell line, U-CH1 (2, 220). Compared to their effect in chordoma cells, these drug's induction of apoptosis was less distinct in skin fibroblasts that derived from the same patient as the chordoma cell line, MUG-Chor1 (2). Furthermore, SAHA and LBH589 induced a cell cycle arrest in the S and the G2/M-phase (2). In line with the literature, LBH589 was active at lower concentrations as compared to SAHA, which indicated that LBH589 was very potent (2, 274). Compared to SAHA and LBH589, the third pan-HDAC inhibitor tested, PXD101, failed to exert major apoptotic effects or to induce a cell cycle arrest (2). These differences in response were interesting, as all drugs tested were pan-HDAC inhibitors (2, 181, 200, 201). Yet, existing data suggest that pan-HDAC inhibitors might not affect all HDACs equally (2, 202, 275). Dejligberg *et al.* (2008) (276) showed that depletion of HDAC1 induced an increased resistance to PXD101 (but not to SAHA) in HeLa cells (2). However, the authors did not observe similar effects after depletion of HDACs 2 and 3 (2, 276). HDAC1 was only focally expressed in the nucleus of a minority of our chordoma samples, so it is interesting to speculate as to whether there might be a similar correlation between the absence of HDAC1 and resistance to PXD101 in chordomas (2).

Targeting HDACs in Sarcomas and Chordoma

Based on promising clinical data on HDAC inhibitors in haematological malignancies (200, 203), several research and tretament groups also studied HDAC inhibitors in solid tumours (200, 277). There have been promising results in various *in vitro* models, as well as in animal models of several types of soft tissue and bone sarcomas (2, 181, 200). We are not the only group that has studied HDACs in chordoma (2). Lee D. H. *et al.* (2013) reported that a combination of HDAC and PDGFR

inhibitors act synergistically in chordoma cell lines (278). Based on promising preclinical data, the HDAC inhibitor, LBH589, was combined with the PDGFR inhibitor, imatinib, in a clinical phase I safety trial on newly diagnosed and recurrent chordoma in the United States (NCT01175109) (https://clinicaltrials.gov/ct2/show/NCT01175109). However, the trial had to be halted prematurely due to unsatisfactory responses and, in particular, due to severe toxicity issues (oral communication from Deric M Park, MD, University of Virginia). These observations were in line with results from other solid tumours; when HDAC inhibitors were tested in clinical trials against solid tumours, the results were disappointing, and there were severe side effects, as reviewed by a team of Leiden oncologists (277). The effective concentrations obtained in solid tumours were low, and cardiac toxicities appeared to be a particular issue (277). The origins of these differences in action in haematological and solid malignancies are not understood. However, the authors discuss that HDAC inhibitors might not be able to permeate solid tumours, and/or their half-lives might not allow them to effectively do so (277). Also, they might not target these tumours selectively (277). What is more, sufficient biomarkers for response are still lacking, as is the case with many targeted therapeutics. For that reasons, interest in HDAC inhibitors in solid tumours and in chordoma has markedly declined, although further research might bring them back on stage, particularly in a combinatory setting (277).

The EGFR/ERBB Family in Cancer

In the early 1980s, the EGFR/ERBB family was implicated in cancer when the avian erythroblastosis tumour virus (an oncogenic retrovirus in birds (279)) was found to encode for an aberrant form of the human *EGFR* (113). Hyperactivated tyrosine kinase activity of ERBB family members has since been reported to result in unregulated growth stimulation and tumourigenesis in various cancer types, including breast, lung, stomach, brain, head and neck, pancreatic and colorectal cancer (112, 114, 122). A tumour becomes oncogenically addicted to EGFR/ERBB signalling due to a constitutive activation of the receptor (e.g. by an activating mutation) or due to the hyperactivation of EGFR/ERBB signalling because of an overexpression of either the ligands or the receptors (113). Whereas only a small proportion of tumours with hyperactivated EGFR signalling (9-20%) is likely to respond to EGFR inhibition, the majority (88-94%) of tumours with sensitising *EGFR* mutations have been shown to respond to anti-EGFR tyrosine kinase inhibitors (TKIs) (113).

Overexpression of EGFR may be caused by polysomy or amplification of the *EGFR* gene, which is located on the short arm of chromosome 7 (7p12) (113, 280). EGFR overexpression has been reported to be a strong prognostic indicator in several cancers, such as head and neck squamous carcinoma (113, 281, 282), renal cell carcinoma (283, 284) and prostate cancer (280). In these

neoplasms, protein (over-)expression and polysomy (rather than *EGFR* gene amplification) seem to be implicated in disease pathology (280-284). Also, in other cancers, such as ovarian, cervical, bladder and esophageal cancer, elevated EGFR expression has been reported to correlate with prognosis (113). In gastric, endometrial and colorectal cancer, EGFR expression was shown to be a modest predictor (113). In colorectal cancers, several meta-analyses indicated a positive correlation of *EGFR* copy number gain and therapeutic response to anti-EGFR targeted therapeutics (245, 285). However, heterogeneous scoring systems and problems in the reproducibility of FISH scoring systems were stated as limiting factors in interpreting these results (245, 286). Sesboüe *et al.* (2012) noted that gene amplifications, which result from an aberrant DNA replication, form a key mechanism of oncogene activation (286). Gene amplification leads to several hundreds of copies of a gene that are either integrated in extrachromosomal double minutes (these are small fragments of extrachromosomal DNA) or in chromosomal homogeneously staining regions (HSRs) (286). Characteristically, the *EGFR*/chromosome7-ratio is expected to be >2 in the presence of a true amplification (286). In contrast, gene copy number gains correspond to a gene copy number >2 without altering the gene/chromosome ratio (286). Copy number gains can occur for various reasons, ranging from segmental chromosomal duplications to an increase of the chromosome number to polyploidisation (286). Gene copy number gains thus reflect a general genomic instability within a tumour rather than a specific oncogene activator mechanism, although also copy number gains can be associated with elevated protein levels (286). For that reason, the authors claim that the evaluation of FISH results, which is the most commonly used method for the detection of copy number variations (CNVs) and gene amplifications, must rely on accurate criteria to distinguish between true amplifications and chromosome 7 aneusomy (286). Accurate and well-defined criteria are crucial for a comparison of different study results in order to draw reliable prognostic conclusions from them (286).

Apart from the aforementioned cancers, *EGFR* copy number gains and protein overexpression were also reported to be of some predictive value for the response to EGFR TKIs in NSCLC (287, 288). However, authors such as Grob *et al.* (2013) (289) and Mansuet-Lupo *et al.* (2014) (290) have recently noted that remarkable intratumoural heterogeneities of *EGFR* copy number gains have been observed in NSCLC samples. Thus, small biopsy samples might not allow pathologists to reliably determine *EGFR* copy number gains, thereby restricting the predictive value of this aberration (289, 290). In contrast, the *EGFR* mutational status did not display intratumoural heterogeneities (290). Particularly in NSCLC, somatic mutations in the *EGFR* gene are known to sensitise tumours to treatment with EGFR TKIs (291). The prevalence of *EGFR* mutations in NSCLC (adenocarcinoma)

ranges from 10.4% (Italy) to 50% (Japan) to 39% (Taiwan), according to local study reports (291). *EGFR* mutations are restricted to four exons (exons 18 – 21), with deletions in exon 19 and point mutations in exon 21 accounting for more than 90% of mutations (291). Observational studies have linked point mutations at codon 719 of exon 18, deletions in exon 19, and point mutations at codons 858 and 861 of exon 21 to neoplasms that are responsive to treatment with gefitinib (291). Thus, these somatic *EGFR* mutations determine clinical response to EGFR TKIs and are therefore regarded as the most robust biomarkers for EGFR targeting (291-293).

Apart from EGFR, other ERBB family members have also been implicated in cancer development. ERBB2 (HER2/neu) expression, along with estrogen receptor (ER) and progesterone receptor (PR) status, has been established as a biomarker for routine use in clinical practice in breast cancer (116, 293). Amplification or overexpression of the *ERBB2* gene, which is located in the long arm of chromosome 17 (17q12) (116), has been reported to occur in approximately 15-30% of breast cancers and in 10-30% of gastric/gastroesophageal cancers (116). *ERBB2* amplification has been associated with a shorter disease-free and overall survival in these patients, and it has also been implicated in the pathogenesis of various other cancers (116). There have been reports of activating *ERBB2* mutations in a small subset of NSCLC patients (approximately 6%, particularly in never-smokers (122)) and breast cancer patients (approximately 1.6%) (122). Being incapable of ligand induced activation on its own, ERBB2 is known to form highly potent heterodimers with other ERBB family members, such as EGFR and ERBB3 (HER3) (114, 116, 117). HER2 targeting therapies, such as trastuzumab (Herceptin®, Roche), a monoclonal antibody which binds to an extracellular domain of the HER2 receptor; lapatinib (Tykerb®/Tyverb®, GSK), a dual EGFR/ERBB2 small molecule inhibitor; and the combination of both (294), have shown to be beneficial in the treatment of HER2-positive breast cancer and have been approved by the FDA for this application (116). Although HER2 has been shown to be expressed by a subset of chordomas (3, 171, 172), neither we nor other authors have been able to detect *HER2* activating mutations or amplifications (3, 11, 171, 172).

ERBB3 (HER3) has recently attracted attention for its putative role in cancer development and resistance to cancer therapeutics, such as EGFR/ERBB inhibitors (117, 250, 251). Activating mutations in *HER3* have been reported in various types of cancer, such as gastric, colon and bladder cancer, and NSCLC (251). ERBB3 lacks intrinsic kinase activity and can thus only induce cell signalling via heterodimerization with other ERBB family members, of which ERBB2 forms the most important partner (117, 250, 251). A key mechanisms of ERBB3-induced therapy failure seems to lie in its compensatory activation of common RTK downstream pathways (e.g. AKT/mTOR,

RAS/RAF/MAPK and JAK/STAT signalling) in the presence of EGFR or ERBB2 blocking agents (117). ERBB3 has been linked to tamoxifen resistance in breast cancers (117, 250, 251). It has been shown to increase in expression and relocate to the plasma membrane upon TKI treatment of HER2-amplified breast cancer models (250). ERBB3 has further been reported to contribute to gefitinib resistance in *MET*-amplified lung cancer, as well as to *de novo* resistance to cetuximab in colorectal cancers that express high levels of the ERBB3-activating ligand, HRG (117).

To study possible effects of EGFR/ERBB3 heterodimers in chordoma, we added the EGFR-specific ligand, EGF, to our cell culture medium (114) and conducted Western blot analysis. We observed an upregulation of phospho-ERBB3 as a result of heterodimerization of EGFR and ERBB3 receptors. This heterodimerization was observed in two chordoma cell lines resistant to EGFR TKIs (U-CH2 and JHC7) but not in three responsive cell lines (MUG-Chor1, U-CH1 and U-CH7). However, this experiment was conducted as a pilot study investigating potential resistance mechanisms in chordoma, and data on U-CH10 and UM-Chor1 are currently still lacking. Our most promising compound, sapitinib (AZD8931, AstraZeneca), is a reversible EGFR/ERBB2/ERBB3 inhibitor (235). The fact that sapitinib did not perform better on resistant chordoma cell lines compared to erlotinib, gefitinib or other EGFR inhibitors that have not been reported to co-target ERBB3 (**Table 11, Table 13**) (295, 296) raises doubts as to whether ERBB3 forms a key mechanism of resistance in these lines. To date, no specific ERBB3-targeting therapeutics exist, but inhibitory monoclonal antibodies and bispecific antibodies co-targeting EGFR and ERBB3 are currently under development and in (pre-) clinical evaluation (117, 250). However, preliminary data indicate that ERBB3 targeting antibodies have only limited potency (251). Nevertheless, the role of ERBB3 bypass signalling in EGFR TKI resistance seems interesting to pursue in chordoma, although this was clearly beyond the scope of this project.

In contrast to the aforementioned ERBB family members, the fourth member, ERBB4, has been correlated to a favourable prognosis and more differentiated phenotype in various diseases (297, 298). Alternative splicing of the ERBB4 gene transcript (with the *ERBB4* gene localised on chromosome 2q33.3-34) leads to different isoforms of this receptor protein, which show different organ distributions and are believed to exert functional differences (298, 299). Whereas EGFR is physiologically centrally involved in the ductal differentiation of the breast, ERBB4 plays a role in the alveolic maturation of the mammary gland during pregnancy and lactation, which might explain why pregnancy and a prolonged lactation have been reported to reduce the overall breast cancer risk (297). Furthermore, ERBB4 is known to be involved in the development of organs such as the heart and the brain (297, 299), where it shows the highest expression throughout life (298). For that

reason, it is not surprising that ERBB4 has also been implicated in cardiovascular and psychiatric diseases (297, 299). ERBB4 expression has also been reported in several types of carcinomas (such as colon, lung, ovary, pancreas, endometrium and stomach cancer), as well as in soft tissue sarcomas and paediatric brain tumours (298). Sixty-six percent of medulloblastomas and approximately 75% of ependymomas were positive for ERBB4 (298). However, the prognostic significance of these observations seem to vary based on the tumour type involved. In mammary carcinomas, ERBB4 expression seems to indicate a higher differentiated tumour grade and a more favourable outcome (298), while the opposite was observed for medulloblastomas and ependymomas (298). In these neoplasms, ERBB4 seems to indicate a poor prognosis (298). Mendoza-Naranjo *et al.* (2013) (300) reported a transcriptional ERBB4 overexpression in chemoresistant and/or metastatic Ewing's sarcoma cell lines. The authors found that ERBB4 expression was correlated to a significantly reduced disease-free survival in Ewing's sarcoma (300).

As outlined above, the EGFR/ERBB family plays an important role in the tumourigenesis of many solid tumours, and selective inhibitors are available, making them an attractive therapeutic target (112). For that reason, EGFR has also been studied in chordomas.

EGFR Expression in Chordomas

Several authors have studied the expression of EGFR and its activated form, phospho-EGFR, in chordomas (3, 51, 171, 172, 252). Shalaby *et al.* (2011) reported immunohistochemical expression of EGFR in 69% of 173 clinical chordoma samples (3). Phospho-EGFR was detected in 52% of non-skull based and 43% of skull-based samples, respectively (3). Weinberger *et al.* (2005) reported the expression of EGFR in all 12 samples analysed (252). Tamborini *et al.* (2010) showed that EGFR was present in 80% of 22 chordomas studied (171). Furthermore, they reported activation of EGFR, ERBB2 and ERBB4 (but not ERBB3) in RTK arrays performed on surgical chordoma specimens (171). Dewaele *et al.* (2011) described EGFR as the most frequently activated RTK in chordomas, particularly in advanced chordomas, with 67% (26 of 39) of their samples immunopositive for EGFR (172). Furthermore, 38% (16 of 42) specimens displayed *EGFR* polysomy, and four (9.5%) showed FISH amplification, although no activating *EGFR* mutations could be detected (172). In line with these findings, other authors also failed to detect recurrent point mutations in *EGFR* and relevant downstream effectors, such as *KRAS*, *NRAS*, *HRAS* or *BRAF* (3) (10, 171-173, 215, 301).

PI3K/AKT/mTOR Signalling in Chordoma

There is increasing evidence of mTORC1 signalling activation in chordomas, which might contribute to tumourigenesis in this neoplasm (6, 153, 169). Rinner *et al.* (2013) described the loss of the

PIK3CA locus on chromosome 3 (3q26) in all ten chordoma samples analysed (221). Mutations in *PI3KCA* have been detected in a small subset (approximately 1%) of 30 chordomas that have undergone whole genome sequencing with compared normal tissue at the Wellcome Sanger Trust Institute, Hinxton, UK (unpublished data from Professor Flanagan's laboratory at the UCL Cancer Institute, London, UK, which is displayed in the Catalogue of Somatic Mutations in Cancer (COSMIC) database: http://cancer.sanger.ac.uk/cosmic/browse/tissue#sn=bone&ss=all&hn=chordoma&sh=all&in=t&src=tissue&all_data=n; last checked: 14/06/2016). The loss of *PTEN* (10q23) with its subsequent constitutive activation of AKT signalling belongs to the most frequently described genetic alterations in chordoma (169, 170, 172, 173, 215). In line with this, the COSMIC database reports *PTEN* mutations in 2% of chordoma samples (http://cancer.sanger.ac.uk/cosmic/browse/tissue#sn=bone&ss=all&hn=chordoma&sh=all&in=t&src=tissue&all_data=n).

Presneau *et al.* (2009) tested mTOR pathway activity in 50 clinical chordoma samples (6). The authors stated that 65% of chordomas might potentially be responsive to mTOR antagonists, although they did not observe hyperactivation of this pathway (6). Han *et al.* (2009) reported activation of AKT and mTORC1 signalling in ten sporadic sacral chordomas and in U-CH1 (169). AKT/mTORC1 signalling was associated with a significantly reduced protein expression of the tumour suppressor, PTEN (169). They also found that the mTOR inhibitor, rapamycin, inhibited mTORC1 signalling and suppressed proliferation of chordoma-derived cell lines (169). Schwab *et al.* (2009) reported activation of the PI3K/mTOR pathway in 13 chordomas and showed that the dual PI3K/mTOR inhibitor, PI-103, inhibited this pathway in U-CH1 (153). Dewaele *et al.* (2011) confirmed activation of PI3K/AKT signalling downstream of EGFR (172). Stacchiotti *et al.* (2009) reported that ten patients suffering from advanced progressive chordoma were treated with a combination of the PDGFR inhibitor, imatinib (400 mg/day), and the mTOR inhibitor, sirolimus (2 mg/day) (302). Both drugs were generally well-tolerated (302). Nine patients were available for response evaluation (302). One patient showed a partial response, according to Response Evaluation Criteria in Solid Tumours (RECIST), seven showed stable disease and one patient suffered from progressive disease (302). In MRI, seven tumours showed a minor partial response (≥10% decrease in four cases), one was stable and one was progressive (302). Seven patients had a PET response, and 89% reported a clinical benefit (302). Based on this study, it has been assumed that imatinib is more efficacious for chordoma treatment in combination with an mTOR inhibitor, and so a phase II study

of imatinib plus everolimus has been conducted (EUDRACT-2010-021755-34) (15). Recruitment for this study ended in January 2016, and data analysis is currently ongoing.

RAS/RAF/MAPK Signalling in Chordoma

There is evidence for activation of this pathway in chordomas (4, 11, 169). However, as mentioned above, several groups have failed to reveal recurring point mutations in *KRAS*, *NRAS*, *HRAS* and *BRAF* (3, 10, 11, 171-173). Rinner *et al.* (2013) found hypermethylation of *RASSF1* (RAS association domain family protein 1), a *RAS* related tumour suppressor gene, in chordomas as compared to normal blood (170). Physiological functions of this gene include DNA repair and cell cycle control, and transcriptional silencing by promotor methylation has been reported for several tumour types, particularly breast and colorectal cancer (170).

STAT3 Signalling in Chordoma

Apart from PI3K/AKT/mTOR and RAS/RAF/MAPK signalling, STAT3 signalling has also been implicated in chordoma pathogenesis. Yang *et al.* (2009) described a nuclear staining positivity for phopho-STAT3 in all 70 chordoma samples investigated (303). The authors furthermore found that phospho-STAT3 positivity was correlated with a worse clinical outcome (303). What is more, they described inhibitory effects of the STAT3 inhibitor, SD-1029, in three chordoma cell lines (303). SD-1029 acted synergistically in combination with doxorubicin and cisplatin (303). In 2010, the same group reported STAT3 activation in another 13 chordoma samples and similar functional results with a different STAT3 inhibitor (2-cyano-3,12-dioxooleana-1,9 (11)-dien-28-oic acid-methyl ester; CDDOMe) (177). Dobsahi *et al.* (2007), who studied EGFR and its downstream pathways in various types of sarcomas, reported activation of STAT3 signalling, particularly in tumours of epithelial nature, including synovial sarcomas and chordomas (176). However, this assumption was based on a very limited sample size, which consisted of one and two cases of each of these entities, respectively (176). In summary, there is some evidence for the activation of STAT3 signalling in chordomas, which must be further explored. In our experiments, we found that phosphorylated AKT, ERK1/2 and STAT3 were present in all of our chordoma cell lines (**Figure 20**), supporting existing data on an activation of these pathways in chordoma (4, 6, 11, 169, 172, 177, 303). Whereas PI3K/AKT/mTOR and RAS/RAF/MAPK signalling were dose-dependently suppressed in response to treatment with EGFR inhibitors, this was not the case for phospho-STAT3 (11). Based on our data, we could not determine whether this is indicative of STAT3 signalling's minor relevance for EGFR downstream signalling in chordoma, or whether phospho-STAT3 expression is influenced by another mechanism in this disease. However, phospho-STAT3 was suppressed when we combined

the EGFR inhibitor, sapitinib, and the MET inhibitor, crizotinib, in the EGFR TKI resistant cell line, U-CH2 (**Figure 23**). This finding supports the claim that the role of STAT3 signalling in this disease needs further clarification.

Targeting EGFR/ERBB Signalling in Chordoma

EGFR expression in chordoma been confirmed by several authors (3, 51, 171, 252). Furthermore, inhibitors have also been studied in this disease (51, 54-59, 212, 304). Positive results for gefitinib and erlotinib have been reported *in vitro* for the chordoma cell line, U-CH1 (304). Erlotinib has further been shown to significantly inhibit tumour growth *in vivo* in a patient-derived chordoma mouse xenograft compared to DMSO-treated controls (304). In H&E stained sections of these erlotinib-treated xenografts, chordoma cell lobules appeared to be less dense compared to the controls (304). EGFR inhibitors have also been studied in clinical settings, although mainly as isolated case reports (54-59). Singhal *et al.* (2009) described tumour shrinkage upon erlotinib (Tarceva®) treatment in a patient with progressive recurrent sacral chordoma (57). The neoplasm had not responded to imatinib or the vascular disrupting agent, CYT997 (Selleckchem), so the patient was treated with a standard dose of erlotinib (150 mg/day) (57). Sequencing of the tumour failed to reveal mutations in *EGFR* (exons 18 – 24) (57). The authors reported a grade 2 skin rash, which improved over time (57). There were no signs of upcoming resistance within the reported 11 months of treatment (57)].

Other authors reported clinical and radiological improvements upon combinatory treatment with the monoclonal antibody, cetuximab, and the small molecule inhibitor, gefitinib, in cases of advanced chordoma (56, 59). Hof *et al.* (2006) (56) treated a patient who suffered from a recurrent sacral chordoma, which was associated with lung metastases and a positive inguinal lymph node. The patient received cetuximab (Erbitrux®, Merck KGaA, Darmstadt, Germany) 500 mg (250 mg/m^2, delivered as weekly intravenous infusion) and gefitinib (Iressa®, AstraZeneca, AstraZeneca, Wedel, Germany) 250 mg orally daily (56). The patient had rejected surgery due to anticipated neural lesions and had thus been treated with photon beam irradiation (56). The authors reported a partial regression of the tumour and the pulmonary metastases after two months of treatment with cetuximab/gefitinib (56). However, the therapy had to be discontinued for a month due to side effects (skin rash and gastrointestinal symptoms) (56). When it was continued, the sacral tumour remained stable in size, but the lung metastases further decreased by 10% of their volume, and the tumour-related symptoms were also regressive (56). The authors stated that there was no treatment failure due to upcoming resistance within the reported nine-month observation period (56). Linden *et al.* (2009) (59) also describe the clinical improvement of symptoms related to a spinal cord compression

induced by a primary chordoma located in the second cervical vertebra of a female patient. The patient had undergone debulking surgery and photon beam irradiation but experienced progressive neurological impairments due to a 6.5 x 5.5 cm large residual re-progressing tumour mass (59). Similar to the previous patient (56), this patient was also treated with weekly cetuximab infusions and daily doses of gefitinib (250 mg) (59). After a week's treatment, anal sphincter control returned, and after two weeks, the patient was able to walk supported by a walking frame (59). Also, in this case, anti-EGFR therapy had to be paused for a couple of weeks due to cutaneous side effects (59). After 4 months of treatment, MRI scans showed regression of the spinal cord compression, and the tumour had shrunk to 4.9 x 4.1 cm (59). Other published reports have shown positive effects for erlotinib treatment in combination with the anti-angiogenic drug, bevacizumab (Avastin®) (54, 55). Asklund *et al.* (2011) reported an intracranial lesion that had been non-invasively diagnosed as chordoma and that progressed under radio- and chemotherapy and under combination treatment with erlotinib and cetuximab (54). Due to progression and toxicity issues, the therapeutic regimen was amended to erlotinib (150 mg once daily) and bevacizumab (10 mg/kg once weekly), which resulted in a PET response and a slight tumour shrinkage on MRI (54). In 2014, the same group reported a long-term follow-up of this patient, who had received this combination treatment for 11 months and was free of any tumour-related symptoms until the last follow-up 4.5 years later (55). In addition, the authors described two other patients with histologically verified chordomas who responded to the same combination treatment (55). Launay *et al.* (2011) reported a case of metastasising sacral chordoma that had progressed under imatinib treatment, so that oral treatment with erlotinib (150 mg daily) was initiated (58). After three months, the patient experienced clinical improvement and pain relief (58). Several of the tumour nodules had decreased in size, whereas others stayed stable (58). After 12 months of treatment, which was the last follow-up reported, all target lesions except one were clinically and radiologically stable, and the treatment had been well-tolerated (58).

Recently, Aleksic *et al.* (2016) (305) reported durable response of an EGFR wild-type spinal chordoma to a combined inhibition of EGFR (erlotinib,) and IGF-1R (linsitinib, OSI-906) in course of the phase I OSI-906-103 trial. The authors, who cited our previous work on IGF-1R (1, 305), reported that the female adult patient had been treated with this combination for 18 months, until a partial response according to RECIST criteria was observed (305). The treatment was well-tolerated and the patient remained stable on treatment for a total of five years (305).

In 2013, Stacchiotti *et al.* (51) conducted the first (and only) clinical trial involving an EGFR inhibitor in chordoma patients. In this non-randomised phase II clinical trial, the FDA-approved dual EGFR/ERBB2 inhibitor, lapatinib (Tykerb®/Tyverb®, GSK), was administered to 18 patients with

advanced EGFR-positive chordoma (1500 mg/daily) (51, 212, 306). EGFR positivity was defined as immunohistochemical positivity for EGFR (51, 212). The majority of these patients (n = 16) had previously been treated with imatinib (51). The response rates were evaluated according to Choi criteria, which measures density changes within a tumour rather than actual volumetric changes (307, 308), and which had been chosen as the primary endpoint of this study (51, 307). However, lapatinib exerted only a moderate clinical response, with six patients (33.3%) showing partial response and seven (38.9%) stable disease (51). The median progression-free survival in this study was six months (according to Choi criteria), and the median overall survival was 25 months (51). None of the patients showed tumour shrinkage, and thus response, according to RECIST criteria (51) (308). This moderate clinical response of lapatinib was paralleled by the limited potency and selectivity this compound exerted *in vitro* in our focused compound screen, in which this drug had not come up as a hit when screened at a single concentration (11). When tested alongside other FDA-approved EGFR inhibitors at a later stage of the project, lapatinib exerted inferior potency (11). Possible reasons for this moderate *in vitro* response of lapatinib compared to other EGFR small molecule inhibitors might lie in its chemical structure, which differs from the other FDA-approved inhibitors, as discussed below. Apart from the choice of an appropriate drug candidate, Lebellec *et al.* (2015) addressed another issue, the choice of appropriate endpoints and trial designs for orphan diseases like chordoma (212).

Outcomes from our Focused Compound Screen Suggest that EGFR/ERBB Inhibitors Form a Potential New Treatment Option for Patients with Chordoma

In the absence of recurrent and/or tractable genetic alterations, we chose a phenotypic screening approach to identify mechanism(s) possibly driving chordoma and/or targets that could be translated into clinical practice (11, 218). When we started this project, three authenticated and well-characterised chordoma cell lines (U-CH1, U-CH2, MUG-Chor1) had become available (220, 221, 223). We screened these lines against 1,097 compounds (11). The majority of these (n=1,046) were small molecule kinase inhibitors (11). Twenty-seven of them mediated a chordoma-selective cell kill effect, which means that they did not target normal dermal fibroblasts (11). Normal adult human dermal fibroblasts were chosen as controls, based on the advice of our collaborators from CRT, as notochordal tissue was not available due to its physiological regression during fetal development (8, 11, 309). The majority (21/27) of chordoma selective compounds were EGFR/ERBB inhibitors (11). This finding was consistent across different compound libraries included in our screen (11) and could be reproduced when a second batch of a selection of these compounds was tested (11). What is more, the targets of our largest compound library (PKIS2, comprising 522 compounds) were only released

by GSK after we had provided them with our screening data, which further strengthens our results. When our non-EGFR hit compounds were analysed by "enrichment in pathways"-analysis, it became apparent that VEGFR-1/2 signalling covered most of their target genes (11). This is in line with isolated case reports stating activity of VEGF inhibitors in chordoma patients (11, 54, 55). However, most of these non-EGFR hits were multi-kinase inhibitors, their targets were ill-defined, and/or the compounds were phenotypically less potent compared to the EGFR/ERBB inhibitors (11). For that reason, we focused on EGFR/ERBB TKIs in our subsequent experiments (11). Given the fact that most of the chordoma-selective hit compounds were tool kinases and would not realistically be developed further for an orphan disease, our collaborators from GSK advised us to test EGFR/ERBB inhibitors which had already been FDA-approved and/or were being studied in clinical trials. These drugs had chance of being repurposed for application in chordoma. For that reason, we included six commercially available EGFR inhibitors: (erlotinib (Roche/Genentech), gefitinib (AstraZeneca, Cambridge, Cambridgeshire, UK), sapitinib (AstraZeneca), lapatinib (GSK), afatinib (Boehringer Ingelheim, Ingelheim, Rhineland-Palatinate, Germany) and poziotinib (Spectrum Pharmaceuticals, Irvine, CA, USA) (11, 122, 229, 231, 310). By then, a total of seven human chordoma cell lines (six originating from sacral tumours and one from a clival tumour) had become available (http://www.chordomafoundation.org/) (224). These included the sacral chordoma cell line, U-CH7, which we had established at the UCL Cancer Institute, London, UK. When the commercial EGFR/ERBB inhibitors were tested on these seven chordoma cell lines, we found that four of the lines (U-CH1, U-CH7, MUG-Chor1, UM-Chor1) were sensitive and three (U-CH2, U-CH10, JHC7) were resistant to EGFR inhibition (11).

As stated above, EGFR was the first tyrosine kinase receptor to be linked to tumourigenesis (73, 114, 244, 311), and therapeutic inhibition of this pathway has shown varying success in the treatment of malignant disease (11, 122, 244, 311). A common cause for EGFR activation lies in the presence of mutations and gene amplification, as observed in NSCLC and glioblastoma (11, 101, 122, 312, 313). However, we did not detect *EGFR* mutations or amplifications in our cell lines panel. This is consistent with other published reports (172, 173) and with unpublished data from 30 whole genomes/whole exomes from Professor Flanagan's laboratory at the UCL Cancer Institute, London, UK (11). The absence of *EGFR* mutations in chordomas is shared with other cancers, such as head and neck squamous cell carcinoma, colorectal and pancreatic cancer, which are known to respond to anti-EGFR therapy to varying degrees (11, 113, 244, 314-319). Similar to these tumours, chordoma cell lines express the activated form of the receptor and show suppression of the downstream EGFR signalling pathways following treatment with EGFR inhibitors (11). The clinical relevance of our *in*

vitro studies is supported by the expression of these markers in patients' samples, which has been documented by various authors (3, 4, 6, 169, 171, 172, 252). Specifically, up to 52% of 173 chordoma samples have been reported to express phospho-EGFR (3, 11, 51, 171, 172, 252), although this is likely to be an underestimate, as phosphorylated protein is unstable (4, 6, 11, 171, 172). The significance of our finding that erlotinib exerted a significant kill effect on four of seven chordoma cell lines tested is supported by the response to erlotinib that was observed in a well-characterised patient-derived chordoma xenograft mouse model (11, 304). Furthermore, this is consistent with the significant growth reduction that sapitinib induced in two xenograft mouse models (11). These *in vitro* and *in vivo* data are strengthened by several well-documented reports of chordoma patients showing partial volumetric regression and/or clinical improvement upon EGFR TKI treatment (11, 54-59, 211). However, a small non-randomised phase II clinical trial involving the FDA-approved dual EGFR/ERBB2 inhibitor, lapatinib (Tykerb®/Tyverb®), on 18 patients with advanced chordoma was only a modest clinical success. According to Choi criteria, only six patients (33.3%) had a partial intratumoural response (11, 51). These results are in line with lapatinib's failure of to exert a kill effect at therapeutic concentrations in all but one of our chordoma cell lines *in vitro* (11). In an attempt to address differences in the phenotypic kill effects observed in response to different EGFR TKIs, our collaborators from GSK analysed a selection of EGFR inhibitory compounds to identify similarities in chemical structures and substituents (11). Their overall finding was that compounds such as sapitinib, gefitinib and erlotinib, had small substituents appended to the aniline ring in the 4-position of the quinazoline ring system and seemed to be more effective than compounds such as lapatinib, which had large substituents in that position. However, these findings derived from a small sample size (11). However, the complex relationship of this potency, selectivity and phenotypic response interplay requires further in-depth study to optimise activity for chordoma patients (11).

EGF has been identified as a direct target of *T*, the expression of which is considered to be critical in chordoma growth and pathogenesis. This might explain why EGFR phosphorylation (phospho-EGFR) is present in chordoma (9, 11). The fact that *T* drives EGF expression could also explain why *T* expression is not suppressed in Western blot analysis in response to EGFR inhibitors, a finding also reported by other authors (3, 11). Early phase clinical trials involving vaccines against *T* in patients with lung cancer and chordoma have reported some evidence of clinical activity (68, 320, 321), and it would be interesting to know whether phospho-EGFR is suppressed in clinical samples from these patients (11). If this were the case, then a combination of this vaccine and EGFR inhibitors could possibly be more effective than each of these agents in monotherapy (11).

In an attempt to understand why three of seven chordoma cell lines were resistant to EGFR inhibitors, we studied some frequent mechanisms by which EGFR TKI resistance has been reported to occur (11, 100, 101, 244). In line with other authors, we were unable to detect downstream mutations in *PIK3CA*, *BRAF*, *KRAS*, *MAPK1* and others (11, 100, 101, 244). Nevertheless, *PIK3CA* alterations and losses have been reported in a minority of chordomas, and so these could be used to stratify patients for future EGFR inhibitor clinical trials (173) (11, 170). *ERBB2* amplification, another reported resistance mechanism (101, 244), was not identified in our chordoma cell line panel (11). Furthermore, loss and decreased expression of the tumour suppressor, PTEN, have been correlated to resistance to EGFR TKIs (11, 244, 245). Several authors have reported a loss of heterozygosity for *PTEN* in chordoma (11, 172, 173, 215, 244, 245, 278, 309, 322). However, our *in vitro* results did not allow us to predict response to EGFR inhibition based on PTEN expression (11). Neither could we correlate protein expression levels of PTEN, E-Cadherin and YAP with the presence and/or absence of resistance to EGFR TKIs in our cell line panel, although this was not studied in depth (11).

EGFR resistance may also be brought about by the activation of bypass signalling pathways, such as MET (11, 101, 244). It is therefore noteworthy that MET signalling was activated in one of our resistant cell lines, U-CH2, and that a combination of the MET inhibitor, crizotinib, and the EGFR inhibitor, sapitinib, exhibited a synergistic effect on cell kill in this cell line (11). The absence of *MET* amplifications or mutations leaves the mechanism of activation unanswered and is in line with results from clinical chordoma samples, in which *MET* amplifications were only detected in two out of 116 specimens (11). However, this has not been studied exhaustively, as MET can be activated by various other mechanisms, such as crosstalks with several receptor tyrosine kinases (11, 137). Resistance mechanisms to EGFR TKIs are versatile, and many of them remain unexplained even in common cancers (11, 101). For that reason, it was beyond the scope of this project to pursue this in greater detail, although resistance issues will have to be addressed if EGFR inhibitors are pursued further for clinical use in chordoma therapy (11).

In summary, the collective data from our phenotypic compound screen showed that EGFR inhibitors represent the group of compounds within our extensive screen that was most effective against chordoma cell growth (11). There have been reports of other therapeutics found to exert activity against chordoma, but ultimately, whether some patients with chordoma benefit from EGFR inhibitors alone or in combination with these other agents, is likely to only be resolved in a prospective, randomised clinical trial (11, 15, 212, 222). We propose that such a study should involve in-depth biological studies of the tumour samples pre- and post-treatment, with the aim of

explaining the mechanism(s) by which some chordomas are primarily resistant or develop secondary resistance to EGFR inhibitors (11).

Limitations of these Studies

We are aware that experimental limitations and hazards apply to our studies (11). Our *in vitro* and *in vivo* experiments were conducted on model systems, which included human chordoma cell lines and xenograft mouse models, both of which do not fully represent conditions found in human neoplasms (323-326). For that reason, both systems suffer from a variety of limitations. As the statistician George E. P. Box appropriately remarked, "Essentially, all models are wrong, some models are useful" (327).

To begin, we used immortalised cell lines grown in monolayer cultures. These cultures do not reflect the three-dimensional organisation and the three-dimensional cell-to-cell interactions present in a neoplasm, nor do they account for its microenvironment and its vascularisation (325, 326). During their immortalisation, cell lines undergo selection for single cell clones, which do not represent the heterogeneities observed within a neoplasm. And, these clones are not likely to mirror a tumour's evolution during drug treatment (324, 326). Due to the lack of a broader variety of available chordoma cell lines, intertumoural heterogeneities are also not sufficiently reflected (324, 325). This lack of a broad range of well-characterised model systems is an acknowledged problem in drug discovery in general (328) and in orphan diseases (such as chordomas) in particular. In an attempt to address different sites of tumour origin, we added the first available clival chordoma cell line (UM-Chor1) to our panel, which consisted of lines derived from sacral neoplasms (11, 220-224) (http://www.chordomafoundation.org/).

Fast-dividing cell clones are selected in course of a cell line's immortalisation, as these overgrow well-differentiated clones (324). Yet, fast-dividing clones are usually preferred for *in vitro* experiments, as these require a large quantity of cells in a comparatively short interval of time (324, 325). Thus, the metabolic features and adaption processes of well-differentiated clones might be lost (324, 326). Furthermore, abrupt exchanges of media and the lack of oxygen under culture conditions do not display physiological conditions (324). Neither does fetal calf serum, which is added to the culture medium to feed the cells (324, 326). Antibiotics and solvents, such as DMSO, are also known to exert negative and even toxic effects on the cells (324, 326). To keep these toxicities low, our collaborators from CRT, who have extensive experience in drug screening, conducted preliminary experiments to determine the effect size of these confounders and to define tolerable cut-off concentrations for these agents. What is more, specialists from CRT frequently quality-controlled the

compounds for degradation and prepared them for proper storage and use. Throughout the process, automated handling and drug-dispensing systems were routinely used to minimise pipetting errors. Furthermore, we tested different batches for a selection of compounds to double-check the reproducibility of our results.

Limitations also apply to our reagents. The WST-1 assay (Roche) is based on the metabolic (mitochondrial) activity of cells, which might not obligatory correlate with cell number (329). For that reason, we double-checked our key findings with lysis-based assays (Cell-Titer-Glo®, Promega), and we could determine a good overall reproducibility (data not shown). In addition, we used reserved batches of WST-1 and fetal bovine serum for tour experiments to minimise variations between the reagents.

It is known that misidentifications and infections of cell lines are a severe issue and cause misleading, non-reproducible results (324). This is why we only included chordoma cell lines in our study once they had been authenticated by the Chordoma Foundation via an independent laboratory (http://www.chordomafoundation.org/). What is more, we frequently validated our cell lines by STR analysis to make sure they had not been mixed up or undergone significant changes in culture. We regularly checked our lines for mycoplasma infections as a matter of routine quality control.

In vivo testings were conducted by a third, independent laboratory, which was chosen by the Chordoma Foundation Drug Screening Pipeline for its reputation for high standards in experimental work and quality control. Nevertheless, it is a well-recognised fact that mice do not sufficiently mirror human beings (325), and that results obtained in comparatively small subcutaneous mouse xenografts do not necessarily match results obtained in large human spinal tumours (325). Also, inbred animal strains, which are immunocompromised and/or genetically altered, are likely to react differently compared to genetically diverse, immunocompetent humans (325).

However, basic limitations of preclinical studies are not likely to be overcome as long as efficient alternatives are lacking. Possible alternatives are being sought by the pharmaceutical industry and researchers alike by creating large, diverse panels of well-characterised cell lines, primary cultures and xenografts, which are supposed to be more likely to reflect heterogeneities within and between tumours (328). In addition, there is a trend towards more sophisticated model systems (e.g. 3D (co-)culture systems and advanced animal models), which are thought to be more likely to mimic natural conditions (325, 330, 331). In orthotopic models, animals grow tumours in their original sites rather than subcutaneously (325, 332), and syngeneic (allograft) animal models possess a functional

immune system (325, 333). However, whether more sophisticated models will actually improve the predictiveness of preclinical studies remains to be seen (325).

Apart from the models applied, our choice of a negative control might also raise questions. Ideally, we would have chosen non-neoplastic notochordal tissue, as this is the tissue from which chordomas originate (15). However, this was not feasible, because notochord is a transient embryonic structure that largely disappears during fetal development (334). For our HDAC study, we therefore chose immortalised fibroblasts that were derived from the same patient as the chordoma cell line we studied (MUG-Chor1). And, for our phenotypic compound screen, we tested normal adult human dermal fibroblasts (NAHDF) from the ATCC (2, 11). Fibroblasts can be found ubiquitously in the human body and in the environment of many tumours (including chordoma), and our collaborators from CRT, who are experts in compound screening, considered them a very suitable choice of control cells for this purpose.

Even though the collective data from our phenotypic screen showed that EGFR inhibitors represented the only group of compounds effective against chordoma, other therapeutics have also been reported to exert activity against chordoma (11, 15, 212, 222). Our findings do not necessarily contradict these reports. Our screen was conducted on a limited number of cell lines, due to the orphan nature of this disease. We included all verified chordoma cell lines that were available and that could be expanded to an extent that would allow them to be tested against our compound panel. Statistically, however, the size of this panel must be regarded as limited (328). What is more, our kinase libraries, which contained a large number and a broad variety of compounds, might not have included sufficient numbers and/or chemotypes of certain therapeutics to allow final conclusions about their activity in chordoma (335). Nor did we test monoclonal antibodies, as this would have changed the setup of our experimental designs, which all collaborators considered to be beyond the scope of this project. Aware of these and other limitations, we imposed a high level of quality control measurements to ensure the generation of robust data (214, 217, 218). Nevertheless, our results need to be interpreted with a critical awareness of these limiting factors, and constant efforts need to be undertaken to minimise and/or to overcome these limitations for future research.

Outlook

Two independent laboratories yielded promising collective data on EGFR inhibitors. The key findings from our phenotypic screen were reproduced by an Italian laboratory that used a similar (phenotypic) screening approach. Those researchers also found that EGFR inhibitors represented the only group of compounds active against chordoma *in vitro*. Even though these data have not been

published to date and are likely to show differences in reported details, this further strengthens the case for EGFR inhibitors in chordoma treatment. What is more, these *in vitro* data have been supported by animal studies. The latter were conducted via the Chordoma Foundation Drug Screening Pipeline at the START laboratories in Texas, USA, and will be released soon. Several well-documented case reports showed tumour regression and symptom relief in patients with chordoma who were treated with EGFR inhibitors. Based on these promising collective data on EGFR inhibitors, a multicentre clinical trial on advanced and metastasising chordoma is planned. This trial, which will be the first prospective, randomised drug trial in chordoma, will involve a second-generation EGFR inhibitor (Afatinib, Gilotrif®, Boehringer Ingelheim). It will be conducted at the centres of Milan, Italy; Leiden, The Netherlands; and London, UK. Currently, feasible endpoints and read-outs for this trial are being discussed. For chordoma patients and researchers alike, this trial is a remarkable achievement, and would not have been possible without collective efforts from international collaborators, funding bodies and supporters who substantially contributed to this underlying work. For that reason, we (Professor Flanagan, our collaborators from Cancer Research Technology, GlaxoSmithKline, and I) were awarded the "Uncommon Collaboration Award" in course of the 5th International Chordoma Research Workshop 2016 in Boston.

Our results have been published in the *Journal of Pathology* (IF 7.4) and are being disseminated at various meetings and conferences. These include the 29th Annual Meeting of the European Muscolo-Skeletal Oncology Society (EMSOS) 2016 in La Baule, France, as well as the 5th International Chordoma Research Workshop 2016 in Boston, MA, USA; the University College London (UCL) Annual Conference 2016; and others. Subsequent studies will focus on biomarkers for resistance and response, improved model systems and combination therapies, and these studies are currently in the planning stage.

In summary, the approaches we have chosen to identify therapeutic targets for chordoma have become more functional and comprehensive during the time I spent on this thesis. Both IGF-1R and HDACs seemed to be promising candidates at the time when I started these studies. However, these targets have not live up to clinicians' expectations when they were inhibited in clinical trials: So was IGF-1R dropped after having shown only moderate responses in various sarcoma types (132, 133), and HDACs were ineffective and toxic the treatment of solid tumours (277). Nevertheless, both targets might be of interest for future combinatory approaches (277, 305). In order to minimise potentially misleading hypotheses regarding the nature and/or the structure of a target, we then undertook a phenotypic screen on more than 1,000 kinase inhibitors. From this screen, the EGFR/ERBB family emerged as key target class inhibiting chordoma growth *in vitro* and *in vivo*. Two independent laboratories have also yielded promising data on EGFR inhibitors in this disease.

Based on our collective work, there is now going to be a prospective, randomised clinical trial involving an EGFR inhibitor in patients with advanced chordoma. This is an important achievement, as it will be the first prospective, multicentre trial in this orphan disease. There are many people and institutions from various countries who have contributed to this achievement, and that have enabled patients, clinicians and researchers alike to hope that EGFR inhibitors will prove beneficial for patients with chordoma. Therefore, I am happy that this work is part of these contributions and would like to thank all people, institutions, and funding bodies for the support they have provided during the work on this thesis.

References

1.r Scheipl S, Froehlich EV, Leithner A*, et al.* Does insulin-like growth factor 1 receptor (IGF-1R) targeting provide new treatment options for chordomas? A retrospective clinical and immunohistochemical study. Histopathology. 2012 May;60(6):999-1003.

2.r Scheipl S, Lohberger B, Rinner B*, et al.* Histone deacetylase inhibitors as potential therapeutic approaches for chordoma: an immunohistochemical and functional analysis. J Orthop Res. 2013 Dec;31(12):1999-2005.

3.r Shalaby A, Presneau N, Ye H*, et al.* The role of epidermal growth factor receptor in chordoma pathogenesis: a potential therapeutic target. J Pathol. 2011 Feb;223(3):336-346.

4.r Shalaby AA, Presneau N, Idowu BD*, et al.* Analysis of the fibroblastic growth factor receptor-RAS/RAF/MEK/ERK-ETS2/brachyury signalling pathway in chordomas. Mod Pathol. 2009 Aug;22(8):996-1005.

5.r Pillay N, Plagnol V, Tarpey PS*, et al.* A common single-nucleotide variant in T is strongly associated with chordoma. Nat Genet. 2012 Nov;44(11):1185-1187.

6.r Presneau N, Shalaby A, Idowu B*, et al.* Potential therapeutic targets for chordoma: PI3K/AKT/TSC1/TSC2/mTOR pathway. Br J Cancer. 2009 May 5;100(9):1406-1414.

7.r Presneau N, Shalaby A, Ye H*, et al.* Role of the transcription factor T (brachyury) in the pathogenesis of sporadic chordoma: a genetic and functional-based study. J Pathol. 2011 Feb;223(3):327-335.

8.r Vujovic S, Henderson S, Presneau N*, et al.* Brachyury, a crucial regulator of notochordal development, is a novel biomarker for chordomas. J Pathol. 2006 Jun;209(2):157-165.

9.r Nelson AC, Pillay N, Henderson S*, et al.* An integrated functional genomics approach identifies the regulatory network directed by brachyury (T) in chordoma. J Pathol. 2012 Nov;228(3):274-285.

10.r Flanagan A, Yamaguchi T. Chordoma. In: Fletcher C, Bridge J, Hogendoorn P, Mertens F, editors. World Health Organization Classification of Tumours of Soft Tissue and Bone. 4th Edition ed. Lyon: WHO, IARC Press; 2013. p. 328, 329.

11.r Scheipl S, Barnard M, Cottone L*, et al.* EGFR inhibitors identified as a potential treatment for chordoma in a focused compound screen. J Pathol. 2016 Apr 22;239(3):320-334.

12.r Walcott BP, Nahed BV, Mohyeldin A*, et al.* Chordoma: current concepts, management, and future directions. Lancet Oncol. 2012 Feb;13(2):e69-76.

13.r Williams BJ, Raper DM, Godbout E*, et al.* Diagnosis and treatment of chordoma. J Natl Compr Canc Netw. 2013 Jun 1;11(6):726-731.

14.r Smoll NR, Gautschi OP, Radovanovic I*, et al.* Incidence and relative survival of chordomas: the standardized mortality ratio and the impact of chordomas on a population. Cancer. 2013 Jun 1;119(11):2029-2037.

15.r Stacchiotti S, Sommer J. Building a global consensus approach to chordoma: a position paper from the medical and patient community. Lancet Oncol. 2015 Feb;16(2):e71-e83.

16.r Nibu Y, Jose-Edwards DS, Di Gregorio A. From notochord formation to hereditary chordoma: the many roles of Brachyury. Biomed Res Int. 2013;2013:826435.

17.r Bone sarcomas: ESMO Clinical Practice Guidelines for diagnosis, treatment and follow-up. Ann Oncol. 2014 Sep;25 Suppl 3:iii113-123.

18.r Chugh R, Tawbi H, Lucas DR*, et al.* Chordoma: the nonsarcoma primary bone tumor. Oncologist. 2007 Nov;12(11):1344-1350.

19.r Yang XR, Ng D, Alcorta DA*, et al.* T (brachyury) gene duplication confers major susceptibility to familial chordoma. Nat Genet. 2009 Nov;41(11):1176-1178.

20.r Bhadra AK, Casey AT. Familial chordoma. A report of two cases. J Bone Joint Surg Br. 2006 May;88(5):634-636.

21.r Kelley MJ, Korczak JF, Sheridan E*, et al.* Familial chordoma, a tumor of notochordal remnants, is linked to chromosome 7q33. Am J Hum Genet. 2001 Aug;69(2):454-460.

22.r Casali PG, Stacchiotti S, Sangalli C*, et al.* Chordoma. Curr Opin Oncol. 2007 Jul;19(4):367-370.

23.r Muro K, Das S, Raizer JJ. Chordomas of the craniospinal axis: multimodality surgical, radiation and medical management strategies. Expert Rev Neurother. 2007 Oct;7(10):1295-1312.

24.r Sciubba DM, Chi JH, Rhines LD*, et al.* Chordoma of the spinal column. Neurosurg Clin N Am. 2008 Jan;19(1):5-15.

25.r Tirabosco R, Mangham DC, Rosenberg AE*, et al.* Brachyury expression in extra-axial skeletal and soft tissue chordomas: a marker that distinguishes chordoma from mixed tumor/myoepithelioma/parachordoma in soft tissue. Am J Surg Pathol. 2008 Apr;32(4):572-580.

26.r Lauer SR, Edgar MA, Gardner JM*, et al.* Soft tissue chordomas: a clinicopathologic analysis of 11 cases. Am J Surg Pathol. 2013 May;37(5):719-726.

27.r Suzuki H, Yamashiro K, Takeda H*, et al.* Extra-axial soft tissue chordoma of wrist. Pathol Res Pract. 2011 May 15;207(5):327-331.

28.r Yamaguchi T, Watanabe-Ishiiwa H, Suzuki S*, et al.* Incipient chordoma: a report of two cases of early-stage chordoma arising from benign notochordal cell tumors. Mod Pathol. 2005 Jul;18(7):1005-1010.

29.r Amer HZ, Hameed M. Intraosseous benign notochordal cell tumor. Arch Pathol Lab Med. 2010 Feb;134(2):283-288.

30.r Deshpande V, Nielsen GP, Rosenthal DI*, et al.* Intraosseous benign notochord cell tumors (BNCT): further evidence supporting a relationship to chordoma. Am J Surg Pathol. 2007 Oct;31(10):1573-1577.

31.r Nishiguchi T, Mochizuki K, Tsujio T*, et al.* Lumbar vertebral chordoma arising from an intraosseous benign notochordal cell tumour: radiological findings and histopathological description with a good clinical outcome. Br J Radiol. 2010 Mar;83(987):e49-53.

32.r Lee-Jones L, Aligianis I, Davies PA*, et al.* Sacrococcygeal chordomas in patients with tuberous sclerosis complex show somatic loss of TSC1 or TSC2. Genes Chromosomes Cancer. 2004 Sep;41(1):80-85.

33.r Leung AK, Robson WL. Tuberous sclerosis complex: a review. J Pediatr Health Care. 2007 Mar-Apr;21(2):108-114.

34.r McMaster ML, Goldstein AM, Parry DM. Clinical features distinguish childhood chordoma associated with tuberous sclerosis complex (TSC) from chordoma in the general paediatric population. J Med Genet. 2011 Jul;48(7):444-449.

35.r Papagelopoulos PJ, Mavrogenis AF, Galanis EC*, et al.* Chordoma of the spine: clinicopathological features, diagnosis, and treatment. Orthopedics. 2004 Dec;27(12):1256-1263; quiz 1264-1255.

36.r Yamaguchi T, Suzuki S, Ishiiwa H*, et al.* Intraosseous benign notochordal cell tumours: overlooked precursors of classic chordomas? Histopathology. 2004 Jun;44(6):597-602.

37.r Showell C, Binder O, Conlon FL. T-box genes in early embryogenesis. Dev Dyn. 2004 Jan;229(1):201-218.

38.r McMaster ML, Goldstein AM, Bromley CM*, et al.* Chordoma: incidence and survival patterns in the United States, 1973-1995. Cancer Causes Control. 2001 Jan;12(1):1-11.

39.r Whelan J, McTiernan A, Cooper N*, et al.* Incidence and survival of malignant bone sarcomas in England 1979-2007. Int J Cancer. 2012 Aug 15;131(4):E508-517.

40.r Webber C, Gospodarowicz M, Sobin LH*, et al.* Improving the TNM classification: findings from a 10-year continuous literature review. Int J Cancer. 2014 Jul 15;135(2):371-378.

41.r Juenemann KP, Lue TF, Schmidt RA*, et al.* Clinical significance of sacral and pudendal nerve anatomy. J Urol. 1988 Jan;139(1):74-80.

42.r Fourney DR, Gokaslan ZL. Current management of sacral chordoma. Neurosurg Focus. 2003 Aug 15;15(2):E9.

43.r Puri A, Agarwal MG, Shah M*, et al.* Decision making in primary sacral tumors. Spine J. 2009 May;9(5):396-403.

44.r DeLaney TF, Liebsch NJ, Pedlow FX*, et al.* Long-term results of Phase II study of high dose photon/proton radiotherapy in the management of spine chordomas, chondrosarcomas, and other sarcomas. J Surg Oncol. 2014 Aug;110(2):115-122.

45.r Allen AM, Pawlicki T, Dong L*, et al.* An evidence based review of proton beam therapy: the report of ASTRO's emerging technology committee. Radiother Oncol. 2012 Apr;103(1):8-11.

46.r Lodge M, Pijls-Johannesma M, Stirk L*, et al.* A systematic literature review of the clinical and cost-effectiveness of hadron therapy in cancer. Radiother Oncol. 2007 May;83(2):110-122.

47.r Al-Rahawan MM, Siebert JD, Mitchell CS*, et al.* Durable complete response to chemotherapy in an infant with a clival chordoma. Pediatr Blood Cancer. 2012 Aug;59(2):323-325.

48.r Bayrak OF, Aydemir E, Gulluoglu S*, et al.* The effects of chemotherapeutic agents on differentiated chordoma cells. J Neurosurg Spine. 2011 Dec;15(6):620-624.

49.r Scimeca PG, James-Herry AG, Black KS*, et al.* Chemotherapeutic treatment of malignant chordoma in children. J Pediatr Hematol Oncol. 1996 May;18(2):237-240.

50.r Fleming GF, Heimann PS, Stephens JK*, et al.* Dedifferentiated chordoma. Response to aggressive chemotherapy in two cases. Cancer. 1993 Aug 1;72(3):714-718.

51.r Stacchiotti S, Tamborini E, Lo Vullo S*, et al.* Phase II study on lapatinib in advanced EGFR-positive chordoma. Ann Oncol. 2013 Jul;24(7):1931-1936.

52.r George S, Merriam P, Maki RG*, et al.* Multicenter phase II trial of sunitinib in the treatment of nongastrointestinal stromal tumor sarcomas. J Clin Oncol. 2009 Jul 1;27(19):3154-3160.

53.r Bompas E, Le Cesne A, Tresch-Bruneel E*, et al.* Sorafenib in patients with locally advanced and metastatic chordomas: a phase II trial of the French Sarcoma Group (GSF/GETO). Ann Oncol. 2015 Oct;26(10):2168-2173.

54.r Asklund T, Danfors T, Henriksson R. PET response and tumor stabilization under erlotinib and bevacizumab treatment of an intracranial lesion non-invasively diagnosed as likely chordoma. Clin Neuropathol. 2011 Sep-Oct;30(5):242-246.

55.r Asklund T, Sandstrom M, Shahidi S*, et al.* Durable stabilization of three chordoma cases by bevacizumab and erlotinib. Acta Oncol. 2014 Jul;53(7):980-984.

56.r Hof H, Welzel T, Debus J. Effectiveness of cetuximab/gefitinib in the therapy of a sacral chordoma. Onkologie. 2006 Dec;29(12):572-574.

57.r Singhal N, Kotasek D, Parnis FX. Response to erlotinib in a patient with treatment refractory chordoma. Anticancer Drugs. 2009 Nov;20(10):953-955.

58.r Launay SG, Chetaille B, Medina F*, et al.* Efficacy of epidermal growth factor receptor targeting in advanced chordoma: case report and literature review. BMC Cancer. 2011;11:423.

59.r Linden O, Stenberg L, Kjellen E. Regression of cervical spinal cord compression in a patient with chordoma following treatment with cetuximab and gefitinib. Acta Oncol. 2009;48(1):158-159.

60.r Toporkiewicz M, Meissner J, Matusewicz L*, et al.* Toward a magic or imaginary bullet? Ligands for drug targeting to cancer cells: principles, hopes, and challenges. Int J Nanomedicine. 2015;10:1399-1414.

61.r Cao Y, DePinho RA, Ernst M*, et al.* Cancer research: past, present and future. Nat Rev Cancer. 2011 Oct;11(10):749-754.

62.r Jaffe N. Osteosarcoma: Review of the Past, Impact on the Future.The American Experience. In: Jaffe N, Bruland ØS, Bielack S, editors. Pediatric and Adolescent Osteosarcoma New York: Springer; 2009. p. 239-262.

63.r Ozaki T. Diagnosis and treatment of Ewing sarcoma of the bone: a review article. J Orthop Sci. 2015 Mar;20(2):250-263.

64.r Huang M, Shen A, Ding J*, et al.* Molecularly targeted cancer therapy: some lessons from the past decade. Trends Pharmacol Sci. 2014 Jan;35(1):41-50.

65.r Naldini L. Gene therapy returns to centre stage. Nature. 2015 Oct 15;526(7573):351-360.

66.r Cross D, Burmester JK. Gene therapy for cancer treatment: past, present and future. Clin Med Res. 2006 Sep;4(3):218-227.

67.r Heery CR, Singh BH, Rauckhorst M*, et al.* Phase I trial of a yeast-based therapeutic cancer vaccine (GI-6301) targeting the transcription factor brachyury. Cancer Immunol Res. 2015 Jun 30.

68.r Hamilton DH, Litzinger MT, Jales A*, et al.* Immunological targeting of tumor cells undergoing an epithelial-mesenchymal transition via a recombinant brachyury-yeast vaccine. Oncotarget. 2013 Oct;4(10):1777-1790.

69.r Robbins PF, Morgan RA, Feldman SA*, et al.* Tumor regression in patients with metastatic synovial cell sarcoma and melanoma using genetically engineered lymphocytes reactive with NY-ESO-1. J Clin Oncol. 2011 Mar 1;29(7):917-924.

70.r Veldwijk MR, Berlinghoff S, Laufs S*, et al.* Suicide gene therapy of sarcoma cell lines using recombinant adeno-associated virus 2 vectors. Cancer Gene Ther. 2004 Aug;11(8):577-584.

71.r Scott AM, Wolchok JD, Old LJ. Antibody therapy of cancer. Nat Rev Cancer. 2012 Apr;12(4):278-287.

72.r Strebhardt K, Ullrich A. Paul Ehrlich's magic bullet concept: 100 years of progress. Nat Rev Cancer. 2008 Jun;8(6):473-480.

73.r Cohen S. Nobel lecture. Epidermal growth factor. Biosci Rep. 1986 Dec;6(12):1017-1028.

74.r Smith MR. Rituximab (monoclonal anti-CD20 antibody): mechanisms of action and resistance. Oncogene. 2003 Oct 20;22(47):7359-7368.

75.r Mok CC. Rituximab for the treatment of rheumatoid arthritis: an update. Drug Des Devel Ther. 2014;8:87-100.

76.r Arteaga CL, Sliwkowski MX, Osborne CK*, et al.* Treatment of HER2-positive breast cancer: current status and future perspectives. Nat Rev Clin Oncol. 2012 Jan;9(1):16-32.

77.r Cohen MH, Williams G, Johnson JR*, et al.* Approval summary for imatinib mesylate capsules in the treatment of chronic myelogenous leukemia. Clin Cancer Res. 2002 May;8(5):935-942.

78.r Marcucci G, Perrotti D, Caligiuri MA. Understanding the molecular basis of imatinib mesylate therapy in chronic myelogenous leukemia and the related mechanisms of resistance. Commentary re: A. N.

Mohamed et al., The effect of imatinib mesylate on patients with Philadelphia chromosome-positive chronic myeloid leukemia with secondary chromosomal aberrations. Clin. Cancer Res., 9: 1333-1337, 2003. Clin Cancer Res. 2003 Apr;9(4):1248-1252.

79.r Guilhot F. Indications for imatinib mesylate therapy and clinical management. Oncologist. 2004;9(3):271-281.

80.r Bhamidipati PK, Kantarjian H, Cortes J*, et al.* Management of imatinib-resistant patients with chronic myeloid leukemia. Ther Adv Hematol. 2013 Apr;4(2):103-117.

81.r Kantarjian HM, Talpaz M, O'Brien S*, et al.* Imatinib mesylate for Philadelphia chromosome-positive, chronic-phase myeloid leukemia after failure of interferon-alpha: follow-up results. Clin Cancer Res. 2002 Jul;8(7):2177-2187.

82.r Koh JS, Trent J, Chen L*, et al.* Gastrointestinal stromal tumors: overview of pathologic features, molecular biology, and therapy with imatinib mesylate. Histol Histopathol. 2004 Apr;19(2):565-574.

83.r Nakamura I, Kariya Y, Okada E*, et al.* A Novel Chromosomal Translocation Associated With COL1A2-PDGFB Gene Fusion in Dermatofibrosarcoma Protuberans: PDGF Expression as a New Diagnostic Tool. JAMA Dermatol. 2015 Dec 1;151(12):1330-1337.

84.r Riechmann L, Clark M, Waldmann H*, et al.* Reshaping human antibodies for therapy. Nature. 1988 Mar 24;332(6162):323-327.

85.r Imai K, Takaoka A. Comparing antibody and small-molecule therapies for cancer. Nat Rev Cancer. 2006 Sep;6(9):714-727.

86.r Saletti P, Molinari F, Dosso SD*, et al.* EGFR signaling in colorectal cancer: a clinical perspective. Gastrointestinal Cancer: Targets and Therapy. 2015;5:21-38.

87.r Schmiedel J, Blaukat A, Li S*, et al.* Matuzumab binding to EGFR prevents the conformational rearrangement required for dimerization. Cancer Cell. 2008 Apr;13(4):365-373.

88.r Olayioye MA, Neve RM, Lane HA*, et al.* The ErbB signaling network: receptor heterodimerization in development and cancer. EMBO J. 2000 Jul 3;19(13):3159-3167.

89.r Callahan MK, Wolchok JD, Allison JP. Anti-CTLA-4 antibody therapy: immune monitoring during clinical development of a novel immunotherapy. Semin Oncol. 2010 Oct;37(5):473-484.

90.r Funt SA, Page DB, Wolchok JD*, et al.* CTLA-4 antibodies: new directions, new combinations. Oncology (Williston Park). 2014 Nov;28 Suppl 3:6-14.

91.r Schirrmann T, Steinwand M, Wezler X*, et al.* CD30 as a therapeutic target for lymphoma. BioDrugs. 2014 Apr;28(2):181-209.

92.r Alinari L, Lapalombella R, Andritsos L*, et al.* Alemtuzumab (Campath-1H) in the treatment of chronic lymphocytic leukemia. Oncogene. 2007 May 28;26(25):3644-3653.

93.r Ahn NG, Resing KA. Cell biology. Lessons in rational drug design for protein kinases. Science. 2005 May 27;308(5726):1266-1267.

94.r Zhang J, Yang PL, Gray NS. Targeting cancer with small molecule kinase inhibitors. Nat Rev Cancer. 2009 Jan;9(1):28-39.

95.r Cheng HC, Qi RZ, Paudel H*, et al.* Regulation and function of protein kinases and phosphatases. Enzyme Res. 2011;2011:794089.

96.r Shchemelinin I, Sefc L, Necas E. Protein kinases, their function and implication in cancer and other diseases. Folia Biol (Praha). 2006;52(3):81-100.

97.r Josso N, di Clemente N. Serine/threonine kinase receptors and ligands. Curr Opin Genet Dev. 1997 Jun;7(3):371-377.

98.r Zhao B, Chen YG. Regulation of TGF-beta Signal Transduction. Scientifica (Cairo). 2014;2014:874065.

99.r Schöffski P, Cornillie J, Wozniak A*, et al.* Soft Tissue Sarcoma: An Update on Systemic Treatment Options for Patients with Advanced Disease. Oncology Research and Treatment. 2014;37:355–362.

100.r Stewart EL, Tan SZ, Liu G*, et al.* Known and putative mechanisms of resistance to EGFR targeted therapies in NSCLC patients with EGFR mutations-a review. Transl Lung Cancer Res. 2015 Feb;4(1):67-81.

101.r Camidge DR, Pao W, Sequist LV. Acquired resistance to TKIs in solid tumours: learning from lung cancer. Nat Rev Clin Oncol. 2014 Aug;11(8):473-481.

102.r Burrell RA, Swanton C. Tumour heterogeneity and the evolution of polyclonal drug resistance. Mol Oncol. 2014 Sep 12;8(6):1095-1111.

103.r Liegl B, Kepten I, Le C*, et al.* Heterogeneity of kinase inhibitor resistance mechanisms in GIST. J Pathol. 2008 Sep;216(1):64-74.

104.r Huang L, Fu L. Mechanisms of resistance to EGFR tyrosine kinase inhibitors. Acta Pharm Sin B. 2015 Sep;5(5):390-401.

105.r Zhang Z, Lee JC, Lin L*, et al.* Activation of the AXL kinase causes resistance to EGFR-targeted therapy in lung cancer. Nat Genet. 2012 Aug;44(8):852-860.

106.r Ng KP, Hillmer AM, Chuah CT*, et al.* A common BIM deletion polymorphism mediates intrinsic resistance and inferior responses to tyrosine kinase inhibitors in cancer. Nat Med. 2012 Apr;18(4):521-528.

107.r Flaherty KT, Wargo JA, Bivona TG. YAP in MAPK pathway targeted therapy resistance. Cell Cycle. 2015;14(12):1765-1766.

108.r McGranahan N, Swanton C. Biological and therapeutic impact of intratumor heterogeneity in cancer evolution. Cancer Cell. 2015 Jan 12;27(1):15-26.

109.r Zielinski C, Knapp S, Mascaux C*, et al.* Rationale for targeting the immune system through checkpoint molecule blockade in the treatment of non-small-cell lung cancer. Ann Oncol. 2013 May;24(5):1170-1179.

110.r Han W, Lo HW. Landscape of EGFR signaling network in human cancers: biology and therapeutic response in relation to receptor subcellular locations. Cancer Lett. 2012 May 28;318(2):124-134.

111.r Herbst RS. Review of epidermal growth factor receptor biology. Int J Radiat Oncol Biol Phys. 2004;59(2 Suppl):21-26.

112.r Tebbutt N, Pedersen MW, Johns TG. Targeting the ERBB family in cancer: couples therapy. Nat Rev Cancer. 2013 Sep;13(9):663-673.

113.r Jutten B, Rouschop KM. EGFR signaling and autophagy dependence for growth, survival, and therapy resistance. Cell Cycle. 2014;13(1):42-51.

114.r Normanno N, De Luca A, Bianco C*, et al.* Epidermal growth factor receptor (EGFR) signaling in cancer. Gene. 2006 Jan 17;366(1):2-16.

115.r Schneider MR, Yarden Y. Structure and function of epigen, the last EGFR ligand. Semin Cell Dev Biol. 2014 Apr;28:57-61.

116.r Iqbal N. Human Epidermal Growth Factor Receptor 2 (HER2) in Cancers: Overexpression and Therapeutic Implications. Mol Biol Int. 2014;2014:852748.

117.r Ma J, Lyu H, Huang J*, et al.* Targeting of erbB3 receptor to overcome resistance in cancer treatment. Mol Cancer. 2014;13:105.

118.r Schlessinger J. Cell signaling by receptor tyrosine kinases. Cell. 2000 Oct 13;103(2):211-225.

119.r Kang J-H. Protein Kinase C (PKC) Isozymes and Cancer. New Journal of Science. 2014;2014:36 pages.

120.r Griner EM, Kazanietz MG. Protein kinase C and other diacylglycerol effectors in cancer. Nat Rev Cancer. 2007 Apr;7(4):281-294.

121.r Yu H, Lee H, Herrmann A*, et al.* Revisiting STAT3 signalling in cancer: new and unexpected biological functions. Nat Rev Cancer. 2014 Nov;14(11):736-746.

122.r Roskoski R, Jr. The ErbB/HER family of protein-tyrosine kinases and cancer. Pharmacol Res. 2014 Jan;79:34-74.

123.r Luo M, Fu LW. Redundant kinase activation and resistance of EGFR-tyrosine kinase inhibitors. Am J Cancer Res. 2014;4(6):608-628.

124.r Avnet S, Sciacca L, Salerno M*, et al.* Insulin receptor isoform A and insulin-like growth factor II as additional treatment targets in human osteosarcoma. Cancer Res. 2009 Mar 15;69(6):2443-2452.

125.r Chitnis MM, Yuen JS, Protheroe AS*, et al.* The type 1 insulin-like growth factor receptor pathway. Clin Cancer Res. 2008 Oct 15;14(20):6364-6370.

126.r Duan Z, Choy E, Harmon D*, et al.* Insulin-like growth factor-I receptor tyrosine kinase inhibitor cyclolignan picropodophyllin inhibits proliferation and induces apoptosis in multidrug resistant osteosarcoma cell lines. Mol Cancer Ther. 2009 Aug;8(8):2122-2130.

127.r Riedemann J, Macaulay VM. IGF1R signalling and its inhibition. Endocr Relat Cancer. 2006 Dec;13 Suppl 1:S33-43.

128.r Rikhof B, de Jong S, Suurmeijer AJ*, et al.* The insulin-like growth factor system and sarcomas. J Pathol. 2009 Mar;217(4):469-482.

129.r Salisbury AJ, Macaulay VM. Development of molecular agents for IGF receptor targeting. Horm Metab Res. 2003 Nov-Dec;35(11-12):843-849.

130.r Scotlandi K, Picci P. Targeting insulin-like growth factor 1 receptor in sarcomas. Curr Opin Oncol. 2008 Jul;20(4):419-427.

131.r Chmielowski B. Insulin-like growth factor 1 receptor inhibitors: where do we come from? What are we? Where are we going? Cancer. 2014 Aug 15;120(16):2384-2387.

132.r Pappo AS, Patel SR, Crowley J*, et al.* R1507, a monoclonal antibody to the insulin-like growth factor 1 receptor, in patients with recurrent or refractory Ewing sarcoma family of tumors: results of a phase II Sarcoma Alliance for Research through Collaboration study. J Clin Oncol. 2011 Dec 1;29(34):4541-4547.

133.r Pappo AS, Vassal G, Crowley JJ*, et al.* A phase 2 trial of R1507, a monoclonal antibody to the insulin-like growth factor-1 receptor (IGF-1R), in patients with recurrent or refractory rhabdomyosarcoma, osteosarcoma, synovial sarcoma, and other soft tissue sarcomas: results of a Sarcoma Alliance for Research Through Collaboration study. Cancer. 2014 Aug 15;120(16):2448-2456.

134.r van Maldegem AM, Bovee JV, Peterse EF*, et al.* Ewing sarcoma: The clinical relevance of the insulin-like growth factor 1 and the poly-ADP-ribose-polymerase pathway. Eur J Cancer. 2016 Jan;53:171-180.

135.r Frasca F, Pandini G, Scalia P*, et al.* Insulin receptor isoform A, a newly recognized, high-affinity insulin-like growth factor II receptor in fetal and cancer cells. Mol Cell Biol. 1999 May;19(5):3278-3288.

136.r Wullschleger S, Loewith R, Hall MN. TOR signaling in growth and metabolism. Cell. 2006 Feb 10;124(3):471-484.

137.r Organ SL, Tsao MS. An overview of the c-MET signaling pathway. Ther Adv Med Oncol. 2011 Nov;3(1 Suppl):S7-S19.

138.r Krymskaya VP, Goncharova EA. PI3K/mTORC1 activation in hamartoma syndromes: therapeutic prospects. Cell Cycle. 2009 Feb 1;8(3):403-413.

139.r Lane HA, Breuleux M. Optimal targeting of the mTORC1 kinase in human cancer. Curr Opin Cell Biol. 2009 Apr;21(2):219-229.

140.r Yang X, Yang C, Farberman A*, et al.* The mammalian target of rapamycin-signaling pathway in regulating metabolism and growth. J Anim Sci. 2008 Apr;86(14 Suppl):E36-50.

141.r Tee AR, Blenis J. mTOR, translational control and human disease. Semin Cell Dev Biol. 2005 Feb;16(1):29-37.

142.r Inoki K, Corradetti MN, Guan KL. Dysregulation of the TSC-mTOR pathway in human disease. Nat Genet. 2005 Jan;37(1):19-24.

143.r Anagnostou VK, Bepler G, Syrigos KN*, et al.* High expression of mammalian target of rapamycin is associated with better outcome for patients with early stage lung adenocarcinoma. Clin Cancer Res. 2009 Jun 15;15(12):4157-4164.

144.r Garcia JA, Danielpour D. Mammalian target of rapamycin inhibition as a therapeutic strategy in the management of urologic malignancies. Mol Cancer Ther. 2008 Jun;7(6):1347-1354.

145.r Giles FJ, Albitar M. Mammalian target of rapamycin as a therapeutic target in leukemia. Curr Mol Med. 2005 Nov;5(7):653-661.

146.r Herberger B, Berger W, Puhalla H*, et al.* Simultaneous blockade of the epidermal growth factor receptor/mammalian target of rapamycin pathway by epidermal growth factor receptor inhibitors and rapamycin results in reduced cell growth and survival in biliary tract cancer cells. Mol Cancer Ther. 2009 Jun;8(6):1547-1556.

147.r Hidalgo M, Rowinsky EK. The rapamycin-sensitive signal transduction pathway as a target for cancer therapy. Oncogene. 2000 Dec 27;19(56):6680-6686.

148.r Mita MM, Mita A, Rowinsky EK. Mammalian target of rapamycin: a new molecular target for breast cancer. Clin Breast Cancer. 2003 Jun;4(2):126-137.

149.r Panwalkar A, Verstovsek S, Giles FJ. Mammalian target of rapamycin inhibition as therapy for hematologic malignancies. Cancer. 2004 Feb 15;100(4):657-666.

150.r Zhang HY, Zhang PN, Sun H. Aberration of the PI3K/AKT/mTOR signaling in epithelial ovarian cancer and its implication in cisplatin-based chemotherapy. Eur J Obstet Gynecol Reprod Biol. 2009 Sep;146(1):81-86.

151.r Zhang YJ, Dai Q, Sun DF*, et al.* mTOR signaling pathway is a target for the treatment of colorectal cancer. Ann Surg Oncol. 2009 Sep;16(9):2617-2628.

152.r Zou ZQ, Zhang XH, Wang F*, et al.* A novel dual PI3Kalpha/mTOR inhibitor PI-103 with high antitumor activity in non-small cell lung cancer cells. Int J Mol Med. 2009 Jul;24(1):97-101.

153.r Schwab J, Antonescu C, Boland P*, et al.* Combination of PI3K/mTOR inhibition demonstrates efficacy in human chordoma. Anticancer Res. 2009 Jun;29(6):1867-1871.

154.r Baldo P, Cecco S, Giacomin E*, et al.* mTOR pathway and mTOR inhibitors as agents for cancer therapy. Curr Cancer Drug Targets. 2008 Dec;8(8):647-665.

155.r Fasolo A, Sessa C. mTOR inhibitors in the treatment of cancer. Expert Opin Investig Drugs. 2008 Nov;17(11):1717-1734.

156.r LoPiccolo J, Blumenthal GM, Bernstein WB*, et al.* Targeting the PI3K/Akt/mTOR pathway: effective combinations and clinical considerations. Drug Resist Updat. 2008 Feb-Apr;11(1-2):32-50.

157.r Radaelli S, Stacchiotti S, Casali PG*, et al.* Emerging therapies for adult soft tissue sarcoma. Expert Rev Anticancer Ther. 2014 Jun;14(6):689-704.

158.r Demetri GD, Chawla SP, Ray-Coquard I*, et al.* Results of an international randomized phase III trial of the mammalian target of rapamycin inhibitor ridaforolimus versus placebo to control metastatic sarcomas in patients after benefit from prior chemotherapy. J Clin Oncol. 2013 Jul 1;31(19):2485-2492.

159.r Sanfilippo R, Dei Tos AP, Casali PG. Myxoid liposarcoma and the mammalian target of rapamycin pathway. Curr Opin Oncol. 2013 Jul;25(4):379-383.

160.r Davies H, Bignell GR, Cox C*, et al.* Mutations of the BRAF gene in human cancer. Nature. 2002 Jun 27;417(6892):949-954.

161.r Gray-Schopfer V, Wellbrock C, Marais R. Melanoma biology and new targeted therapy. Nature. 2007 Feb 22;445(7130):851-857.

162.r Ciampi R, Nikiforov YE. Alterations of the BRAF gene in thyroid tumors. Endocr Pathol. 2005 Fall;16(3):163-172.

163.r Eigentler TK, Meier F, Garbe C. Protein kinase inhibitors in melanoma. Expert Opin Pharmacother. 2013 Nov;14(16):2195-2201.

164.r Bhatia P, Friedlander P, Zakaria EA*, et al.* Impact of BRAF mutation status in the prognosis of cutaneous melanoma: an area of ongoing research. Ann Transl Med. 2015 Feb;3(2):24.

165.r Ribas A, Flaherty KT. BRAF targeted therapy changes the treatment paradigm in melanoma. Nat Rev Clin Oncol. 2011 Jul;8(7):426-433.

166.r Pietrantonio F, Petrelli F, Coinu A*, et al.* Predictive role of BRAF mutations in patients with advanced colorectal cancer receiving cetuximab and panitumumab: a meta-analysis. Eur J Cancer. 2015 Mar;51(5):587-594.

167.r Robinson SD, O'Shaughnessy JA, Cowey CL*, et al.* BRAF V600E-mutated lung adenocarcinoma with metastases to the brain responding to treatment with vemurafenib. Lung Cancer. 2014 Aug;85(2):326-330.

168.r Brustugun OT, Khattak AM, Tromborg AK*, et al.* BRAF-mutations in non-small cell lung cancer. Lung Cancer. 2014 Apr;84(1):36-38.

169.r Han S, Polizzano C, Nielsen GP*, et al.* Aberrant hyperactivation of akt and Mammalian target of rapamycin complex 1 signaling in sporadic chordomas. Clin Cancer Res. 2009 Mar 15;15(6):1940-1946.

170.r Rinner B, Weinhaeusel A, Lohberger B*, et al.* Chordoma characterization of significant changes of the DNA methylation pattern. PLoS One. 2013;8(3):e56609.

171.r Tamborini E, Virdis E, Negri T*, et al.* Analysis of receptor tyrosine kinases (RTKs) and downstream pathways in chordomas. Neuro Oncol. 2010 Aug;12(8):776-789.

172.r Dewaele B, Maggiani F, Floris G*, et al.* Frequent activation of EGFR in advanced chordomas. Clin Sarcoma Res. 2011 Jul 25;1(1):4.

173.r Choy E, MacConaill LE, Cote GM*, et al.* Genotyping cancer-associated genes in chordoma identifies mutations in oncogenes and areas of chromosomal loss involving CDKN2A, PTEN, and SMARCB1. PLoS One. 2014;9(7):e101283.

174.r Yu H, Kortylewski M, Pardoll D. Crosstalk between cancer and immune cells: role of STAT3 in the tumour microenvironment. Nat Rev Immunol. 2007 Jan;7(1):41-51.

175.r Qi QR, Yang ZM. Regulation and function of signal transducer and activator of transcription 3. World J Biol Chem. 2014 May 26;5(2):231-239.

176.r Dobashi Y, Suzuki S, Sugawara H*, et al.* Involvement of epidermal growth factor receptor and downstream molecules in bone and soft tissue tumors. Hum Pathol. 2007 Jun;38(6):914-925.

177.r Yang C, Hornicek FJ, Wood KB*, et al.* Blockage of Stat3 with CDDO-Me inhibits tumor cell growth in chordoma. Spine (Phila Pa 1976). 2010 Aug 15;35(18):1668-1675.

178.r Wendt MK, Balanis N, Carlin CR*, et al.* STAT3 and epithelial-mesenchymal transitions in carcinomas. JAKSTAT. 2014 Jan 1;3(1):e28975.

179.r Colomiere M, Ward AC, Riley C*, et al.* Cross talk of signals between EGFR and IL-6R through JAK2/STAT3 mediate epithelial-mesenchymal transition in ovarian carcinomas. Br J Cancer. 2009 Jan 13;100(1):134-144.

180.r Wu J, Patmore DM, Jousma E*, et al.* EGFR-STAT3 signaling promotes formation of malignant peripheral nerve sheath tumors. Oncogene. 2014 Jan 9;33(2):173-180.

181.r Kim H, Kim SN, Park YS*, et al.* HDAC inhibitors downregulate MRP2 expression in multidrug resistant cancer cells: implication for chemosensitization. Int J Oncol. 2011 Mar;38(3):807-812.

182.r Jaenisch R, Bird A. Epigenetic regulation of gene expression: how the genome integrates intrinsic and environmental signals. Nat Genet. 2003 Mar;33 Suppl:245-254.

183.r Slack JM. Conrad Hal Waddington: the last Renaissance biologist? Nat Rev Genet. 2002 Nov;3(11):889-895.

184.r Jirtle RL, Skinner MK. Environmental epigenomics and disease susceptibility. Nat Rev Genet. 2007 Apr;8(4):253-262.

185.r Feinberg AP, Ohlsson R, Henikoff S. The epigenetic progenitor origin of human cancer. Nat Rev Genet. 2006 Jan;7(1):21-33.

186.r Tessarz P, Kouzarides T. Histone core modifications regulating nucleosome structure and dynamics. Nat Rev Mol Cell Biol. 2014 Nov;15(11):703-708.

187.r Deaton AM, Bird A. CpG islands and the regulation of transcription. Genes Dev. 2011 May 15;25(10):1010-1022.

188.r Gardiner-Garden M, Frommer M. CpG islands in vertebrate genomes. J Mol Biol. 1987 Jul 20;196(2):261-282.

189.r Sarma K, Reinberg D. Histone variants meet their match. Nat Rev Mol Cell Biol. 2005 Feb;6(2):139-149.

190.r Weber CM, Henikoff S. Histone variants: dynamic punctuation in transcription. Genes Dev. 2014 Apr 1;28(7):672-682.

191.r Latham JA, Dent SY. Cross-regulation of histone modifications. Nat Struct Mol Biol. 2007 Nov;14(11):1017-1024.

192.r Neeli I, Khan SN, Radic M. Histone deimination as a response to inflammatory stimuli in neutrophils. J Immunol. 2008 Feb 1;180(3):1895-1902.

193.r Christophorou MA, Castelo-Branco G, Halley-Stott RP*, et al.* Citrullination regulates pluripotency and histone H1 binding to chromatin. Nature. 2014 Mar 6;507(7490):104-108.

194.r Lee W, Teckie S, Wiesner T*, et al.* PRC2 is recurrently inactivated through EED or SUZ12 loss in malignant peripheral nerve sheath tumors. Nat Genet. 2014 Nov;46(11):1227-1232.

195.r Zhang M, Wang Y, Jones S*, et al.* Somatic mutations of SUZ12 in malignant peripheral nerve sheath tumors. Nat Genet. 2014 Nov;46(11):1170-1172.

196.r Blackledge NP, Rose NR, Klose RJ. Targeting Polycomb systems to regulate gene expression: modifications to a complex story. Nat Rev Mol Cell Biol. 2015 Nov;16(11):643-649.

197.r Behjati S, Tarpey PS, Presneau N*, et al.* Distinct H3F3A and H3F3B driver mutations define chondroblastoma and giant cell tumor of bone. Nat Genet. 2013 Dec;45(12):1479-1482.

198.r Yuen BT, Knoepfler PS. Histone H3.3 mutations: a variant path to cancer. Cancer Cell. 2013 Nov 11;24(5):567-574.

199.r Lu C, Jain SU, Hoelper D*, et al.* Histone H3K36 mutations promote sarcomagenesis through altered histone methylation landscape. Science. 2016 May 13;352(6287):844-849.

200.r Lane AA, Chabner BA. Histone deacetylase inhibitors in cancer therapy. J Clin Oncol. 2009 Nov 10;27(32):5459-5468.

201.r Ma X, Ezzeldin HH, Diasio RB. Histone deacetylase inhibitors: current status and overview of recent clinical trials. Drugs. 2009 Oct 1;69(14):1911-1934.

202.r Marks PA, Xu WS. Histone deacetylase inhibitors: Potential in cancer therapy. J Cell Biochem. 2009 Jul 1;107(4):600-608.

203.r Benedetti R, Conte M, Iside C*, et al.* Epigenetic-based therapy: From single- to multi-target approaches. Int J Biochem Cell Biol. 2015 Dec;69:121-131.

204.r Grant S, Easley C, Kirkpatrick P. Vorinostat. Nat Rev Drug Discov. 2007 Jan;6(1):21-22.

205.r VanderMolen KM, McCulloch W, Pearce CJ*, et al.* Romidepsin (Istodax, NSC 630176, FR901228, FK228, depsipeptide): a natural product recently approved for cutaneous T-cell lymphoma. J Antibiot (Tokyo). 2011 Aug;64(8):525-531.

206.r Lee HZ, Kwitkowski VE, Del Valle PL*, et al.* FDA Approval: Belinostat for the Treatment of Patients with Relapsed or Refractory Peripheral T-cell Lymphoma. Clin Cancer Res. 2015 Jun 15;21(12):2666-2670.

207.r Laubach JP, Moreau P, San-Miguel JF*, et al.* Panobinostat for the Treatment of Multiple Myeloma. Clin Cancer Res. 2015 Nov 1;21(21):4767-4773.

208.r Jenuwein T, Allis CD. Translating the histone code. Science. 2001 Aug 10;293(5532):1074-1080.

209.r Stacchiotti S, Longhi A, Ferraresi V*, et al.* Phase II study of imatinib in advanced chordoma. J Clin Oncol. 2012 Mar 20;30(9):914-920.

210.r Hindi N, Casali PG, Morosi C*, et al.* Imatinib in advanced chordoma: A retrospective case series analysis. Eur J Cancer. 2015 Nov;51(17):2609-14.

211.r Houessinon A, Boone M, Constans JM*, et al.* Sustained response of a clivus chordoma to erlotinib after imatinib failure. Case Rep Oncol. 2015 Jan-Apr;8(1):25-29.

212.r Lebellec L, Aubert S, Zairi F*, et al.* Molecular targeted therapies in advanced or metastatic chordoma patients: facts and hypotheses. Crit Rev Oncol Hematol. 2015 Jul;95(1):125-131.

213.r Patel AC. Clinical relevance of target identity and biology: implications for drug discovery and development. J Biomol Screen. 2013 Dec;18(10):1164-1185.

214.r Swinney DC. Phenotypic vs. target-based drug discovery for first-in-class medicines. Clin Pharmacol Ther. 2013 Apr;93(4):299-301.

215.r Le LP, Nielsen GP, Rosenberg AE*, et al.* Recurrent chromosomal copy number alterations in sporadic chordomas. PLoS One. 2011;6(5):e18846.

216.r Hallor KH, Staaf J, Jonsson G*, et al.* Frequent deletion of the CDKN2A locus in chordoma: analysis of chromosomal imbalances using array comparative genomic hybridisation. Br J Cancer. 2008 Jan 29;98(2):434-442.

217.r Moffat JG, Rudolph J, Bailey D. Phenotypic screening in cancer drug discovery - past, present and future. Nat Rev Drug Discov. 2014 Aug;13(8):588-602.

218.r Zheng W, Thorne N, McKew JC. Phenotypic screens as a renewed approach for drug discovery. Drug Discov Today. 2013 Nov;18(21-22):1067-1073.

219.r Vane JR, Botting RM. The mechanism of action of aspirin. Thromb Res. 2003 Jun 15;110(5-6):255-258.

220.r Scheil S, Bruderlein S, Liehr T*, et al.* Genome-wide analysis of sixteen chordomas by comparative genomic hybridization and cytogenetics of the first human chordoma cell line, U-CH1. Genes Chromosomes Cancer. 2001 Nov;32(3):203-211.

221.r Rinner B, Froehlich EV, Buerger K*, et al.* Establishment and detailed functional and molecular genetic characterisation of a novel sacral chordoma cell line, MUG-Chor1. Int J Oncol. 2012 Feb;40(2):443-451.

222.r von Witzleben A, Goerttler LT, Marienfeld R*, et al.* Preclinical Characterization of Novel Chordoma Cell Systems and Their Targeting by Pharmocological Inhibitors of the Cdk4/6 Cell Cycle Pathway. Cancer Res. 2015 Sep; 75: 3823–3831.

223.r Brüderlein S, Sommer JB, Meltzer PS*, et al.* Molecular characterization of putative chordoma cell lines. Sarcoma. 2010;2010:630129.

224.r Hsu W, Mohyeldin A, Shah SR*, et al.* Generation of chordoma cell line JHC7 and the identification of Brachyury as a novel molecular target. J Neurosurg. 2011 Oct;115(4):760-769.

225.r Ji J, Chen X, Leung SY*, et al.* Comprehensive analysis of the gene expression profiles in human gastric cancer cell lines. Oncogene. 2002 Sep 19;21(42):6549-6556.

226.r Drewry DH, Willson TM, Zuercher WJ. Seeding collaborations to advance kinase science with the GSK Published Kinase Inhibitor Set (PKIS). Curr Top Med Chem. 2014;14(3):340-342.

227.r Elkins JM, Fedele V, Szklarz M*, et al.* Comprehensive characterization of the Published Kinase Inhibitor Set. Nat Biotechnol. 2015 Oct 26.

228.r Matsunaga T, Wada Y, Endo S*, et al.* Aldo-Keto Reductase 1B10 and Its Role in Proliferation Capacity of Drug-Resistant Cancers. Front Pharmacol. 2012;3:5.

229.r Kurata T, Tsurutani J, Fujisaka Y*, et al.* Inhibition of EGFR, HER2 and HER3 signaling with AZD8931 alone and in combination with paclitaxel: phase i study in Japanese patients with advanced solid malignancies and advanced breast cancer. Invest New Drugs. 2014 Oct;32(5):946-954.

230.r Tjulandin S, Moiseyenko V, Semiglazov V*, et al.* Phase I, dose-finding study of AZD8931, an inhibitor of EGFR (erbB1), HER2 (erbB2) and HER3 (erbB3) signaling, in patients with advanced solid tumors. Invest New Drugs. 2014 Feb;32(1):145-153.

231.r Noh YH, Lim HS, Jung JA*, et al.* Population pharmacokinetics of HM781-36 (poziotinib), pan-human EGF receptor (HER) inhibitor, and its two metabolites in patients with advanced solid malignancies. Cancer Chemother Pharmacol. 2015 Jan;75(1):97-109.

232.r Kazandjian D, Blumenthal GM, Chen HY*, et al.* FDA approval summary: crizotinib for the treatment of metastatic non-small cell lung cancer with anaplastic lymphoma kinase rearrangements. Oncologist. 2014 Oct;19(10):e5-11.

233.r Chou TC. Theoretical basis, experimental design, and computerized simulation of synergism and antagonism in drug combination studies. Pharmacol Rev. 2006 Sep;58(3):621-681.

234.r Davies JM, Robinson AE, Cowdrey C*, et al.* Generation of a patient-derived chordoma xenograft and characterization of the phosphoproteome in a recurrent chordoma. J Neurosurg. 2014 Feb;120(2):331-336.

235.r Hickinson DM, Klinowska T, Speake G*, et al.* AZD8931, an equipotent, reversible inhibitor of signaling by epidermal growth factor receptor, ERBB2 (HER2), and ERBB3: a unique agent for simultaneous ERBB receptor blockade in cancer. Clin Cancer Res. 2010 Feb 15;16(4):1159-1169.

236.r McIlwain DR, Berger T, Mak TW. Caspase functions in cell death and disease. Cold Spring Harbor perspectives in biology. [Review]. 2013 Apr;5(4):a008656.

237.r Chaitanya GV, Steven AJ, Babu PP. PARP-1 cleavage fragments: signatures of cell-death proteases in neurodegeneration. Cell communication and signaling : CCS. 2010;8:31.

238.r Folkes AJ, Ahmadi K, Alderton WK*, et al.* The identification of 2-(1H-indazol-4-yl)-6-(4-methanesulfonyl-piperazin-1-ylmethyl)-4-morpholin-4-yl-t hieno[3,2-d]pyrimidine (GDC-0941) as a potent, selective, orally bioavailable inhibitor of class I PI3 kinase for the treatment of cancer. J Med Chem. 2008 Sep 25;51(18):5522-5532.

239.r Seefeld MA, Rouse MB, McNulty KC*, et al.* Discovery of 5-pyrrolopyridinyl-2-thiophenecarboxamides as potent AKT kinase inhibitors. Bioorg Med Chem Lett. 2009 Apr 15;19(8):2244-2248.

240.r Stellwagen JC, Adjabeng GM, Arnone MR*, et al.* Development of potent B-RafV600E inhibitors containing an arylsulfonamide headgroup. Bioorg Med Chem Lett. 2011 Aug 1;21(15):4436-4440.

241.r Gellibert F, Fouchet MH, Nguyen VL*, et al.* Design of novel quinazoline derivatives and related analogues as potent and selective ALK5 inhibitors. Bioorg Med Chem Lett. 2009 Apr 15;19(8):2277-2281.

242.r Ranieri G, Mammi M, Donato Di Paola E*, et al.* Pazopanib a tyrosine kinase inhibitor with strong anti-angiogenetic activity: a new treatment for metastatic soft tissue sarcoma. Crit Rev Oncol Hematol. 2014 Feb;89(2):322-329.

243.r Subramanian A, Tamayo P, Mootha VK*, et al.* Gene set enrichment analysis: a knowledge-based approach for interpreting genome-wide expression profiles. Proc Natl Acad Sci U S A. 2005 Oct 25;102(43):15545-15550.

244.r Chong CR, Janne PA. The quest to overcome resistance to EGFR-targeted therapies in cancer. Nat Med. 2013 Nov;19(11):1389-1400.

245.r Yang ZY, Wu XY, Huang YF*, et al.* Promising biomarkers for predicting the outcomes of patients with KRAS wild-type metastatic colorectal cancer treated with anti-epidermal growth factor receptor monoclonal antibodies: a systematic review with meta-analysis. Int J Cancer. 2013 Oct 15;133(8):1914-1925.

246.r Moroishi T, Hansen CG, Guan KL. The emerging roles of YAP and TAZ in cancer. Nat Rev Cancer. 2015 Feb;15(2):73-79.

247.r Yu FX, Guan KL. The Hippo pathway: regulators and regulations. Genes Dev. 2013 Feb 15;27(4):355-371.

248.r Song S, Honjo S, Jin J*, et al.* The Hippo Coactivator YAP1 Mediates EGFR Overexpression and Confers Chemoresistance in Esophageal Cancer. Clin Cancer Res. 2015 Jun 1;21(11):2580-2590.

249.r He C, Mao D, Hua G*, et al.* The Hippo/YAP pathway interacts with EGFR signaling and HPV oncoproteins to regulate cervical cancer progression. EMBO Mol Med. 2015 Nov;7(11):1426-1449.

250.r Kol A, Terwisscha van Scheltinga AG, Timmer-Bosscha H*, et al.* HER3, serious partner in crime: therapeutic approaches and potential biomarkers for effect of HER3-targeting. Pharmacol Ther. 2014 Jul;143(1):1-11.

251.r Gala K, Chandarlapaty S. Molecular pathways: HER3 targeted therapy. Clin Cancer Res. 2014 Mar 15;20(6):1410-1416.

252.r Weinberger PM, Yu Z, Kowalski D*, et al.* Differential expression of epidermal growth factor receptor, c-Met, and HER2/neu in chordoma compared with 17 other malignancies. Arch Otolaryngol Head Neck Surg. 2005 Aug;131(8):707-711.

253.r Sekyi-Otu A, Bell RS, Ohashi C*, et al.* Insulin-like growth factor 1 (IGF-1) receptors, IGF-1, and IGF-2 are expressed in primary human sarcomas. Cancer Res. 1995 Jan 1;55(1):129-134.

254.r Toretsky JA, Kalebic T, Blakesley V*, et al.* The insulin-like growth factor-I receptor is required for EWS/FLI-1 transformation of fibroblasts. J Biol Chem. 1997 Dec 5;272(49):30822-30827.

255.r Kim SY, Toretsky JA, Scher D*, et al.* The role of IGF-1R in pediatric malignancies. Oncologist. 2009 Jan;14(1):83-91.

256.r Scotlandi K. Targeted therapies in Ewing's sarcoma. Adv Exp Med Biol. 2006;587:13-22.

257.r Kurmasheva RT, Dudkin L, Billups C*, et al.* The insulin-like growth factor-1 receptor-targeting antibody, CP-751,871, suppresses tumor-derived VEGF and synergizes with rapamycin in models of childhood sarcoma. Cancer Res. 2009 Oct 1;69(19):7662-7671.

258.r Mitsuhashi T AH, Hasegawa T. Insulin-like growth factor (IGF)-I and IGF-I receptor (IGF-IR) are consistently expressed in the most of chordomas. Mod Pathol. 2008;21(1s):15A-16A.

259.r Mitsuhashi T WM, Sasano H, Ono M. The expression of insulin-like growth factor-1 (IGF-1), IGF-1 receptor and transforming growth factor-beta in chordoma. Mod Pathol. 2006;19(3s):6.

260.r Sommer J, Itani DM, Homlar KC*, et al.* Methylthioadenosine phosphorylase and activated insulin-like growth factor-1 receptor/insulin receptor: potential therapeutic targets in chordoma. J Pathol. 2010 Apr;220(5):608-617.

261.r Shang Y, Mao Y, Batson J*, et al.* Antixenograft tumor activity of a humanized anti-insulin-like growth factor-I receptor monoclonal antibody is associated with decreased AKT activation and glucose uptake. Mol Cancer Ther. 2008 Sep;7(9):2599-2608.

262.r Kolb EA, Gorlick R. Development of IGF-IR Inhibitors in Pediatric Sarcomas. Curr Oncol Rep. 2009 Jul;11(4):307-313.

263.r Tognon CE, Sorensen PH. Targeting the insulin-like growth factor 1 receptor (IGF1R) signaling pathway for cancer therapy. Expert Opin Ther Targets. 2012 Jan;16(1):33-48.

264.r Ma H, Zhang T, Shen H*, et al.* The adverse events profile of anti-IGF-1R monoclonal antibodies in cancer therapy. Br J Clin Pharmacol. 2014 Jun;77(6):917-928.

265.r Fassnacht M, Berruti A, Baudin E*, et al.* Linsitinib (OSI-906) versus placebo for patients with locally advanced or metastatic adrenocortical carcinoma: a double-blind, randomised, phase 3 study. Lancet Oncol. 2015 Apr;16(4):426-435.

266.r Mulvihill MJ, Cooke A, Rosenfeld-Franklin M*, et al.* Discovery of OSI-906: a selective and orally efficacious dual inhibitor of the IGF-1 receptor and insulin receptor. Future Med Chem. 2009 Sep;1(6):1153-1171.

267.r Miller ML, Molinelli EJ, Nair JS*, et al.* Drug synergy screen and network modeling in dedifferentiated liposarcoma identifies CDK4 and IGF1R as synergistic drug targets. Sci Signal. 2013 Sep 24;6(294):ra85.

268.r van Gaal JC, Roeffen MH, Flucke UE*, et al.* Simultaneous targeting of insulin-like growth factor-1 receptor and anaplastic lymphoma kinase in embryonal and alveolar rhabdomyosarcoma: a rational choice. Eur J Cancer. 2013 Nov;49(16):3462-3470.

269.r Duan Z, Choy E, Nielsen GP*, et al.* Differential expression of microRNA (miRNA) in chordoma reveals a role for miRNA-1 in Met expression. J Orthop Res. 2010 Jun;28(6):746-752.

270.r Boyault C, Sadoul K, Pabion M*, et al.* HDAC6, at the crossroads between cytoskeleton and cell signaling by acetylation and ubiquitination. Oncogene. 2007 Aug 13;26(37):5468-5476.

271.r Matthias P, Yoshida M, Khochbin S. HDAC6 a new cellular stress surveillance factor. Cell Cycle. 2008 Jan 1;7(1):7-10.

272.r Kwon S, Zhang Y, Matthias P. The deacetylase HDAC6 is a novel critical component of stress granules involved in the stress response. Genes Dev. 2007 Dec 15;21(24):3381-3394.

273.r Kawaguchi Y, Kovacs JJ, McLaurin A*, et al.* The deacetylase HDAC6 regulates aggresome formation and cell viability in response to misfolded protein stress. Cell. 2003 Dec 12;115(6):727-738.

274.r Khan N, Jeffers M, Kumar S*, et al.* Determination of the class and isoform selectivity of small-molecule histone deacetylase inhibitors. Biochem J. 2008 Jan 15;409(2):581-589.

275.r Hrzenjak A, Moinfar F, Kremser ML*, et al.* Histone deacetylase inhibitor vorinostat suppresses the growth of uterine sarcomas in vitro and in vivo. Mol Cancer. 2010;9:49.

276.r Dejligbjerg M, Grauslund M, Litman T*, et al.* Differential effects of class I isoform histone deacetylase depletion and enzymatic inhibition by belinostat or valproic acid in HeLa cells. Mol Cancer. 2008;7:70.

277.r Slingerland M, Guchelaar HJ, Gelderblom H. Histone deacetylase inhibitors: an overview of the clinical studies in solid tumors. Anticancer Drugs. 2014 Feb;25(2):140-149.

278.r Lee DH, Zhang Y, Kassam AB*, et al.* Combined PDGFR and HDAC Inhibition Overcomes PTEN Disruption in Chordoma. PLoS One. 2015;10(8):e0134426.

279.r Bassiri M, Privalsky ML. Mutagenesis of the avian erythroblastosis virus erbB coding region: an intact extracellular domain is not required for oncogenic transformation. J Virol. 1986 Aug;59(2):525-530.

280.r Schlomm T, Kirstein P, Iwers L*, et al.* Clinical significance of epidermal growth factor receptor protein overexpression and gene copy number gains in prostate cancer. Clin Cancer Res. 2007 Nov 15;13(22 Pt 1):6579-6584.

281.r Pectasides E, Rampias T, Kountourakis P*, et al.* Comparative prognostic value of epidermal growth factor quantitative protein expression compared with FISH for head and neck squamous cell carcinoma. Clin Cancer Res. 2011 May 1;17(9):2947-2954.

282.r Szabo B, Nelhubel GA, Karpati A*, et al.* Clinical significance of genetic alterations and expression of epidermal growth factor receptor (EGFR) in head and neck squamous cell carcinomas. Oral Oncol. 2011 Jun;47(6):487-496.

283.r Dordevic G, Matusan Ilijas K, Hadzisejdic I*, et al.* EGFR protein overexpression correlates with chromosome 7 polysomy and poor prognostic parameters in clear cell renal cell carcinoma. J Biomed Sci. 2012;19:40.

284.r Minner S, Rump D, Tennstedt P*, et al.* Epidermal growth factor receptor protein expression and genomic alterations in renal cell carcinoma. Cancer. 2012 Mar 1;118(5):1268-1275.

285.r Jiang Z, Li C, Li F*, et al.* EGFR gene copy number as a prognostic marker in colorectal cancer patients treated with cetuximab or panitumumab: a systematic review and meta analysis. PLoS One. 2013;8(2):e56205.

286.r Sesboue R, Le Pessot F, Di Fiore F*, et al.* EGFR alterations and response to anti-EGFR therapy: is it a matter of gene amplification or gene copy number gain? Br J Cancer. 2012 Jan 17;106(2):426-427; author reply 428.

287.r Dahabreh IJ, Linardou H, Kosmidis P*, et al.* EGFR gene copy number as a predictive biomarker for patients receiving tyrosine kinase inhibitor treatment: a systematic review and meta-analysis in non-small-cell lung cancer. Ann Oncol. 2011 Mar;22(3):545-552.

288.r Carlson JJ, Garrison LP, Ramsey SD*, et al.* Epidermal growth factor receptor genomic variation in NSCLC patients receiving tyrosine kinase inhibitor therapy: a systematic review and meta-analysis. J Cancer Res Clin Oncol. 2009 Nov;135(11):1483-1493.

289.r Grob TJ, Hoenig T, Clauditz TS*, et al.* Frequent intratumoral heterogeneity of EGFR gene copy gain in non-small cell lung cancer. Lung Cancer. 2013 Mar;79(3):221-227.

290.r Mansuet-Lupo A, Zouiti F, Alifano M*, et al.* Intratumoral distribution of EGFR mutations and copy number in metastatic lung cancer, what impact on the initial molecular diagnosis? J Transl Med. 2014;12:131.

291.r Westwood M, Joore M, Whiting P*, et al.* Epidermal growth factor receptor tyrosine kinase (EGFR-TK) mutation testing in adults with locally advanced or metastatic non-small cell lung cancer: a systematic review and cost-effectiveness analysis. Health Technol Assess. 2014 2014/05/15;18(32).

292.r Murray S, Karavasilis V, Bobos M*, et al.* Molecular predictors of response to tyrosine kinase inhibitors in patients with Non-Small-Cell Lung Cancer. J Exp Clin Cancer Res. 2012;31:77.

293.r Chung C, Christianson M. Predictive and prognostic biomarkers with therapeutic targets in breast, colorectal, and non-small cell lung cancers: a systemic review of current development, evidence, and recommendation. J Oncol Pharm Pract. 2014 Feb;20(1):11-28.

294.r Blackwell KL, Burstein HJ, Storniolo AM*, et al.* Overall survival benefit with lapatinib in combination with trastuzumab for patients with human epidermal growth factor receptor 2-positive metastatic breast cancer: final results from the EGF104900 Study. J Clin Oncol. 2012 Jul 20;30(21):2585-2592.

295.r Dowell J, Minna JD, Kirkpatrick P. Erlotinib hydrochloride. Nat Rev Drug Discov. 2005 Jan;4(1):13-14.

296.r Cohen MH, Williams GA, Sridhara R*, et al.* FDA drug approval summary: gefitinib (ZD1839) (Iressa) tablets. Oncologist. 2003;8(4):303-306.

297.r Chuu CP, Chen RY, Barkinge JL*, et al.* Systems-level analysis of ErbB4 signaling in breast cancer: a laboratory to clinical perspective. Mol Cancer Res. 2008 Jun;6(6):885-891.

298.r Carpenter G. ErbB-4: mechanism of action and biology. Exp Cell Res. 2003 Mar 10;284(1):66-77.

299.r Veikkolainen V, Vaparanta K, Halkilahti K*, et al.* Function of ERBB4 is determined by alternative splicing. Cell Cycle. 2011 Aug 15;10(16):2647-2657.

300.r Mendoza-Naranjo A, El-Naggar A, Wai DH*, et al.* ERBB4 confers metastatic capacity in Ewing sarcoma. EMBO Mol Med. 2013 Jul;5(7):1019-1034.

301.r Fischer C, Scheipl S, Zopf A*, et al.* Mutation Analysis of Nine Chordoma Specimens by Targeted Next-Generation Cancer Panel Sequencing. J Cancer. 2015;6(10):984-989.

302.r Stacchiotti S, Marrari A, Tamborini E*, et al.* Response to imatinib plus sirolimus in advanced chordoma. Ann Oncol. 2009 Nov;20(11):1886-1894.

303.r Yang C, Schwab JH, Schoenfeld AJ*, et al.* A novel target for treatment of chordoma: signal transducers and activators of transcription 3. Mol Cancer Ther. 2009 Sep;8(9):2597-2605.

304.r Siu IM, Ruzevick J, Zhao Q*, et al.* Erlotinib inhibits growth of a patient-derived chordoma xenograft. PLoS One. 2013;8(11):e78895.

305.r Aleksic T, Browning L, Woodward M*, et al.* Durable Response of Spinal Chordoma to Combined Inhibition of IGF-1R and EGFR. Front Oncol. 2016;6:98.

306.r Medina PJ, Goodin S. Lapatinib: a dual inhibitor of human epidermal growth factor receptor tyrosine kinases. Clin Ther. 2008 Aug;30(8):1426-1447.

307.r Choi H, Charnsangavej C, Faria SC*, et al.* Correlation of computed tomography and positron emission tomography in patients with metastatic gastrointestinal stromal tumor treated at a single institution with imatinib mesylate: proposal of new computed tomography response criteria. J Clin Oncol. 2007 May 1;25(13):1753-1759.

308.r Eisenhauer EA, Therasse P, Bogaerts J*, et al.* New response evaluation criteria in solid tumours: revised RECIST guideline (version 1.1). Eur J Cancer. 2009 Jan;45(2):228-247.

309.r Sun X, Hornicek F, Schwab JH. Chordoma: an update on the pathophysiology and molecular mechanisms. Curr Rev Musculoskelet Med. 2015 Oct;8: 344–352.

310.r de Marinis F, Catania C, Passaro A. Afatinib in NSCLC harbouring EGFR mutations. Lancet Oncol. 2014 Apr;15(4):e148-149.

311.r Hynes NE, Lane HA. ERBB receptors and cancer: the complexity of targeted inhibitors. Nat Rev Cancer. 2005 May;5(5):341-354.

312.r Mitsudomi T, Yatabe Y. Epidermal growth factor receptor in relation to tumor development: EGFR gene and cancer. FEBS J. 2010 Jan;277(2):301-308.

313.r Padfield E, Ellis HP, Kurian KM. Current Therapeutic Advances Targeting EGFR and EGFRvIII in Glioblastoma. Front Oncol. 2015;5:5.

314.r Hansen AR, Siu LL. Epidermal growth factor receptor targeting in head and neck cancer: have we been just skimming the surface? J Clin Oncol. 2013 Apr 10;31(11):1381-1383.

315.r Sacco AG, Cohen EE. Current Treatment Options for Recurrent or Metastatic Head and Neck Squamous Cell Carcinoma. J Clin Oncol. 2015 Oct 10;33(29):3305-3313.

316.r Smilek P, Neuwirthova J, Jarkovsky J*, et al.* Epidermal growth factor receptor (EGFR) expression and mutations in the EGFR signaling pathway in correlation with anti-EGFR therapy in head and neck squamous cell carcinomas. Neoplasma. 2012;59(5):508-515.

317.r Keren S, Shoude Z, Lu Z*, et al.* Role of EGFR as a prognostic factor for survival in head and neck cancer: a meta-analysis. Tumour Biol. 2014 Mar;35(3):2285-2295.

318.r Sasaki T, Hiroki K, Yamashita Y. The role of epidermal growth factor receptor in cancer metastasis and microenvironment. Biomed Res Int. 2013;2013:546318.

319.r Seton-Rogers S. Tumorigenesis: Pushing pancreatic cancer to take off. Nat Rev Cancer. 2012 Nov;12(11):739.

320.r Heery CR, Singh BH, Rauckhorst M*, et al.* Phase I Trial of a Yeast-Based Therapeutic Cancer Vaccine (GI-6301) Targeting the Transcription Factor Brachyury. Cancer Immunol Res. 2015 Nov;3(11):1248-1256.

321.r Hamilton DH, Litzinger MT, Fernando RI*, et al.* Cancer vaccines targeting the epithelial-mesenchymal transition: tissue distribution of brachyury and other drivers of the mesenchymal-like phenotype of carcinomas. Semin Oncol. 2012 Jun;39(3):358-366.

322.r Therkildsen C, Bergmann TK, Henrichsen-Schnack T*, et al.* The predictive value of KRAS, NRAS, BRAF, PIK3CA and PTEN for anti-EGFR treatment in metastatic colorectal cancer: A systematic review and meta-analysis. Acta Oncol. 2014 Jul;53(7):852-864.

323.r Hartung T, Daston G. Are in vitro tests suitable for regulatory use? Toxicol Sci. 2009 Oct;111(2):233-237.

324.r Hartung T. Food for thought... on cell culture. ALTEX. 2007;24(3):143-152.

325.r Kamb A. What's wrong with our cancer models? Nat Rev Drug Discov. 2005 Feb;4(2):161-165.

326.r Zang R, Li D, Tang I*, et al.* Cell-Based Assays in High-Throughput Screening for Drug Discovery. International Journal of Biotechnology for Wellness Industries. 2012;1:31-51.

327.r Box GEP, Draper NR. New York, NY: John Wiley & Sons; 1987.

328.r Wilding JL, Bodmer WF. Cancer cell lines for drug discovery and development. Cancer Res. 2014 May 1;74(9):2377-2384.

329.r Quent VM, Loessner D, Friis T*, et al.* Discrepancies between metabolic activity and DNA content as tool to assess cell proliferation in cancer research. J Cell Mol Med. 2010 Apr;14(4):1003-1013.

330.r Pampaloni F, Reynaud EG, Stelzer EH. The third dimension bridges the gap between cell culture and live tissue. Nat Rev Mol Cell Biol. 2007 Oct;8(10):839-845.

331.r Shamir ER, Ewald AJ. Three-dimensional organotypic culture: experimental models of mammalian biology and disease. Nat Rev Mol Cell Biol. 2014 Oct;15(10):647-664.

332.r Bibby MC. Orthotopic models of cancer for preclinical drug evaluation: advantages and disadvantages. Eur J Cancer. 2004 Apr;40(6):852-857.

333.r Dranoff G. Experimental mouse tumour models: what can be learnt about human cancer immunology? Nat Rev Immunol. 2012 Jan;12(1):61-66.

334.r Salisbury JR. The pathology of the human notochord. J Pathol. 1993;171(4):253-255.

335.r Scannell JW, Blanckley A, Boldon H*, et al.* Diagnosing the decline in pharmaceutical R&D efficiency. Nat Rev Drug Discov. 2012 Mar;11(3):191-200.

Appendix 1

Suppl. Table 1. STR profiles. Adapted from Scheipl *et al.* (2016) (11). **(A) STR profiles of cell lines used in the experiments 2015.**

STR-Analysis	U-CH1		U-CH2		U-CH7		U-CH10		JCH7		MUG-Chor1		UM-Chor1		NCI-N87	
Marker	**Allele 1**	**Allele 2**	**Allele 1**	**Allele 2**	**Allele 1**	**Allele 2**	**Allele 1**	**Allele 2**	**Allele 1**	**Allele 2**	**Allele 1**	**Allele 2**	**Allele 1**	**Allele 2**	**Allele 1**	**Allele 2**
D3S1358	15		17		17		15	16	17		14	17	18		14	
TH01	7		9.3		7		8	9	6	8	9.3		7	9.3	7	9
D21S11	28	29	29	30	30	33.2	29	31	27	31.2	29	33.2	27	31	30	
D18S51	15		12	18	16		13		12		17	23	14		17	
Penta E	7	10	12	15	12	15	18		15		5	12	7		5	
D5S818	11	12	10	11	12	13	11		13		11	12	9	13	12	13
D13S137	11	13	11		10		9	13	11		11		12		8	11
D7S820	9	12	8	12	10	11	10		7	10	8	11	11		10	11
D16S539	12	13	12		10	12	11	13	11		11	14	12		9	13
CSF1PO	10	11	11	12	12		10	11	11		11		11	12	8	12
Penta D	11		12	13	12	13	9	13	6	11	13		8	9	12	
AMEL	X	Y	X		X	Y	X		X		X		X	Y	X	Y
vWA	17		17		16	17	16		17		15		15		15	16
D8S1179	10	15	13		14	16	8	13	13	14	11	12	12	13	14	15
TPOX	8	11	8		8	11	11		10	11	8		8	9	9	11
FGA	20	21	21	22.2	22	24	24		21	23	21	26	19	23	20	21
D19S433	14		15.2	17	13	14	13	15	13	13.2	13	14	14	16	14	14.2
D2S1338	17	18	24		23		19		18	20	18	20	18	20	23	24

(B) STR profiles of cell lines used in the experiments 2014.

STR-Analysis	U-CH1		U-CH2		MUG-Chor1		U-CH7 Cell Line UCL		U-CH7 Primary Tumour	
Marker	**Allele 1**	**Allele 2**	**Allele 1**	**Allele 2**	**Allele 1**	**Allele 2**	**Allele 1**	**Allele 2**	**Allele 1**	**Allele 2**
D3S1358	15		17		14	17	17		16	17
TH01	7		9.3		9.3		7		7	
D21S11	28	29	29	30	29	33.2	30	33.2	30	33.2
D18S51	15		12	18	17	23	16		16	18
Penta E	7	10	12	15	5	12	12	15	12	15
D5S818	11	12	10	11	11	12	12	13	12	13
D13S137	11	13	11		11		10		10	12
D7S820	9	12	8	12	8	11	10	11	10	11
D16S539	12	13	12		11	14	10	12	10	12
CSF1PO	10	11	11	12	11		12		12	
Penta D	11		12	13	13		12	13	12	13
AMEL	X	Y	X		X		X	Y	X	Y
vWA	17		17		15		16	17	16	17
D8S1179	10	15	13		11	12	14	16	14	16
TPOX	8	11	8		8		8	11	8	11
FGA	20	21	21	22.2	21	26	22	24	22	24
D19S433	14		15.2	17	13	14	13	14	13	14
D2S1338	17	18	24		18		23		23	

Suppl. Table 2. List of compounds included in the single concentration screen (n=1,097). Adapted from Scheipl *et al.* (2016) (11).

	Supplier ID or Commercial Name	Library	Supplier	U-CH1		MUG-Chor1		U-CH2	
Number				Mean M%I	SD	Mean M%I	SD	Mean M%I	SD
1	S1065*	Anticancer	SelleckChem	69	6	56	5	64	9
2	S1009*	Anticancer	SelleckChem	78	5	37	10	61	20
3	S1037	Anticancer	SelleckChem	35	4	10	15	0	19
4	S1638	Anticancer	SelleckChem	26	2	-4	8	14	3
5	S1215*	Anticancer	SelleckChem	87	11	104	0	101	1
6	S1141	Anticancer	SelleckChem	4	4	15	5	8	6
7	S1142*	Anticancer	SelleckChem	63	5	75	3	86	3
8	S1003*	Anticancer	SelleckChem	57	30	29	5	9	7
9	S1004	Anticancer	SelleckChem	15	7	10	10	2	7
10	S1208*	Anticancer	SelleckChem	94	2	42	6	67	4
11	S1490*	Anticancer	SelleckChem	56	38	59	9	83	7
12	S1060*	Anticancer	SelleckChem	80	19	71	6	76	7
13	S1555*	Anticancer	SelleckChem	82	2	59	10	76	5
14	S1085*	Anticancer	SelleckChem	80	23	83	5	27	15
15	S1010	Anticancer	SelleckChem	15	1	14	11	30	12
16	S1013*	Anticancer	SelleckChem	50	69	98	4	96	2
17	S1084	Anticancer	SelleckChem	12	9	-7	8	1	31
18	S1261	Anticancer	SelleckChem	23	2	-6	13	-2	7
19	S1018	Anticancer	SelleckChem	-13	43	10	13	8	4
20	S1194	Anticancer	SelleckChem	20	2	36	7	7	11
21	S1021	Anticancer	SelleckChem	9	12	11	11	33	4
22	S1200*	Anticancer	SelleckChem	58	59	-12	12	8	2
23	S1022*	Anticancer	SelleckChem	33	39	32	7	53	6
24	S1148*	Anticancer	SelleckChem	59	39	49	8	64	2
25	S1225	Anticancer	SelleckChem	30	15	36	11	45	1
26	S1120*	Anticancer	SelleckChem	20	32	28	6	56	4
27	S1230*	Anticancer	SelleckChem	76	3	40	10	72	7
28	S1082*	Anticancer	SelleckChem	47	9	47	6	67	13
29	S1360*	Anticancer	SelleckChem	48	3	27	5	53	4
30	S1026	Anticancer	SelleckChem	27	6	17	12	12	3
31	S1028*	Anticancer	SelleckChem	64	7	37	9	16	17
32	S1361	Anticancer	SelleckChem	-9	28	4	7	2	4
33	S1220*	Anticancer	SelleckChem	25	33	6	7	85	2
34	S1220*	Anticancer	SelleckChem	43	32	67	7	4	4
35	S1035	Anticancer	SelleckChem	34	20	8	16	23	18
36	S1487*	Anticancer	SelleckChem	36	9	26	5	55	6
37	S1185	Anticancer	SelleckChem	6	1	5	4	10	7
38	S1515*	Anticancer	SelleckChem	80	25	86	5	64	14
39	S1040	Anticancer	SelleckChem	13	3	11	13	0	13
40	S1118	Anticancer	SelleckChem	5	2	6	11	-1	9

41	S1236	Anticancer	SelleckChem	28	30	3	12	0	6
42	S1130	Anticancer	SelleckChem	37	10	17	3	48	6
43	S1223*	Anticancer	SelleckChem	27	35	45	5	65	7
44	567805, Src Kinase Inhibitor I	Calbiochem	Merck Millipore	23	4	35	9	23	5
45	658552, AG 1478*	Calbiochem	Merck Millipore	61	3	35	11	24	9
46	365250, Go6976	Calbiochem	Merck Millipore	28	12	15	14	24	5
47	371970, HA-1077	Calbiochem	Merck Millipore	9	8	18	8	23	11
48	203290, GF103209X	Calbiochem	Merck Millipore	3	9	12	16	29	6
49	688000, Y-27632	Calbiochem	Merck Millipore	2	12	9	9	11	10
50	513000, PD 98059	Calbiochem	Merck Millipore	8	6	21	13	17	9
51	658390, Tyrphostin 1	Calbiochem	Merck Millipore	7	4	17	10	15	6
52	658550, AG 1295	Calbiochem	Merck Millipore	20	7	13	3	18	6
53	658401, AG 490	Calbiochem	Merck Millipore	11	7	6	3	11	7
54	440202, LY 294002	Calbiochem	Merck Millipore	32	4	14	11	41	10
55	371963, H-89	Calbiochem	Merck Millipore	14	8	14	8	25	2
56	422708, KN-93	Calbiochem	Merck Millipore	7	3	7	8	12	19
57	559388, SB-202190	Calbiochem	Merck Millipore	-11	9	-11	7	11	14
58	317200, DMBI	Calbiochem	Merck Millipore	6	9	-2	9	13	7
59	658551, AG 1296	Calbiochem	Merck Millipore	11	15	9	4	18	4
60	196870, BAY 11-7082	Calbiochem	Merck Millipore	4	6	18	12	10	12
61	420119, SP 600125	Calbiochem	Merck Millipore	9	6	10	6	19	5
62	402085, Indirubin-3'-monoxime	Calbiochem	Merck Millipore	17	5	-4	21	8	3
63	422000, Kenpaullone	Calbiochem	Merck Millipore	5	9	3	2	14	3
64	260961, NU7026	Calbiochem	Merck Millipore	12	2	12	8	19	5
65	328007, FR180204	Calbiochem	Merck Millipore	-5	7	15	9	14	4
66	328008	Calbiochem	Merck Millipore	1	1	16	6	12	5
67	676489	Calbiochem	Merck Millipore	-5	11	13	9	11	6

68	365251, Go6983	Calbiochem	Merck Millipore	13	8	13	3	27	5
69	401481	Calbiochem	Merck Millipore	15	19	33	9	40	2
70	217696, Cdk1 Inhibitor, CGP74514A*	Calbiochem	Merck Millipore	4	20	9	1	61	9
71	203600, Bohemine	Calbiochem	Merck Millipore	-11	37	7	6	9	11
72	234503, Compound 52	Calbiochem	Merck Millipore	-15	36	7	4	11	1
73	527450, PKR Inhibitor*	Calbiochem	Merck Millipore	36	25	66	16	65	6
74	528100, PI-103*	Calbiochem	Merck Millipore	84	6	55	8	65	9
75	118500	Calbiochem	Merck Millipore	6	10	-6	7	13	11
76	118501	Calbiochem	Merck Millipore	13	8	22	5	20	9
77	121767, AG 1024	Calbiochem	Merck Millipore	14	8	11	17	12	5
78	121790, AGL 2043	Calbiochem	Merck Millipore	-7	14	11	5	17	18
79	124011*	Calbiochem	Merck Millipore	80	7	21	11	38	60
80	124012, Triciribine	Calbiochem	Merck Millipore	14	6	30	1	2	3
81	124018	Calbiochem	Merck Millipore	27	3	11	12	34	1
82	124020	Calbiochem	Merck Millipore	-5	8	17	8	19	4
83	126870, Alsterpaullone	Calbiochem	Merck Millipore	6	22	25	18	36	15
84	126871*	Calbiochem	Merck Millipore	60	18	50	11	73	0
85	128125, Aloisine A (RP107)	Calbiochem	Merck Millipore	-14	34	14	7	24	6
86	128135, Aloisine (RP106)	Calbiochem	Merck Millipore	-15	26	-3	7	13	3
87	164640, Aminopurvalanol A	Calbiochem	Merck Millipore	-2	14	-2	1	17	23
88	171260	Calbiochem	Merck Millipore	-13	15	2	9	4	5
89	189404	Calbiochem	Merck Millipore	-8	25	4	11	16	10
90	189405[#]	Calbiochem	Merck Millipore	17	14	10	3	13	12
91	189405[#]	Calbiochem	Merck Millipore	-14	37	6	3	9	4
92	189406	Calbiochem	Merck Millipore	16	9	11	12	32	5
93	197221	Calbiochem	Merck	3	2	6	6	5	1

			Millipore						
94	203297, Bisindolylmaleimide IV	Calbiochem	Merck Millipore	-3	9	11	6	14	3
95	203696, BPIQ-I	Calbiochem	Merck Millipore	45	5	32	12	22	10
96	217695	Calbiochem	Merck Millipore	12	11	4	3	7	1
97	217714	Calbiochem	Merck Millipore	-14	5	7	7	7	8
98	217720	Calbiochem	Merck Millipore	15	3	12	10	17	6
99	218696, D4476	Calbiochem	Merck Millipore	-2	2	16	16	20	11
100	218710, TBCA	Calbiochem	Merck Millipore	13	6	14	7	13	11
101	219476	Calbiochem	Merck Millipore	6	55	19	13	33	6
102	219477, NSC 625987	Calbiochem	Merck Millipore	-8	5	-4	11	1	26
103	219478*	Calbiochem	Merck Millipore	-4	6	-10	9	66	12
104	219479, TG003	Calbiochem	Merck Millipore	-2	4	-5	6	9	13
105	219491*	Calbiochem	Merck Millipore	75	6	30	12	67	2
106	220486	Calbiochem	Merck Millipore	10	4	3	5	6	6
107	234505*	Calbiochem	Merck Millipore	62	4	29	4	29	8
108	238803	Calbiochem	Merck Millipore	6	6	13	10	23	10
109	238804, NU6140	Calbiochem	Merck Millipore	28	5	20	10	30	7
110	260962	Calbiochem	Merck Millipore	-1	5	5	8	11	16
111	260964	Calbiochem	Merck Millipore	-5	11	6	9	4	10
112	266788	Calbiochem	Merck Millipore	-7	10	6	12	3	7
113	324673	Calbiochem	Merck Millipore	7	15	22	13	20	5
114	324674*	Calbiochem	Merck Millipore	62	5	60	7	77	6
115	324840*	Calbiochem	Merck Millipore	61	5	44	13	26	4
116	328009	Calbiochem	Merck Millipore	21	7	11	4	15	3
117	341251, Fascaplysin, synthetic*	Calbiochem	Merck Millipore	103	3	107	4	101	0

118	343020	Calbiochem	Merck Millipore	-9	9	-8	11	3	9
119	343021	Calbiochem	Merck Millipore	10	16	-13	11	4	14
120	343022	Calbiochem	Merck Millipore	-22	31	-18	9	7	13
121	344036	Calbiochem	Merck Millipore	-27	28	-5	8	1	8
122	361540	Calbiochem	Merck Millipore	-15	37	-5	12	9	7
123	361541	Calbiochem	Merck Millipore	14	10	7	2	11	6
124	361549	Calbiochem	Merck Millipore	34	2	24	10	22	5
125	361550	Calbiochem	Merck Millipore	35	6	6	12	35	12
126	361551	Calbiochem	Merck Millipore	12	20	3	7	18	10
127	361553	Calbiochem	Merck Millipore	-10	7	0	11	-4	13
128	361554, TWS119	Calbiochem	Merck Millipore	-5	13	9	6	12	13
129	361555	Calbiochem	Merck Millipore	11	19	26	15	32	5
130	371806, GTP-14564	Calbiochem	Merck Millipore	10	5	11	5	10	1
131	371957, Isogranulatimide	Calbiochem	Merck Millipore	10	2	12	8	14	5
132	375670, Herbimycin A, Streptomyces sp.*	Calbiochem	Merck Millipore	55	9	44	14	77	2
133	400090, IC261*	Calbiochem	Merck Millipore	8	45	41	9	70	6
134	402081, Indirubin Derivative E804	Calbiochem	Merck Millipore	44	6	10	9	40	1
135	407248	Calbiochem	Merck Millipore	-1	16	-15	14	-2	21
136	407601	Calbiochem	Merck Millipore	-6	10	-13	17	0	13
137	420099	Calbiochem	Merck Millipore	-13	38	12	2	28	14
138	420104	Calbiochem	Merck Millipore	29	67	28	9	28	4
139	420121	Calbiochem	Merck Millipore	-16	32	-3	4	13	12
140	420123	Calbiochem	Merck Millipore	6	10	12	6	11	6
141	420126	Calbiochem	Merck Millipore	11	8	22	4	44	8
142	420129	Calbiochem	Merck Millipore	12	9	3	5	20	4
143	420135	Calbiochem	Merck	-5	11	-2	8	-1	5

			Millipore						
144	420136*	Calbiochem	Merck Millipore	30	8	38	7	72	5
145	420298, K-252a, Nocardiopsis sp.*	Calbiochem	Merck Millipore	77	6	29	11	69	7
146	422706, KN-62	Calbiochem	Merck Millipore	7	7	13	9	14	1
147	428205	Calbiochem	Merck Millipore	-2	9	1	15	29	3
148	440203, LY 303511	Calbiochem	Merck Millipore	8	5	9	8	11	9
149	444937	Calbiochem	Merck Millipore	1	18	0	14	1	3
150	444938	Calbiochem	Merck Millipore	5	4	-9	15	14	8
151	444939	Calbiochem	Merck Millipore	0	10	2	11	0	20
152	448101	Calbiochem	Merck Millipore	-25	30	-11	14	6	9
153	454861	Calbiochem	Merck Millipore	-16	19	-7	11	15	16
154	475863*	Calbiochem	Merck Millipore	-8	23	0	7	55	21
155	481406	Calbiochem	Merck Millipore	-3	47	31	12	22	8
156	506121	Calbiochem	Merck Millipore	6	4	13	11	11	4
157	506126	Calbiochem	Merck Millipore	12	5	-19	11	0	1
158	513030, PD 169316	Calbiochem	Merck Millipore	-19	9	-12	9	1	7
159	513035, PD 158780*	Calbiochem	Merck Millipore	56	2	9	21	13	4
160	513040, PD 174265*	Calbiochem	Merck Millipore	55	6	30	16	18	2
161	521231	Calbiochem	Merck Millipore	-16	18	-4	5	15	12
162	521232	Calbiochem	Merck Millipore	30	4	19	6	29	2
163	521233*	Calbiochem	Merck Millipore	40	3	51	11	84	2
164	521234	Calbiochem	Merck Millipore	24	9	21	7	23	2
165	521275*	Calbiochem	Merck Millipore	105	4	105	4	100	0
166	527455	Calbiochem	Merck Millipore	-8	25	-8	16	1	12
167	528106	Calbiochem	Merck Millipore	1	17	-11	10	1	14
168	528108	Calbiochem	Merck Millipore	-14	37	-8	19	-2	16

169	529574, PP3	Calbiochem	Merck Millipore	-30	27	-6	13	1	17
170	529581, PP1 Analog II, 1NM-PP1	Calbiochem	Merck Millipore	5	3	5	5	11	5
171	539648, Staurosporine, N-benzoyl-*	Calbiochem	Merck Millipore	81	8	44	5	95	0
172	539652	Calbiochem	Merck Millipore	7	8	14	10	13	9
173	539654	Calbiochem	Merck Millipore	0	6	-18	7	10	2
174	540500, Purvalanol A	Calbiochem	Merck Millipore	-9	5	3	12	14	12
175	553210, Rapamycin	Calbiochem	Merck Millipore	39	0	6	8	44	2
176	555553	Calbiochem	Merck Millipore	-9	3	6	5	6	7
177	555554	Calbiochem	Merck Millipore	4	7	17	6	23	1
178	559387, SB-202747	Calbiochem	Merck Millipore	-4	6	1	4	0	2
179	559389, SB-203580	Calbiochem	Merck Millipore	3	1	4	11	16	0
180	559396, SB-220025	Calbiochem	Merck Millipore	15	7	4	6	31	2
181	559402, SB-218078	Calbiochem	Merck Millipore	21	16	5	18	49	1
182	565625, SC-68376	Calbiochem	Merck Millipore	-17	35	-13	13	-7	6
183	567305 SKF-86002	Calbiochem	Merck Millipore	-28	26	-14	12	-5	17
184	567731	Calbiochem	Merck Millipore	-8	8	-10	11	1	13
185	569397, Staurosporine, Streptomyces sp.#*	Calbiochem	Merck Millipore	94	14	88	7	100	0
186	569397, Staurosporine, Streptomyces sp.#	Calbiochem	Merck Millipore	102	5	75	12	100	0
187	570250, STO-609	Calbiochem	Merck Millipore	21	8	4	2	18	7
188	572635, SU6656	Calbiochem	Merck Millipore	3	3	18	16	8	7
189	572650, SU9516	Calbiochem	Merck Millipore	-17	2	-6	4	7	7
190	572660 SU11652	Calbiochem	Merck Millipore	-18	7	8	17	41	4
191	574711	Calbiochem	Merck Millipore	-5	2	4	13	10	8
192	574712	Calbiochem	Merck Millipore	-4	2	5	1	10	7
193	574713	Calbiochem	Merck	-7	9	6	4	-2	5

			Millipore						
194	616373	Calbiochem	Merck Millipore	14	14	28	10	15	4
195	616451	Calbiochem	Merck Millipore	-2	2	21	15	20	1
196	616453	Calbiochem	Merck Millipore	18	10	37	10	25	5
197	658440, AG 112	Calbiochem	Merck Millipore	2	10	-14	7	-7	8
198	676480	Calbiochem	Merck Millipore	-25	28	-12	12	-8	3
199	676481	Calbiochem	Merck Millipore	-16	5	-14	14	-5	10
200	676485	Calbiochem	Merck Millipore	-6	8	-9	17	-4	12
201	676487	Calbiochem	Merck Millipore	-19	34	3	12	-3	10
202	220285, Chelerythrine Chloride	Calbiochem	Merck Millipore	3	8	1	11	13	2
203	S1207, AV-951(Tivozanib)		SelleckChem	17	12	-4	3	30	2
204	GW632580X	PKIS	GSK	21	19	6	7	-1	6
205	GW620972X	PKIS	GSK	20	21	6	14	9	8
206	SB-220025-R*	PKIS	GSK	12	8	-26	8	33	11
207	SB-220025-A	PKIS	GSK	5	5	-30	26	7	6
208	SKF-86002-A2	PKIS	GSK	5	4	-3	15	3	13
209	GW282974X	PKIS	GSK	13	10	34	39	3	21
210	GW769076X	PKIS	GSK	3	5	-3	9	1	12
211	GW775608X	PKIS	GSK	6	8	-11	3	8	8
212	GW549390X	PKIS	GSK	11	17	-14	52	9	20
213	GW572399X	PKIS	GSK	5	10	-4	9	-16	27
214	GW572401X	PKIS	GSK	-3	12	-21	12	-8	29
215	GW575533A	PKIS	GSK	-1	6	25	26	-6	21
216	GW577921A	PKIS	GSK	11	8	0	9	0	8
217	GW580509X	PKIS	GSK	13	7	-12	3	2	10
218	GW621431X	PKIS	GSK	1	3	4	17	17	17
219	GW621970X	PKIS	GSK	4	14	1	2	-6	10
220	GW622055X	PKIS	GSK	5	8	-7	16	-1	12
221	GW627512B	PKIS	GSK	4	6	11	8	7	12
222	GW627834A	PKIS	GSK	17	31	6	3	3	7
223	GW631581B	PKIS	GSK	0	4	-4	13	-6	15
224	GW632046X	PKIS	GSK	10	13	-2	3	11	15
225	GW641155A	PKIS	GSK	5	3	22	15	-6	10
226	GW678313X	PKIS	GSK	11	10	0	10	11	9
227	GSK718429A	PKIS	GSK	2	7	3	8	-1	9
228	GW572738X	PKIS	GSK	3	4	4	11	-2	10
229	GW846105X	PKIS	GSK	13	9	-3	21	-10	18
230	SB-347804	PKIS	GSK	9	4	0	10	17	24

231	SB-657836-AAA	PKIS	GSK	5	2	-2	5	1	7
232	SB-814597	PKIS	GSK	14	17	-2	44	18	36
233	GSK586581A	PKIS	GSK	5	7	12	13	12	18
234	GSK605714A	PKIS	GSK	-5	6	-24	12	-3	16
235	GSK620503A	PKIS	GSK	3	4	13	20	7	12
236	GSK625137A	PKIS	GSK	16	12	-4	13	-1	3
237	GSK635416A	PKIS	GSK	2	1	5	22	11	13
238	GSK711701A	PKIS	GSK	2	2	2	9	3	9
239	GW549034X	PKIS	GSK	5	2	-2	6	12	12
240	GW785404X	PKIS	GSK	-3	7	-7	8	0	15
241	SB-734117	PKIS	GSK	11	7	10	10	-15	36
242	SB-736290	PKIS	GSK	11	10	2	3	13	8
243	SB-736302	PKIS	GSK	6	6	7	14	13	24
244	SB-738561	PKIS	GSK	6	9	21	36	4	12
245	SB-737198*	PKIS	GSK	6	10	36	23	5	9
246	SB-744941	PKIS	GSK	4	0	-1	11	-11	22
247	SB-750140*	PKIS	GSK	13	8	9	5	40	5
248	SB-751148	PKIS	GSK	11	13	3	6	5	9
249	SB-751399	PKIS	GSK	3	9	22	26	1	13
250	SB-333612	PKIS	GSK	6	6	-12	2	0	4
251	SB-358518	PKIS	GSK	8	5	-6	8	3	8
252	SB-360741	PKIS	GSK	4	4	-6	11	-3	18
253	SB-361058	PKIS	GSK	4	7	-5	5	7	9
254	SB-376719	PKIS	GSK	2	7	12	15	0	14
255	SB-390523	PKIS	GSK	3	6	-16	13	0	9
256	SB-390527	PKIS	GSK	3	4	1	8	9	2
257	SB-409513	PKIS	GSK	14	8	-17	11	0	9
258	SB-409514	PKIS	GSK	3	3	1	13	-3	8
259	SKF-62604	PKIS	GSK	11	10	4	28	-3	14
260	GW819230X	PKIS	GSK	1	18	-17	30	19	36
261	GSK319347A	PKIS	GSK	7	14	2	31	3	34
262	SB-725317*	PKIS	GSK	-6	10	45	5	1	13
263	SB-732941	PKIS	GSK	1	1	7	6	6	19
264	SB-735465	PKIS	GSK	6	7	3	9	8	19
265	SB-735467	PKIS	GSK	3	7	2	5	2	16
266	SB-738482	PKIS	GSK	21	20	-2	3	10	13
267	SB-739452	PKIS	GSK	10	8	-1	8	3	8
268	SB-741905	PKIS	GSK	5	7	-5	20	-2	11
269	SB-742864	PKIS	GSK	6	5	21	15	20	20
270	SB-742865	PKIS	GSK	9	6	-3	8	12	5
271	GW651576X	PKIS	GSK	2	4	4	6	-12	27
272	GW659893X	PKIS	GSK	10	16	-9	13	-7	8
273	GW703087X	PKIS	GSK	24	30	7	4	12	19
274	GW772405X	PKIS	GSK	12	9	-4	6	7	16
275	GW794726X	PKIS	GSK	1	8	4	7	12	7
276	GW799251X	PKIS	GSK	15	28	-15	20	0	4
277	GW807930X	PKIS	GSK	11	10	1	7	8	10

278	GSK1000163A	PKIS	GSK	9	14	13	17	6	9
279	GSK1007102B*	PKIS	GSK	43	25	57	54	74	18
280	GSK938890A	PKIS	GSK	10	8	-11	3	5	8
281	GSK943949A	PKIS	GSK	10	3	1	5	15	18
282	GSK949675A	PKIS	GSK	19	12	0	44	6	21
283	GW824645A	PKIS	GSK	10	8	-7	13	-1	11
284	GW831090X	PKIS	GSK	9	19	1	12	-13	25
285	GW831091X	PKIS	GSK	7	1	-17	9	1	13
286	GW406731X	PKIS	GSK	11	9	2	20	-4	7
287	GW427984X	PKIS	GSK	-2	5	-3	14	-4	27
288	GW432441X	PKIS	GSK	13	17	5	14	4	26
289	GW435821X	PKIS	GSK	7	4	-17	3	-6	13
290	GW439255X	PKIS	GSK	9	16	0	12	-11	13
291	GW441806A	PKIS	GSK	6	7	-3	6	14	21
292	GW445012X	PKIS	GSK	-6	6	-11	25	0	29
293	GW445014X	PKIS	GSK	6	8	-8	14	-5	12
294	GW445015X	PKIS	GSK	9	5	-10	6	-5	4
295	GW445017X	PKIS	GSK	-2	6	-5	14	-6	28
296	GW450241X	PKIS	GSK	8	4	-3	10	-6	13
297	GW458344A	PKIS	GSK	2	6	-1	4	5	7
298	GW459057A	PKIS	GSK	8	4	-4	8	4	13
299	GW743024X	PKIS	GSK	7	13	0	9	4	7
300	GW782907X	PKIS	GSK	3	4	-6	10	5	14
301	GW782912X	PKIS	GSK	0	7	1	11	3	11
302	GW785974X	PKIS	GSK	6	6	-2	23	15	19
303	GW796920X	PKIS	GSK	-2	3	-3	8	12	6
304	GW796921X	PKIS	GSK	-7	7	-5	7	-9	30
305	GW806776X	PKIS	GSK	2	6	25	15	4	10
306	GW701032X	PKIS	GSK	8	19	7	24	-11	42
307	GW708893X	PKIS	GSK	16	6	-10	15	13	11
308	GW734508X	PKIS	GSK	1	2	-4	7	5	12
309	GW607117X	PKIS	GSK	11	7	-13	5	10	8
310	GW856804X	PKIS	GSK	11	7	-4	4	-1	7
311	GSK237700A	PKIS	GSK	16	8	-11	30	3	7
312	GSK237701A*	PKIS	GSK	40	19	-4	12	54	33
313	GSK317314A*	PKIS	GSK	11	12	5	14	57	5
314	GSK317315A	PKIS	GSK	6	2	11	4	20	7
315	GSK326090A*	PKIS	GSK	20	5	24	5	38	42
316	GSK571989A*	PKIS	GSK	19	6	0	16	72	7
317	GSK579289A*	PKIS	GSK	32	16	4	7	52	32
318	GSK978744A*	PKIS	GSK	8	6	27	29	50	7
319	GW843682X	PKIS	GSK	3	6	4	6	0	9
320	GW852849X	PKIS	GSK	8	16	-2	5	-9	25
321	GSK180736A	PKIS	GSK	-2	10	-7	6	11	15
322	GSK270822A	PKIS	GSK	-1	11	0	6	22	17
323	GSK299115A	PKIS	GSK	-1	9	6	39	6	11
324	GSK466314A	PKIS	GSK	2	8	16	19	21	14

325	GSK466317A	PKIS	GSK	4	4	11	21	13	9
326	GW461104A*	PKIS	GSK	29	22	30	23	-4	8
327	GW569530A	PKIS	GSK	7	8	19	27	-9	11
328	GR105659X	PKIS	GSK	8	5	7	8	14	9
329	GW275616X	PKIS	GSK	3	11	3	13	11	11
330	GW278681X	PKIS	GSK	6	5	3	8	10	23
331	GW301789X	PKIS	GSK	7	13	-8	10	1	7
332	GW442130X	PKIS	GSK	8	4	-8	13	5	26
333	GW679410X	PKIS	GSK	6	9	-3	23	15	9
334	GW680975X	PKIS	GSK	0	8	28	27	11	14
335	GW682841X	PKIS	GSK	-5	8	-2	10	5	18
336	GW695874X	PKIS	GSK	0	6	15	15	0	30
337	GW711782X	PKIS	GSK	1	3	11	15	7	31
338	GW410563A*	PKIS	GSK	12	14	35	5	4	5
339	GW612286X*	PKIS	GSK	10	8	37	10	13	4
340	GW654652C	PKIS	GSK	7	10	9	29	2	16
341	GW770220A	PKIS	GSK	13	8	-16	4	0	3
342	GW771127A	PKIS	GSK	4	13	4	0	12	21
343	GSK953913A	PKIS	GSK	3	12	11	20	3	12
344	GSK980961A	PKIS	GSK	15	15	-1	18	1	2
345	GW806742X	PKIS	GSK	9	7	-6	9	5	18
346	GW809897X	PKIS	GSK	7	4	1	8	9	6
347	GW830263A	PKIS	GSK	8	6	-9	3	5	14
348	GW830365A	PKIS	GSK	5	3	1	5	0	7
349	GW830900A	PKIS	GSK	9	13	-1	14	5	6
350	GSK248233A	PKIS	GSK	8	16	2	19	12	15
351	GSK269962B*	PKIS	GSK	14	9	17	2	34	12
352	GW589961A	PKIS	GSK	9	11	-6	21	-19	28
353	GW607049C	PKIS	GSK	-5	7	-39	22	-3	7
354	GW659386A	PKIS	GSK	5	10	-30	8	-2	12
355	GW673715X	PKIS	GSK	2	3	-1	11	-5	27
356	GW680908A	PKIS	GSK	7	8	-5	9	0	12
357	GW683134A	PKIS	GSK	21	21	-7	18	-5	8
358	GW693917A	PKIS	GSK	5	17	-17	8	2	10
359	GW694234A	PKIS	GSK	3	2	2	19	-1	5
360	GW694590A	PKIS	GSK	1	4	-15	7	-9	15
361	GW700494A	PKIS	GSK	2	3	6	13	11	11
362	GW701427A	PKIS	GSK	0	3	-13	6	1	10
363	GW709042A	PKIS	GSK	7	6	-26	10	7	11
364	GSK1023156A	PKIS	GSK	-1	7	-6	7	3	7
365	GSK1030058A	PKIS	GSK	7	5	-9	11	8	8
366	GSK1030059A	PKIS	GSK	9	11	11	5	-8	19
367	GSK1030061A	PKIS	GSK	8	6	-5	8	9	17
368	GSK1030062A	PKIS	GSK	7	8	4	7	-8	13
369	GSK204925A	PKIS	GSK	11	8	-3	15	10	14
370	GSK312948A	PKIS	GSK	8	6	-15	20	-7	13
371	GW804482X	PKIS	GSK	9	9	-3	7	-6	20

372	GW853606X	PKIS	GSK	-5	8	-15	17	0	31
373	GW853609X	PKIS	GSK	6	9	0	6	2	23
374	GW693481X	PKIS	GSK	7	7	5	15	13	6
375	GW780159X	PKIS	GSK	9	11	2	11	-7	19
376	GW785804X	PKIS	GSK	2	7	4	2	16	8
377	GW786460X	PKIS	GSK	6	6	19	13	13	6
378	GSK554170A	PKIS	GSK	6	5	7	19	13	13
379	GSK561866B	PKIS	GSK	10	5	1	11	8	8
380	GSK614526A*	PKIS	GSK	10	4	0	12	35	15
381	GSK619487A	PKIS	GSK	3	11	26	33	18	24
382	GW876790X	PKIS	GSK	2	9	19	9	26	9
383	SB-759335-B	PKIS	GSK	4	7	-7	11	0	11
384	SB-400868-A	PKIS	GSK	15	11	16	12	-5	11
385	SB-431533	PKIS	GSK	12	12	-7	22	3	24
386	SB-431542-A	PKIS	GSK	-4	17	7	4	4	25
387	SKF-86055	PKIS	GSK	12	20	-9	16	-2	21
388	GR269666A	PKIS	GSK	1	9	-22	20	-2	22
389	GW282449A*	PKIS	GSK	37	16	53	9	3	10
390	GW301888X	PKIS	GSK	18	24	7	6	2	11
391	GW820759X	PKIS	GSK	7	5	1	17	-16	43
392	GW575808A	PKIS	GSK	9	11	3	7	3	14
393	GW759710A	PKIS	GSK	15	21	4	5	-1	18
394	GW782612X	PKIS	GSK	20	23	8	30	0	18
395	GW642125X	PKIS	GSK	8	7	4	15	19	17
396	GW642138X	PKIS	GSK	14	7	-6	17	19	25
397	GW578748X	PKIS	GSK	19	24	-5	11	8	9
398	GW644007X	PKIS	GSK	1	6	4	9	2	9
399	GW784307A	PKIS	GSK	-5	5	3	12	15	9
400	GW794607X	PKIS	GSK	-3	14	-8	13	-10	31
401	GW809885X	PKIS	GSK	12	9	-6	8	0	6
402	GW811168X	PKIS	GSK	-9	13	4	5	-8	14
403	GW817394X	PKIS	GSK	17	21	5	8	3	11
404	GW817396X	PKIS	GSK	6	4	14	26	-8	23
405	GW829874X	PKIS	GSK	1	8	-2	8	10	7
406	GW829877X	PKIS	GSK	6	4	2	15	5	4
407	SB-772077-B	PKIS	GSK	5	1	12	13	21	18
408	GW284372X	PKIS	GSK	18	13	33	38	4	5
409	GW458787A	PKIS	GSK	-4	12	9	11	-3	36
410	GW567808A	PKIS	GSK	15	12	1	15	0	6
411	GW568377A	PKIS	GSK	3	4	-5	4	6	4
412	GW574782A	PKIS	GSK	-8	16	-11	12	-7	31
413	GW574783B	PKIS	GSK	11	5	7	11	1	6
414	GW576484X	PKIS	GSK	9	6	-4	23	-17	25
415	GW576609A*	PKIS	GSK	46	13	47	7	6	9
416	GW576924A	PKIS	GSK	-8	9	29	9	-10	20
417	GW580496A	PKIS	GSK	0	1	-3	7	-5	14
418	GW583373A*	PKIS	GSK	14	23	39	4	3	22

419	GW615311X	PKIS	GSK	3	6	26	13	5	16
420	GW616030X*	PKIS	GSK	30	14	38	22	6	12
421	GW621823A	PKIS	GSK	11	10	25	0	-6	6
422	GW633459A	PKIS	GSK	9	14	19	16	8	6
423	GSK2220400A*	PKIS	GSK	11	8	52	27	8	12
424	SB-437013	PKIS	GSK	-4	2	8	8	10	9
425	SB-630812	PKIS	GSK	0	5	-3	11	19	16
426	SB-633825	PKIS	GSK	14	11	4	10	-9	18
427	GW768505A	PKIS	GSK	5	18	-1	15	-2	29
428	GW770249A	PKIS	GSK	10	6	7	3	11	3
429	GW770249X	PKIS	GSK	9	8	0	8	-5	12
430	GW795486X	PKIS	GSK	6	4	-8	10	-7	14
431	GW795493X	PKIS	GSK	16	12	-4	10	11	9
432	GW275944X	PKIS	GSK	2	8	10	22	-8	19
433	GW276655X	PKIS	GSK	2	2	2	8	-3	20
434	GW280670X	PKIS	GSK	20	27	-9	3	-1	7
435	GW282536X	PKIS	GSK	1	12	-14	14	-18	17
436	GW290597X	PKIS	GSK	6	6	-6	9	6	17
437	GW297361X	PKIS	GSK	-5	4	-5	7	-4	9
438	GW300653X	PKIS	GSK	3	2	-6	14	-3	4
439	GW300657X	PKIS	GSK	2	5	2	7	-4	7
440	GW300660X	PKIS	GSK	2	4	-4	15	6	11
441	GW301784X	PKIS	GSK	18	17	13	11	-11	4
442	GW305178X	PKIS	GSK	2	3	-5	11	2	21
443	GW335962X	PKIS	GSK	7	7	-2	4	-2	9
444	GW352430A	PKIS	GSK	5	7	-3	9	-5	2
445	GW396574X	PKIS	GSK	1	12	9	42	-18	10
446	GW416469X	PKIS	GSK	6	6	10	15	-13	21
447	GW416981X	PKIS	GSK	10	11	19	7	2	8
448	SB-239272	PKIS	GSK	5	7	-8	32	1	37
449	SB-242717	PKIS	GSK	1	3	-15	10	2	19
450	SB-242718	PKIS	GSK	0	2	-11	13	-10	17
451	SB-242719	PKIS	GSK	-2	4	3	5	5	14
452	SB-242721	PKIS	GSK	4	18	3	32	10	13
453	SB-245392	PKIS	GSK	2	2	-4	7	12	12
454	SB-250715	PKIS	GSK	5	8	18	7	-1	20
455	SB-251505	PKIS	GSK	10	9	9	37	-1	29
456	SB-251527	PKIS	GSK	-5	11	-15	1	5	24
457	SB-253226	PKIS	GSK	4	5	-7	16	3	10
458	SB-253228	PKIS	GSK	-4	11	7	4	3	13
459	SB-254169	PKIS	GSK	-5	9	-14	11	-5	13
460	SB-264865	PKIS	GSK	5	5	-2	24	9	8
461	SB-264866	PKIS	GSK	6	5	5	3	4	16
462	SB-278538	PKIS	GSK	6	8	5	12	3	20
463	SB-278539	PKIS	GSK	3	6	2	13	8	12
464	SB-284847-BT	PKIS	GSK	8	15	-4	11	7	7
465	SB-285234-W	PKIS	GSK	19	17	-1	12	17	23

466	GSK317354A	PKIS	GSK	2	7	0	19	3	14
467	SB-210313	PKIS	GSK	3	5	-7	3	12	13
468	SB-216385	PKIS	GSK	1	1	-9	7	-8	17
469	SB-220455	PKIS	GSK	1	2	-2	14	9	20
470	SB-221466	PKIS	GSK	4	11	-16	5	8	6
471	SB-223133	PKIS	GSK	2	0	-4	14	15	12
472	SB-226879	PKIS	GSK	2	4	1	8	16	10
473	SB-236687	PKIS	GSK	6	3	3	11	17	13
474	GSK200398A	PKIS	GSK	-7	9	6	0	1	16
475	GSK238583A	PKIS	GSK	11	9	-6	17	18	12
476	GSK259178A	PKIS	GSK	16	19	24	38	2	9
477	GW869810X	PKIS	GSK	11	9	-15	3	-9	14
478	GW784752X	PKIS	GSK	-7	7	8	2	-1	12
479	GW813360X	PKIS	GSK	3	5	1	29	5	14
480	GI261520A	PKIS	GSK	-1	6	7	16	10	17
481	GW680191X*	PKIS	GSK	57	9	39	31	6	3
482	GW440139A*	PKIS	GSK	6	5	37	7	16	28
483	GW559768X	PKIS	GSK	-3	10	1	15	30	13
484	SB-476429-A	PKIS	GSK	1	13	-42	16	4	20
485	SB-610251-B	PKIS	GSK	7	6	-25	35	-2	14
486	GSK182497A	PKIS	GSK	5	6	-8	6	-2	14
487	GSK192082A	PKIS	GSK	7	3	-6	12	-7	11
488	GSK238063A	PKIS	GSK	4	2	33	23	-1	14
489	GSK300014A	PKIS	GSK	-1	11	6	8	3	28
490	GSK969786A	PKIS	GSK	-5	6	5	9	-2	16
491	GW684626B	PKIS	GSK	6	8	-18	4	2	22
492	GW693881A	PKIS	GSK	3	7	-5	6	10	6
493	GW784684X	PKIS	GSK	22	17	22	60	7	37
494	SB-675259-M*	PKIS	GSK	-8	10	52	10	20	33
495	SB-678557-A	PKIS	GSK	1	4	25	10	-15	9
496	SB-686709-A	PKIS	GSK	-6	11	35	12	7	19
497	SB-698596-AC	PKIS	GSK	-3	5	38	7	19	19
498	SB-711237	PKIS	GSK	1	4	-7	10	-8	18
499	SB-732881*	PKIS	GSK	-1	10	37	8	41	14
500	SB-732881-H*	PKIS	GSK	0	5	41	20	65	16
501	SB-739245-AC	PKIS	GSK	-1	9	7	15	-8	12
502	SB-743899	PKIS	GSK	6	9	5	7	2	7
503	GW441756X	PKIS	GSK	12	16	8	25	8	2
504	GSK1173862A*	PKIS	GSK	9	7	54	15	5	9
505	GSK1220512A	PKIS	GSK	1	11	22	29	8	8
506	GSK1326255A	PKIS	GSK	1	8	9	2	3	9
507	GSK1392956A	PKIS	GSK	10	21	-8	4	-1	36
508	GSK994854A	PKIS	GSK	7	7	10	7	3	5
509	GW837331X	PKIS	GSK	12	9	16	6	-2	7
510	GW861893X	PKIS	GSK	10	6	5	11	-3	14
511	GW874091X	PKIS	GSK	6	15	-24	12	5	19
512	GW513184X	PKIS	GSK	10	6	0	2	-5	36

513	GW643971X	PKIS	GSK	7	4	-3	12	-1	6
514	GW801372X	PKIS	GSK	6	6	3	15	29	30
515	GW806290X*	PKIS	GSK	60	7	70	5	68	5
516	GW807982X	PKIS	GSK	3	5	15	6	3	9
517	GW810372X	PKIS	GSK	18	12	-6	7	7	8
518	GW810576X*	PKIS	GSK	44	33	24	32	47	38
519	GW811761X	PKIS	GSK	6	10	-7	7	7	7
520	GW819077X	PKIS	GSK	-2	8	4	4	-8	12
521	GW827099X	PKIS	GSK	6	4	6	1	0	21
522	GW827102X	PKIS	GSK	15	17	11	25	6	18
523	GW827105X	PKIS	GSK	9	5	-11	16	-3	10
524	GW827106X	PKIS	GSK	10	5	1	10	3	5
525	GW827396X	PKIS	GSK	-1	9	-17	7	-12	45
526	GW828525X	PKIS	GSK	8	7	1	7	3	7
527	GW828529X	PKIS	GSK	15	21	2	8	8	7
528	GW829055X	PKIS	GSK	5	7	12	8	14	6
529	GW829115X	PKIS	GSK	8	13	-13	25	0	13
530	GW829906X	PKIS	GSK	1	2	10	3	9	8
531	GW832467X	PKIS	GSK	5	7	8	14	8	14
532	GW833373X	PKIS	GSK	9	13	-3	5	17	5
533	GSK1713088A	PKIS	GSK	9	7	5	35	-2	12
534	GSK1751853A	PKIS	GSK	6	6	31	15	4	6
535	GSK2213727A*	PKIS	GSK	3	2	38	10	14	11
536	GSK2219385A	PKIS	GSK	11	6	19	22	-8	19
537	GSK1511931A	PKIS	GSK	17	20	13	21	-1	8
538	GSK1819799A	PKIS	GSK	2	5	1	13	-5	14
539	GSK2110236A*	PKIS	GSK	4	13	63	1	-7	24
540	GSK2163632A*	PKIS	GSK	10	6	51	32	-11	47
541	GSK2186269A*	PKIS	GSK	72	52	51	70	66	60
542	GW279320X	PKIS	GSK	3	4	-7	10	5	12
543	GW589933X	PKIS	GSK	5	2	-9	16	0	10
544	GW561436X	PKIS	GSK	5	6	-4	26	0	12
545	GW568326X	PKIS	GSK	8	6	10	21	-1	15
546	GW581744X	PKIS	GSK	8	8	-3	7	5	5
547	GW618013A	PKIS	GSK	6	15	-12	16	7	20
548	GW683003X	PKIS	GSK	15	8	6	6	-15	14
549	GW683109X	PKIS	GSK	9	10	0	11	-1	8
550	GW683768X*	PKIS	GSK	-1	4	46	11	22	14
551	GW708336X	PKIS	GSK	5	5	1	4	2	6
552	GW778894X*	PKIS	GSK	58	5	55	20	73	1
553	GW779439X*	PKIS	GSK	59	3	60	29	65	7
554	GW780056X*	PKIS	GSK	63	10	46	48	69	6
555	GW781673X	PKIS	GSK	14	10	0	15	-10	14
556	GW805758X	PKIS	GSK	7	15	-9	15	-9	3
557	GW305074X	PKIS	GSK	9	8	-2	4	8	10
558	GW405841X	PKIS	GSK	-3	3	0	4	14	18
559	GW406108X	PKIS	GSK	12	10	-2	12	15	14

560	GW407323A	PKIS	GSK	4	2	7	26	-19	40
561	GW429374A	PKIS	GSK	8	5	8	3	1	12
562	SB-614067-R	PKIS	GSK	-11	17	-28	18	-15	27
563	SB-682330-A	PKIS	GSK	3	11	-12	24	-5	7
564	GW434756X	PKIS	GSK	8	10	-2	10	5	9
565	GW296115X	PKIS	GSK	7	7	-18	19	21	19
566	GW284408X	PKIS	GSK	7	6	4	12	0	17
567	GW569293E	PKIS	GSK	5	7	-2	38	-1	17
568	SB-590885-AAD	PKIS	GSK	-2	5	-25	12	1	5
569	GW824645A	PKIS2	GSK	9	15	23	21	7	3
570	GW659386A	PKIS2	GSK	1	5	-27	2	-3	31
571	GW683134A	PKIS2	GSK	1	0	17	7	32	12
572	GW574783B*	PKIS2	GSK	59	9	47	2	13	2
573	GW779439X*	PKIS2	GSK	80	5	73	11	66	25
574	AH20685XX	PKIS2	GSK	22	4	22	1	17	7
575	AH2635	PKIS2	GSK	10	6	18	10	9	14
576	AH5015X	PKIS2	GSK	11	2	4	4	18	7
577	GI230329A*	PKIS2	GSK	62	3	43	9	22	14
578	GI261656A	PKIS2	GSK	-4	1	9	5	20	6
579	GI262866A	PKIS2	GSK	12	2	12	9	19	3
580	GI98581X	PKIS2	GSK	3	2	21	5	12	14
581	GSK1014915A	PKIS2	GSK	4	7	-4	4	12	11
582	GSK1024304A	PKIS2	GSK	33	9	22	10	11	23
583	GSK1024306A	PKIS2	GSK	16	5	12	8	21	2
584	GSK1033723A	PKIS2	GSK	9	5	16	5	10	15
585	GSK1034945A	PKIS2	GSK	14	1	11	3	26	1
586	GSK1122999D	PKIS2	GSK	8	3	14	5	16	13
587	GSK1229496A	PKIS2	GSK	31	6	15	8	25	11
588	GSK1229782A	PKIS2	GSK	21	3	17	6	4	12
589	GSK1229959A*	PKIS2	GSK	89	2	69	8	84	1
590	GSK1269851A	PKIS2	GSK	7	13	31	4	23	18
591	GSK1287544A*	PKIS2	GSK	18	2	27	1	46	4
592	GSK1292139B	PKIS2	GSK	8	0	25	30	17	1
593	GSK1307810A*	PKIS2	GSK	12	1	34	6	49	9
594	GSK1321561A	PKIS2	GSK	-8	1	17	4	27	2
595	GSK1321565A	PKIS2	GSK	13	8	30	1	31	4
596	GSK1322949A*	PKIS2	GSK	38	2	53	3	82	6
597	GSK1323434A	PKIS2	GSK	8	0	21	4	30	2
598	GSK1325775A	PKIS2	GSK	10	2	31	12	35	19
599	GSK1326180A	PKIS2	GSK	-35	36	13	5	14	3
600	GSK1379706A	PKIS2	GSK	7	6	20	0	4	19
601	GSK1379708A	PKIS2	GSK	4	8	15	4	12	4
602	GSK1379710A	PKIS2	GSK	9	3	7	13	7	18
603	GSK1379712A	PKIS2	GSK	10	5	17	8	12	4
604	GSK1379713A	PKIS2	GSK	5	5	19	3	3	11
605	GSK1379714A	PKIS2	GSK	10	3	23	1	16	12
606	GSK1379715A	PKIS2	GSK	26	6	27	13	11	8

607	GSK1379716A	PKIS2	GSK	10	6	5	5	22	1
608	GSK1379717A	PKIS2	GSK	15	1	-3	10	9	3
609	GSK1379720A	PKIS2	GSK	6	1	8	5	20	3
610	GSK1379721A	PKIS2	GSK	13	2	-1	18	20	10
611	GSK1379722A	PKIS2	GSK	9	2	9	3	10	3
612	GSK1379723A	PKIS2	GSK	10	1	11	4	-2	16
613	GSK1379724A	PKIS2	GSK	8	2	5	7	16	1
614	GSK1379725A	PKIS2	GSK	7	1	9	3	10	1
615	GSK1379727A	PKIS2	GSK	0	3	12	3	18	1
616	GSK1379729A	PKIS2	GSK	3	5	8	7	18	14
617	GSK1379730A	PKIS2	GSK	4	2	7	1	13	6
618	GSK1379731A	PKIS2	GSK	6	1	9	16	9	9
619	GSK1379732A	PKIS2	GSK	1	2	11	1	11	1
620	GSK1379735A	PKIS2	GSK	4	4	11	4	4	6
621	GSK1379737A*	PKIS2	GSK	30	1	40	12	18	2
622	GSK1379738A	PKIS2	GSK	14	7	18	1	7	18
623	GSK1379741A	PKIS2	GSK	6	1	11	0	6	4
624	GSK1379742A	PKIS2	GSK	9	0	8	5	14	0
625	GSK1379745A	PKIS2	GSK	5	2	-2	14	7	2
626	GSK1379746A	PKIS2	GSK	7	7	17	7	15	2
627	GSK1379748A	PKIS2	GSK	-1	15	10	3	20	2
628	GSK1379751A	PKIS2	GSK	6	2	9	1	11	9
629	GSK1379753A	PKIS2	GSK	-8	15	5	0	9	0
630	GSK1379754A	PKIS2	GSK	9	1	11	15	5	0
631	GSK1379757A	PKIS2	GSK	-22	2	3	15	10	0
632	GSK1379760A	PKIS2	GSK	1	5	14	6	0	2
633	GSK1379761A	PKIS2	GSK	3	6	16	2	16	8
634	GSK1379762A	PKIS2	GSK	2	0	14	3	4	12
635	GSK1379763A	PKIS2	GSK	6	11	15	5	8	12
636	GSK1379765A	PKIS2	GSK	-1	1	14	10	7	13
637	GSK1379766A	PKIS2	GSK	16	5	20	2	18	15
638	GSK1379767A	PKIS2	GSK	16	0	17	5	11	4
639	GSK1379788A	PKIS2	GSK	9	1	-8	12	18	11
640	GSK1379800A	PKIS2	GSK	12	6	-10	20	17	1
641	GSK1379812A	PKIS2	GSK	0	12	-11	7	13	2
642	GSK1379825A	PKIS2	GSK	7	9	-6	19	14	14
643	GSK1379859A	PKIS2	GSK	-24	6	5	5	9	4
644	GSK1379860A	PKIS2	GSK	6	6	-3	9	0	0
645	GSK1379874A	PKIS2	GSK	-12	0	-3	2	7	2
646	GSK1379878A	PKIS2	GSK	-1	6	13	8	9	3
647	GSK1379879A	PKIS2	GSK	-6	13	4	10	12	2
648	GSK1379880A	PKIS2	GSK	1	3	6	4	10	4
649	GSK1379882A	PKIS2	GSK	2	0	7	6	8	1
650	GSK1379883A	PKIS2	GSK	2	3	8	7	8	7
651	GSK1379896A	PKIS2	GSK	5	2	5	0	11	1
652	GSK1379899A	PKIS2	GSK	3	1	15	3	4	1
653	GSK1379901A	PKIS2	GSK	16	1	25	11	21	5

654	GSK1379944A	PKIS2	GSK	7	2	19	2	7	13
655	GSK1383280A*	PKIS2	GSK	21	11	25	4	69	5
656	GSK1383281A*	PKIS2	GSK	20	5	37	3	61	4
657	GSK1389063A*	PKIS2	GSK	29	3	21	15	56	12
658	GSK1398460A*	PKIS2	GSK	0	9	33	3	13	13
659	GSK1398463A	PKIS2	GSK	0	24	24	0	8	1
660	GSK1398467A	PKIS2	GSK	19	4	20	4	-6	1
661	GSK1398468A	PKIS2	GSK	1	12	9	10	6	0
662	GSK1398470A*	PKIS2	GSK	16	2	39	1	-2	36
663	GSK1398471A	PKIS2	GSK	-2	13	21	2	15	2
664	GSK1398472A	PKIS2	GSK	12	1	30	5	6	20
665	GSK1398473A	PKIS2	GSK	11	2	22	12	9	8
666	GSK1398474A	PKIS2	GSK	18	3	31	11	14	2
667	GSK1398475A*	PKIS2	GSK	24	5	42	4	13	1
668	GSK1398477A*	PKIS2	GSK	13	5	32	2	24	1
669	GSK1440913A	PKIS2	GSK	0	4	7	5	10	10
670	GSK1487252A	PKIS2	GSK	29	4	24	5	38	10
671	GSK1520489A*	PKIS2	GSK	62	10	60	13	90	6
672	GSK1535721A	PKIS2	GSK	11	9	-13	23	16	2
673	GSK1558669A*	PKIS2	GSK	17	10	37	2	90	1
674	GSK1576028A*	PKIS2	GSK	66	7	65	5	68	3
675	GSK1581427A*	PKIS2	GSK	25	8	28	13	51	1
676	GSK1581428A*	PKIS2	GSK	36	8	27	17	49	12
677	GSK1627798A*	PKIS2	GSK	69	4	41	7	65	11
678	GSK1645872A*	PKIS2	GSK	46	4	25	22	32	1
679	GSK1645895A	PKIS2	GSK	-10	12	3	9	15	5
680	GSK1649598A*	PKIS2	GSK	11	7	12	6	45	10
681	GSK1653537A	PKIS2	GSK	-11	4	2	5	12	4
682	GSK1653539A	PKIS2	GSK	-10	4	12	3	4	3
683	GSK1660437A*	PKIS2	GSK	29	1	17	12	43	4
684	GSK1660450B*	PKIS2	GSK	37	3	19	2	28	7
685	GSK1669917A	PKIS2	GSK	5	4	11	1	8	7
686	GSK1669921A*	PKIS2	GSK	86	2	60	5	80	5
687	GSK1693850A*	PKIS2	GSK	82	6	43	10	70	13
688	GSK1723980B*	PKIS2	GSK	31	5	-7	23	51	5
689	GSK175726A	PKIS2	GSK	-8	14	-9	14	-2	18
690	GSK1804250A	PKIS2	GSK	2	16	18	28	22	21
691	GSK189015A	PKIS2	GSK	-14	23	-3	18	-5	9
692	GSK190937A	PKIS2	GSK	2	7	9	20	-2	22
693	GSK1917008A	PKIS2	GSK	-15	17	-3	5	0	5
694	GSK198271A*	PKIS2	GSK	67	1	28	9	11	3
695	GSK2008607A*	PKIS2	GSK	-6	16	9	6	50	5
696	GSK204559A	PKIS2	GSK	-1	3	17	12	-2	6
697	GSK204607A	PKIS2	GSK	3	1	12	2	11	4
698	GSK204919A	PKIS2	GSK	4	6	25	10	15	1
699	GSK205189A	PKIS2	GSK	8	4	17	5	10	1
700	GSK2137462A	PKIS2	GSK	0	0	-6	28	13	7

701	GSK2177277A*	PKIS2	GSK	2	0	21	2	56	3
702	GSK2181306A	PKIS2	GSK	14	8	11	4	5	4
703	GSK2188764A	PKIS2	GSK	0	5	3	14	10	21
704	GSK2189892A	PKIS2	GSK	15	11	-7	24	14	17
705	GSK2192730A	PKIS2	GSK	5	8	-7	15	7	3
706	GSK2193613A	PKIS2	GSK	11	7	-9	20	-5	14
707	GSK2197149A	PKIS2	GSK	-6	7	-9	8	13	0
708	GSK2206003A	PKIS2	GSK	3	2	5	12	-6	22
709	GSK2219329A	PKIS2	GSK	-18	21	-6	6	8	2
710	GSK2221681A	PKIS2	GSK	-4	4	7	9	-3	19
711	GSK2224810A	PKIS2	GSK	-13	9	-6	1	10	2
712	GSK2225749A	PKIS2	GSK	-5	4	21	11	15	15
713	GSK2227430A	PKIS2	GSK	4	1	13	7	14	5
714	GSK2228768A	PKIS2	GSK	3	2	18	9	10	13
715	GSK223675A	PKIS2	GSK	7	4	30	1	22	4
716	GSK223810A	PKIS2	GSK	7	0	15	0	4	11
717	GSK2250882A	PKIS2	GSK	10	2	16	2	8	1
718	GSK2258759A	PKIS2	GSK	14	10	11	1	10	7
719	GSK2269905A	PKIS2	GSK	13	12	2	12	35	0
720	GSK2276055A	PKIS2	GSK	28	5	6	6	9	13
721	GSK2283293A	PKIS2	GSK	-2	13	-3	5	8	10
722	GSK2286062A	PKIS2	GSK	-3	12	-3	8	-21	19
723	GSK2286096A	PKIS2	GSK	3	18	-9	22	7	4
724	GSK2286295A	PKIS2	GSK	11	3	-3	15	1	10
725	GSK2286775B	PKIS2	GSK	-9	7	-14	17	8	2
726	GSK2288359A	PKIS2	GSK	-11	0	0	20	-20	12
727	GSK2289044B	PKIS2	GSK	3	5	0	12	24	4
728	GSK2291363A	PKIS2	GSK	10	4	15	12	20	18
729	GSK2296823A	PKIS2	GSK	15	5	9	4	35	0
730	GSK2297099A	PKIS2	GSK	14	1	7	11	19	28
731	GSK2297428A	PKIS2	GSK	10	4	14	9	17	5
732	GSK2297430A	PKIS2	GSK	13	2	15	9	20	11
733	GSK2297542A	PKIS2	GSK	21	5	9	2	31	9
734	GSK2297543A	PKIS2	GSK	20	0	14	9	18	7
735	GSK2298859A	PKIS2	GSK	17	7	-11	10	25	2
736	GSK2299009A	PKIS2	GSK	4	5	-12	20	-11	9
737	GSK2306394A	PKIS2	GSK	1	18	-5	5	17	5
738	GSK2328680A	PKIS2	GSK	3	1	-6	33	9	6
739	GSK2333389A	PKIS2	GSK	8	8	-7	11	26	2
740	GSK2334006A	PKIS2	GSK	1	2	-12	12	-1	20
741	GSK2336394A	PKIS2	GSK	-13	23	-2	6	11	13
742	GSK2342769A	PKIS2	GSK	10	7	-12	8	9	25
743	GSK2344444A	PKIS2	GSK	22	5	-4	5	38	2
744	GSK2347225A	PKIS2	GSK	11	1	0	15	11	19
745	GSK2358994A	PKIS2	GSK	10	4	-3	2	29	1
746	GSK2363608B	PKIS2	GSK	17	5	18	1	28	13
747	GSK2373690A*	PKIS2	GSK	31	3	17	4	45	4

748	GSK2373693A	PKIS2	GSK	13	7	14	6	23	5
749	GSK2373723A*	PKIS2	GSK	46	0	22	10	49	4
750	GSK2375584A	PKIS2	GSK	30	2	23	0	33	5
751	GSK2376236A	PKIS2	GSK	11	10	-4	5	26	16
752	GSK2576924A	PKIS2	GSK	12	6	-14	6	9	7
753	GSK257997A	PKIS2	GSK	-7	20	9	20	0	15
754	GSK2587663A	PKIS2	GSK	-2	8	0	14	-17	17
755	GSK2592465A	PKIS2	GSK	-4	24	-7	20	-11	3
756	GSK2593067A	PKIS2	GSK	-18	1	-9	0	-28	1
757	GSK2593074A	PKIS2	GSK	-11	9	-11	19	2	6
758	GSK260205A	PKIS2	GSK	7	5	5	13	9	0
759	GSK2603346A	PKIS2	GSK	-17	8	1	3	2	1
760	GSK2603358A	PKIS2	GSK	-10	16	14	2	-12	24
761	GSK2606414A	PKIS2	GSK	6	0	7	9	12	5
762	GSK2606590A	PKIS2	GSK	4	6	25	6	14	7
763	GSK2608885A	PKIS2	GSK	0	3	18	6	13	5
764	GSK2608899A	PKIS2	GSK	3	0	19	5	9	7
765	GSK2634140A	PKIS2	GSK	6	5	18	7	15	2
766	GSK2634758A	PKIS2	GSK	14	4	17	8	3	6
767	GSK2635225A	PKIS2	GSK	-10	12	-8	11	6	3
768	GSK2645446A	PKIS2	GSK	-5	17	-22	19	-9	9
769	GSK292658A*	PKIS2	GSK	51	21	26	5	22	11
770	GSK299495A*	PKIS2	GSK	63	5	27	27	19	19
771	GSK301329A	PKIS2	GSK	-4	14	-5	2	5	12
772	GSK301362A	PKIS2	GSK	-5	2	-2	17	-32	21
773	GSK306886A	PKIS2	GSK	-10	21	-7	4	1	9
774	GSK312879A	PKIS2	GSK	-2	1	5	0	-17	15
775	GSK323521A*	PKIS2	GSK	76	16	63	3	59	6
776	GSK323543A*	PKIS2	GSK	84	0	81	6	40	27
777	GSK326180A*	PKIS2	GSK	66	8	35	3	31	7
778	GSK327238A*	PKIS2	GSK	83	2	80	2	62	9
779	GSK336313A	PKIS2	GSK	0	5	7	4	8	3
780	GSK336735A*	PKIS2	GSK	74	0	58	3	48	5
781	GSK346294A*	PKIS2	GSK	19	7	18	2	43	19
782	GSK350559A*	PKIS2	GSK	13	1	51	9	18	6
783	GSK357952A*	PKIS2	GSK	41	14	19	8	20	14
784	GSK361061A*	PKIS2	GSK	55	1	19	8	20	7
785	GSK361065A	PKIS2	GSK	-10	18	-5	13	-5	7
786	GSK364507A	PKIS2	GSK	-4	6	-3	11	-25	16
787	GSK398099A	PKIS2	GSK	-7	14	-8	14	-13	1
788	GSK429286A	PKIS2	GSK	-19	3	4	17	-9	2
789	GSK448459A*	PKIS2	GSK	11	6	23	4	55	31
790	GSK479719A*	PKIS2	GSK	41	0	2	13	22	60
791	GSK483724A*	PKIS2	GSK	44	7	33	4	65	13
792	GSK507274A	PKIS2	GSK	3	13	3	14	-3	18
793	GSK507358A	PKIS2	GSK	-15	2	11	6	8	6
794	GSK534911A	PKIS2	GSK	-4	4	32	8	30	6

795	GSK534913A	PKIS2	GSK	0	1	28	10	27	0
796	GSK562689A	PKIS2	GSK	20	4	22	15	22	12
797	GSK580432A*	PKIS2	GSK	53	5	23	1	81	1
798	GSK581271A	PKIS2	GSK	19	3	17	5	4	3
799	GSK641502A*	PKIS2	GSK	61	49	22	1	71	2
800	GSK683281A	PKIS2	GSK	6	6	-5	30	-16	9
801	GSK846226A	PKIS2	GSK	-12	25	-8	10	8	3
802	GSK902056A	PKIS2	GSK	3	6	-1	19	-15	27
803	GSK907232A*	PKIS2	GSK	35	14	18	9	71	3
804	GSK955403A	PKIS2	GSK	-10	5	-12	29	-24	11
805	GSK977617A	PKIS2	GSK	-19	14	3	8	7	5
806	GSK977620A	PKIS2	GSK	-2	3	12	15	-7	13
807	GSK986310C	PKIS2	GSK	-17	11	-3	0	10	4
808	GSK993273A	PKIS2	GSK	5	2	4	12	-6	26
809	GW271431X	PKIS2	GSK	0	7	21	7	14	1
810	GW272142A	PKIS2	GSK	-2	0	12	6	2	5
811	GW273749A	PKIS2	GSK	4	6	19	1	13	2
812	GW275568A	PKIS2	GSK	-1	1	13	2	-10	14
813	GW281179X	PKIS2	GSK	22	9	19	9	21	8
814	GW282450A	PKIS2	GSK	11	4	10	5	0	11
815	GW284543A	PKIS2	GSK	-9	17	-10	6	8	14
816	GW320571X	PKIS2	GSK	9	2	-12	3	-9	25
817	GW345098X	PKIS2	GSK	-4	15	1	11	2	3
818	GW407034X	PKIS2	GSK	1	10	-4	3	-22	12
819	GW412617A	PKIS2	GSK	-12	18	-10	13	-11	4
820	GW424170A	PKIS2	GSK	-12	1	-16	0	-9	36
821	GW440132A	PKIS2	GSK	-12	11	4	10	0	1
822	GW440135A	PKIS2	GSK	-12	1	-4	6	-25	17
823	GW440137A	PKIS2	GSK	-10	3	2	6	8	10
824	GW440138A*	PKIS2	GSK	21	14	39	1	26	30
825	GW440146A	PKIS2	GSK	8	4	16	15	15	21
826	GW440148A*	PKIS2	GSK	36	33	17	5	61	56
827	GW457859A	PKIS2	GSK	-3	1	8	11	10	4
828	GW461484A	PKIS2	GSK	4	1	8	3	3	6
829	GW461487A	PKIS2	GSK	16	2	7	1	-1	0
830	GW466413A	PKIS2	GSK	-17	22	-21	8	-6	11
831	GW468513X	PKIS2	GSK	1	5	-22	10	8	6
832	GW475620X	PKIS2	GSK	-10	20	-12	6	6	6
833	GW482059X	PKIS2	GSK	-7	3	-22	14	-24	11
834	GW493036X	PKIS2	GSK	11	18	1	1	-2	9
835	GW494601A	PKIS2	GSK	-9	0	2	18	-27	10
836	GW494610A	PKIS2	GSK	-23	2	-6	0	19	1
837	GW494702A	PKIS2	GSK	-11	4	-16	27	-27	25
838	GW497681X	PKIS2	GSK	-31	9	-7	5	-9	11
839	GW514784X	PKIS2	GSK	-3	4	-1	6	-11	20
840	GW514786X	PKIS2	GSK	5	4	7	2	13	2
841	GW515532X	PKIS2	GSK	2	3	15	11	12	8

842	GW525701A*	PKIS2	GSK	33	7	50	3	75	0
843	GW548057X	PKIS2	GSK	0	6	19	2	7	1
844	GW551191X	PKIS2	GSK	-2	6	6	6	9	2
845	GW552771X	PKIS2	GSK	7	4	9	0	2	14
846	GW554060X	PKIS2	GSK	1	8	-11	9	-1	17
847	GW557777X	PKIS2	GSK	-12	5	7	7	37	3
848	GW560106X	PKIS2	GSK	-8	17	-1	7	8	4
849	GW560109X	PKIS2	GSK	-14	6	-5	11	-6	14
850	GW560116X	PKIS2	GSK	-18	22	-10	11	5	11
851	GW560459X	PKIS2	GSK	-14	1	-16	0	-35	12
852	GW567140X	PKIS2	GSK	-17	12	-4	0	-10	3
853	GW567142A	PKIS2	GSK	-11	6	-6	4	-15	17
854	GW567143X	PKIS2	GSK	-19	10	-6	3	-3	5
855	GW567145X	PKIS2	GSK	-14	15	3	12	-9	31
856	GW567148X	PKIS2	GSK	-8	1	1	4	14	2
857	GW569716A*	PKIS2	GSK	50	0	40	9	13	4
858	GW576604X	PKIS2	GSK	-1	1	20	12	13	2
859	GW577382X	PKIS2	GSK	-8	3	-6	2	1	4
860	GW578342X	PKIS2	GSK	8	4	1	7	-1	4
861	GW579362A	PKIS2	GSK	3	24	19	6	20	8
862	GW582764A*	PKIS2	GSK	44	14	6	4	21	17
863	GW582868A	PKIS2	GSK	-8	10	-4	2	10	5
864	GW583340C*	PKIS2	GSK	44	3	24	3	-13	10
865	GW591947A	PKIS2	GSK	-12	18	-8	3	-5	7
866	GW595885X	PKIS2	GSK	-3	4	-1	18	-19	26
867	GW599550X	PKIS2	GSK	-22	8	-1	13	-5	4
868	GW608005X	PKIS2	GSK	2	2	-12	30	-22	21
869	GW621581X	PKIS2	GSK	-9	4	0	8	0	0
870	GW622475X	PKIS2	GSK	-7	6	-5	21	10	11
871	GW630813X	PKIS2	GSK	-2	15	6	1	13	2
872	GW630823A	PKIS2	GSK	-1	4	3	8	14	2
873	GW635815X	PKIS2	GSK	2	5	15	0	15	2
874	GW639905A	PKIS2	GSK	2	6	-7	42	1	4
875	GW654607A	PKIS2	GSK	1	3	7	8	17	5
876	GW659008A	PKIS2	GSK	13	7	10	5	-6	9
877	GW659009A	PKIS2	GSK	-2	5	-6	6	-1	10
878	GW663929X	PKIS2	GSK	0	14	4	6	11	10
879	GW664114X	PKIS2	GSK	2	0	14	5	13	11
880	GW679395X	PKIS2	GSK	3	16	0	7	-12	2
881	GW679396X	PKIS2	GSK	-10	1	-12	0	-24	16
882	GW679662X	PKIS2	GSK	-8	1	-10	13	-11	1
883	GW680061X	PKIS2	GSK	-6	11	2	3	-21	32
884	GW680338X	PKIS2	GSK	-19	5	9	1	-2	3
885	GW680903X	PKIS2	GSK	0	24	13	22	22	62
886	GW681170A	PKIS2	GSK	-6	2	6	2	-1	1
887	GW681251X	PKIS2	GSK	-7	5	8	14	11	8
888	GW682569X	PKIS2	GSK	10	2	23	9	18	3

889	GW684083X	PKIS2	GSK	10	9	22	1	25	28
890	GW684088X	PKIS2	GSK	-2	7	18	0	38	49
891	GW684374X	PKIS2	GSK	7	10	4	1	23	40
892	GW684941X	PKIS2	GSK	23	29	21	1	24	35
893	GW689066X	PKIS2	GSK	8	5	9	5	15	25
894	GW692089A	PKIS2	GSK	-4	17	0	12	14	25
895	GW693028X	PKIS2	GSK	3	5	19	7	21	21
896	GW693542X	PKIS2	GSK	12	1	16	5	-4	10
897	GW694077X	PKIS2	GSK	23	9	20	3	43	27
898	GW696155X	PKIS2	GSK	23	22	24	4	27	8
899	GW697465A	PKIS2	GSK	6	6	6	5	8	8
900	GW697999A	PKIS2	GSK	9	15	13	2	16	1
901	GW701424A*	PKIS2	GSK	35	39	25	2	36	36
902	GW702865X	PKIS2	GSK	-9	3	0	1	1	3
903	GW707818B*	PKIS2	GSK	26	2	34	9	9	8
904	GW709199X	PKIS2	GSK	-7	20	10	4	9	10
905	GW709213X	PKIS2	GSK	4	28	-3	6	40	37
906	GW767488X*	PKIS2	GSK	41	46	-4	12	37	49
907	GW768504A	PKIS2	GSK	5	10	6	12	5	10
908	GW775604X	PKIS2	GSK	9	4	27	24	0	4
909	GW775610X	PKIS2	GSK	3	0	1	8	1	1
910	GW776245A	PKIS2	GSK	9	0	21	6	10	3
911	GW777257X*	PKIS2	GSK	21	9	36	3	34	12
912	GW781483X*	PKIS2	GSK	31	10	43	0	45	13
913	GW784041A*	PKIS2	GSK	5	34	35	2	36	10
914	GW787226A	PKIS2	GSK	14	42	6	16	22	23
915	GW789449X	PKIS2	GSK	9	37	2	29	29	9
916	GW792479X	PKIS2	GSK	6	33	12	12	30	18
917	GW800172X	PKIS2	GSK	9	11	9	5	27	32
918	GW809893X*	PKIS2	GSK	27	56	35	4	61	15
919	GW810083X	PKIS2	GSK	3	14	15	5	22	18
920	GW810437X	PKIS2	GSK	2	5	18	1	15	24
921	GW810445X	PKIS2	GSK	-4	19	16	2	-3	13
922	GW810578X*	PKIS2	GSK	72	9	30	17	40	34
923	GW811603A	PKIS2	GSK	-6	3	-2	1	4	19
924	GW812171X	PKIS2	GSK	7	9	17	8	3	17
925	GW813244A	PKIS2	GSK	-6	1	3	1	-1	9
926	GW813349X	PKIS2	GSK	0	1	2	1	9	22
927	GW818933X	PKIS2	GSK	3	3	6	1	9	18
928	GW818941X	PKIS2	GSK	3	9	9	8	16	27
929	GW819776X	PKIS2	GSK	5	2	3	10	-4	11
930	GW823670X	PKIS2	GSK	-11	3	-5	28	-2	12
931	GW827654A	PKIS2	GSK	-9	5	2	8	16	3
932	GW828205X	PKIS2	GSK	-11	7	3	6	2	13
933	GW828206X	PKIS2	GSK	-6	9	4	0	12	5
934	GW829058X	PKIS2	GSK	2	14	16	7	10	1
935	GW829116X	PKIS2	GSK	29	13	-8	5	13	26

936	GW829350X	PKIS2	GSK	-2	6	-3	8	5	2
937	GW829351X	PKIS2	GSK	3	1	-3	6	-1	8
938	GW830707A	PKIS2	GSK	7	18	21	23	13	3
939	GW830899A	PKIS2	GSK	6	3	13	0	9	2
940	GW835314X	PKIS2	GSK	-3	25	18	17	16	13
941	GW839464X	PKIS2	GSK	8	30	8	6	24	17
942	GW854278X	PKIS2	GSK	-14	31	21	1	18	32
943	GW855857X*	PKIS2	GSK	-9	37	34	3	49	34
944	GW856795X	PKIS2	GSK	-7	50	10	3	15	24
945	GW856805X	PKIS2	GSK	-16	74	12	2	23	14
946	GW857175X	PKIS2	GSK	17	30	30	27	35	41
947	GW867253X	PKIS2	GSK	9	41	7	28	24	15
948	GW867587X	PKIS2	GSK	13	9	27	1	24	21
949	GW867588X	PKIS2	GSK	-13	22	21	2	7	3
950	GW868318X	PKIS2	GSK	-9	4	-9	6	19	22
951	GW869516X	PKIS2	GSK	20	18	21	5	26	19
952	GW869640X*	PKIS2	GSK	-10	10	33	6	11	13
953	GW869641X	PKIS2	GSK	3	6	15	23	2	18
954	GW869979X	PKIS2	GSK	-2	3	-3	7	10	23
955	GW872411X*	PKIS2	GSK	22	1	32	5	16	9
956	GW873004X	PKIS2	GSK	1	15	2	1	7	6
957	GW876019X	PKIS2	GSK	11	5	28	16	0	14
958	GW876731X*	PKIS2	GSK	37	17	41	5	58	13
959	SB-202620	PKIS2	GSK	-5	12	0	7	4	11
960	SB-210486	PKIS2	GSK	-1	18	5	0	-9	13
961	SB-211742	PKIS2	GSK	-4	11	-5	5	-7	10
962	SB-211743	PKIS2	GSK	14	15	24	23	14	3
963	SB-213663	PKIS2	GSK	-26	12	4	1	8	0
964	SB-217146-A	PKIS2	GSK	-9	23	0	8	5	10
965	SB-217360	PKIS2	GSK	-12	15	-1	5	9	1
966	SB-217780	PKIS2	GSK	-6	16	-2	3	23	13
967	SB-219952	PKIS2	GSK	-4	21	-4	5	5	13
968	SB-219980	PKIS2	GSK	4	15	-10	2	8	3
969	SB-222516	PKIS2	GSK	2	12	-1	7	6	9
970	SB-222517	PKIS2	GSK	-4	16	10	20	-5	10
971	SB-222903	PKIS2	GSK	-13	27	4	4	1	10
972	SB-223132	PKIS2	GSK	-10	20	-5	8	-10	8
973	SB-226605	PKIS2	GSK	1	36	6	1	28	18
974	SB-229482	PKIS2	GSK	-28	46	12	0	4	13
975	SB-236560	PKIS2	GSK	-26	51	-2	9	25	6
976	SB-238039-R	PKIS2	GSK	30	15	11	1	33	27
977	SB-245391	PKIS2	GSK	-5	28	6	15	1	12
978	SB-249175	PKIS2	GSK	-11	30	-2	10	0	13
979	SB-282852	PKIS2	GSK	-1	28	1	6	8	15
980	SB-282975-A	PKIS2	GSK	9	5	6	1	14	19
981	SB-284851-BT	PKIS2	GSK	-9	37	0	14	2	9
982	SB-284852-BT	PKIS2	GSK	-5	31	-9	11	11	14

983	SB-300079	PKIS2	GSK	6	8	12	1	1	4
984	SB-317651	PKIS2	GSK	-3	10	21	7	16	20
985	SB-317658	PKIS2	GSK	-9	1	-13	10	-6	16
986	SB-317661	PKIS2	GSK	5	9	7	7	5	10
987	SB-326892	PKIS2	GSK	15	1	-4	3	-3	15
988	SB-331032	PKIS2	GSK	2	7	-1	1	5	17
989	SB-333613	PKIS2	GSK	11	2	10	5	-2	12
990	SB-334860	PKIS2	GSK	9	4	7	2	9	14
991	SB-334865	PKIS2	GSK	1	8	-5	16	-14	6
992	SB-340867	PKIS2	GSK	0	11	-9	2	-2	32
993	SB-341528	PKIS2	GSK	-7	3	-2	5	-11	11
994	SB-341556	PKIS2	GSK	8	4	18	17	1	3
995	SB-342409	PKIS2	GSK	-20	4	7	1	12	3
996	SB-342411	PKIS2	GSK	-13	18	0	7	1	6
997	SB-360737	PKIS2	GSK	-7	6	-8	10	-9	12
998	SB-373598	PKIS2	GSK	3	4	-1	5	-3	11
999	SB-376715	PKIS2	GSK	-18	28	-10	1	-3	2
1000	SB-381891	PKIS2	GSK	-5	10	-5	1	8	1
1001	SB-381904	PKIS2	GSK	2	13	1	10	6	11
1002	SB-386023-B	PKIS2	GSK	-13	14	-8	13	-8	3
1003	SB-390526	PKIS2	GSK	0	7	-3	0	-15	19
1004	SB-390530	PKIS2	GSK	7	4	-3	7	-13	14
1005	SB-390532	PKIS2	GSK	-1	24	3	3	18	26
1006	SB-390534	PKIS2	GSK	-31	35	-5	13	5	16
1007	SB-390765	PKIS2	GSK	-31	40	0	17	0	12
1008	SB-390766	PKIS2	GSK	-9	20	3	12	16	26
1009	SB-390767	PKIS2	GSK	-22	21	-11	18	13	9
1010	SB-390769	PKIS2	GSK	-7	20	5	4	-10	15
1011	SB-390770	PKIS2	GSK	0	14	2	12	0	13
1012	SB-390771	PKIS2	GSK	15	7	10	1	28	23
1013	SB-404290	PKIS2	GSK	-14	0	0	5	-5	4
1014	SB-404321	PKIS2	GSK	-4	17	-23	15	-12	4
1015	SB-405367	PKIS2	GSK	13	3	18	2	-3	11
1016	SB-408010	PKIS2	GSK	-11	12	7	28	12	17
1017	SB-428218-A	PKIS2	GSK	-1	0	-11	13	-10	13
1018	SB-477794-AAA	PKIS2	GSK	-1	41	-4	6	22	11
1019	SB-517081	PKIS2	GSK	6	5	-5	1	-9	12
1020	SB-517389	PKIS2	GSK	-1	11	-3	15	-6	11
1021	SB-548492	PKIS2	GSK	7	5	6	1	-6	10
1022	SB-589132	PKIS2	GSK	1	3	5	2	-6	9
1023	SB-601273*	PKIS2	GSK	49	46	12	12	44	52
1024	SB-601436	PKIS2	GSK	-2	10	-7	2	-10	8
1025	SB-610250	PKIS2	GSK	-2	14	-14	7	-8	8
1026	SB-625086-M	PKIS2	GSK	9	6	17	15	8	4
1027	SB-627772-A	PKIS2	GSK	-15	1	3	10	14	3
1028	SB-642057	PKIS2	GSK	-7	5	17	13	5	17
1029	SB-642124-AAA	PKIS2	GSK	-6	3	-6	2	-8	0

1030	SB-660566	PKIS2	GSK	-19	12	-8	0	-5	1
1031	SB-684387-B	PKIS2	GSK	-21	27	-11	4	-11	19
1032	SB-693162	PKIS2	GSK	1	12	-9	1	3	2
1033	SB-693578	PKIS2	GSK	3	7	-5	1	3	7
1034	SB-707548-A	PKIS2	GSK	13	10	25	3	-1	10
1035	SB-708998	PKIS2	GSK	3	8	-3	6	-8	31
1036	SB-708999	PKIS2	GSK	3	12	0	1	-20	7
1037	SB-710363	PKIS2	GSK	5	28	14	1	27	12
1038	SB-710397-B	PKIS2	GSK	-24	34	-2	6	12	12
1039	SB-710903	PKIS2	GSK	-31	40	-21	19	11	2
1040	SB-711239	PKIS2	GSK	-23	26	-16	27	5	18
1041	SB-711805	PKIS2	GSK	-17	28	-6	21	-4	9
1042	SB-711880	PKIS2	GSK	-19	26	-2	14	-7	15
1043	SB-731254-M	PKIS2	GSK	14	4	2	3	5	19
1044	SB-731284	PKIS2	GSK	7	6	2	3	5	26
1045	SB-731579	PKIS2	GSK	-19	34	9	22	22	25
1046	SB-732932	PKIS2	GSK	-17	17	-7	9	-12	14
1047	SB-733371	PKIS2	GSK	5	7	12	1	-5	11
1048	SB-733416	PKIS2	GSK	-4	14	0	1	10	17
1049	SB-733887	PKIS2	GSK	-27	3	-16	25	-16	22
1050	SB-733894	PKIS2	GSK	-16	2	-4	1	-11	9
1051	SB-734909	PKIS2	GSK	-14	2	-11	0	-22	30
1052	SB-735216	PKIS2	GSK	3	4	-2	1	-13	14
1053	SB-735297	PKIS2	GSK	6	6	1	7	-7	9
1054	SB-735464	PKIS2	GSK	5	6	12	2	12	25
1055	SB-736398	PKIS2	GSK	-3	3	1	1	-8	8
1056	SB-736715	PKIS2	GSK	-5	4	-5	4	6	18
1057	SB-737447	PKIS2	GSK	-7	10	-9	11	-2	15
1058	SB-737856	PKIS2	GSK	12	8	9	9	2	3
1059	SB-738004	PKIS2	GSK	-4	4	10	27	26	2
1060	SB-738481	PKIS2	GSK	-23	3	6	16	-11	7
1061	SB-742034-AC	PKIS2	GSK	-15	1	-1	11	-20	26
1062	SB-742251	PKIS2	GSK	-9	12	-11	1	-14	2
1063	SB-742352-AC	PKIS2	GSK	-19	35	-8	2	-10	5
1064	SB-742609	PKIS2	GSK	2	10	-10	0	4	6
1065	SB-743341	PKIS2	GSK	0	10	-1	6	-1	6
1066	SB-747651-A	PKIS2	GSK	25	12	24	21	21	7
1067	SB-750250-M	PKIS2	GSK	0	13	-4	1	-8	14
1068	SKF-104365	PKIS2	GSK	9	7	32	7	10	4
1069	SKF-104493-B2	PKIS2	GSK	7	19	7	4	21	22
1070	SKF-105561	PKIS2	GSK	-33	40	3	8	1	12
1071	SKF-105942	PKIS2	GSK	-31	26	-18	18	-15	8
1072	SKF-106164-A2	PKIS2	GSK	-15	18	-11	35	-5	6
1073	SKF-12778	PKIS2	GSK	-13	27	-21	20	-2	10
1074	SKF-18267	PKIS2	GSK	-14	21	-9	3	14	17
1075	SKF-18355	PKIS2	GSK	7	6	2	10	0	14
1076	SKF-31736	PKIS2	GSK	19	21	-1	9	22	25

1077	SKF-96418	PKIS2	GSK	-24	34	2	1	-4	9
1078	SKF-97184	PKIS2	GSK	-27	58	10	14	-5	5
1079	SKF-97236	PKIS2	GSK	11	7	14	2	10	14
1080	SKF-97255	PKIS2	GSK	-27	18	7	12	-5	12
1081	SKF-97263	PKIS2	GSK	-12	9	-18	3	-13	19
1082	SKF-97293	PKIS2	GSK	-4	6	-5	27	4	15
1083	SKF-97359	PKIS2	GSK	1	7	-7	4	-12	11
1084	SKF-97416	PKIS2	GSK	-4	8	3	8	-5	10
1085	SKF-97510	PKIS2	GSK	4	0	1	1	-7	8
1086	SKF-97560	PKIS2	GSK	7	2	4	2	10	24
1087	SKF-97620	PKIS2	GSK	1	5	1	0	5	8
1088	SKF-97623	PKIS2	GSK	4	1	-3	5	10	18
1089	GI1261590A*	PKIS2	GSK	38	2	27	6	20	2
1090	F9005, Fulfenamic Acid	AKR1B10	Sigma	ND	ND	ND	ND	ND	ND
1091	D6899, Diclofenac Sodium Salt	AKR1B10	Sigma	ND	ND	ND	ND	ND	ND
1092	S8139, Sulindac	AKR1B10	Sigma	ND	ND	ND	ND	ND	ND
1093	C2755, Cortisone	AKR1B10	Sigma	ND	ND	ND	ND	ND	ND
1094	M4267, Mefenamic Acid	AKR1B10	Sigma	ND	ND	ND	ND	ND	ND
1095	B6938, BisdemethoxycurcUmin	AKR1B10	Sigma	ND	ND	ND	ND	ND	ND
1096	P7265, PGA1	AKR1B10	Sigma	ND	ND	ND	ND	ND	ND
1097	O5504, Oleanolic Acid	AKR1B10	Sigma	ND	ND	ND	ND	ND	ND

Footnote to Suppl. Table 2. 154 inhibitory hit compounds are marked with an asterisk (*). BT: Batch Reference. Mean M%I: Mean Maximum Percentage Inhibition. SD: Standard Deviation. Inhibitory hits (n=154) above the selected thresholds (see main text) are marked with an asterisk (*). Identical compounds of different batches are labelled with a hash tag (#). ND: Not done: AKR1B10 inhibitors were tested in an EC_{50} format only, so that no single-point screening data is available for these compounds.

Suppl. Table 3. Enrichment in pathway analysis. (A) Enrichment in pathways of targets of non-EGFR hit compounds. Number genes in comparison: n=5. Adapted from Scheipl *et al.* (2016) (11).

Gene Set Name	# Genes in Gene Set (K)	Description	# Genes in Overlap (k)	k/K	p-value	FDR q-value	Genes					# Compounds
KEGG_COLORECTAL_CANCER	62	Colorectal cancer	4	0.065	1.5E-11	9.73E-09	AKT1	PIK3CA	BRAF	TGFBR1		**4**
PID_VEGFR-1_2_PATHWAY	69	Signaling events mediated by VEGFR-1 and VEGFR-2	4	0.058	2.32E-11	9.73E-09	AKT1	PIK3CA	BRAF		KDR	**4**
KEGG_PANCREATIC_CANCER	70	Pancreatic cancer	4	0.057	2.46E-11	9.73E-09	AKT1	PIK3CA	BRAF	TGFBR1		**4**
KEGG_CHRONIC_MYELOID_LEUKEMIA	73	Chronic myeloid leukemia	4	0.055	2.93E-11	9.73E-09	AKT1	PIK3CA	BRAF	TGFBR1		**4**
KEGG_FOCAL_ADHESION	201	Focal adhesion	4	0.02	1.77E-09	4.71E-07	AKT1	PIK3CA	BRAF		KDR	**4**
ST_ADRENERGIC	36	Adrenergic Pathway	3	0.083	4.41E-09	9.77E-07	AKT1	PIK3CA	BRAF			3
ST_DIFFERENTIATION_PATHWAY_IN_PC12_CELLS	45	Differentiation Pathway in PC12 Cells; this is a specific case of PAC1 Receptor Pathway.	3	0.067	8.76E-09	0.0000166	AKT1	PIK3CA	BRAF			3
KEGG_PATHWAYS_IN_CANCER	328	Pathways in cancer	4	0.012	1.27E-08	0.0000181	AKT1	PIK3CA	BRAF	TGFBR1		**4**
KEGG_ENDOMETRIAL_CANCER	52	Endometrial cancer	3	0.058	1.36E-08	0.0000181	AKT1	PIK3CA	BRAF			3

KEGG_MTOR_SIGNALING_PATHWAY	52	mTOR signaling pathway	3	0.058	1.36E-08	0.00000181	AKT1	PIK3CA	BRAF			3
KEGG_NON_SMALL_CELL_LUNG_CANCER	54	Non-small cell lung cancer	3	0.056	1.53E-08	0.00000185	AKT1	PIK3CA	BRAF			3
KEGG_ACUTE_MYELOID_LEUKEMIA	60	Acute myeloid leukemia	3	0.05	2.11E-08	0.00000234	AKT1	PIK3CA	BRAF			3
KEGG_GLIOMA	65	Glioma	3	0.046	2.69E-08	0.00000276	AKT1	PIK3CA	BRAF			3
KEGG_RENAL_CELL_CARCINOMA	70	Renal cell carcinoma	3	0.043	3.38E-08	0.00000313	AKT1	PIK3CA	BRAF			3
KEGG_MELANOMA	71	Melanoma	3	0.042	3.53E-08	0.00000313	AKT1	PIK3CA	BRAF			3
PID_AVB3_INTEGRIN_PATHWAY	75	Integrins in angiogenesis	3	0.04	4.16E-08	0.00000339	AKT1	PIK3CA		KDR		3
KEGG_VEGF_SIGNALING_PATHWAY	76	VEGF signaling pathway	3	0.04	4.34E-08	0.00000339	AKT1	PIK3CA		KDR		3
ST_INTEGRIN_SIGNALING_PATHWAY	82	Integrin Signaling Pathway	3	0.037	5.46E-08	0.00000404	AKT1	PIK3CA	BRAF			3
KEGG_PROGESTERONE_MEDIATED_OOCYTE_MATURATION	86	Progesterone-mediated oocyte maturation	3	0.035	6.31E-08	0.00000435	AKT1	PIK3CA	BRAF			3
KEGG_ERBB_SIGNALING_PATHWAY	87	ErbB signaling pathway	3	0.035	6.54E-08	0.00000435	AKT1	PIK3CA	BRAF			3
KEGG_PROSTATE_CANCER	89	Prostate cancer	3	0.034	0.00000007	0.00000443	AKT1	PIK3CA	BRAF			3
PID_ERBB1_DOWNSTREAM_PATHWAY	105	ErbB1 downstream signaling	3	0.029	1.16E-07	0.00000698	AKT1	PIK3CA	BRAF			3
REACTOME_SIGNALING_BY_FGFR	112	Genes involved in Signaling by FGFR	3	0.027	0.00000014	0.00000812	AKT1	PIK3CA	BRAF			3
KEGG_NEUROTROPHIN_SIGNALING_PATHWAY	126	Neurotrophin signaling pathway	3	0.024	0.0000002	0.0000109	AKT1	PIK3CA	BRAF			3
REACTOME_SIGNALING_BY_FGFR_IN_DISEASE	127	Genes involved in Signaling by FGFR in disease	3	0.024	2.05E-07	0.0000109	AKT1	PIK3CA	BRAF			3
KEGG_INSULIN_SIGNALING_PATHWAY	137	Insulin signaling pathway	3	0.022	2.58E-07	0.0000127	AKT1	PIK3CA	BRAF			3

REACTOME_NGF_SIGNALLING_VIA_TRKA_FROM_THE_PLASMA_MEMBRANE	137	Genes involved in NGF signalling via TRKA from the plasma membrane	3	0.022	2.58E-07	0.0000127	AKT1	PIK3CA	BRAF	3
BIOCARTA_TRKA_PATHWAY	12	Trka Receptor Signaling Pathway	2	0.167	6.25E-07	0.0000297	AKT1	PIK3CA		2
KEGG_CHEMOKINE_SIGNALING_PATHWAY	190	Chemokine signaling pathway	3	0.016	6.91E-07	0.0000317	AKT1	PIK3CA	BRAF	3
BIOCARTA_LONGEVITY_PATHWAY	15	The IGF-1 Receptor and Longevity	2	0.133	9.94E-07	0.0000441	AKT1	PIK3CA		2
REACTOME_SIGNALLING_BY_NGF	217	Genes involved in Signalling by NGF	3	0.014	0.00000103	0.0000442	AKT1	PIK3CA	BRAF	3
BIOCARTA_ACH_PATHWAY	16	Role of nicotinic acetylcholine receptors in the regulation of apoptosis	2	0.125	0.00000114	0.0000458	AKT1	PIK3CA		2
BIOCARTA_BCELLSURVIVAL_PATHWAY	16	B Cell Survival Pathway	2	0.125	0.00000114	0.0000458	AKT1	PIK3CA		2
BIOCARTA_HCMV_PATHWAY	17	Human Cytomegalovirus and Map Kinase Pathways	2	0.118	0.00000129	0.0000476	AKT1	PIK3CA		2
SA_PTEN_PATHWAY	17	PTEN is a tumor suppressor that dephosphorylates the lipid messenger phosphatidylinositol triphosphate.	2	0.118	0.00000129	0.0000476	AKT1	PIK3CA		2
SA_TRKA_RECEPTOR	17	The TrkA receptor binds nerve growth factor to activate MAP kinase pathways and promote cell growth.	2	0.118	0.00000129	0.0000476	AKT1	PIK3CA		2
BIOCARTA_ERK5_PATHWAY	18	Role of Erk5 in Neuronal Survival	2	0.111	0.00000145	0.0000507	AKT1	PIK3CA		2
BIOCARTA_PTEN_PATHWAY	18	PTEN dependent cell cycle arrest and apoptosis	2	0.111	0.00000145	0.0000507	AKT1	PIK3CA		2

BIOCARTA_IGF1MTOR_PATHWAY	20	Skeletal muscle hypertrophy is regulated via AKT/mTOR pathway	2	0.1	0.0000018	0.0000613	AKT1	PIK3CA			2
KEGG_MAPK_SIGNALING_PATHWAY	267	MAPK signaling pathway	3	0.011	0.00000192	0.0000624	AKT1		BRAF	TGFBR1	3
BIOCARTA_TFF_PATHWAY	21	Trefoil Factors Initiate Mucosal Healing	2	0.095	0.00000199	0.0000624	AKT1	PIK3CA			2
PID_ECADHERIN_KERATINOCYTE_PATHWAY	21	E-cadherin signaling in keratinocytes	2	0.095	0.00000199	0.0000624	AKT1	PIK3CA			2
BIOCARTA_AKT_PATHWAY	22	AKT Signaling Pathway	2	0.091	0.00000219	0.0000624	AKT1	PIK3CA			2
BIOCARTA_GCR_PATHWAY	22	Corticosteroids and cardioprotection	2	0.091	0.00000219	0.0000624	AKT1	PIK3CA			2
PID_HEDGEHOG_2PATHWAY	22	Signaling events mediated by the Hedgehog family	2	0.091	0.00000219	0.0000624	AKT1	PIK3CA			2
REACTOME_CD28_DEPENDENT_PI3K_AKT_SIGNALING	22	Genes involved in CD28 dependent PI3K/Akt signaling	2	0.091	0.00000219	0.0000624	AKT1	PIK3CA			2
BIOCARTA_CTCF_PATHWAY	23	CTCF: First Multivalent Nuclear Factor	2	0.087	0.00000239	0.0000624		PIK3CA		TGFBR1	2
BIOCARTA_GLEEVEC_PATHWAY	23	Inhibition of Cellular Proliferation by Gleevec	2	0.087	0.00000239	0.0000624	AKT1	PIK3CA			2
BIOCARTA_IGF1R_PATHWAY	23	Multiple antiapoptotic pathways from IGF-1R signaling lead to BAD phosphorylation	2	0.087	0.00000239	0.0000624	AKT1	PIK3CA			2
BIOCARTA_MTOR_PATHWAY	23	mTOR Signaling Pathway	2	0.087	0.00000239	0.0000624	AKT1	PIK3CA			2

Footnote to Suppl. Table 3 (A). The analysis is based on the compounds' key targets (n=5, **Table 10**). # = number; FDR: false discovery rate**.**

(B) Enrichment in pathways of targets of non-EGFR hit compounds. Number of genes in comparison: n=13. Adapted from Scheipl *et al.* (2016) (11).

Gene Set Name	# Genes in Gene Set (K)	Description	# Genes in Overlap (k)	k/K	p-value	FDR q-value	Genes					# Compounds
KEGG_COLORECTAL_CANCER	62	Colorectal cancer	4	0.065	1.5E-11	9.73E-09	AKT1	PIK3CA	BRAF	TGFBR1		**4**
PID_VEGFR-1_2_PATHWAY	69	Signaling events mediated by VEGFR-1 and VEGFR-2	4	0.058	2.32E-11	9.73E-09	AKT1	PIK3CA	BRAF		KDR	**4**
KEGG_PANCREATIC_CANCER	70	Pancreatic cancer	4	0.057	2.46E-11	9.73E-09	AKT1	PIK3CA	BRAF	TGFBR1		**4**
KEGG_CHRONIC_MYELOID_LEUKEMIA	73	Chronic myeloid leukemia	4	0.055	2.93E-11	9.73E-09	AKT1	PIK3CA	BRAF	TGFBR1		**4**
KEGG_FOCAL_ADHESION	201	Focal adhesion	4	0.02	1.77E-09	4.71E-07	AKT1	PIK3CA	BRAF		KDR	**4**
ST_ADRENERGIC	36	Adrenergic Pathway	3	0.083	4.41E-09	9.77E-07	AKT1	PIK3CA	BRAF			3
ST_DIFFERENTIATION_PATHWAY_IN_PC12_CELLS	45	Differentiation Pathway in PC12 Cells; this is a specific case of PAC1 Receptor Pathway.	3	0.067	8.76E-09	0.0000016	AKT1	PIK3CA	BRAF			3
KEGG_PATHWAYS_IN_CANCER	328	Pathways in cancer	4	0.012	1.27E-08	0.0000018 1	AKT1	PIK3CA	BRAF	TGFBR1		**4**
KEGG_ENDOMETRIAL_CANCER	52	Endometrial cancer	3	0.058	1.36E-08	0.0000018 1	AKT1	PIK3CA	BRAF			3
KEGG_MTOR_SIGNALING_PATHWAY	52	mTOR signaling pathway	3	0.058	1.36E-08	0.0000018 1	AKT1	PIK3CA	BRAF			3
KEGG_NON_SMALL_CELL_LUNG_CANCER	54	Non-small cell lung cancer	3	0.056	1.53E-08	0.0000018 5	AKT1	PIK3CA	BRAF			3
KEGG_ACUTE_MYELOID_LEUKEMIA	60	Acute myeloid leukemia	3	0.05	2.11E-08	0.0000023 4	AKT1	PIK3CA	BRAF			3
KEGG_GLIOMA	65	Glioma	3	0.046	2.69E-08	0.0000027 6	AKT1	PIK3CA	BRAF			3
KEGG_RENAL_CELL_CARCINOMA	70	Renal cell carcinoma	3	0.043	3.38E-08	0.0000031 3	AKT1	PIK3CA	BRAF			3
KEGG_MELANOMA	71	Melanoma	3	0.042	3.53E-08	0.0000031	AKT1	PIK3CA	BRAF			3

						3					
PID_AVB3_INTEGRIN_PATHWAY	75	Integrins in angiogenesis	3	0.04	4.16E-08	0.0000033 9	AKT1	PIK3CA		KDR	3
KEGG_VEGF_SIGNALING_PATHWAY	76	VEGF signaling pathway	3	0.04	4.34E-08	0.0000033 9	AKT1	PIK3CA		KDR	3
ST_INTEGRIN_SIGNALING_PATHWAY	82	Integrin Signaling Pathway	3	0.037	5.46E-08	0.0000040 4	AKT1	PIK3CA	BRAF		3
KEGG_PROGESTERONE_MEDIATED_OOCYTE_MATURATION	86	Progesterone-mediated oocyte maturation	3	0.035	6.31E-08	0.0000043 5	AKT1	PIK3CA	BRAF		3
KEGG_ERBB_SIGNALING_PATHWAY	87	ErbB signaling pathway	3	0.035	6.54E-08	0.0000043 5	AKT1	PIK3CA	BRAF		3
KEGG_PROSTATE_CANCER	89	Prostate cancer	3	0.034	0.0000000 7	0.0000044 3	AKT1	PIK3CA	BRAF		3
PID_ERBB1_DOWNSTREAM_PATHWAY	105	ErbB1 downstream signaling	3	0.029	1.16E-07	0.0000069 8	AKT1	PIK3CA	BRAF		3
REACTOME_SIGNALING_BY_FGFR	112	Genes involved in Signaling by FGFR	3	0.027	0.0000001 4	0.0000081 2	AKT1	PIK3CA	BRAF		3
KEGG_NEUROTROPHIN_SIGNALING_PATHWAY	126	Neurotrophin signaling pathway	3	0.024	0.0000002	0.0000109	AKT1	PIK3CA	BRAF		3
REACTOME_SIGNALING_BY_FGFR_IN_DISEASE	127	Genes involved in Signaling by FGFR in disease	3	0.024	2.05E-07	0.0000109	AKT1	PIK3CA	BRAF		3
KEGG_INSULIN_SIGNALING_PATHWAY	137	Insulin signaling pathway	3	0.022	2.58E-07	0.0000127	AKT1	PIK3CA	BRAF		3
REACTOME_NGF_SIGNALLING_VIA_TRKA_FROM_THE_PLASMA_MEMBRANE	137	Genes involved in NGF signalling via TRKA from the plasma membrane	3	0.022	2.58E-07	0.0000127	AKT1	PIK3CA	BRAF		3
BIOCARTA_TRKA_PATHWAY	12	Trka Receptor Signaling Pathway	2	0.167	6.25E-07	0.0000297	AKT1	PIK3CA			2
KEGG_CHEMOKINE_SIGNALING_PATHWAY	190	Chemokine signaling pathway	3	0.016	6.91E-07	0.0000317	AKT1	PIK3CA	BRAF		3
BIOCARTA_LONGEVITY_PATHWAY	15	The IGF-1 Receptor and Longevity	2	0.133	9.94E-07	0.0000441	AKT1	PIK3CA			2
REACTOME_SIGNALLING_BY_NGF	217	Genes involved in Signalling by NGF	3	0.014	0.0000010 3	0.0000442	AKT1	PIK3CA	BRAF		3

BIOCARTA_ACH_PATHWAY	16	Role of nicotinic acetylcholine receptors in the regulation of apoptosis	2	0.125	0.00000114	0.0000458	AKT1	PIK3CA				2
BIOCARTA_BCELLSURVIVAL_PATHWAY	16	B Cell Survival Pathway	2	0.125	0.00000114	0.0000458	AKT1	PIK3CA				2
BIOCARTA_HCMV_PATHWAY	17	Human Cytomegalovirus and Map Kinase Pathways	2	0.118	0.00000129	0.0000476	AKT1	PIK3CA				2
SA_PTEN_PATHWAY	17	PTEN is a tumor suppressor that dephosphorylates the lipid messenger phosphatidylinositol triphosphate.	2	0.118	0.00000129	0.0000476	AKT1	PIK3CA				2
SA_TRKA_RECEPTOR	17	The TrkA receptor binds nerve growth factor to activate MAP kinase pathways and promote cell growth.	2	0.118	0.00000129	0.0000476	AKT1	PIK3CA				2
BIOCARTA_ERK5_PATHWAY	18	Role of Erk5 in Neuronal Survival	2	0.111	0.00000145	0.0000507	AKT1	PIK3CA				2
BIOCARTA_PTEN_PATHWAY	18	PTEN dependent cell cycle arrest and apoptosis	2	0.111	0.00000145	0.0000507	AKT1	PIK3CA				2
BIOCARTA_IGF1MTOR_PATHWAY	20	Skeletal muscle hypertrophy is regulated via AKT/mTOR pathway	2	0.1	0.0000018	0.0000613	AKT1	PIK3CA				2
KEGG_MAPK_SIGNALING_PATHWAY	267	MAPK signaling pathway	3	0.011	0.00000192	0.0000624	AKT1		BRAF	TGFBR1		3
BIOCARTA_TFF_PATHWAY	21	Trefoil Factors Initiate Mucosal Healing	2	0.095	0.00000199	0.0000624	AKT1	PIK3CA				2
PID_ECADHERIN_KERATINOCYTE_PATHWAY	21	E-cadherin signaling in keratinocytes	2	0.095	0.00000199	0.0000624	AKT1	PIK3CA				2

BIOCARTA_AKT_PATHWAY	22	AKT Signaling Pathway	2	0.091	0.00000219	0.0000624	AKT1	PIK3CA		2
BIOCARTA_GCR_PATHWAY	22	Corticosteroids and cardioprotection	2	0.091	0.00000219	0.0000624	AKT1	PIK3CA		2
PID_HEDGEHOG_2PATHWAY	22	Signaling events mediated by the Hedgehog family	2	0.091	0.00000219	0.0000624	AKT1	PIK3CA		2
REACTOME_CD28_DEPENDENT_PI3K_AKT_SIGNALING	22	Genes involved in CD28 dependent PI3K/Akt signaling	2	0.091	0.00000219	0.0000624	AKT1	PIK3CA		2
BIOCARTA_CTCF_PATHWAY	23	CTCF: First Multivalent Nuclear Factor	2	0.087	0.00000239	0.0000624		PIK3CA	TGFBR1	2
BIOCARTA_GLEEVEC_PATHWAY	23	Inhibition of Cellular Proliferation by Gleevec	2	0.087	0.00000239	0.0000624	AKT1	PIK3CA		2
BIOCARTA_IGF1R_PATHWAY	23	Multiple antiapoptotic pathways from IGF-1R signaling lead to BAD phosphorylation	2	0.087	0.00000239	0.0000624	AKT1	PIK3CA		2
BIOCARTA_MTOR_PATHWAY	23	mTOR Signaling Pathway	2	0.087	0.00000239	0.0000624	AKT1	PIK3CA		2

Footnote to Suppl. Table 3 (B). The analysis is based on all of the compounds' targets (n=13, **Table 10**). Adapted from Scheipl et al. (2016) (11). FDR: false discovery rate; #: number.

Appendix 2

Published Papers

The three papers by Scheipl *et al.* (2012), (2013) and (2016) that have been published in course of this thesis are subsequently attached (1, 2, 11):

1. Scheipl, S; Barnard, M; Cottone, L; Jorgensen, M; Drewry, DH; Zuercher, WJ; Turlais, F; Ye, H; Leite, AP; Smith, JA; Leithner, A; Möller, P; Brüderlein, S; Guppy, N; Amary, F; Tirabosco, R; Strauss, SJ; Pillay, N; Flanagan, AM, 2016. EGFR inhibitors Identified as a Potential Treatment for Chordoma in a Focused Compound Screen. J Pathol. 2016; 239(3):320-334. Doi:10.1002/path.4729
2. Scheipl, S; Lohberger, B; Rinner, B; Froehlich, EV; Beham, A; Quehenberger, F; Lazáry, A; Pal Varga, P; Haybaeck, J; Leithner, A; Liegl, B, 2013. Histone deacetylase inhibitors as potential therapeutic approaches for chordoma: an immunohistochemical and functional analysis. J Orthop Res. 2013; 31(12):1999-2005. Doi:10.1002/jor.22447
3. Scheipl, S; Froehlich, EV; Leithner, A; Beham, A; Quehenberger, F; Mokry, M; Stammberger, H; Varga, PP; Lazary, A; Windhager, R; Gattenloehner, S; Liegl, B, 2012
   Does insulin-like growth factor 1 receptor (IGF-1R) targeting provide new treatment options for chordomas? A retrospective clinical and immunohistochemical study. Histopathology. 2012; 60(6):999-1003. Doi:10.1111/j.1365-2559.2012.04186.x

Appendix 3

Reference Library (CD)

Full texts/PDFs of all references are provided on the attached CD.

Permissions (CD)

Permissions of copyright holders and co-authors to the published papers are provided on the attached CD:

- Permission Wiley IGF-1R
- Permission Wiley HDAC
- Permission Wiley EGFR
- Permission Wiley Figure 5
- Permission Wiley Figure 6
- Permission of co-authors of the manuscripts (Scheipl *et al.* (2012) (1), Scheipl *et al.* (2013) (2), Scheipl *et al.* (2016) (11))